

Copyright
by
Hilary Ruth Plake
2004

**The Dissertation Committee for Hilary Ruth Plake Certifies that this is the
approved version of the following dissertation:**

**Synthesis and Evaluation of Conformationally Constrained Peptide
Replacements and Studies Toward the Total Synthesis of Kidamycin**

Committee:

Stephen F. Martin, Supervisor

Eric V. Anslyn

Lara Mahal

Dean Appling

Sean Kerwin

**Synthesis and Evaluation of Conformationally Constrained Peptide
Replacements and Studies Toward the Total Synthesis of Kidamycin**

by

Hilary Ruth Plake, B. A.

Dissertation

Presented to the Faculty of the Graduate School of

The University of Texas at Austin

in Partial Fulfillment

of the Requirements

for the Degree of

Doctor of Philosophy

The University of Texas at Austin

August 2004

Dedication

In 1976 a dissertation was “dedicated to a person not yet born.”

With the same love and inspiration, this time the dissertation is dedicated to you, Mom.

Acknowledgements

There are so many people who made this adventure over the last five years possible. First and foremost I have to thank my excellent advisor, Professor Stephen F. Martin for his support, knowledge and encouragement during these five years. His influence has made me a better writer, thinker and scientist. He is very dedicated to his excellent research group and it shows in the work that they produce. I am indebted to him for his precious time that he spent reading and critiquing the early stages of the dissertation. I also want to thank the entire Martin research group whose knowledge and expertise is unmatched for their help with my research through their friendship, entertainment and superior intellect. In particular, my “Lab 2” colleges are amazing and wonderful people. I am also grateful for Nina Antikainen and Aaron Benfield who taught me everything I ever needed to know about biochemistry and molecular biology. I was also fortunate to have three superb undergraduate students assist me with my research. Thomas Sundberg, Angela Woodward and Neda Nosrati all made substantial contributions to this dissertation. I also acknowledge the excellent NMR and Mass Spec departments at the University of Texas at Austin. The Women in Chemistry and Women in Natural Sciences organizations were excellent resources and special thanks go to Martin T, Laura C, Nina A. Apolonio A., Jen D., Hui L. Rod A., Chris N. and Karl W. for their time spent proof reading this dissertation.

Outside of Welch hall, I thank all of my roommates Sissa, Christine, Karl and Heather who were very understanding and supportive during these five years. There is no way I would have been successful without the support from my great friends: including Nina, Rich, Jason, Shawn, Apolonio, Janan, Michelle, Lauren, Dan, Neipp, Maya, Sue, Lindsay, Bridgette and Adrian who made life in Austin enjoyable, Rachel Porges, my own personal public relations expert, who I could always count on for those special word choices. I definitely want to acknowledge Professor Kosta Steliou at Boston University for allowing me to discover that I loved organic chemistry and John Buchanan, Ph. D. who ignited my desire for synthesis and who is a great scientist, mentor and friend.

Finally, I acknowledge my entire family who made this whole thing possible, especially Emily whose drive and strength inspires me, the memory of my Father that keeps me smiling each and everyday and my Grandma, Mom, and Jim for their unconditional love and support. And finally, I am grateful to David Beck for his undying commitment to keep me smiling, strong and successful. Without the support from all of you, I would have never finished, Thanks!

Synthesis and Evaluation of Conformationally Constrained Peptide Replacements and Studies Toward the Total Synthesis of Kidamycin

Publication No. _____

Hilary Ruth Plake, Ph. D.

The University of Texas at Austin, 2004

Supervisor: Stephen F. Martin

A series of conformationally constrained pseudopeptides derivative of the tripeptide pYVN were designed and synthesized. The conformationally restricted compounds contained either *trans*- or *cis*-cyclopropanes as replacements to enforce locally extended and reverse turn peptide conformations, respectively. In addition, the proper flexible control molecules were prepared. All compounds were evaluated for the ability to bind to the Grb2-SH2 domain in order to determine the energetic consequences of introducing a conformational constraint into peptide ligands. No difference in the $\Delta G_{\text{binding}}$ between the *trans*-cyclopropane and its control partner was observed. Surprisingly, there was an entropic disadvantage when comparing the binding energetics of the constrained and flexible pseudopeptides. Therefore, the introduction of the cyclopropane constraint was associated with an entropic disadvantage in the system, which is the opposite of conventional wisdom. An X-ray crystal structure of the *trans*-cyclopropane containing ligand bound to the Grb2-SH2 domain was obtained and

discussed. On the other hand, *cis*-cyclopropane containing pseudopeptides do not seem to enforce the desired turn conformation of the ligand.

A method to allow access to unsymmetrical *C*-aryl glycoside natural products was developed through employing a disposal tether to enforce the desired regioselectivity in a [4+2] cycloaddition between benzyne and glycosyl-substituted furan. Application of this novel strategy toward the synthesis of kidamycin is discussed. Additional synthetic routes, including utilizing Suzuki's *O* → *C* glycoside rearrangement are also provided. Studies toward the synthesis of sugar ring E and F are illustrated.

Table of Contents

Chapter 1. After 25 Years, Are Conformational	
Constraints Really Worth the Energy?	1
1.1 Introduction.....	1
1.1.1 Energetics of Binding	1
1.1.2 Methods of Determining Binding Energetics	9
1.1.3 Theory Behind Conformational Constraints.....	10
1.2 Examples of Simple Conformational Constraints.....	19
1.3 Examples of Side Chain to Side Chain Conformational Constraints ..	26
1.4 Examples of Backbone to Backbone Conformational Constraints.....	34
1.5 Examples of Conformational Constraints Where the Thermodynamic Parameters of Binding Were Measured.....	40
1.6 The Introduction of Cyclopropanes as Conformational Constraints ..	45
1.6.1 Introduction: Cyclopropanes Restrict Both Peptide Backbone and Side Chain Orientation.....	46
1.6.2 Introduction of Cyclopropane Conformational Constraints into Peptide Ligands	54
1.7 Conclusions.....	64
Chapter 2. Cyclopropane-Derived Pseudopeptides for the Grb2-SH2 Domain	67
2.1 Introduction.....	67
2.1.1 The Grb2-SH2 Domain.....	67
2.1.2 Ligands for the Grb2-SH2 Domain.....	71
2.2 Design of Cyclopropane-Containing Ligands for Grb2-SH2 Domain	72
2.3 Synthesis of pY Cyclopropane and Control Ligands.....	77
2.4 Synthesis of pY+1 Cyclopropane and Control Ligands	87
2.4.1 First Generation Synthesis of 2.006	87
2.4.2 Second Generation Synthesis of the 2.006	94
2.4.3 First Generation Synthesis of 2.007	101

2.4.4	Second Generation Synthesis of 2.007	105
2.5	Synthesis of pY+1 Second Generation Ligands 2.008 and 2.009	106
2.5.1	Synthesis of Mono-Methyl Cyclopropane 2.008	107
2.5.2	Synthesis of Reduced Abu Control Ligand 2.009	110
2.6	Summary	112
Chapter 3. The Thermodynamic and Structural Evaluation of		
	Cyclopropane-Derived Pseudopeptides for Grb2-SH2 Domain	114
3.1	Introduction	114
3.2	Isothermal Microcalorimetry Evaluations	115
3.2.1	pY Pseudopeptides	117
3.2.2	pY+1 Pseudopeptides	119
3.3	X-ray Structures	120
3.3.1	Introduction	120
3.3.2	X-ray Structures of 2.004 Bound to Grb2-SH2 Domain	121
3.3.3	Conclusions from X-ray Structure	133
3.4	Summary and Conclusions	133
Chapter 4. Studies Toward the Synthesis of C-Aryl Glycosides		
4.1	Introduction of C-Aryl Glycosides	137
4.1.1	Kidamycin	137
4.2	The Tethered Benzyne Cycloaddition Methodology	139
4.2.1	Application to Group I C-Aryl Glycosides	145
4.2.2	Application to Group II C-Aryl Glycosides	149
4.2.3	Conclusions	151
4.3	Studies Toward the Synthesis of Kidamycin	151
4.3.1	Retrosynthesis	151
4.3.2	Application of the Tether Methodology to Group III C-Aryl Glycosides	153
4.3.3	Problem with Tether Methodology	159
4.3.4	Synthetic Studies of Ring E: Anglosamine	164

4.3.5	Synthetic Studies of Ring F: <i>N,N</i> -Dimethylvancosamine	169
4.4	Conclusions and Future Directions	174
Chapter 5	Experimentals	175
5.1	Biological Materials and Methods	175
5.1.1	Materials	175
5.1.2	Methods	175
5.1.3	Isothermal Titration Calorimetry:	176
5.1.4	In P:	177
5.2	Organic Synthesis	178
5.2.1	General	178
5.2.2	Compounds	180
Appendix		251
ITC		251
References		269
Vita		290

Chapter 1. After 25 Years, Are Conformational Constraints Really Worth the Energy?

1.1 INTRODUCTION

A major goal in developing leads for drug candidates is to design and prepare molecules with enhanced binding affinities. It is common practice in medicinal laboratories to incorporate conformational constraints into flexible ligands, typically by introducing a ring.¹⁻⁶ However, the true energetic consequences of introducing a cyclic conformational constraint have not been rigorously evaluated. This chapter will showcase and critically evaluate examples of conformational constraints found in the literature.

1.1.1 Energetics of Binding

When a protein (P) and ligand (L) interact under equilibrium conditions, the strength of the ligand-protein complex (PL) is expressed by an association constant K_a , Equation 1.1.



The Gibb's free energy of binding ($\Delta G_{\text{binding}}$) is obtained from the difference between the free energy of the ligand-protein complex relative to the combined free energies of the ligand and protein in solution. The $\Delta G_{\text{binding}}$ is related to K_a according to Equation 1.2 where R is the gas constant and T is the temperature in Kelvin.

$$\Delta G_{\text{binding}} = -RT \ln K_a \quad (1.2)$$

The $\Delta G_{\text{binding}}$ is composed of two thermodynamic components, the enthalpy of binding ($\Delta H_{\text{binding}}$) and entropy of binding ($\Delta S_{\text{binding}}$), Equation 1.3.

$$\Delta G_{\text{binding}} = \Delta H_{\text{binding}} - T \Delta S_{\text{binding}} \quad (1.3)$$

The $\Delta H_{\text{binding}}$ is the sum of the strength of all the non-covalent interactions between the protein and the ligand formed during binding, relative to the sum of the strength of all the interactions of the protein and the ligand with the solvent prior to complexation. The entropic component takes into account the disorder (degrees of freedom) of ligand, protein and solvent during the complex formation.

The enthalpic components of binding are determined by weak interactions, which are individually worth at least one order of magnitude less than the amount of energy required to break a covalent bond.⁷ There are many different types of weak interactions involved in the formation of ligand-protein complexes, which include electrostatic, hydrogen bond, and van der Waals interactions. These interactions have been estimated for common functional groups found in biological systems (ie. hydrocarbons, ammonium, phosphate, hydroxyl, and carboxylate, etc.).⁸

Electrostatic interactions, the Coulombic interaction between two opposing charges, are the strongest of the non-covalent interactions and are worth about 12 kcal mol⁻¹.⁷ Such interactions include ionic bonds, salt linkages, salt bridges or ionic pairs, with the optimal distance between the two charges being 2.8 Å.⁹ The most common charged moieties found in biological systems are ammonium, carboxylate and phosphate groups. Additionally, metal ions can be involved in electrostatic interactions; iron, calcium, and magnesium ions are most common. In determining the electrostatic

contribution to binding, one must take into account the difference between the electrostatic interactions of the protein and ligand before and after complexation.

A hydrogen bond between functional groups is not as strong as the electrostatic interaction and is worth about 2 – 11 kcal mol⁻¹.⁷ This is dependent upon the direction and distance between the species as discussed below. It is considered a dipole-dipole interaction involving the sharing of hydrogen atoms by two other atoms, the hydrogen donor and hydrogen acceptor. In biological systems hydrogen bonds are usually encountered between nitrogen and oxygen heteroatoms. The optimal distance between most hydrogen donors and acceptors is 2.7 – 3.1 Å.⁹ Before the ligand-protein complex is formed, the functional groups of the ligand and protein are involved in highly ordered hydrogen bonds with the surrounding water molecules of the solvent. On complexation, these hydrogen bonds are disrupted, and are replaced by hydrogen bonds between the ligand and the protein. The water molecules that were previously involved in interactions with the ligand and protein become involved in hydrogen bonds within the bulk solvent. The hydrogen bonding contribution to $\Delta G_{\text{binding}}$ depends on the difference between the energies of these hydrogen bonds.

Pauling first highlighted the importance of hydrogen bonding, and he reported that the values of hydrogen bond contributions vary.¹⁰ The strongest hydrogen bond is formed when the hydrogen acceptor and donor are co-linear within a range of 130 – 180°.¹¹ Fersht and Williams have reported that hydrogen bonding between neutral charge atoms contributes 0.5 – 1.5 kcal mol⁻¹ to the $\Delta G_{\text{binding}}$, an amount that corresponds to a 2- to 15-fold increase in binding affinity.^{12,13} On the other hand, charge assisted hydrogen bonds may be worth as much as 2.4 – 4.7 kcal mol⁻¹, and a corresponding 3000-fold increase in affinity.^{11,12} A charge assisted hydrogen bond is a hydrogen bond between a charged species (carboxylate or ammonium) and a hydrogen

atom. The hydrogen bond between two amides is estimated to be worth 0.5 – 1.9 kcal mol⁻¹.^{14,15}

On the other hand, van der Waals interactions between functional groups are much weaker than hydrogen bonds and are worth about 1 kcal mol⁻¹.⁹ They are non-specific attractive forces caused by the natural occurrence of the change of charge around an atom (induced dipole-induced dipole interactions) and are sometimes referred to as London dispersion forces. The optimal range for a van der Waals interaction is 3 – 4 Å.⁹ Kuntz has estimated that the maximal contribution of van der Waals interaction to $\Delta G_{\text{binding}}$ is 1 kcal mol⁻¹ per atom.¹⁶

There are three main entropic components to the $\Delta G_{\text{binding}}$. When the protein and ligand interact, there is a loss of overall rotational and translational entropy in forming the complex. The rotational and translational entropy refer to the tumbling and translation of the molecules through space, respectively. The energetic contributions of translational and rotational entropy to $\Delta G_{\text{binding}}$ are unfavorable for the formation of the complex. Both the ligand and protein have more translational and rotational freedom in solution than in the protein-ligand complex, with the overall loss in the energy estimated to be worth 14 kcal mol⁻¹.^{8,17,18}

The conformational entropy refers to the internal motion, bond stretches and rotations of the protein, ligand, and complex. It is commonly believed that both the ligand and protein lose conformational entropy upon forming the complex.^{17,19-21} The conformational entropy of protein side chain residues is known to be an important factor for estimating binding affinities.²² However, most research has been focused on the loss of conformational entropy for the ligand upon complexation. It has been estimated that each rotatable bond that is rigidified upon binding of the protein and ligand has an associated $\Delta G_{\text{binding}}$ penalty of 0.7 – 1.6 kcal mol⁻¹ due to loss of conformational

entropy.^{8,13,23-25} For example, the conformational entropy lost upon binding is estimated to be worth $3.7 - 4.9 \text{ cal mol}^{-1}$ per rotor lost for a hydrocarbon residue.¹⁷ The amount of conformational entropy lost by the ligand during binding is the basis for the theory that scientists cite when introducing conformational constraints (see Section 1.1.3).

All three forms of entropy and enthalpy are involved in the hydrophobic effect which plays a critical role in $\Delta G_{\text{binding}}$. This effect has both an enthalpic and entropic component; however, the contribution of the hydrophobic effect is mostly attributed to entropy. Upon binding, the strength of the newly formed hydrogen bonds in the ligand-protein complex and between water molecules of the solvent contributes to the enthalpic portion of the hydrophobic effect. Water molecules form more hydrogen bonds with other water molecules in the bulk solvent than with the protein or ligand surfaces, as many as $3 - 4$ hydrogen bonds per water molecule.¹¹ Solvation of the protein and ligand rupture some of these water-water hydrogen bonds, which are recovered upon formation of the ligand-protein complex. Reports in the literature for the enthalpic contribution of the hydrophobic effect vary, but it has been reported to be worth up to $0.5 \text{ kcal mol}^{-1} \text{ \AA}^{-2}$.¹¹

The entropic component of the hydrophobic effect stems from the entropy gained by releasing ordered water molecules from the protein and ligand surfaces into bulk solvent upon complexation. The hydrogen bonding network in the bulk solvent is dynamic and thus bulk water is relatively disordered. However, there is an unfavorable, highly static structure of water molecules surrounding the protein and ligand in solution, and this cage-like structure is entropically less favorable.⁷ During the binding of protein and ligand, entropy is gained as cage-like water molecules are released into the bulk solvent.

The energy of this hydration entropic term has two components. The first of these is the amount of surface area that is in contact with the solvent, known as the solvent-accessible surface area (SAS). The unbound protein surface is surrounded by water molecules; however, upon binding of a ligand, the SAS of the protein exposed to solvent is minimized. The SAS of a protein can be calculated using several methods.²⁶⁻³¹ The Δ SAS is calculated atom by atom as the difference in the SAS between the complex and the sum of the SAS of the protein and ligand and can be partitioned into polar and nonpolar components: O, N, and S atoms are defined as polar while all carbon atoms are defined as nonpolar.²⁸ The total energy gained by Δ SAS_{non-polar} during the binding event is estimated to be worth about 22 – 28 cal mol⁻¹ Å⁻².^{32,33}

The second term related to the entropy of hydration is the atomic solvation parameter (ASP) which defines the energy of transferring atomic surfaces to water and sometimes referred to as the energy of solvent transfer.⁷ The energy of solvent transfer for the ligand can be derived from the partition coefficient P of the small molecules, which is the equilibrium constant between the concentration of the molecule in water and in organic solvent and is related to the free energy of ASP (Δ G_{ASP}), Equation 1.4 and 1.5.

$$P = \frac{[\text{Ligand in organic}]}{[\text{Ligand in aqueous}]} \quad (1.4)$$

$$\Delta G_{\text{ASP}} = -RT \ln P \quad (1.5)$$

The value P for many common functional groups has been calculated,³⁴⁻³⁶ and can be determined by octanol-water partition experiments.³⁷ The solvation energies for many organic and biological molecules has also been predicted.³⁰ The ASP values can also be

determined for surfaces of proteins.⁷ The total contribution of the hydrophobic effect to $\Delta G_{\text{binding}}$, both enthalpic and entropic, has been estimated to be between 0 – 3 kcal mol⁻¹ Å⁻², the strongest being for a completely buried heavy atom.^{11,13,16}

Enthalpy-entropy compensation has been widely reported in many biological systems and in molecular recognition events.^{33,38} It is observed as a linear relationship between the $\Delta H_{\text{binding}}$ and $\Delta S_{\text{binding}}$, and its origin is currently debated in the literature. Some researchers report that it is an extra thermodynamic parameter involved in the protein and ligand binding, an unexpected linear correlation between $\Delta H_{\text{binding}}$ and $\Delta S_{\text{binding}}$ values.³⁹ For example, when interactions between a ligand and protein are strongest, the $\Delta H_{\text{binding}}$ is negative, and the ligand is tightly held by the protein. However, this tight interaction is accompanied by higher order and hence a less favorable $\Delta S_{\text{binding}}$.^{14,40} Williams attributes enthalpy-entropy compensation to cooperativity in binding where more positive cooperativity manifests itself in a more favorable enthalpy but a less favorable entropy.⁴¹ Some researchers associate the enthalpy-entropy compensation with weak intramolecular interactions.^{11,42} However, some believe that enthalpy-entropy compensation may be an artifact of experimental error, particularly when van't Hoff plots (see Section 1.1.2 for definition) are used to determine $\Delta H_{\text{binding}}$ and $\Delta S_{\text{binding}}$.^{33,38} Due to experimental limitations, K values measured using isothermal titration calorimetry (ITC, see Section 1.1.2 for definition) typically range between 10² to 10⁸ M⁻¹ creating a 'window' in which interactions are confined. Thus, the range of observable $\Delta H_{\text{binding}}$ values is limited and may give rise to an observed linear relationship between the $\Delta H_{\text{binding}}$ and $\Delta S_{\text{binding}}$.³⁹ In fact, $\Delta S_{\text{binding}}$ is usually obtained by measuring $\Delta H_{\text{binding}}$, so any error in the measurement of enthalpy will affect the value of entropy and may result in a linear relationship between the enthalpy and entropy.⁴³ In order for the compensation to be considered a real phenomenon, the experimental

temperature must be outside of the confidence interval for the compensation temperature T_c , where T_c is the linear relationship between $\Delta H_{\text{binding}}$ and $\Delta S_{\text{binding}}$ (Equation 1.6).^{44,45}

$$T_c = \frac{[\Delta\Delta H_{\text{binding}}]}{[\Delta\Delta S_{\text{binding}}]} \quad (1.6)$$

The 95% confidence interval for T_c is $T_c \pm 2\sigma$, where σ is the estimated standard error in T_c . If the experimental temperature is within $T_c \pm 2\sigma$, the enthalpy-entropy compensation may not be a real phenomenon and the linear correlation between $\Delta H_{\text{binding}}$ and $\Delta S_{\text{binding}}$ is probably due to the experimental method.

The change in heat capacity (ΔC_p) upon binding is also an important thermodynamic parameter to consider when comparing protein and ligand interactions. Heat capacity is the amount of heat required to increase the temperature of a substance by 1 degree Kelvin. It is also the temperature dependence of the $\Delta H_{\text{binding}}$ (Equation 1.7).

$$\Delta C_p = \frac{\Delta H_{\text{binding}}}{T} \quad (1.7)$$

There is a direct and experimentally useful correlation between the ΔC_p and the ΔS_{AS} where measuring ΔC_p provides a useful method for probing the structural effects of the complex formation.⁴⁶ A negative ΔC_p is attributed to the burial of nonpolar surfaces upon protein and ligand binding, whereas a positive ΔC_p is attributed to the burial of polar surfaces.⁴⁷ Large ΔC_p effects are also associated with the hydrophobic effect.³⁹ Similar ΔC_p s for different ligands binding to a protein suggest that there is no large structural perturbation between the respective binding events.⁴⁸

1.1.2 Methods of Determining Binding Energetics

Scientists use different methods to measure the binding interactions between proteins and ligands. In some cases the dissociation constant K_d of binding is directly measured, where K_d is the reciprocal of K_a . When measuring the ability of an inhibitor to bind to a protein, many researchers express the results in IC_{50} , which is the inhibitor concentration required to cause 50% inhibition. The inhibition constant K_i is related to both K_d and IC_{50} by the Cheng-Prusoff Equation where C is the concentration of the substrate that is inhibited (Equation 1.8).⁸

$$K_i = \frac{IC_{50}}{(1 + C/K_d)} = \frac{[PI]}{[P][I]} \quad (1.8)$$

When either the substrate concentration is small or K_d is large, K_i will be approximately equal to IC_{50} .

Researchers use isothermal titration calorimetry (ITC) to measure the energetics of binding at a constant temperature and determine each thermodynamic parameter of the binding event, including K_a , $\Delta G_{\text{binding}}$, $\Delta H_{\text{binding}}$, and $\Delta S_{\text{binding}}$.^{11,39,49-52} The heat released or absorbed during the binding event is monitored by the calorimeter.^{11,53,54} The reference cell contains only buffer while the sample cell contains buffer plus protein. An injection system is filled with the ligand. During an ITC experiment, the ligand is injected into the sample cell and the time dependence of the electric power ($\mu\text{cal sec}^{-1}$) necessary to maintain constant temperature between the reference and sample cells after each injection of ligand is recorded by the instrument. Peaks correspond to the heat released, or absorbed, during the binding event.⁵² Negative peaks are associated with exothermic interactions while positive peaks are associated with endothermic interactions. The heat released or absorbed after each injection is obtained by calculating

the area under each peak and provides a binding curve that furnishes the K_a , stoichiometry and ΔH of binding through nonlinear least squares analysis done by the Origin program.^{50,52} Simple calculations then afford $\Delta G_{\text{binding}}$ and $\Delta S_{\text{binding}}$. Each ITC experiment should be repeated at least three times and the values averaged. In order to account for any heat of dilution during the experiment, a blank titration, ligand titrated into buffer solution, should also be obtained and the values subtracted from each ligand into protein titration.

Van't Hoff plots offer another method to measure the thermodynamic parameters of binding. Binding affinities are measured at different temperatures from which $\Delta H_{\text{binding}}$ and $\Delta S_{\text{binding}}$ values can be extracted from a linear plot of $\ln K_a$ versus $1/T$ where $-\Delta H_{\text{binding}}/R$ is the slope and $\Delta S_{\text{binding}}/R$ is the intercept.^{55,56} However, in biological systems $\Delta G_{\text{binding}}$ only exhibits a low temperature dependence, and a reliable determination of $\Delta H_{\text{binding}}$ and $\Delta S_{\text{binding}}$ may not be possible with van't Hoff plots. For example, where ITC shows a temperature dependence of $\Delta H_{\text{binding}}$ and $T\Delta S_{\text{binding}}$, van't Hoff plots often show non-linear behavior for $\Delta G_{\text{binding}}$ as a function of reciprocal temperature.^{11,38}

1.1.3 Theory Behind Conformational Constraints

There are a limited number of strategies medicinal chemist can use to strengthen the interactions between the protein and ligand and provide compounds with higher potency. The enthalpic contribution to $\Delta G_{\text{binding}}$ can be increased by strengthening the electrostatic, hydrogen bond and/or van der Waals interactions in the ligand-protein complex relative to those between the unbound ligand and protein with the solvent. The entropic component of $\Delta G_{\text{binding}}$ can be made less positive through increasing the hydrophobic effect upon binding, which can be accomplished by adding hydrocarbons to the ligand. By adding more nonpolar surface to the ligand, interactions between the

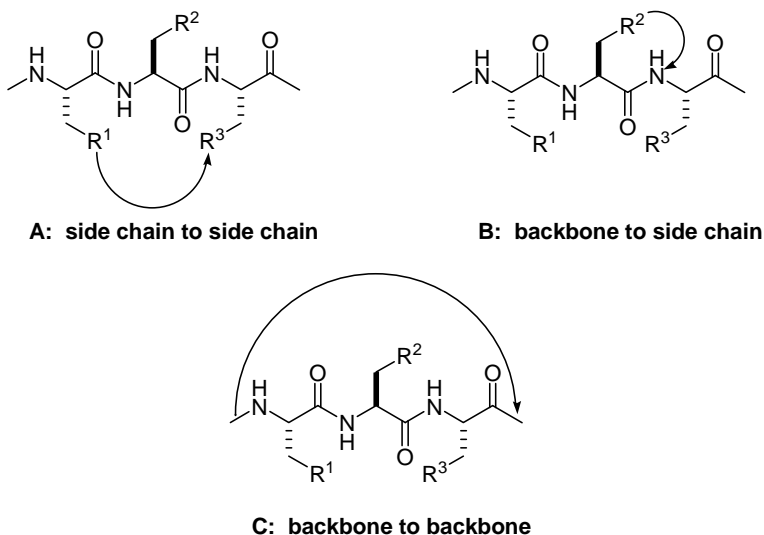
ligand and the solvent become unfavorable which results in a greater entropic advantage for the binding event. The translational and rotational entropic components of binding cannot be easily changed. However, it is conventional wisdom that by synthetically pre-organizing a ligand into the biologically active conformation, the impact of the conformational entropic penalty of $\Delta G_{\text{binding}}$ will be minimized. Everything else being equal, a conformationally constrained molecule should have a higher binding affinity because it is associated with a smaller conformational entropic cost upon binding.²³ The idea of introducing conformational constraints in peptide ligands to rigidify them into their biologically active conformation was first hypothesized in 1979, and many medicinal chemists have used this hypothesis to assist in the development and design of molecules that bind more tightly to proteins.⁵⁷

In solution, peptides are highly flexible; the peptide bond can adopt either a *trans*- or *cis*- conformation, usually *trans*- due to sterics, and the amino acid side chain can orient itself in many directions. The torsional angles associated with the amide nitrogen- $C\alpha$ bond and the $C\alpha$ -carbonyl carbon bond are defined as ϕ and ψ , respectively. The torsional angle associated with the $C\alpha$ - $C\beta$ bond is χ_1 .

There are three different designs used to introduce conformational constraints into peptide ligands to rigidify or pre-organize them in their biologically active conformations (Figure 1.1). The first of these is side chain to side chain constraint, in which two side chains are linked together to form a macrocycle. Alternatively, a side chain can be connected to the backbone via a bridge, creating a side chain to backbone constraint. A backbone to backbone macrocyclization can also be used to rigidify the ligand.

Figure 1.1: Different designs used to introduce conformational constraints into peptides.

A) side chain to side chain, B) backbone to side chain, C) backbone to backbone⁵⁸



There are many synthetic methods used to introduce cyclic conformational constraints into peptides.¹ Backbone to backbone cyclization can be achieved by macrolactamization. Side chain to side chain connections can be accomplished using disulfide bridges, ring closing metathesis and amide bonds. Many different linkages are used in designing side chain to backbone cyclizations including ethers, amines and carbocycle moieties. Ideally, the cyclization should not perturb any of the direct interactions between the ligand and protein or the solvent, otherwise the increased or decreased binding affinity of the cyclic molecule could be due to these interactions and not the pre-organization caused by the introduction of the conformational constraint.

Fairlie has stated that “a central principle in medicinal chemistry is that molecules, which are conformationally pre-organized or fixed into a shape that is

recognized by a receptor, will have higher affinity for that receptor due to the reduced entropy penalty for adopting the receptor-binding shape.”² Additionally, in the development of host-guest complexes, pre-organization is proposed to be a central determinant of the binding of metal ions to spherands, cryptands, corands, and podands.⁵⁹ According to this theory, the entropic penalty for binding of a cyclic compound should be dramatically less than that for an acyclic counterpart. This penalty has been estimated to be 0.7 – 1.6 kcal mol⁻¹ per rotor.^{8,13,23-25} However, the position on the ligand where the conformational constraint is introduced needs to be considered carefully. The constraint should not perturb any of the protein-ligand interactions crucial for binding affinity. In addition, Bartlett has stated that in some cases a highly flexible bridge might induce more conformational mobility, making the cycle more flexible than its non-restricted partner.⁶⁰ In addition, a poorly designed bridge may distort the binding region, which could impact the energetics of binding and make it difficult to determine the energetic effect of introducing a conformational constraint.⁶¹ Although no one has critically evaluated its usefulness, the implementation of conformational constraints is common practice in many medicinal chemistry laboratories and is still considered an important step in drug discovery.

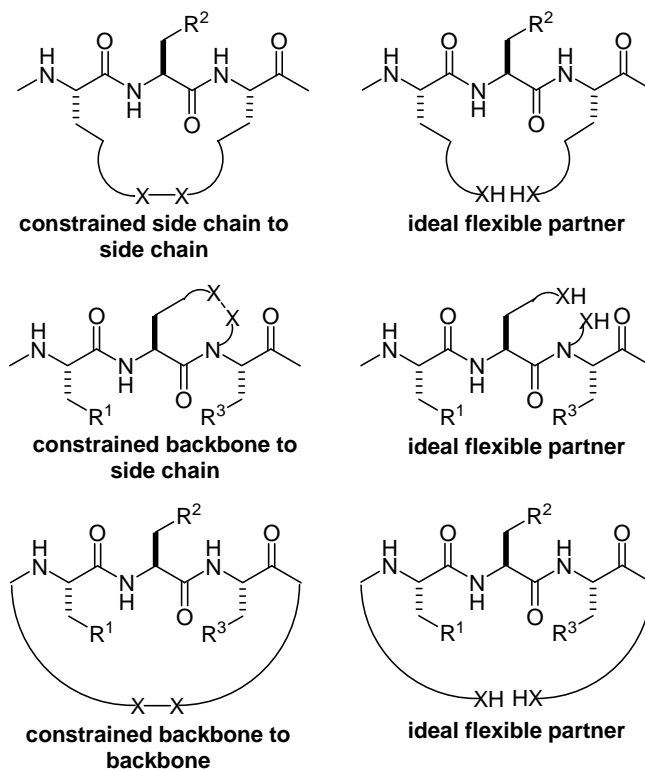
In addition to increasing affinity through reduction of the entropic penalty of binding, the introduction of a conformational constraint has many other advantages. By adding unnatural constraints, proteases may not degrade the constrained molecule as quickly, and the ligand might be expected to survive longer *in vivo*. Backbone to backbone cyclization may remove the ionized C- and N- termini of the peptide resulting in a more facile crossing of the ligand through membrane barriers.⁶² There are also reports that constrained molecules have better membrane permeation and oral bioavailability.⁶³ The flexibility of native peptides renders them relatively nonselective

in binding, so, incorporation of conformational constraints into linear peptides may force their structure into the binding conformation of one particular receptor, thus making them more selective and eliminating undesired biological side effects. In addition, introducing conformational constraints can provide important information about the structure of the bound ligand. For example, one ligand with a particular restricted conformation may bind with higher affinity to the protein than a ligand with a different restricted conformation. Therefore, the bioactive ligand conformation mostly likely resembles the conformation constrained in the higher affinity ligand. On the other hand, by locking otherwise flexible amino acids into the protein binding conformation, independent structure-activity changes can be made elsewhere in the inhibitor without affecting the overall ligand conformation. Constrained cyclic peptides have also been used as templates to reduce the effect of “induced fit,” which is associated with unpredictable changes in one region of a ligand that influence the ligand-protein interactions at a different region of the ligand.⁶⁴

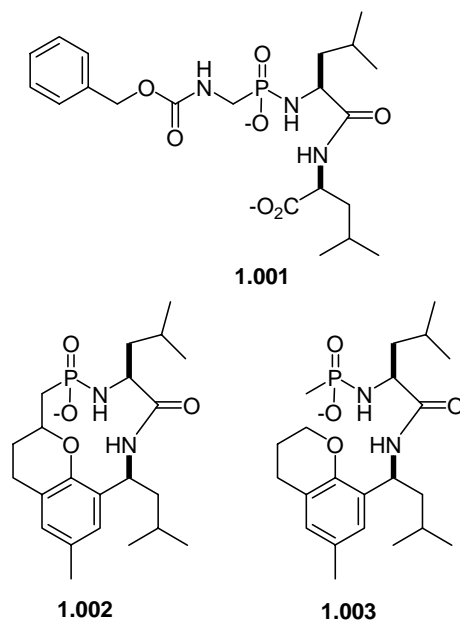
In order to critically evaluate the energetic advantage gained by introducing a conformational constraint, one must have proper control molecules to evaluate the true effect of cyclization on binding and not the effect of the bridge itself. In an ideal situation, the only difference between the rigid and flexible control molecules would be H_2 , the formal hydrogenolysis of one of a bond contained in the cycle (Figure 1.2). However, examples of such systems are difficult to find in the literature. At any rate, there should be minimal structural changes between the constrained molecule and its flexible control. For example, both ligands should contribute the same hydrogen bonds, hydrophobic effect, electrostatic and van der Waals interactions to complex formation. The molecules in each pair should also have similar molecular weights and the same number of heavy atoms (C, N, O, S, P, etc). The molecules should also have the same

relative solvation energies, having the same polar and nonpolar solvent accessible surface areas. For example, a lactam linkage in a macrocycle and an amine and carboxylate groups in an acyclic control may look very similar but they interact differently with a protein and the solvent. The amide bond could have neutral charge hydrogen bond interaction with the protein and the solvent, whereas both the amine and carboxylate groups would have electrostatic and charge assisted hydrogen bond interactions with the protein and the solvent. In addition, the amide, amine and carboxylate groups likely have different relative solvation energies. These differences could be substantial and might affect the binding affinities for the cycle and control, which one cannot anticipate, making it difficult to determine the true impact of introducing a conformational constraint on the binding affinity in such systems.

Figure 1.2: Examples of constrained ligands and their ideal control partners where X = carbon is the best case.



One potential problem to consider when designing ideal control partners for cyclic conformational constraints was illustrated by Bartlett and co-workers who were interested in using macrocyclic conformational constraints to enhance binding to thermolysin.²⁵ A linker was designed to connect the carbon α to the phosphorus atom in **1.001** with the C-terminal carboxylate to form a backbone to side chain bridge providing bicycle **1.002**. The conformational constraint was devised to enforce the biologically active orientation for thermolysin binding. The acyclic analogue **1.003** was envisioned as the control and is related to **1.002** by cleavage of a carbon-carbon bond to the hydropyran ring. Inhibition constants were determined, and **1.002** was found to be a 20 times more potent nanomolar inhibitor of thermolysin than the acyclic molecule **1.003**. X-ray crystal structure analysis of the bound conformations of **1.002** and **1.003** showed that the backbone and side-chain atoms of these molecules are virtually superimposable with each other. However, the aromatic unit of the **1.003** is rotated 168° in comparison with **1.002**, adopting a different position in the thermolysin active site. The important structural data reveals that the difference in affinity between these two molecules is not simply the result of cyclization but also due to different interactions between the two ligands bound to thermolysin. The only chemical difference between the control and macrocyclic ligands was the addition of two hydrogen atoms. In order for the molecules to have the same bound conformation, the length of a carbon-carbon bond in the cycle must increase from the length of a carbon-carbon bond (1.5 Å) to the van der Waals contact distance of a CH group (about 3 - 4 Å). However, in this example the enzyme binding site was not flexible enough to accommodate this substantial change without the “reorientation” of the aromatic unit. Thus, researchers must carefully consider the design of the proper control ligands when evaluating the impact of introducing a conformational constraint.



The above example illustrates that structural information of the binding mode of the constrained ligand is crucial for determining the benefit of introducing the conformational constraint. The introduction of the conformational constraint must stabilize the biologically active conformation for the ligand binding to the protein. Otherwise, as shown, the enhanced binding affinity of the restricted ligand cannot be attributed to minimization of the conformational entropic penalty of binding. When structural data is lacking from an example, it is difficult to interpret the experimental results.

In addition, structural information is essential to verify that the constrained and flexible ligands have uniform binding modes. Otherwise, any energetic advantage associated with the binding of the constrained molecule could be attributed to better binding interactions between the molecule and the protein and not the reduction of the entropic penalty of binding or vice versa. Furthermore, ITC should be used to evaluate the binding affinities of the constrained and control ligands. The ITC experiments can

evaluate the entropic contribution to the binding event and determine if the introduction of the conformational constraint has affected the conformational entropic penalty paid upon ligand binding to the protein.

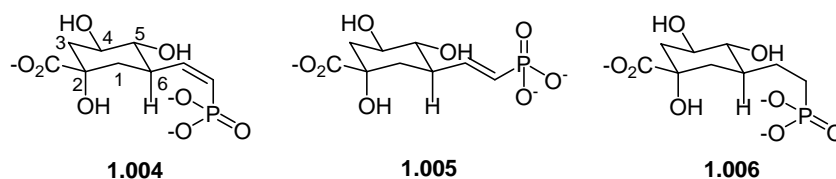
The experimental methods used to obtain the binding affinity data are also crucial to evaluating the effect of introducing a conformational constraint. Using enzyme-based assays, where the binding affinities of ligands to proteins are directly measured, we can compare the values obtained for the constrained and flexible molecules in order to determine the effect of introducing the conformational constraint on affinity. However, many times in the literature cell-based assays are employed to evaluate the pre-organized and control pair. This method indirectly measures binding affinities as there are other factors including membrane binding, transport, and interactions with other cellular enzymes (including proteases) which may cloud the experimental results. For example, in a cell-based assay a constrained ligand may appear to bind tighter to a protein than a flexible control, but it is possible that the constrained ligand is not degraded by cellular proteases present in the assay while the control partner is quickly destroyed. Thus, it would appear that the control molecule did not bind to the protein as well as the constrained ligand, where in reality, the flexible molecule did not have the same access to the protein as the constrained ligand. Therefore, one must rigorously evaluate the experimental methods used to compare the ligand partners before drawing any conclusions as to the effect of introducing a conformational constraint on the binding affinity of the ligands.

In designing new ligands, many medicinal chemists have used the hypothesis that introducing a conformational constraint will reduce the entropic penalty of binding and create molecules with better binding affinity.^{2,23,65-69} Many times a cyclic peptide is prepared and evaluated but the proper control molecules are never considered and

whether or not conformational constraints actually enhanced binding affinity is rarely addressed in the literature. In addition, sometimes scientists don't explicitly describe the results in a manner that makes it obvious that a conformational constraint was used. Thus, it is difficult to find examples where the validity of the pre-organization theory has been evaluated. Presented here is an overview of the field of conformational constraints. Bear in mind that many of the examples presented here do not fit the criteria that allow for the evaluation of the validity of the conformational constraint theory.

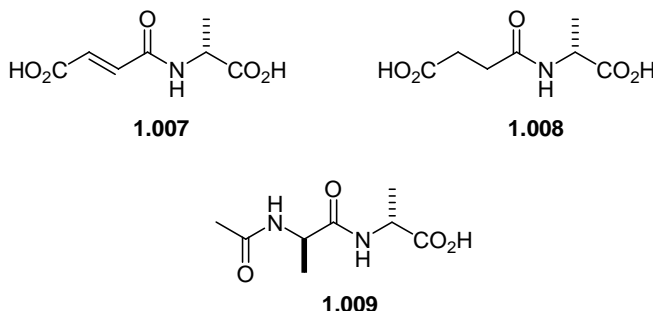
1.2 EXAMPLES OF SIMPLE CONFORMATIONAL CONSTRAINTS

Researchers have introduced conformational constraints into ligands to enhance binding potency. The simplest way to introduce a conformational constraint is through unsaturation. For example, a double bond was introduced into dehydroquinase synthase inhibitor **1.006** providing the *Z*- and *E*-vinyl homophosphonates **1.004** and **1.005**, respectively.⁷⁰ The *Z*-analogue **1.005** bound weakly to dehydroquinase synthase, whereas **1.004** and **1.006** both exhibited micromolar activity with constrained **1.004** being ten-fold more active than flexible **1.006**. In this example, there is no substantial difference in the interactions between the restricted and control ligands with the solvent or the protein. Thus, it seems that by introducing a double bond conformational constraint into the system, the binding affinity was enhanced.



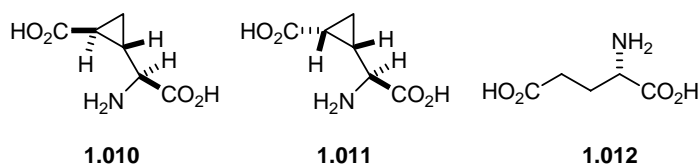
In order to assess the energetic contribution to binding from restricting rotors through introducing a double bond conformational constraint, compounds **1.007** and

1.008 were prepared as analogues of *N*-acetyl-D-alanyl-D-alanine (**1.009**).⁷¹ The binding of these ligands to ristocetin A, a member of the vancomycin group of antibiotics, was measured. Both had millimolar activity with rigid **1.007** being nine times more potent than flexible **1.008**. Once again there is no substantial difference between the two molecules expect for the rigidification from the carbon-carbon double bond, so the difference in binding affinities may be attributed to the number of rotors restricted in **1.007**. The authors speculate that the introduction of the double bond likely increased the barrier of rotation for each single carbon-carbon bond on either side of the double bond restriction. The authors estimate that 1.5 rotors are restricted by introducing the double bond into **1.007** and the free energy per rotor restricted was calculated to be 0.9 kcal mol⁻¹, which is well within the range predicted in the literature for the entropy penalty of binding minimized through the introduction of a conformational constraint (see Section 1.1.3). Thus, once again the introduction of a double bond conformational constraint enhanced binding affinity.

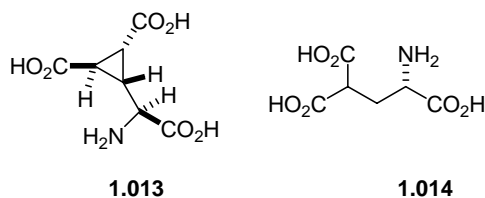


In addition to double bonds, simple carbocycles have been used to install conformational constraints into peptide ligands. For example, cyclopropane containing rigid glutamate analogues have been prepared and analyzed for their affinity to various glutamate receptor subtypes in brain membranes.⁷² The cyclopropane-containing **1.010**

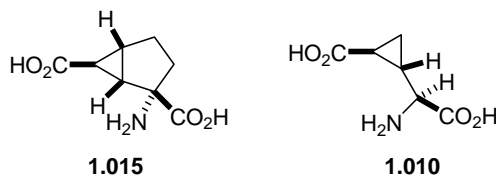
and **1.011** analogues of glutamate and linear **1.012** were evaluated as inhibitors for *N*-methyl-D-aspartate receptors. The cyclopropane **1.010** was not active, whereas the linear **1.012** exhibited nanomolar potency, and the cyclopropane **1.011** was 17 times more active than flexible **1.012**. There is an additional methylene unit present in the rigid compounds but not found in the linear control. How this additional residue effects interactions with the protein or solvent is unknown. Even so, it appears from the data presented here that the introduction of the cyclopropane constraint did increase potency. Unfortunately, however, a cocktail of enzymes was present in the binding assay and thus the true binding affinities cannot be determined or compared in this example.



In another example, cyclopropane **1.010** and control **1.012** were also evaluated as ligands for the metabotropic glutamate (mGlu) receptors.⁷³ The cyclopropane **1.013** and its control **1.014** were also examined. All compounds exhibited micromolar potency and the linear controls **1.012** and **1.014** were as much as 10-fold less potent than the cycles **1.010** and **1.013**. In this example, only cell-based assays were employed which are, unfortunately, inadequate for evaluating the consequences of introducing a cyclopropane conformational constraint as previously discussed.

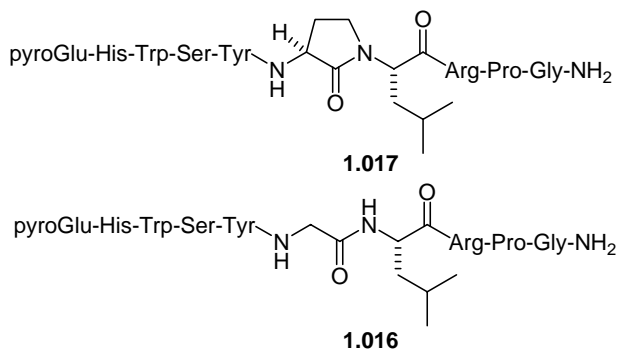


Monn and co-workers also synthesized conformationally constrained glutamic acid analogues as highly potent and selective neurotransmitters for group 2 mGlu receptors.⁷⁴ The glutamic acid skeleton was incorporated into a fused bicyclo[3.1.0]hexane nucleus in **1.015** in order to constrain the glutamate into the conformation required for optimal binding. The cyclopropane-containing glutamic acid **1.010** was used as the flexible control. Modeling suggested that the bicycle closely mimicked the proposed bioactive conformation required to interact with the 2 mGlu receptor. The constrained molecule contains two additional carbon units which are not found in the control and the impact these residues have on protein or solvent interactions is unknown at this time. The bicyclo **1.015** was slightly more active, with nanomolar potency, than the control ligand **1.010**. Again, multiple enzymes were present in the binding assay, which make it difficult to determine the true impact on binding affinity from introducing the conformational constraint.



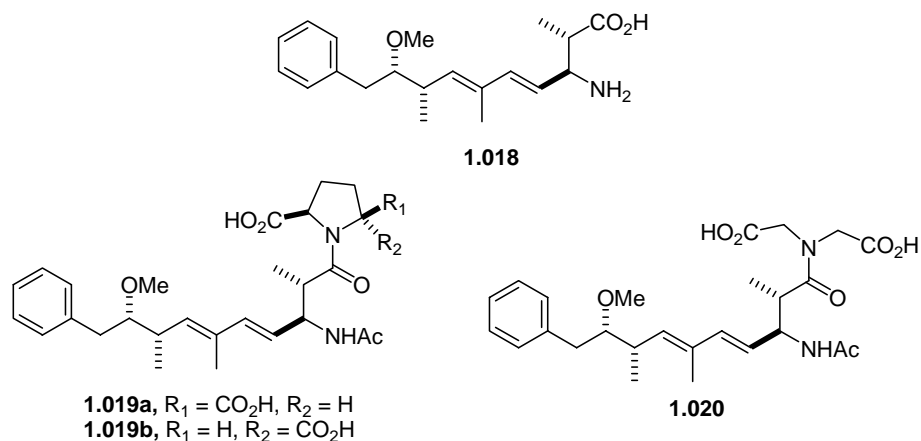
Another example of utilizing a simple carbocycle as a conformational constraint can be found in one of the earliest examples of introducing a conformational constraint into a peptide. A lactam moiety was introduced into the luteinizing hormone-releasing hormone pyroGlu-His-trp-Ser-Tyr-Gly-Leu-Arg-Pro-Gly-NH₂ (**1.016**) to provide ligand **1.017**.⁶⁵ Modeling suggested the close proximity of the pro-*S* hydrogen of Gly⁶ to N-H of Leu⁷ in **1.016** suggesting that these positions were ideally suited for the introduction of the conformational constraint. The five-membered lactam was designed by replacing the

Gly⁶ pro-*S* hydrogen with a methylene group and connecting it to the N of Leu⁷. The lactam ring was proposed to stabilize a β -turn conformation by restricting rotation and forcing the Gly-Leu peptide bond to remain in the required *trans*-conformation. Lactam **1.017** was found to be two to eight times more potent than the acyclic control **1.016** for inducing release of luteinizing hormone *in vivo* and *in vitro*. The structural difference between control **1.016** and **1.017** is two hydrocarbon residues and N-H moiety and the consequence of the interactions with these groups and the protein and solvent is difficult to estimate. In addition, the only assays employed in this study were cell-based thus making it difficult to evaluate the true impact of the conformational constraint on binding affinity. Although it appears from the data that introducing a conformational constraint enhanced binding affinity, issues make it difficult to validate this conclusion.



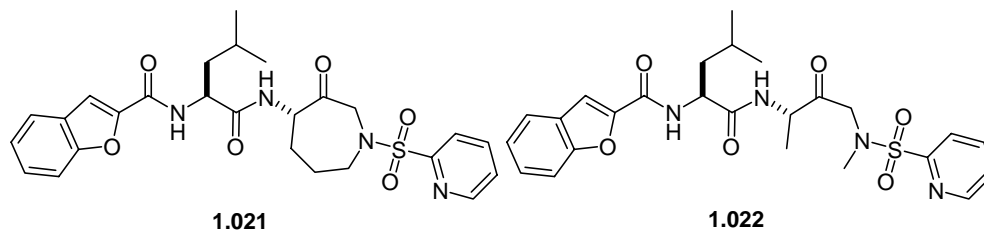
Another example of the introduction of a simple carbocycle conformational constraint involved using a proline ring as a scaffold to design analogues of adda (**1.018**), which is a potent inhibitor of protein phosphatase 1 and 2A (PP1 and PP2A).⁷⁵ Compounds **1.019a**, **1.019b**, and the flexible control **1.020** were prepared and the *cis*-**1.019a** was four-fold more active than *trans*-**1.019b** with both exhibiting micromolar activity. However, the acyclic control **1.020** relative to **1.018** was inactive ($IC_{50} > 100$ μ M). Since the acycle **1.020** was inactive, the authors speculated that the pyrrolidine

heterocycle plays a role in the enhanced potency, perhaps by pre-organizing the active conformation for the two carboxyl groups. Even though it seems that pre-organization enhanced potency in this system, there are two carbon residues different between the control and rigid molecules. The impact of this difference to the binding affinity has not been examined and thus, it is difficult to evaluate the introduction of the conformational constraint in the system.

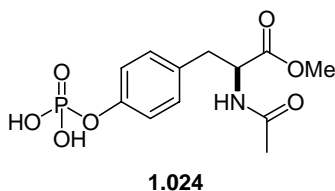
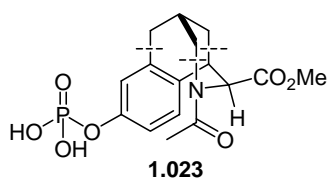


A larger carbocycle, a azepanone ring, was used by Marquis and co-workers to introduce a conformational constraint in inhibitors of cysteine protease cathepsin K providing **1.021**.⁷⁶ Compound **1.022**, which contains the same hydrogen bond donor/acceptor count as **1.021** but has one less methylene unit, was examined as the control. The incorporation of the conformational constraint into **1.022** increased the inhibitor potency by 1000-fold to subnanomolar potency in the *in vitro* cell-based assay, and gave a compound having good oral bioavailability. The authors provide important structural evidence that the cycle **1.021** binds in the biologically active conformation to the protease and the methylene groups of the azepanone ring make no contacts with the protein. This example clearly demonstrates that an enhanced activity is observed on the introduction of a conformational constraint. Unfortunately, only a cell-based assay was

employed in this example which, as previously discussed, is inadequate for determining the effect of introducing a conformational constraint on ligand binding.

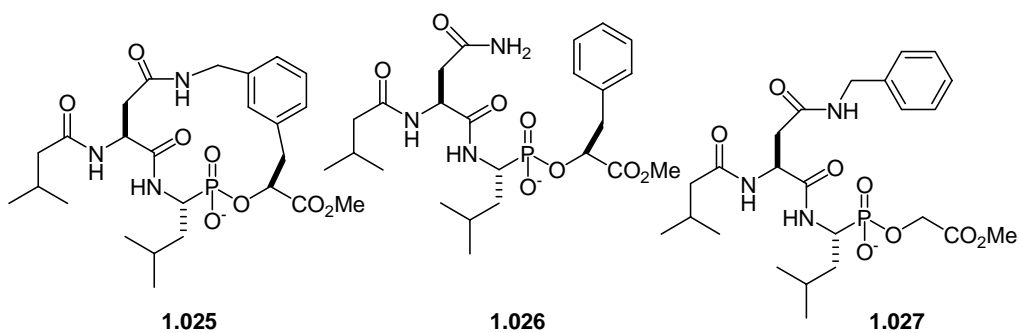


In 2003, Burke and co-workers introduced a carbocyclic conformational constraint into the pY residue of Src homology 2 domain of the growth factor receptor binding protein 2 (Grb2-SH2 domain) binding ligands in order to stabilize the bound conformation.⁷⁷ The installation of the carbocycle in **1.023** constrained the three torsion angles (χ_1 , χ_2 and ϕ) of the ligand's pY residue to values similar to those observed for its biologically active conformation. An X-ray crystal structure of unbound **1.023** showed that this analogue is stabilized into the orientation required for Grb2-SH2 domain binding. The unconstrained phosphorylated *N*-acetyltyrosine methyl ester **1.024** was examined as a control which contained extra methylene residues not present in the constrained system. Comparison of the binding affinity of **1.023** with the conformationally more flexible phosphotyrosine **1.024** revealed no apparent increase in affinity, both compounds were approximately equipotent within experimental error (with low millimolar potency). Unlike the previous examples, the authors claim that a conformational constraint is ineffective in enhancing SH2 domain binding affinity.



1.3 EXAMPLES OF SIDE CHAIN TO SIDE CHAIN CONFORMATIONAL CONSTRAINTS

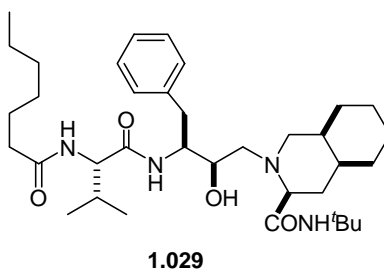
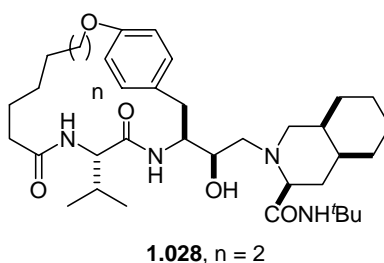
Research groups are also interested in introducing conformational constraints by linking peptide side chain residues. For example, Bartlett and co-workers used a methylene moiety to link two amino acid side chains and form a macrocyclic inhibitor of the aspartic protease penicillopepsin providing **1.025**.⁷⁸⁻⁸⁰ Two different acyclic controls were prepared for the macrocycle. Due to the problems encountered in the thermolysin system previously described (see Section 1.1.3), the linear compounds **1.026** and **1.027** were derived by replacing the methylene units on either side of the phenyl ring of **1.025** with hydrogens in order to enable the controls to adopt the same bound conformation as the macrocycle. The authors speculate that conformational formed with an extra methylene unit in each of the control ligands would not fit into the penicillopepsin active site. The cyclic molecule **1.025** had higher binding affinity than either of the control partners (**1.025**: $K_i = 0.1$ nM, **1.026**: $K_i = 42$ nM, **1.027**: $K_i = 1300$ nM,). However, since the controls had substantially different potencies, this example illustrates the importance of selecting the proper control molecules when determining the effect of introducing a conformational constraint.



The authors estimated the energetic effect on binding caused by introducing the conformational constraint by comparing the number of independent rotations restricted in each ligand and the ligand binding affinities. An average value of 0.9 kcal mol⁻¹ per rotor was calculated. This is within the range estimated for the conformational entropy penalty of binding reduced by pre-organizing a ligand into its biologically active conformation (see Section 1.1.3). In addition, the 3.6 kcal mol⁻¹ binding energy difference between macrocycle **1.025** and control **1.026** is among the highest value reported for the enhancement in binding potency due to the introduction of a conformational constraint. However, **1.026** contains an extra N-H moiety that could provide additional interactions compared with **1.025** and **1.027** and compound **1.025** also contains an additional methylene group compared with the controls **1.026** and **1.027**. These moieties could provide additional energetic interactions in the ligand-protein complex. On the other hand, X-ray structures of **1.025** and **1.026** bound to the protease were solved and the position and conformation of the ligands in the complexes are virtually identical with the most pronounced conformation difference between the two ligands being the χ_2 -angle at the Phe residue.²⁴ In addition, the conformation of the bound cycle closely resembles the solution structure obtained from NMR data. It seems that in solution **1.025** is pre-organized into its bound conformation. Thus, it appears that in the example, the

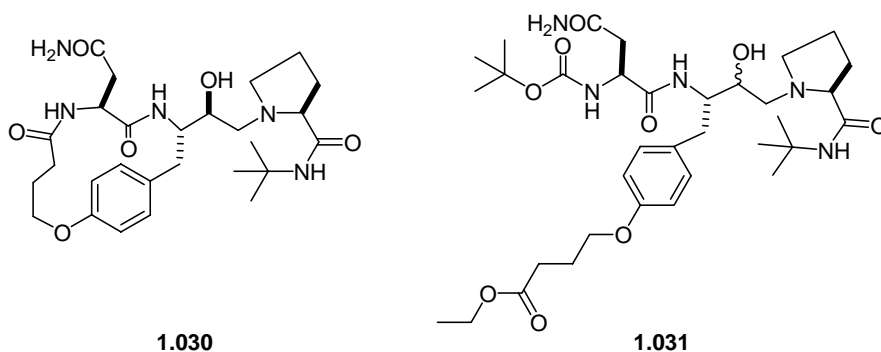
introduction of a side chain to side chain conformational constraint did enhance binding potency.

Research groups have also utilized ether linkages to introduce side chain to side chain conformational constraints. For example, in 1994 a series of nanomolar macrocyclic inhibitors of HIV-1 protease were prepared.⁸¹ Cycle **1.028** was the most active constrained analogue in the series being six times more potent than the control molecule **1.029** in an enzyme-based assay. However, the ether linkage present in cycle **1.028** was not present in the control **1.029** making it difficult to evaluate the effect of introducing a conformational constraint because it is not known how this difference could effect interactions with both the solvent and the protein.

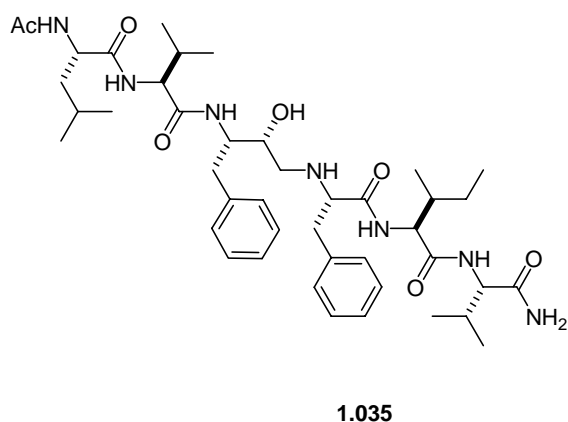
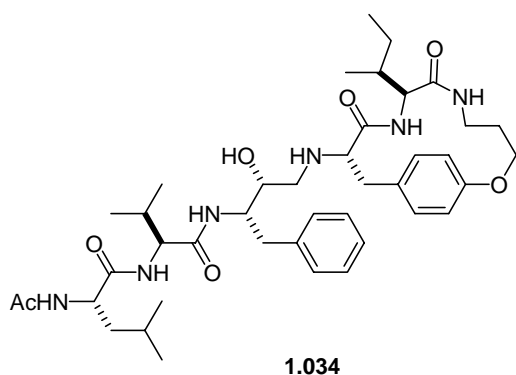
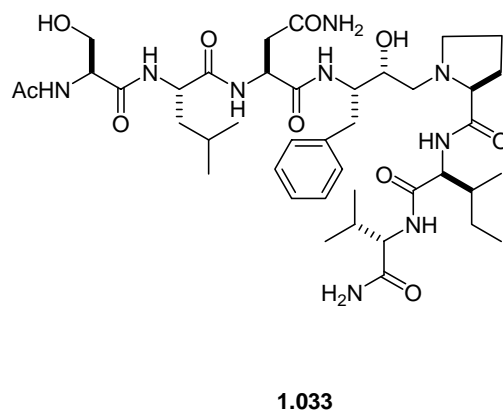
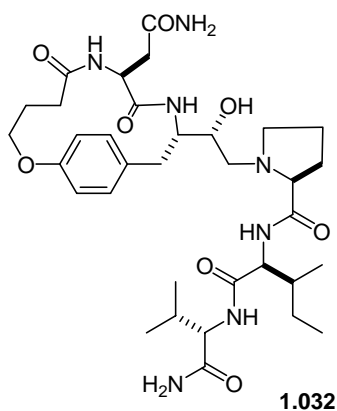


Fairlie and co-workers have also designed numerous cyclic peptide inhibitors of HIV-1 protease using ether side chain to side chain linkages.^{82,83} Macrocyclic compound **1.030** was compared to the Boc-carbamate acycle **1.031**.⁸⁴ The acyclic compound **1.031** was 37 times less active than the cyclic derivative **1.030**, and the authors suggested that the enhanced potency was likely to be an underestimate of the

advantage from introducing the conformational constraint, since the linear compound can potentially make additional interactions with the enzyme via hydrogen bonding of its ester group and hydrophobic effect with the *t*Bu moiety. These statements may be valid; however, in this example the estimation of the impact of introducing the conformational constraint is complicated by many factors.

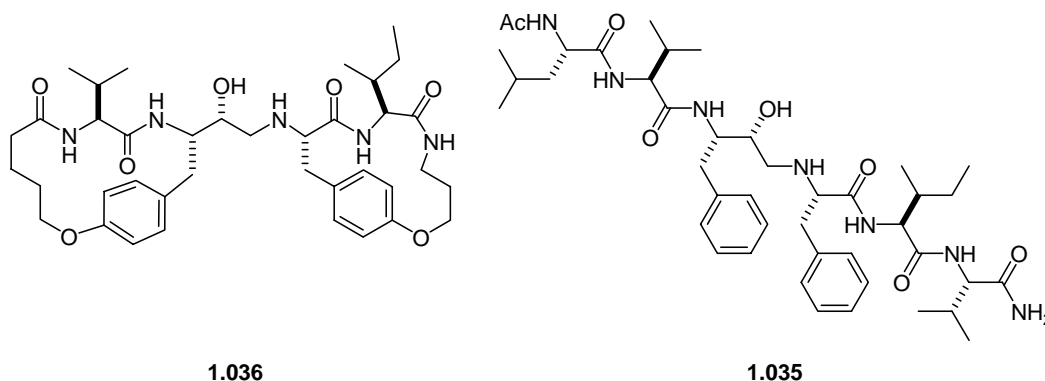


In another example, 15-membered restricted macrocyclic derivatives of Leu-Asn-Phe and Phe-Ile-Val tripeptides **1.032** and **1.034** were also designed as HIV-1 protease inhibitors using ether linkages. The acyclic controls **1.033** and **1.035** were the peptide equivalents of **1.032** and **1.034** minus the ether bridge. Modeling studies suggested that the cyclic and acyclic inhibitors had similar conformations and formed similar contacts with the enzyme. Constrained compound **1.034** was two times more potent than the linear **1.035** in an enzyme-based assay, whereas the macrocycle **1.032** was more active than control **1.033** by 72-fold. It may appear from this example that the introduction of a side chain to side chain conformational constraint enhanced binding affinity; however, since the cycles and controls could have different interactions with the protein and solvent, it is difficult to draw any conclusions.

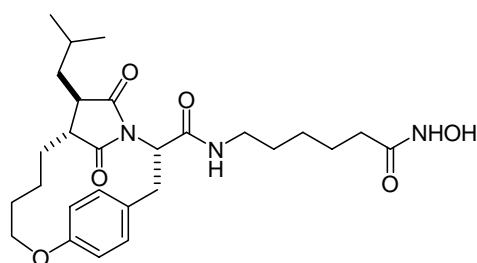


Next the research group designed the conformationally constrained bicyclic HIV-1 protease inhibitor **1.036** containing both macrocyclic components of **1.032** and **1.034** pre-organized in the desired conformations for enzyme binding.⁸⁵ The linear derivative **1.035** was again used as a control, although it lacked the ether linkages present in each of the macrocyclic rings in **1.036**. Molecular modeling and ¹H NMR studies indicated that each ring in **1.036** was constrained in a conformation that superimposed well with the bound conformation of acyclic peptide **1.035**. By constraining the two otherwise flexible tripeptide components in **1.035** to the conformations required for binding, the authors expected a significant entropic and thus energetic advantage for the binding of **1.036** over the acyclic inhibitor **1.035**. However in the biological assay, compounds **1.035** and **1.036** were found to be equipotent having nanomolar potency. Very important X-ray structures

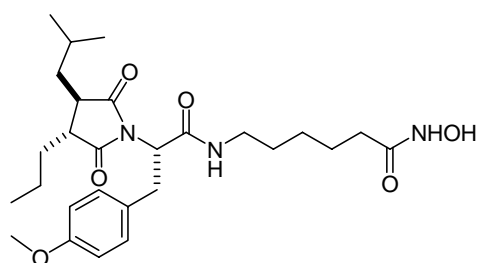
revealed that the cycle **1.036** and the control **1.035** might have different hydrogen bond interactions with the protease. Even so, it appears that an ether linkage conformational constraint did not enhance binding potency in this system.



As another example of introducing a conformational restriction containing an ether linkage, rigid **1.037** was derived through the installation of a carbon-carbon bond in **1.038**. The compounds were prepared as small-molecule inhibitors of histones deacetylases (HDAC) because inhibition of HDAC is a potential strategy for the development of small molecule anticancer agents.⁸⁶ The control and constrained molecules only differ in the number of carbon-carbon bonds. Due to the similar make up of the molecules, the cycle and control should have the same interactions with HDAC and the solvent. Any difference in the binding affinities could then be associated with the introduction of the conformational constraint. Nanomolar inhibitors **1.037** and **1.038** had equal activity against HDAC. Although no structural information was provided to determine if **1.037** and **1.038** bind in similar modes to the protein, it seems that once again the introduction of a conformational constraint did not enhance binding affinity.

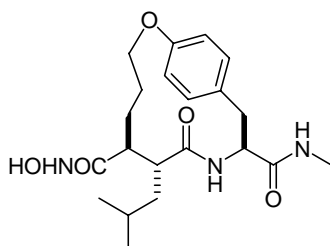


1.037

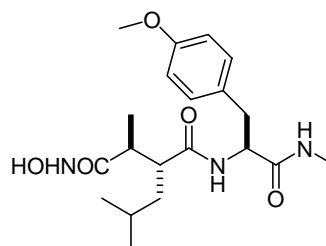


1.038

In another example where side chain to side chain linkage did not enhance binding affinity, the 14-membered macrocyclic hydroxamic acid **1.039** that inhibits tumor necrosis factor α (TNF- α) release was designed as a cyclic analogue of **1.040**. Two methylene residues were used to link the methyl and methoxy moieties in **1.040** to afford **1.039**.⁸⁷ An X-ray structure of an inhibitor-enzyme complex was inspiration for this macrocycle because it revealed the close proximity of the methyl and methoxy ligand groups. The control **1.040** was found to be equipotent as the cyclophane **1.039** in micromolar inhibition of TNF- α release. The important X-ray crystal structure of **1.039** bound to MMP-3 reveals that the 14-membered ring holds all the structural elements in positions analogous to those of **1.040** bound to the protein. Hence, the introduction of a conformational constraint did not change the mode of binding in this system. Since the constrained and control molecules are equipotent and bind to the protein in the same manner, one might assume that there was no impact on binding energetics by introducing this conformational constraint.

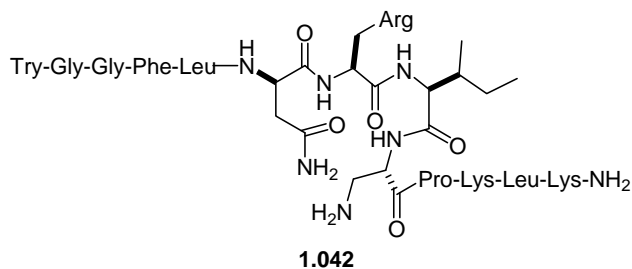
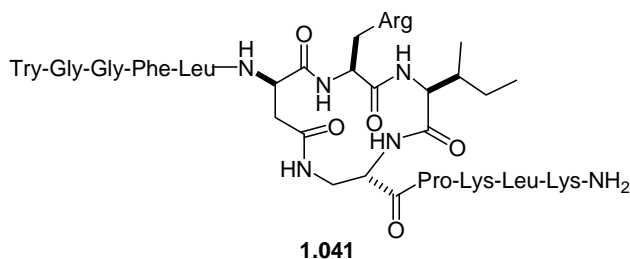


1.039



1.040

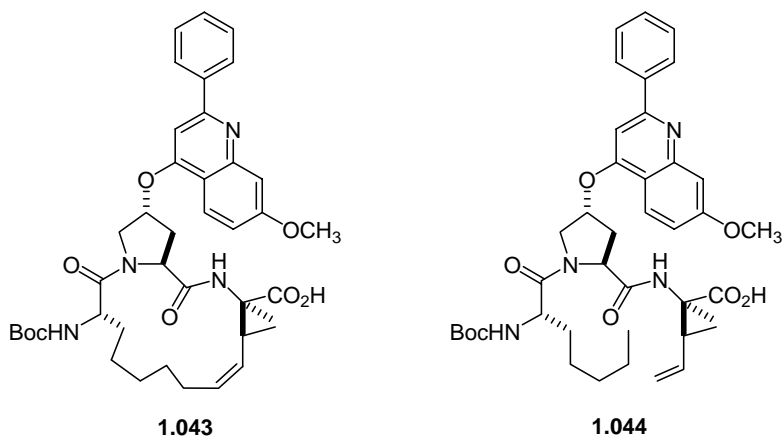
Lactam bridges have also be utilized to introduce side chain to side chain conformational constraints. For many years, Aldrich and co-workers have been interested in synthesizing rigid dynorphin A (Dyn A) analogues as selective κ opioid receptor agonists.⁸⁸ Dyn A-(1-13)NH₂ is a highly flexible peptide with the following amino acid sequence: Tyr-Gly-Gly-Phe-Leu-Arg-Arg-Ile-Arg-Pro-Lys-Leu-Lys-OH. The low selectivity for the κ opioid receptor is partially attributed to the conformational flexibility of the ligand. The *N*-terminus of Dyn A has been estimated to adopt a helical structure from Tyr¹ through Arg⁹ when interacting with κ receptors.⁸⁹ The side chain to side chain cyclic constraints were installed in order to stabilize this structure and the amino acid residues involved in the constraint were carefully selected such they were not critical residues for receptor recognition. Cycle **1.041** was the most potent nanomolar inhibitor for the κ opioid receptor and was six times more active than its linear control partner **1.042** in the cell-based assay. Futhermore, the linear control **1.042** contains a free amine that is not present in the cycle and this moiety could also be positively charged at physiological pH. The impact of interactions between this amine residue and the solvent and protein are unknown. Thus, it is difficult to determine the effect of introducing a conformational constraint in this system.



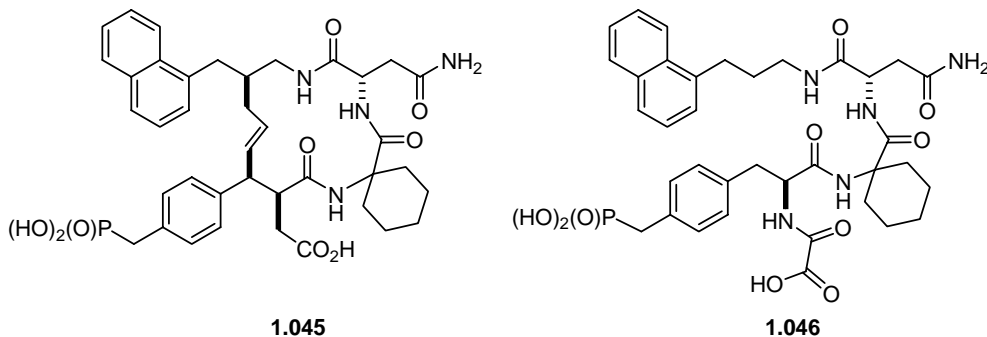
1.4 EXAMPLES OF BACKBONE TO BACKBONE CONFORMATIONAL CONSTRAINTS

Research groups have also been interested in installing backbone to backbone linkages in order to design conformational constraints into peptide ligands. Carbon chains and ester or amide bonds have been used as the bridging units in many constrained molecules. For example, a macrocyclic nanomolar inhibitor of NS3 protease, a potential therapeutic target of hepatitis C virus infection, was synthesized with the hope that 15-membered macrocycle containing a *Z*-double bond would enforce the conformation required to bind to NS3.⁹⁰ The macrocyclic constraint was designed by installing an alkyl chain between backbone atoms. The only difference between **1.043** and its ideal control **1.044** was the breaking of a carbon-carbon bond in the alkyl backbone bridge. *In vitro* IC₅₀ values were determined and constrained **1.043** had 36-fold increased potency over flexible **1.044**. An important X-ray structure of **1.043** bound to the protease was solved and confirmed that **1.043** had a similar bound conformation as other inhibitors

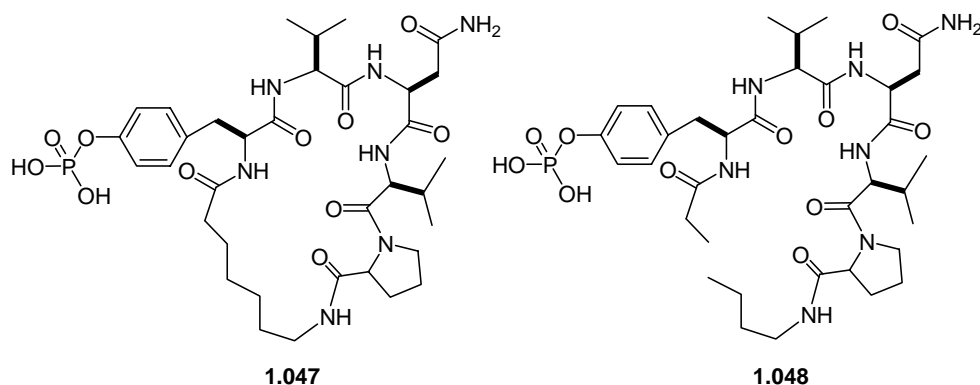
previously reported. In this example, it is clear that the introduction of a conformational constraint enhanced binding affinity.



Burke and co-workers also designed a carbon bridge that linked the backbone atoms of a peptide in order to introduce a conformational constraint. Ligands **1.045** and open-chained analogue **1.046** were evaluated for their ability to bind to the Grb2-SH2 domain.⁹¹ All compounds had nanomolar potency with the macrocycle **1.045** having seven-fold higher binding affinity than its acyclic partner. However, the oxalyl group in **1.046** might interact differently with the domain or solvent than the carboxylate group found in **1.045**. In addition, the hydrocarbon bridge in the macrocycle **1.045** could also provide additional contacts with the protein or solvent. Thus, it is difficult to judge the effect of introducing a conformational constraint in this system.

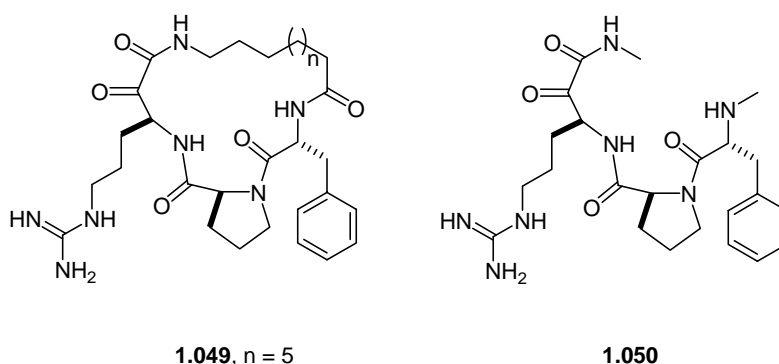


Also using carbon backbone to backbone linkage, Ettmayer made a number of cyclic phospholactams as Grb2-SH2 domain binding antagonists.⁹² In competitive ELISA assays, the macrocycle **1.047** was found to be 2.6-fold more active, with submicromolar potency, than its control **1.048**. Two dimensional NMR studies of the ligands in aqueous solution suggested that the pTyr-Val-Asn motif of **1.047** is stabilized in the β -turn that is required for interaction with Grb2-SH2 domain, whereas in solution the structure of **1.048** is a random coil. There are no major discrepancies between the constrained and control molecules, they both should have the same interactions with the protein and the solvent, and thus, the introduction of a conformational restriction seemed to slightly enhance affinity in this case.



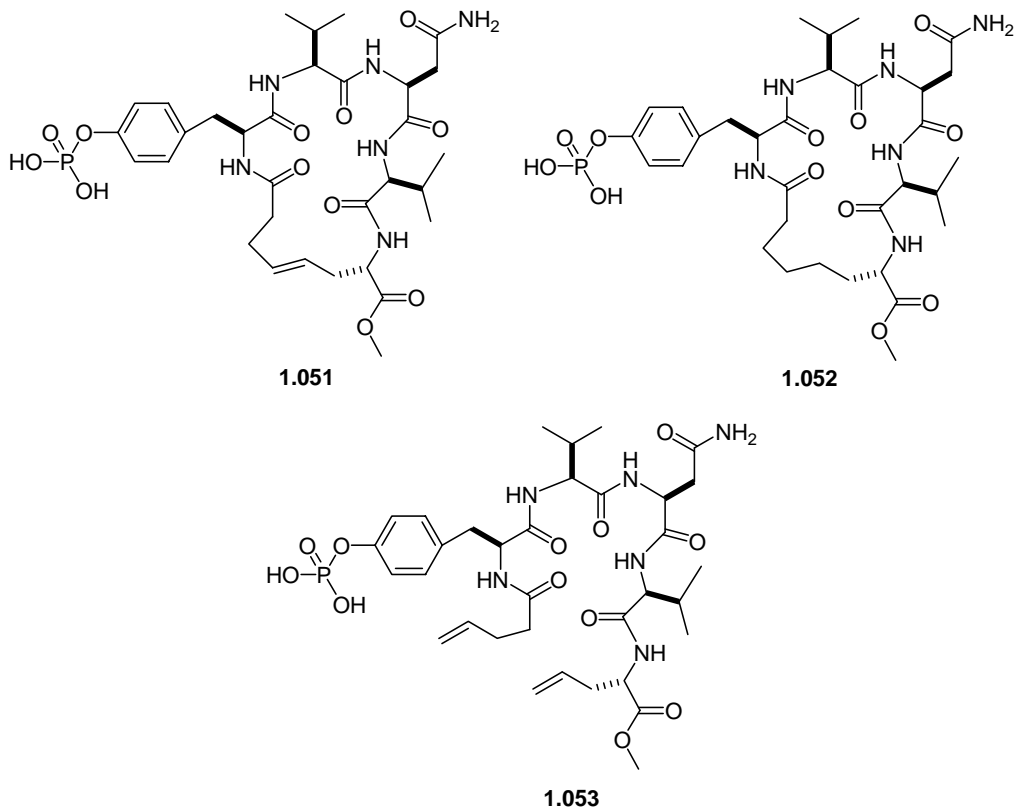
Greco and co-workers also designed backbone to backbone macrocyclic serine protease inhibitors using methylene residues as the bridging atoms with the intent of evaluating the effects of ring size on binding activity.⁹³ Cycle **1.049** was the most active rigid compound with nanomolar potency and the acycle **1.050** served as the linear control; the compounds displayed similar inhibition activity, with only a two-fold difference in potency. However, the control has an amine residue that is not present in the cycle. Based on the X-ray structure of a similar cyclic inhibitor bound to the

protease, this amine in the flexible control **1.050** seems close enough to interact with protein residues potentially giving the control ligand additional interactions with the protease relative to the cyclic derivatives, which were not discussed in this study. It is therefore difficult to estimate the effect of introducing a backbone to backbone conformational constraint in this system.



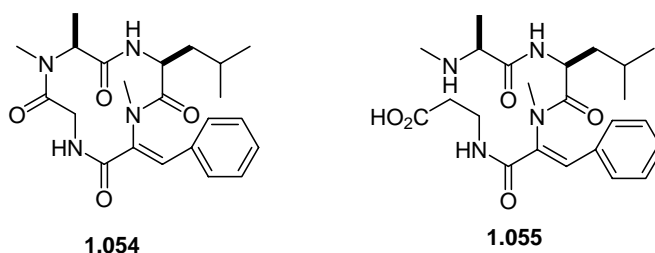
Liskamp also introduced a carbon chain to design a backbone to backbone constraint in **1.053** forming the macrocycles **1.051** and **1.052** in order to enhance Grb2-SH2 domain binding.⁹⁴ The control **1.053**, which was the synthetic precursor for **1.051** and **1.052**, differs from the cyclic compounds by two methylene units. The double bond in **1.051** introduces an additional constraint relative to **1.052**. The binding affinities for **1.051**, **1.052** and **1.053** were measured, and the unsaturated cyclic peptide **1.051** was slightly less active than the linear peptide **1.053**, whereas the reduced cyclic peptide **1.052** was approximately equipotent as the linear peptide **1.053** both exhibiting nanomolar potency. It should be noted, however, that these energetic differences are relatively small. This example, once again, illustrates that conformational constraints do not always enhance binding affinity to SH2 domains. The authors suggest that enthalpy-entropy compensation may be responsible for counteracting any entropy gained through

pre-organization. However, the researchers provide no thermodynamic data to support this hypothesis.



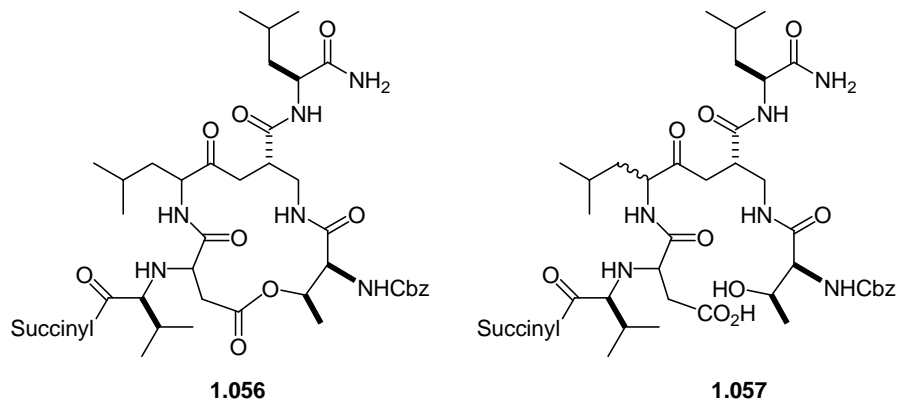
In addition to carbon units, amide bonds have also been used to link the backbone residues of peptides together in order to introduce conformational constraints. In one such example, the bioactive properties of a series of cyclic peptides were determined in a lettuce seeding assay to measure chlorosis induction, a disease condition in plants that is characterized by yellowing.⁹⁵ Tentoxin (**1.054**), which causes chlorosis, is the backbone to backbone macrolactam of the flexible peptide **1.055**. The rigid **1.054** was four-fold more active than the linear control **1.054**. Therefore, the introduction of a conformational constraint seemed to enhance binding potency of the linear peptide. However, there are potentially different interactions between the functional groups of the ligands with the

solvent and/or protein. The cycle **1.054** contains an amide group while the linear **1.055** has carboxylate and amine moieties. The effect each of these groups will have on the binding event makes the evaluation of the backbone to backbone conformational constraint in this system difficult to determine.



Macrolactonization can also be used to introduce a backbone to backbone conformational constraint. For example, Bartlett and co-workers synthesized the novel macrocyclic peptidase inhibitors **1.056** (both *R*- and *S*- enantiomers were prepared) by introducing a conformational constraint into **1.057**.^{60,61} The lactone linkage in **1.056** was cleaved with base to provide the hydroxy acid **1.057**, which was used as a control to determine the energetic effect of macrolactonization on binding. However, the basic conditions caused epimerization giving a 60/40 mixture of diastereomers of **1.057**. The compounds were tested for their ability to inhibit α -chymotrypsin. The diastereomeric mixture **1.057** had a K_i of 1500 μM , whereas the *S*-lactone **1.056** had a K_i of 220 μM , and the *R*-lactone **1.056** had a K_i of 1700 μM . Comparison of the acyclic hydroxy acid **1.057** with the lactone **1.056** indicated that the macrolactonization enhanced the affinity by about a factor of four, assuming that the inhibition observed for the acycle emanates from only one of two epimers present in the mixture. However, one needs to consider that the lactone in **1.056** and the carboxylate and alcohol moieties in **1.057** could interact

differently with protein and solvent, and the true energetic consequences of introducing the macrolactone constraint cannot be explicitly determined from this study.



1.5 EXAMPLES OF CONFORMATIONAL CONSTRAINTS WHERE THE THERMODYNAMIC PARAMETERS OF BINDING WERE MEASURED

Many of the preceding examples suggest that the introduction of a conformational constraint could enhance the binding affinity of a flexible ligand as stated in the theory of pre-organization. However, evidence that this increase affinity is caused by the reduction of the entropic penalty of binding has not been conclusively provided in the literature. In order to determine the true entropic advantage that should accompany the introduction of the conformational constraint, the thermodynamic parameters of the binding of the constrained and control molecules need to be evaluated. There are only a few examples of this in the literature. For example, the effect of introducing a conformational constraints in pp60^{c-src} SH2-domain binding ligands was evaluated using ITC.⁹⁶ The C-terminal portion of the native tetrapeptide ligand (N-Ac-pY-EEI-OH) was rigidified using a piperidine ring in order to define the structural requirement for the hydrophobic pY+3 binding site of the SH2 domain. The flexible analogue **1.059** was prepared as a control, although it contained two additional methylene groups. Binding of the rigid **1.058** was

found to be more enthalpically favorable than the binding of the flexible **1.059** with the $\Delta\Delta H$ being -1.1 kcal mol⁻¹ (Table 1.01). An unanticipated entropic disadvantage from pre-organization was also observed and therefore, this example suggests that the introduction of a conformational constraint may not reduce the entropic penalty of binding. However, the overall binding difference between the pair was almost equal ($\Delta\Delta G = 0.5$ kcal mol⁻¹) suggesting that enthalpy-entropy compensation (see Section 1.1.1) is an important factor and may result in the introduction of a conformational constraint having no effect on binding affinity. In addition, no structural data was provided in this example which is important for determining the effects of introducing the conformational constraint.

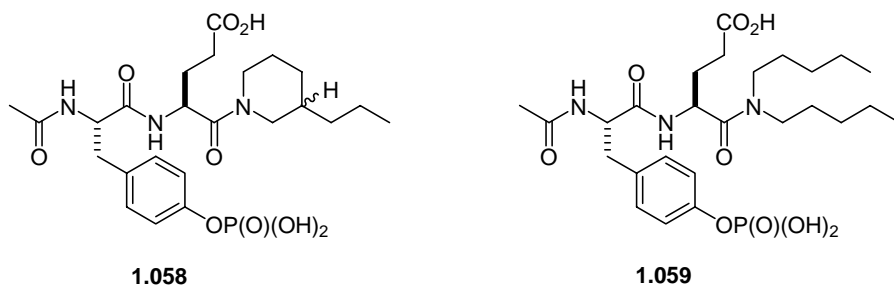


Table 1.01: ITC data for binding to SH2 domain.⁹⁶

compounds	K_d (μM)	ΔG (kcal mol ⁻¹)	ΔH (kcal mol ⁻¹)	ΔS (cal mol ⁻¹ K ⁻¹)
1.058	1.0 ± 0.5	-8.4	-5.4 ± 0.1	10
1.059	0.4 ± 0.1	-8.9	-4.3 ± 0.9	15.3

In another example, Spaller and co-workers designed and studied conformationally constrained ligands for the third PDZ (PDZ3) domain of the postsynaptic density-95 kDa protein, which mediates a variety of protein-protein interactions in eukaryotic cells.⁹⁷ A group of macrocycles was prepared utilizing side

chain to side chain lactam linkages and evaluated using ITC (Table 1.02). The ligands were designed based on the native peptide NH₂-Tyr-Lys-Gln-Thr-Ser-Val-OH (**1.060**). The Gln residue at P₋₃ positions was converted to an amine-bearing side chain X and Ser at position P₋₁ was changed to a carboxylate-bearing side chain Y. Coupling the X and Y side chains formed a lactam bridges providing cyclic compounds where the key binding residues for PDZ3 (Val at P₀ and Thr at P₋₂) were not altered.

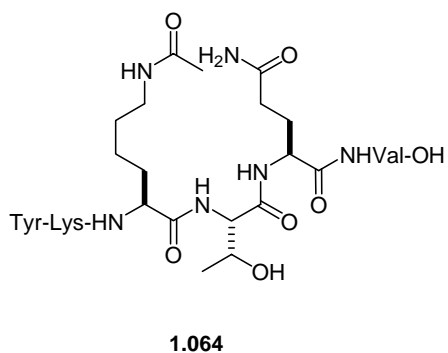
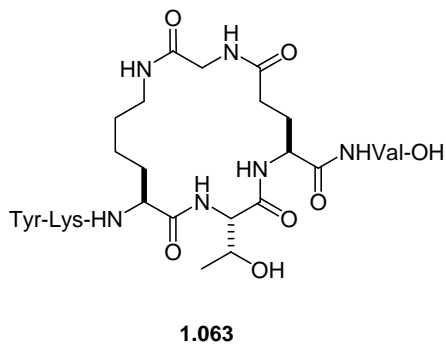
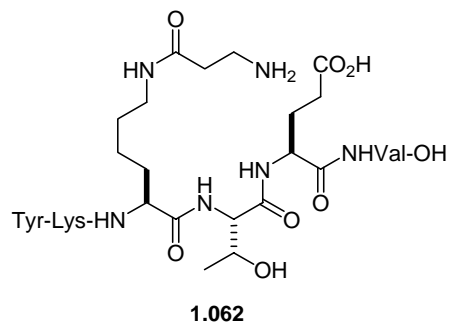
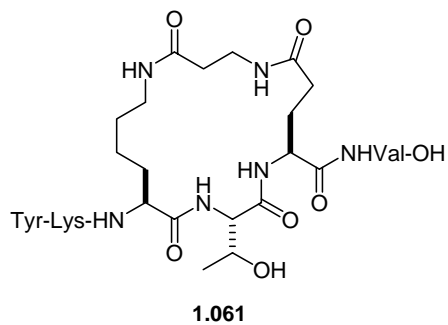
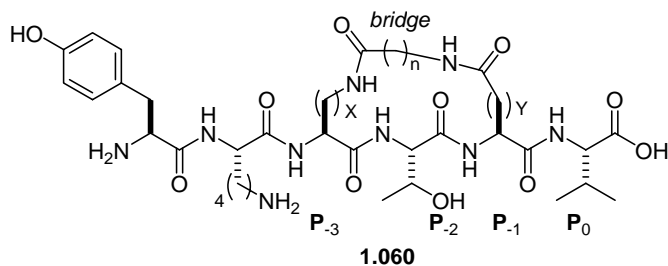


Table 1.02: Binding profile for macrocycles and controls of PDZ3.⁹⁷

compounds	K_d (μM)	ΔG (kcal mol^{-1})	ΔH (kcal mol^{-1})	$T\Delta S$ (kcal mol^{-1})
1.061	4.47 ± 0.26	-7.29 ± 0.03	-2.29 ± 0.01	5.01 ± 0.03
1.062	5.54 ± 0.18	-7.17 ± 0.02	-4.77 ± 0.35	2.4 ± 0.3
1.063	18.5 ± 3.5	-6.45 ± 0.1	-2.47 ± 0.09	4.00 ± 0.01
1.064	5.03 ± 0.18	-7.22 ± 0.02	-3.08 ± 0.09	4.15 ± 0.07

Many cyclic and acyclic pairs in this study showed very similar entropy of binding. However, there was a large, favorable increase in entropy, $T\Delta S = 2.6 \text{ kcal mol}^{-1}$ for the cyclic derivative **1.061** relative to its acyclic control **1.062**. The authors speculate that this increase in entropy might be attributed to a decreased entropic penalty of binding (through rotor restriction). However, in addition to the entropic gain associated with the introduction of the conformational constraint in the **1.061/1.062** pair, there was also an enthalpic loss resulting in a small difference in the overall ΔG . This enthalpy-entropy compensation appears ubiquitous in biological systems and is once again a factor in ligand pre-organization. It should be noted that the control **1.062** is “unavoidably imperfect”, because it contains amine and carboxylate groups, which may participate in dramatically different interactions with the protein and solvent than the amide present in the cyclic partner. Nevertheless, it seems that the conformational constraint might have reduced the entropic penalty of binding but did not enhance the overall binding affinity.

On the other hand, **1.064** was the almost ideal flexible control for macrocycle **1.063** as the only difference between **1.063** and **1.064** was a formal hydrogenolysis of a carbon-nitrogen bond in the macrocyclic ring. There is, however, an extra amide N-H group in the control **1.064** that could participate in interactions with solvent or protein. Interestingly, control **1.064** had a slightly higher affinity than cycle **1.063**, mostly through an enthalpic gain ($\Delta\Delta H = 0.61 \text{ kcal mol}^{-1}$). It appears that in this pair the pre-

organization did not reduce the entropic penalty or increase potency. This research illustrates that the choice of control molecule is crucial to evaluating the energetics of introducing a conformational constraint. However, once again, the researchers did not provide any of the important structural information needed to further evaluate the conformational constraint theory.

Disulfide bonds are naturally used to control the conformation of peptides and proteins, and forming disulfide bonds between proximal cysteine or related residues have been used as a tactic to introduce constraints in peptide ligands. For example, Hruby designed conformationally restricted derivatives of enkephalin by installing disulfide linkages into the flexible dithiols in order to stabilize the β -turn required for activity.⁹⁸⁻¹⁰¹ ITC was used to examine the interaction between the lipid membrane and the cyclic and acyclic peptides **1.065** and **1.066** (Table 1.03).¹⁰² The control **1.066** had more favorable enthalpy of binding to the cell membrane while **1.065** had more favorable entropy of binding. Enthalpy-entropy compensation was once again observed for the pair with the free energy of binding to the cell membrane being very similar for each compound. Although the only difference between the molecules in the pair is the disulfide bridge which is replaced by two hydrogen atoms, the compounds could potentially interact differently with the protein and solvent. In addition, one must consider the stability of the acyclic control, which could be easily oxidized to the corresponding cyclic compound. Despite the fact that no structural data was provided, it seems that in this case the pre-organized compound had an entropic advantage over its control partner but the introduction of a conformational constraint did not enhance overall binding affinity.

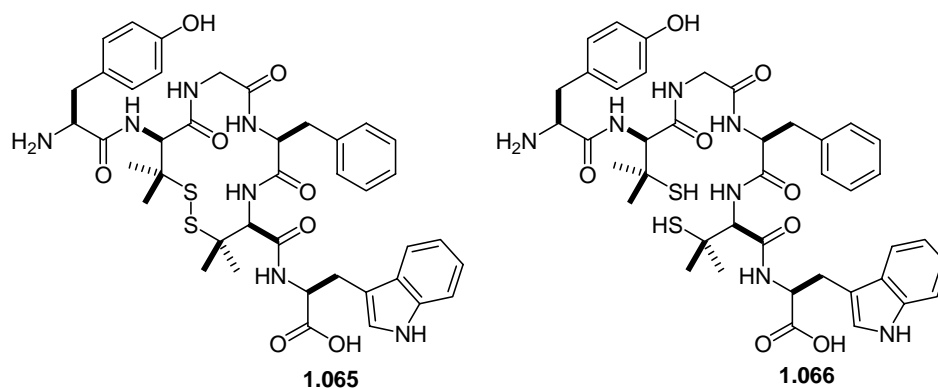


Table 1.03: Thermodynamic parameters for binding cyclic and acyclic enkephalin analogues to POPC/cholesterol.

compounds	K (M^{-1})	ΔG ($kcal\ mol^{-1}$)	ΔH ($kcal\ mol^{-1}$)	ΔS ($cal\ mol^{-1}$)
1.065	385	-5.9	-4.4	5.1
1.066	890	-6.4	-13	-23

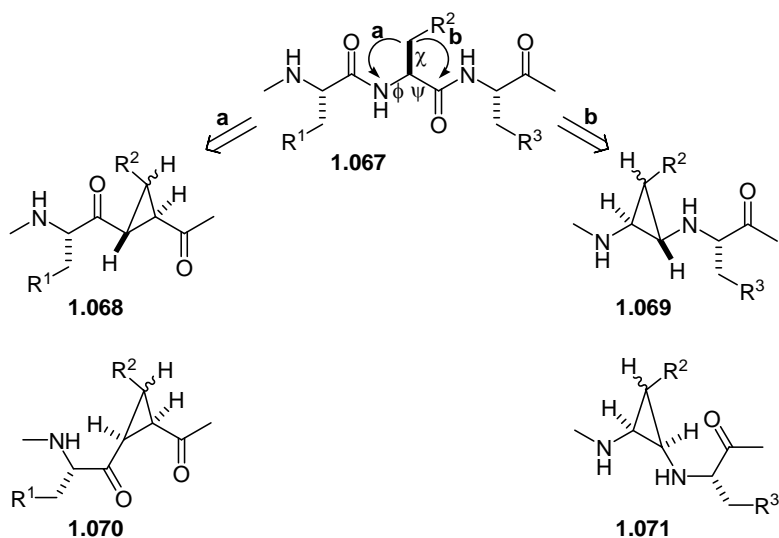
1.6 THE INTRODUCTION OF CYCLOPROPANES AS CONFORMATIONAL CONSTRAINTS

Although there are examples in the literature where the introduction of a conformational constraint has increased binding affinity, but there are also examples where pre-organization does not seem to affect binding potency. In addition, there is little clear cut evidence that a conformational constraint reduces the entropic penalty of binding. Thus, it seems that the two fundamental elements of the conformational constraint theory, namely enhanced binding affinity and minimized entropic penalty, have not been fully examined and may not, in fact, be true. Even so, medicinal chemists still use this unproven theory to design and develop new molecules and drugs. The Martin group has begun to investigate their cyclopropane conformational constraints in order to address these issues more thoroughly. The Martin has explored the use of cyclopropanes to introduce conformational constraints into peptides since the early

1990s. In some but not all cases, the proper control molecules were prepared to evaluate explicitly the effect of introducing a constraint. We have also used thermodynamic and structural data to examine the conformational constraint theory. This section summarizes the results to date.

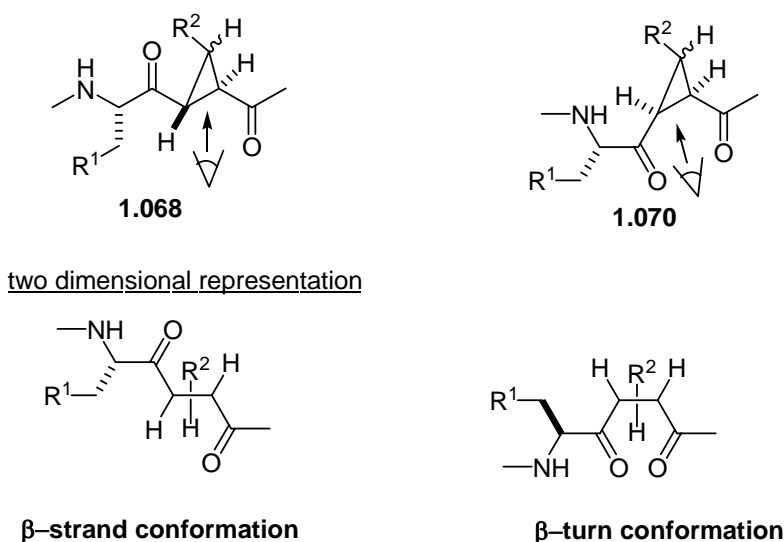
1.6.1 Introduction: Cyclopropanes Restrict Both Peptide Backbone and Side Chain Orientation

In order to lock both the backbone and side chain of a peptide into the biologically active conformation, the Martin group designed 1,2,3-trisubstituted cyclopropanes as conformationally restricted mimics of peptide **1.067**. Many of the conformational constraints that have been reported in the literature restrict only the backbone or side chain moiety of the parent peptide. Using cyclopropanes it is possible to constrain both the peptide backbone and side chain into specific orientations at the same time. In addition, it is straight forward to design and prepare the ideal control partners for these constrained pseudopeptides. The cyclopropane replacements **1.068** and **1.070** were developed by mutating the nitrogen atom of the amide bond in the native peptide **1.067** to carbon and covalently connecting it to C(β) on the side chain (mode **a**). These cyclopropanes are designed to restrict the ϕ and χ_1 torsional angles of the peptide. Replacements **1.069** and **1.071** were derived from the native peptide **1.067** by replacing the amide carbonyl carbon with a sp^3 -carbon and connecting it to the C(β) on the side chain (mode **b**). These cyclopropanes restrict the ψ and χ_1 torsional angles of the peptide.



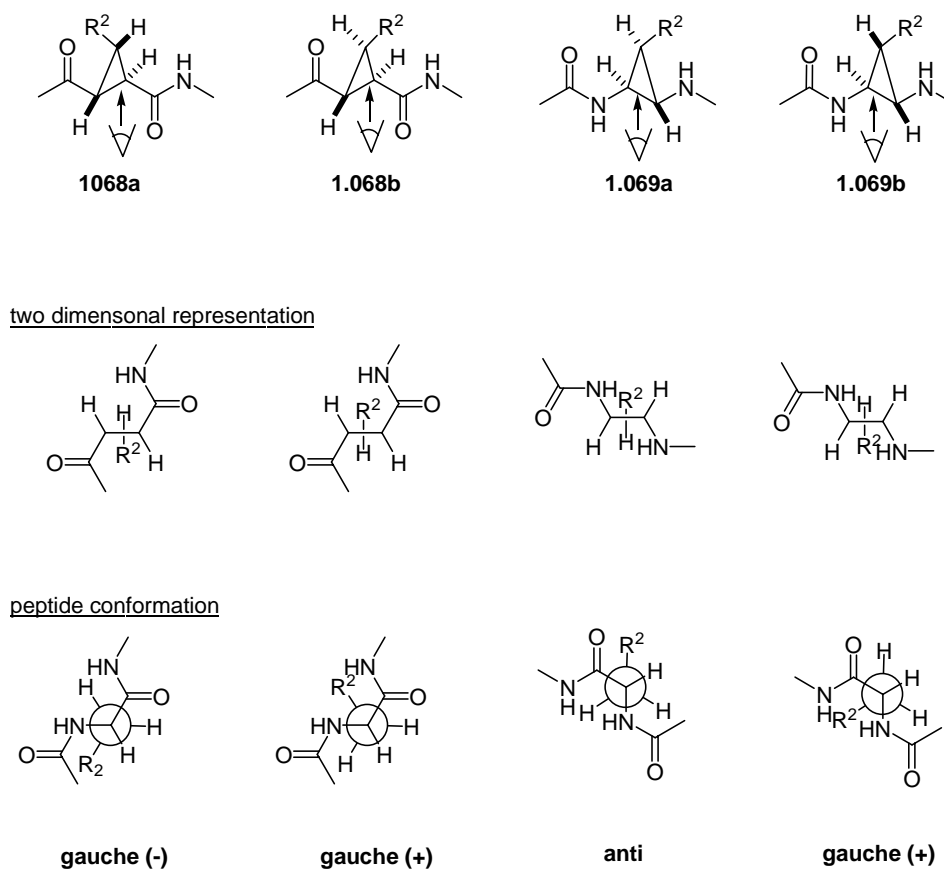
The stereochemistry around the cyclopropane ring plays an important role in determining the conformation of the native peptide that is mimicked. For example, when the backbone atoms on the ring are in a *trans*-orientation as in **1.068** and **1.069** the peptide backbone is locally rigidified in an extended (β -strand) conformation by locking the ϕ or ψ angle at about -132° and 143° , respectively, as evident by X-ray crystal structures.¹⁰³⁻¹⁰⁵ Ideally, the torsional angles for a peptide β -strand of $\phi = -139^\circ$ and $\psi = 135^\circ$.² On the other hand, when the backbone substituents on the cyclopropane **1.070** or **1.071** are *cis*, it has been hypothesized that a β -turn conformation would be stabilized (Figure 1.3).

Figure 1.3: The Two Dimensional representation of the conformation of the *trans*- and *cis*-cyclopropanes.



The stereochemistry at the carbon atom bearing R^2 on the cyclopropane ring determines which direction the side chain will be locked in space. In **1.068a** the conformation of the native peptide that is mimicked by the cyclopropane constraint is gauche (-), which can be seen by looking at the two dimensional, pseudo Fischer projection, representation (Figure 1.4). In the gauche (-) conformation the χ_1 torsional angle is approximately -60° . In a similar fashion, cyclopropanes **1.068b** and **1.069b** mimic a gauche (+) conformation where the χ_1 torsional angle is roughly $+60^\circ$. However, in **1.069a**, an *anti* conformation is mimicked where the χ_1 torsional angle is 180° .

Figure 1.4: The χ_1 angles mimicked by the cyclopropane constraints.



Molecular modeling suggests that all these conformations are stabilized by the cyclopropanes. The geometric properties of replacements can be best illustrated by examining the superimposition of the $-\text{Phe}[\text{COcpCO}]\text{Phe}-$ replacements in Figures 1.5 and 1.6. The *N*-terminal Phe of **1.072** was anchored in the gauche (-) conformation, and the superimposition of **1.072** with the corresponding Phe-Phe dipeptide **1.074** in which the backbone is in an idealized β -strand and both phenyl groups are fixed in gauche (-) orientations. The root-mean-square fit for this rigid superimposition is approximately

0.35Å.¹⁰⁴ The anti-conformation is shown in Figure 1.6 where **1.073** is overlaid with the Phe-Phe dipeptide **1.074**.

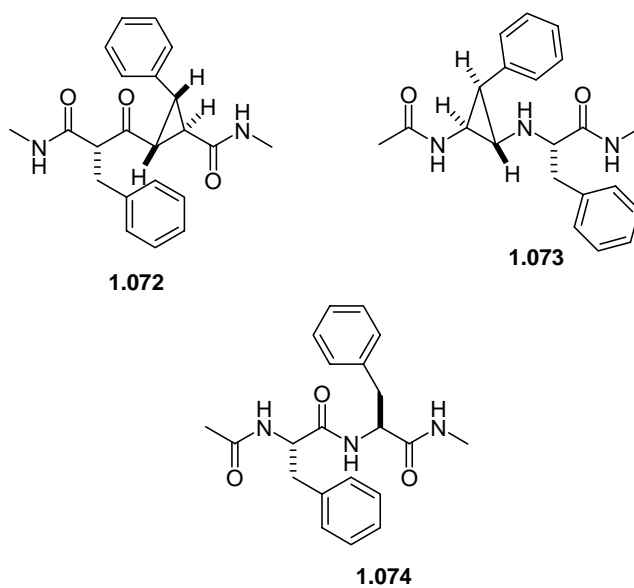


Figure 1.5: The overlay cyclopropane **1.072** with Phe-Phe dipeptide **1.074**.⁵⁸

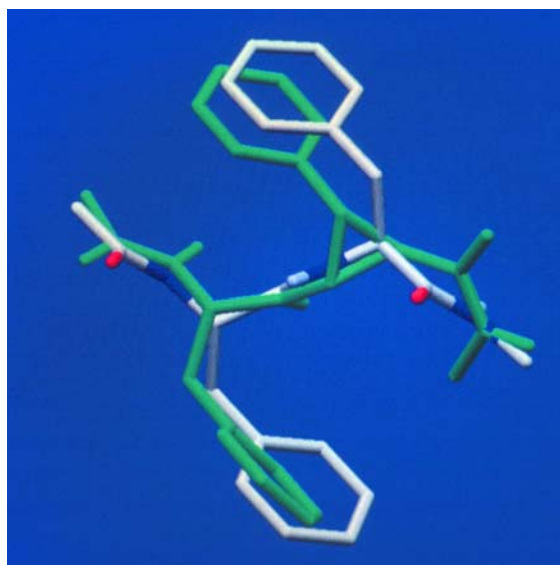
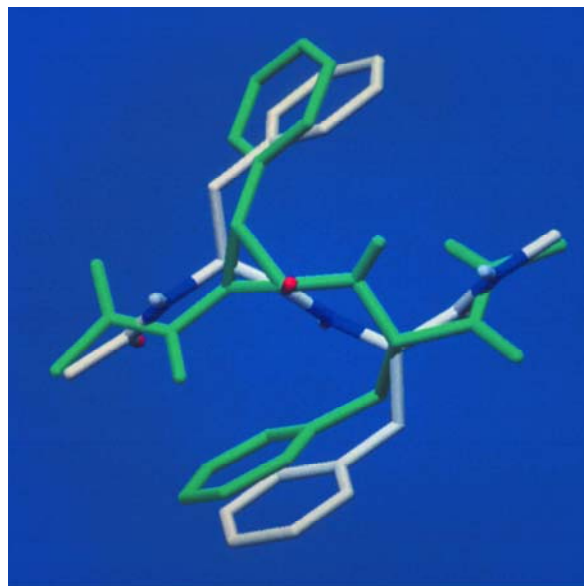


Figure 1.6: The overlay cyclopropane **1.073** with Phe-Phe dipeptide **1.074**.⁵⁸



The cyclopropane in **1.068-1.071** was anticipated to restrict two torsional angles of either ϕ and χ_1 in **1.068** and **1.070** or ψ and χ_1 in **1.069** and **1.071**. In addition, the dicarbonyl pseudopeptides based on **1.068** would have additional restriction of the ϕ_2 and ψ torsional angles due to interactions of the carbonyl π orbitals with the carbon-carbon σ bond of the cyclopropane ring as illustrated in Figure 1.7 and 1.8.^{106,107} This orientation has been seen in X-ray crystal structures of the cyclopropane-containing molecule alone and complexed with proteins.¹⁰³⁻¹⁰⁵ The χ_2 -angle is also restricted due to sterics; however, the ϕ_2 -angle is a more flexible than the same torsional angle in the peptide because the amide was changed to a ketone. It is anticipated that two to three rotors are restricted on the native peptide by introducing the cyclopropane constraint. The total

energetic advantage that arises from restricting the rotors should be about 1.4 kcal mol⁻¹ (see Section 1.1.3).

Figure 1.7: The preferred conformation of a carbonyl on a cyclopropane ring where the *N*-terminus carbonyl bisects the cyclopropane in a compound similar to **1.068**.¹⁰³

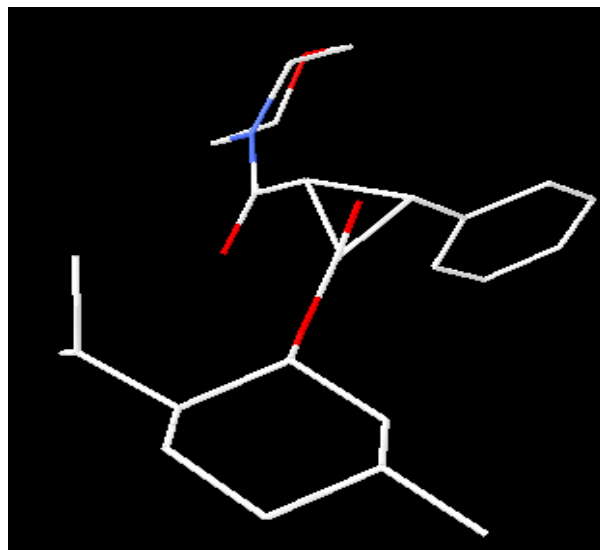
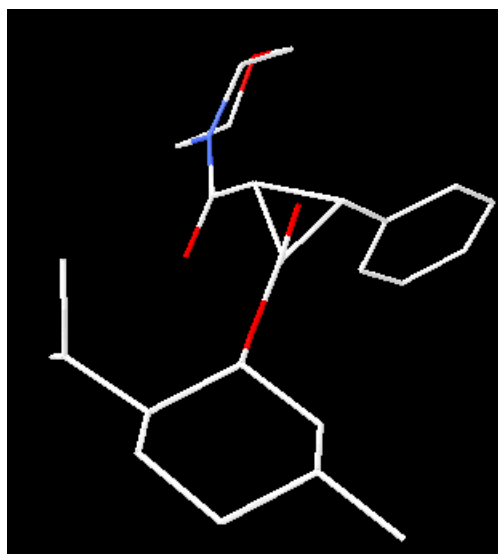
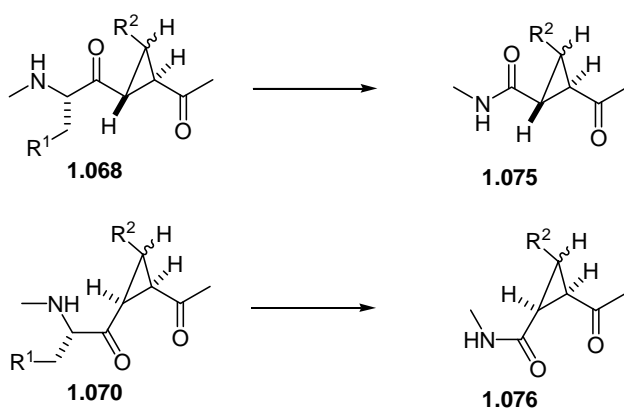


Figure 1.8: The preferred conformation of a carbonyl on a cyclopropane ring where the *C*-terminus carbonyl distorted bisection of the cyclopropane in a compound similar to **1.068**.¹⁰³



Although some hydrogen-bond accepting capability of an amide carbonyl group in mimics **1.068** and **1.070** is maintained by the keto functions, omission of a backbone N-H in these surrogates eliminates possible hydrogen bond donor and acceptor interactions. However, this amide functionality can be maintained by moving the amide nitrogen over two carbons as in **1.075** and **1.076**, thereby converting the keto functionality of the cyclopropanes **1.068** and **1.070** into a retro amide and helping to maintain the hydrogen bond interaction of the peptide backbone.

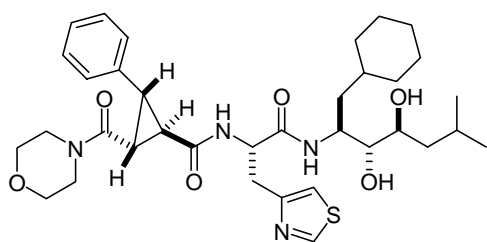


The installation of cyclopropane in **1.067** producing **1.069** and **1.071** requires an amide bond in **1.067** replacing an amino residue. Most of the time neither the carbonyl oxygen nor the N-H of this mutated amide bond in **1.067** interacted directly with the proteins systems evaluated. It seemed reasonable to assess the impact of this aminoethyl substitution. If the newly installed amino group were highly detrimental to binding, second generation ligands could be designed in which an ether could link the residues.

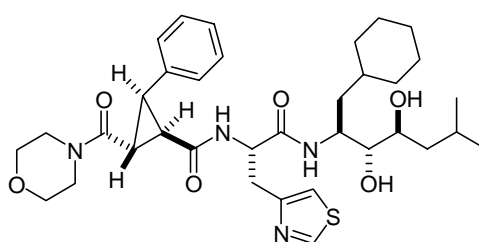
1.6.2 Introduction of Cyclopropane Conformational Constraints into Peptide Ligands

Cyclopropanes have been installed in many different peptide ligands (types **1.068** – **1.071**) with the purpose to obtain ligands with greater binding affinities.^{104,105,108-115} In general the cyclopropane-containing molecules were equipotent but rarely better than their control counterpart.

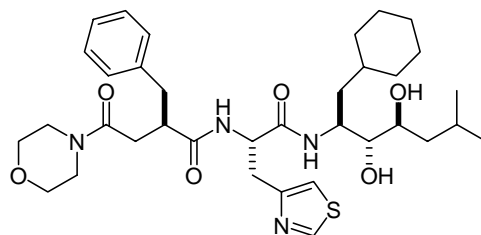
A cyclopropane was first incorporated at the P3 position of renin inhibitors.¹¹³ Cyclopropanes **1.077a-d** and their proper control molecules **1.078** and **1.079** were prepared and evaluated. Cyclopropane **1.077c** and **1.077d** were equipotent and had similar binding affinities as the control **1.079** but these ligands were the least active of all the compounds in question suggesting that the conformations stabilized in these ligands were not appropriate for binding. On the other hand, cyclopropane **1.077a** was 200-fold more active than cyclopropane **1.077b** and thus the conformation stabilized by cyclopropane **1.077a** most resembles the biologically active conformation. However, **1.077a** was found to be about two-fold less active than control **1.078**. Thus, in this case pre-organization provided some insight into the bound ligand conformation but did not increase binding potency compared with the proper control. However, no structural (NMR or X-ray) data for this system was obtained.



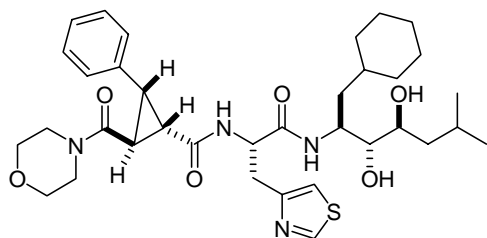
1.077a



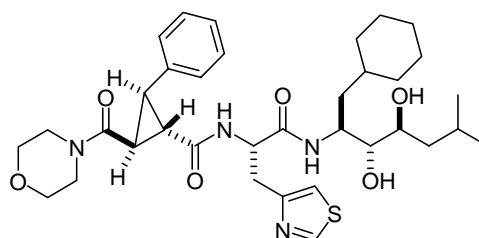
1.077b



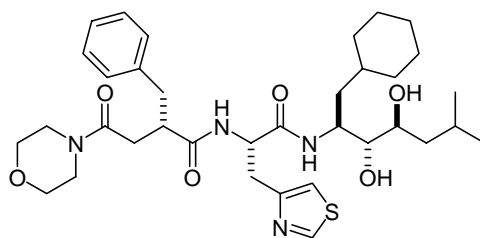
1.078



1.077c



1.077d



1.079

Next a system where the important structural data could be obtained was explored. HIV-1 protease inhibitors were used as a platform to examine the effects of introducing cyclopropanes into peptide ligands.¹⁰⁴ Compounds **1.080**, **1.081** and **1.083** contained two *N*-terminal truncated cyclopropane replacements incorporated at the P2 and P2' subsites of the native ligand that appeared to match the extended conformation

adopted by the peptide upon binding to the protease as shown by X-ray structures of enzyme complexed with inhibitors.^{116,117} The cyclopropanes **1.080** and **1.081** were nearly equipotent to the subnanomolar flexible inhibitor **1.082**, whereas the *N*-methyl cyclopropane ligand **1.083** was a significantly weaker inhibitor than its flexible analogue **1.084**. Two dimensional ¹H NMR studies indicated that **1.080** adopted a well-defined, preferred conformation in solution (DMSO-d₆) in which the peptide backbone was in an extended conformation. This suggests that in solution the cyclopropanes stabilize the biologically active, extended, conformation of the ligand. A three-dimensional X-ray structure of **1.081** complexed with HIV-1 protease was also obtained, and the structure superimposed well onto the bound conformation of a related linear inhibitor **1.084**, particularly in the P2-P2' regions (Figure 1.9). The similar conformations of the bound and solution structure of the cyclopropanes can be seen in Figure 1.10. It seems that the pre-organized conformation of the ligands in solution mimics their biologically active structure. However, the assay data reveals that the incorporation of the cyclopropanes did not enhance the biological potency.

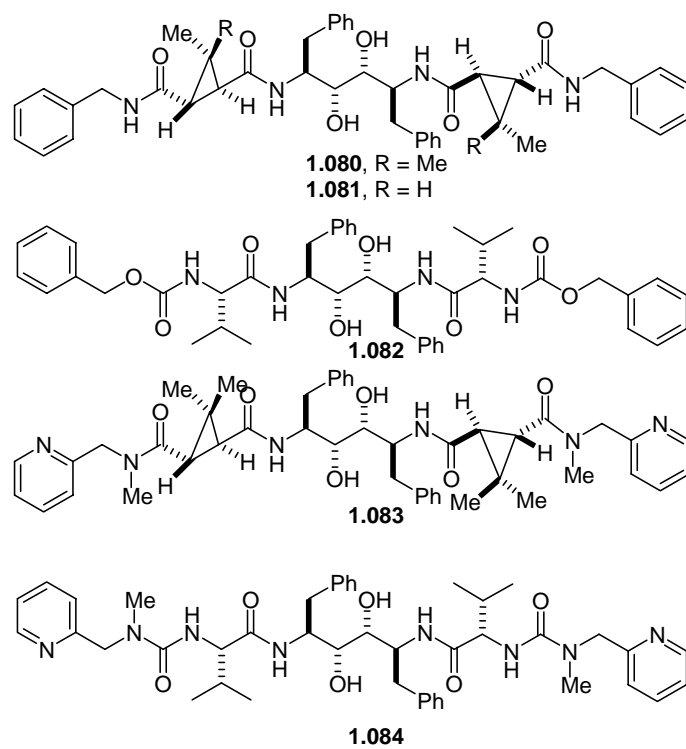


Figure 1.9: Overlay of inhibitors complexed **1.081** (orange) and **1.084** (white) with HIV-1 protease.¹⁰⁴

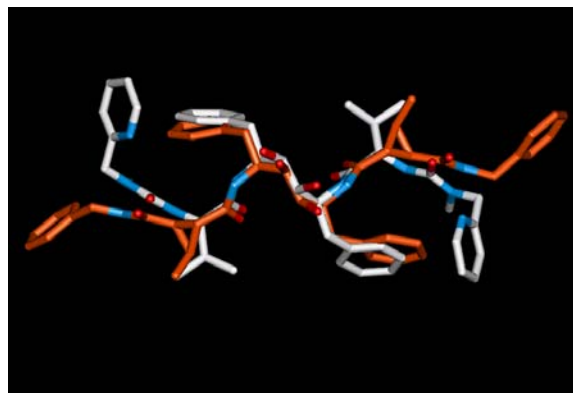
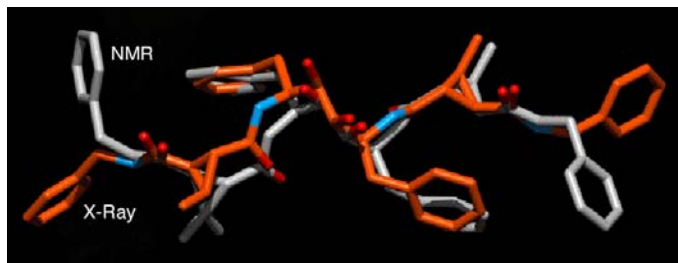


Figure 1.10: Comparison of the X-ray structure of **1.081** complexed with HIV-1 protease and the structure of compound **1.080** in solution determined by NMR.¹⁰⁴



We, like many others, had made the assumption that there should be energetic benefits associated with pre-organizing a ligand into its biologically active conformation, namely, a reduction in conformational entropy paid upon complexation. Favorable entropy of binding was predicted to elicit enhanced binding, provided there were no enthalpic penalties arising from a loss of attractive interactions or the introduction of unfavorable steric interactions in the protein-ligand complex. *However, in most of our experiments, the conformationally constrained cyclopropane ligands were at best equal to their flexible peptide counterparts.* Hence, the primary goal of preparing tighter binding pseudopeptides through introduction of conformational constraints was not achieved. The next question we asked was “Why?”

Because there had been no studies that had directly measured the thermodynamic parameters (K_a , ΔG , ΔH and ΔS) for binding of constrained cyclopropane-containing ligands; a set of experiments were designed to evaluate the energetic consequences by introducing a cyclopropane constraint into peptide ligands using a biological system that could provide useful structural and thermodynamic data. Attention was turned to the Src-SH2 domain system to correlate the structure and energetics of binding. Many X-ray structures of the domain had been solved, and calorimetry measurements had been

performed.¹¹⁸⁻¹²⁰ This domain preferentially binds the phosphotyrosine-containing tetrapeptide Ac-pTyr-Glu-Glu-Ile-OH (**1.085**) in an extended conformation, and the *N*-terminal amide N-H is not involved in binding with the protein; therefore, incorporating a cyclopropane at this residue should have no detrimental effect to the binding affinity.¹¹⁸ The cyclopropane mimics **1.086** and **1.088** were designed to mimic this conformation, while the flexible ligands **1.087** and **1.089** would serve as the controls.¹⁰⁹ The energetics of binding of these compounds were determined by ITC (Table 1.04).¹⁰⁵ The cyclopropane ligands **1.086** and **1.088** bound with approximately equal affinity relative to their corresponding flexible analogues **1.087** and **1.089**. Both cyclopropanes exhibited a significant entropic advantage ($\Delta\Delta S = 5 - 9 \text{ cal mol}^{-1} \text{ K}^{-1}$) of binding over their flexible controls. This favorable entropy corresponds approximately to that predicted for restricting two to three rotors and supports the hypothesis that pre-organization of a ligand in its active conformation does result in a favorable entropic contribution to binding (see Section 1.2). Nevertheless, both cyclopropanes bound to the SH2 domain with significantly less favorable enthalpies ($\Delta\Delta H = 1.4 - 1.9 \text{ kcal mol}^{-1}$) relative to their flexible controls, resulting in approximately equal potency for the pairs. This enthalpy-entropy compensation has been seen in numerous examples throughout this review (see Section 1.1). In addition, the data obtained for mimics **1.088** and **1.089** suggests that elimination of the amide nitrogen when introducing cyclopropanes like **1.068** into native peptide is not detrimental to binding in this case.

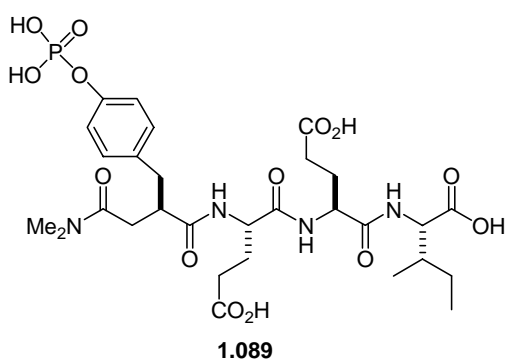
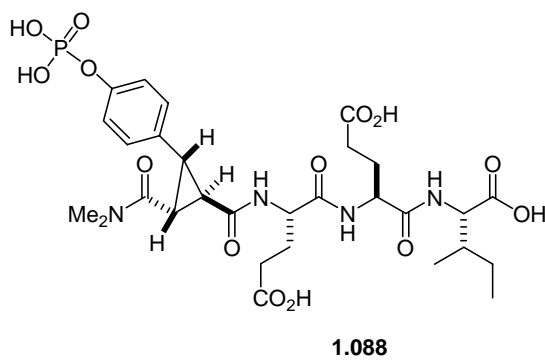
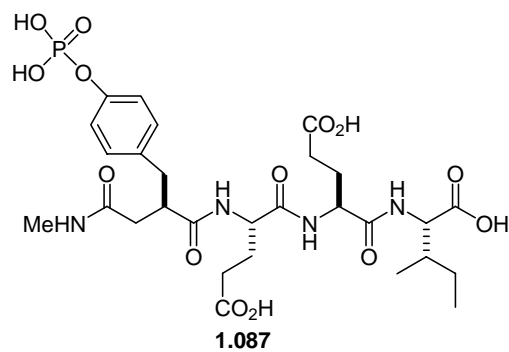
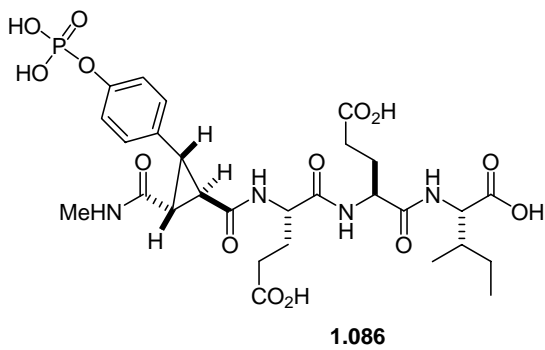
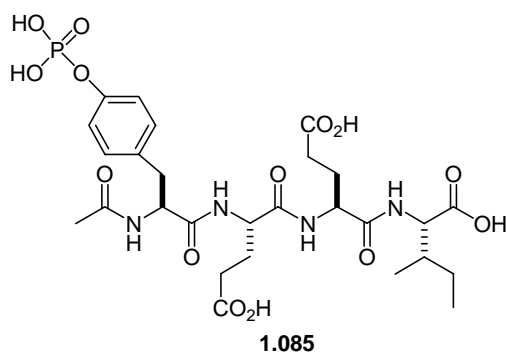
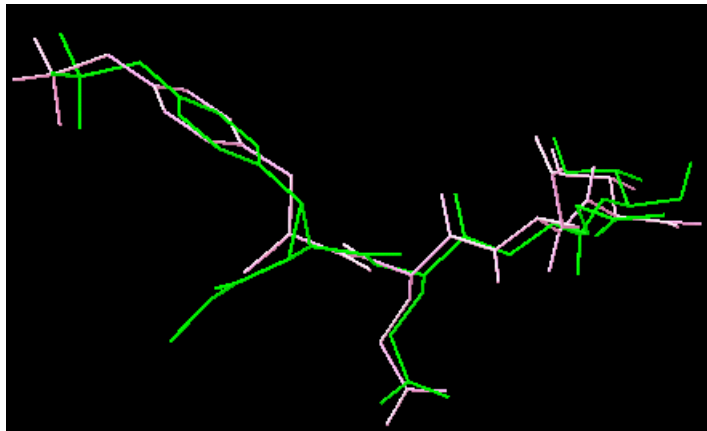


Table 1.04: Thermodynamic profile for the binding of ligands to Src-SH2.^{105,121}

compounds	K_a (M^{-1})	ΔG (kcal mol ⁻¹)	ΔH (kcal mol ⁻¹)	ΔS (cal mol ⁻¹)
1.085	$4.1 (\pm 0.1) \times 10^6$	-9.01 ± 0.01	-6.06 ± 0.05	-9.9 ± 0.2
1.086	$9.7 (\pm 1.5) \times 10^6$	-9.52 ± 0.09	-4.6 ± 0.2	17 ± 1
1.087	$1.7 (\pm 0.6) \times 10^7$	-9.8 ± 0.2	-7.33 ± 0.2	8.3 ± 0.5
1.088	$6.3 (\pm 0.6) \times 10^6$	-9.26 ± 0.06	-5.01 ± 0.05	14.3 ± 0.4
1.089	$1.4 (\pm 0.1) \times 10^7$	-9.72 ± 0.06	-6.92 ± 0.09	9.4 ± 0.4

In order to probe the contribution of introducing the cyclopropane conformational constraints on surfaces of the SH2 domain during binding, the ΔC_p values for compounds **1.086** and **1.087** were determined and were found to be identical within experimental error. This suggests that in the binding of **1.086** and **1.087** to the domain, the same protein surfaces become buried and that **1.086** and **1.087** may bind to the Src-SH2 domain in similar modes (see Section 1.1). A crystal structure of the cyclopropane **1.086** complexed with the SH2 domain shows that the compound binds in a similar manner to the native peptide, and that the biologically active conformation of the native ligand is mimicked by incorporation of a cyclopropane (Figure 1.10). This experiment demonstrated that the incorporation of a cyclopropane did provide an entropic advantage in protein binding, but did not enhance the overall binding affinity, which may be explained by the observed enthalpy-entropy compensation.

Figure 1.10: Overlay of cyclopropane **1.086** shown in green with the native ligand shown in white both bound to Src-SH2 domain.¹²¹



To further explore the phenomenon of enthalpy-entropy compensation in this system, several mutants of **1.086** and **1.087** were prepared that contained different residues at the pY+1, pY+2, and pY+3 positions giving compounds **1.090-1.101**.¹²¹ The thermodynamic data from these ligands revealed no significant differences in ΔG when compared to the ligands (Table 1.05). There were, however, significant variations in the magnitudes of $\Delta\Delta H$ and $\Delta\Delta S$ between each pair with all the cyclopropane-derived molecules showing an entropic advantage. For example, the $\Delta\Delta S$ for the pY+1 Ala variants **1.100** and **1.101** was calculated to be $12.4 \text{ cal mol}^{-1}$ while the $\Delta\Delta S$ is only 2.9 cal mol^{-1} when comparing the cyclic and flexible pY+1 Asp variants **1.094** and **1.095**. There is no structural data for these compounds bound to the SH2 domain. Thus far we cannot comment on the binding modes of each ligand pair to the SH2 domain.

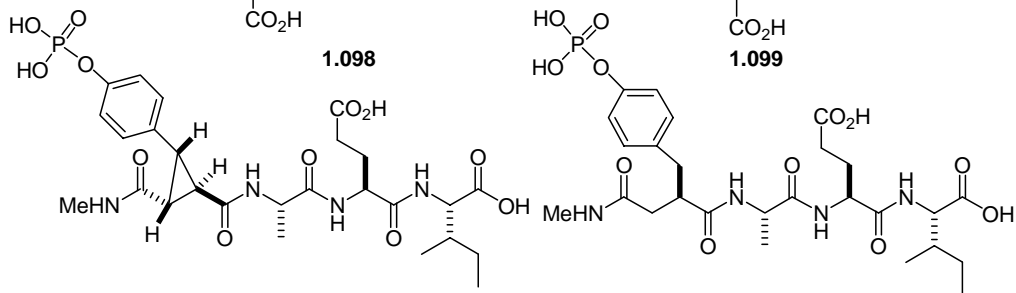
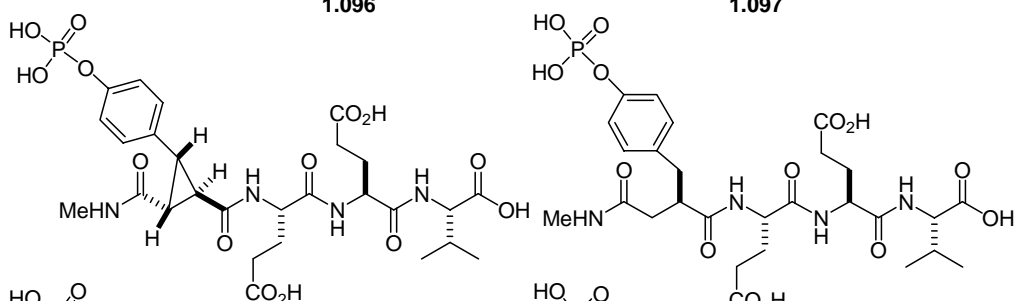
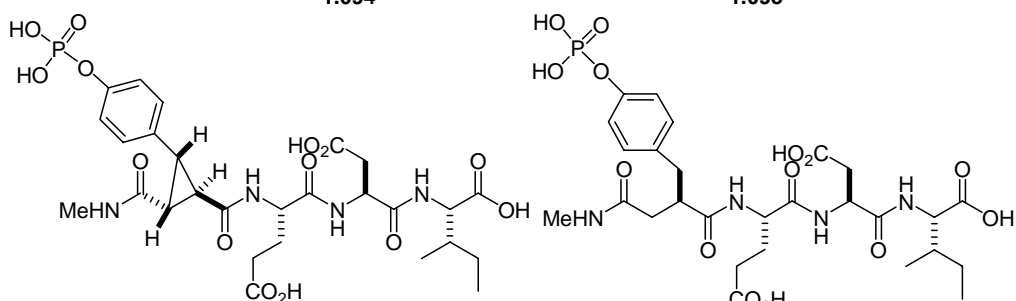
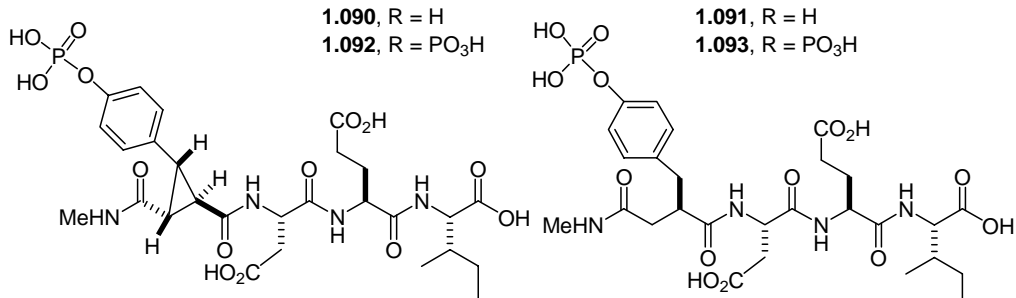
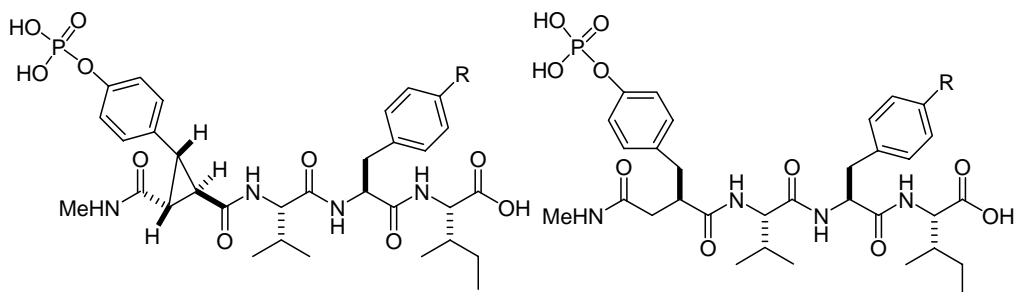


Table 1.05: Thermodynamic binding parameter for Src-SH2 mutant ligands.¹²¹

compounds	K_a (M^{-1})	ΔG (kcal mol ⁻¹)	ΔH (kcal mol ⁻¹)	ΔS (cal mol ⁻¹)
1.090	$3.7 (\pm 0.3) \times 10^6$	-9.95 ± 0.05	-3.47 ± 0.01	18.4 ± 0.2
1.091	$7.7 (\pm 1.6) \times 10^6$	-9.4 ± 0.1	-6.1 ± 0.10	11.0 ± 0.6
1.092	$5.5 (\pm 0.8) \times 10^6$	-7.8 ± 0.1	-1.10 ± 0.05	22.5 ± 0.5
1.093	$5.7 (\pm 1.2) \times 10^6$	-9.1 ± 0.1	-4.79 ± 0.04	14.8 ± 0.6
1.094	$3.0 (\pm 0.1) \times 10^6$	-8.82 ± 0.02	-4.69 ± 0.04	13.9 ± 0.2
1.095	$4.7 (\pm 0.1) \times 10^6$	-9.09 ± 0.01	-5.81 ± 0.05	11.0 ± 0.2
1.096	$5.0 (\pm 0.1) \times 10^6$	-9.13 ± 0.04	-6.09 ± 0.03	10.2 ± 0.1
1.097	$4.8 (\pm 0.2) \times 10^6$	-9.09 ± 0.02	-7.36 ± 0.06	5.9 ± 0.2
1.098	$3.8 (\pm 0.3) \times 10^6$	-8.96 ± 0.05	-3.75 ± 0.04	17.5 ± 0.3
1.099	$6.2 (\pm 0.2) \times 10^6$	-9.26 ± 0.02	-7.02 ± 0.03	7.5 ± 0.2
1.100	$4.1 (\pm 0.1) \times 10^6$	-9.01 ± 0.01	-3.05 ± 0.01	20.0 ± 0.1
1.101	$4.6 (\pm 0.1) \times 10^6$	-9.08 ± 0.02	-6.83 ± 0.08	7.6 ± 0.3

1.7 CONCLUSIONS

The conformational constraint hypothesis, which states that pre-organization of a flexible ligand will enhance binding affinity through reduction of the entropic penalty of binding, is often used in the design of novel ligands. Conformational constraints clearly have their place in drug discovery, as they can increase cell permeability,⁶³ increase selectivity.¹²²⁻¹²⁵ and increase stability. Furthermore, constraints can be used to determine the biologically active conformation of the ligand; however, in the case of HIV-1 protease inhibitors, flexible inhibitors are sometimes more accommodating to mutations of the protease.²³ The validity of the hypothesis is in question. Proper design of the constrained and control molecules is very important. Although not interested in testing the validity of this hypothesis, many research groups have neglected to make the

ideal control molecules to compare explicitly what effect introducing a constraint has on the system. Without the proper control molecules it is very difficult to assess the energetic advantage or disadvantage associated with conformational constraint introduction. In the few cases where such ideal controls are present, the enthalpy and entropy of binding are rarely measured, which makes evaluating the entropic effect of restricting ligand conformation impossible to determine. Any increase in binding cannot be arbitrarily attributed to a more favorable entropy of binding alone. In the few examples where the thermodynamic parameters of binding were determined, there is a balancing act between the entropic and enthalpic terms; any entropy gain is accompanied by an enthalpic penalty, resulting in ligand pairs that are equipotent (i.e. enthalpy-entropy compensation). In many examples, the binding energy difference between the ligand pairs is too small (< 5 -fold or $< 0.7 \text{ kcal mol}^{-1}$) to account for the $0.7 - 1.6 \text{ kcal mol}^{-1}$ stabilization per restricted rotor predicted by the theory for the introduction of a conformational constraint (see Section 1.1.3). In addition, it is not clear how many times the hypothesis has failed because examples that do not increase binding affinity remain unpublished.

Structure-based approaches have generally pursued a “lock and key” model to understand protein/receptor and ligand interactions; however, it is now known that the ligand and the receptor are not rigid when complexed.³² Residual thermal motions in the complex tend to reduce the enthalpy of binding as the atoms move away from their equilibrium positions, while the entropy associated with this residual motion is favorable. Thus, optimizing the design of a conformationally constrained ligand presents a dilemma.²⁵ Should this residual motion be taken advantage of by pre-organizing the ligand only enough to allow for this motion? Or should it be made as inflexible as possible, in order to optimize the enthalpic interactions with the binding site? The

importance of dynamics to binding affinity between a ligand and a protein has never been addressed.

Twenty five years after its introduction into the literature, the legitimacy of conformational constraint theory is under question. Applications of the pre-organization theory could be based solely on chance. In some studies affinity is enhanced with the introduction of a conformational constraint, while in other cases affinity is not changed. Additionally, sometimes entropic advantage is associated with the pre-organization and other times there is not. Scientists should demand and strive to understand what is really occurring rather than relying on luck. The proper experiments required to fully examine and truly validate or invalidate this pre-organization theory need to be designed and implemented.

Chapter 2. Cyclopropane-Derived Pseudopeptides for the Grb2-SH2 Domain

2.1 INTRODUCTION

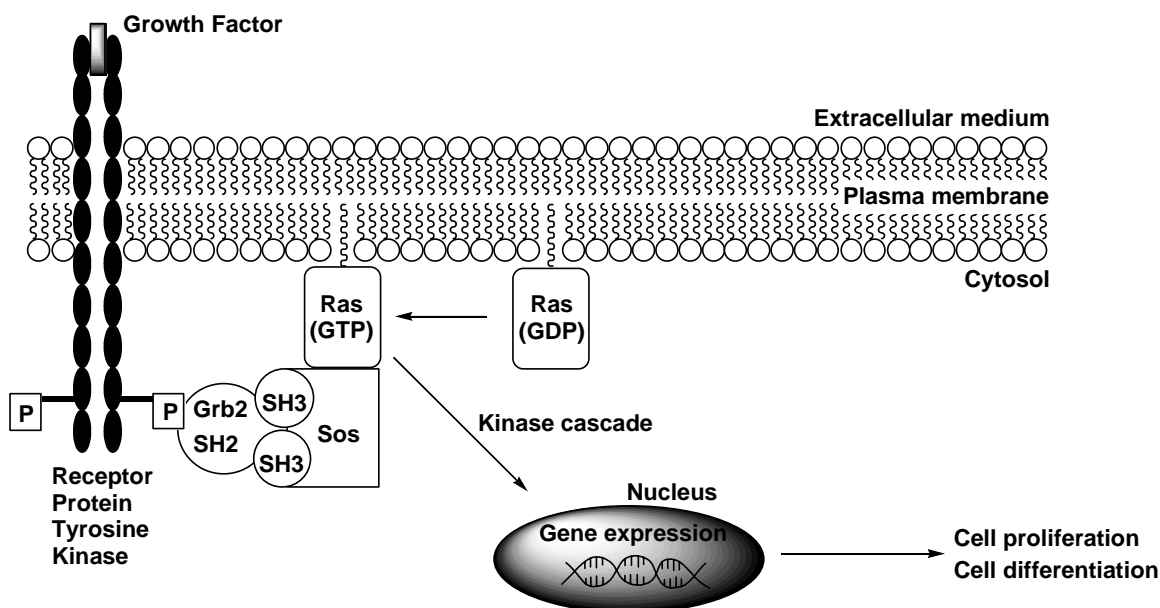
Previous work in the Martin group has established that ligand preorganization does not necessarily lead to higher affinity binding, even though $\Delta S_{\text{binding}}$ is more favorable. In order to further probe the entropic impact of ligand rigidification, we set out to evaluate a different biological system. It was important to identify a system that was structurally well characterized. Furthermore, it was essential that replacement of an amino acid residue with a cyclopropane would not eliminate or modify interactions with the target protein. We also wanted a system where no conformational change of the protein occurred upon ligand complexation, since this type of change might complicate interpretation of the ITC measurements. In addition, a protein that could be used to evaluate the ability of *cis*-cyclopropanes to stabilize a β -turn was of interest. We thus identified the SH2 domain of Grb2 (Grb2-SH2) as a perfect system to continue our evaluation of the energetic and structural consequences of introducing a cyclopropane conformational constraint into a peptide ligand.

2.1.1 The Grb2-SH2 Domain

The growth factor receptor binding protein 2 (Grb2) is an essential intracellular adaptor protein involved in signal transduction cascades inside mammalian cells. The protein itself is devoid of intrinsic enzyme activity.¹²⁶ Grb2 contains a Src homology region 2 (SH2 domain), that is flanked by two Src homology region 3 (SH3) domains on each side. SH2 domains are conserved sequences of approximately 100 amino acids found in various signaling molecules. In unstimulated cells, Grb2 is located in the cytosol complexed with Son of sevenless (Sos) protein through Grb2-SH3 domains that

bind to proline-rich sequences in Sos. When growth factors bind (e.g. epidermal growth factor a 6-kD polypeptide that stimulates the growth of epidermal and epithelial cells¹²⁷) to the extracellular domain of receptor tyrosine kinases, the kinases become activated resulting in autophosphorylation of specific tyrosine residues in the intracellular domain (Figure 2.1).¹²⁸ Grb2 then interacts through its SH2 domain with the phosphorylated residue by recognizing the sequence pTyr-X-Asn-X, wherein X can be almost any residue. The interaction between the Grb2-SH2 domain and a phosphorylated receptor sequence leads to the translocation of the cytoplasmic Grb2-Sos complex to the cell membrane, thus bringing Sos into the vicinity of membrane anchored Ras, a nucleotide exchange factor. Sos can promote the activation of Ras by exchanging Ras bound GDP for GTP. This activation enables a cascade of further signals to the cell nucleus through a series of kinases, eventually resulting in gene expression that governs cell proliferation and differentiation. Importantly, mutations of this Ras pathway have been linked to cancer.¹²⁷

Figure 2.1: Cartoon of the Ras pathway.



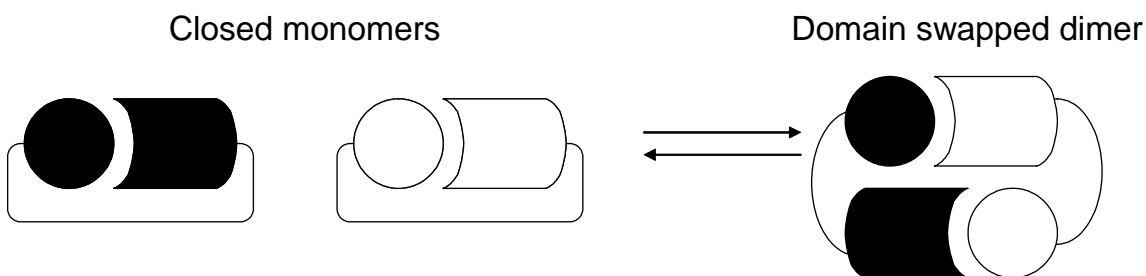
Many X-ray crystal structures of the Grb2-SH2 domain in both bound and unbound forms have been reported.¹²⁹⁻¹³⁴ There are also a number of NMR solution structures of complexes of Grb2-SH2 with peptide ligands.¹³⁵⁻¹³⁸ The crystal structure of the Grb2-SH2 domain complexed with the heptapeptide H₂N-Lys-Pro-Phe-pTyr-Val-Asn-Val-NH₂ was solved in 1996 at 2.1 Å resolution.¹³⁰ The positions of the ligand are labeled relative to the pTyr residue with the Val residue being the pY+1 position and Asn being the pY+2 position. The Grb2-SH2 domain is unique relative to all other SH2 domains because the SH2 domain of Grb2 contains a tryptophan residue (Trp121) that closes the pY+3 (three amino acid residues down from the pTyr residue on the peptide ligand) specificity pocket that is available in other SH2 domains such as Lck and Src.¹³⁰ By blocking this pocket, the backbone of the ligand is forced to change direction after residue pY+1 (one amino acid residue down from the pTyr residue of the peptide ligand), thus adopting a β -turn centered on this residue. Interestingly, the T215W mutant of the

Src-SH2 domain has been crystallized in complex with a dodecapeptide in which the ligand adopts a β -turn binding very similar to that required for a peptide ligand to bind to the Grb2-SH2.¹³⁹

The Grb2-SH2 domain can exist as a domain swapped dimer with the point of rotation at Trp121.^{131,134} A domain swapped dimer is formed when a globular domain of one protein molecule is intertwined with an identical protein chain of another molecule. The swapped domain protein environment is essentially identical to that of the same domain in the protein monomer (Figure 2.2).¹⁴⁰ For the Grb2-SH2 domain the swapping takes place at residues 121-123, with Trp121 located on the *N*-terminus of the hinge loop.¹³¹ Domain swapping is commonly found in the literature, and x-ray structures of dimers and monomers both complexed with and without ligand have been solved for the Grb2-SH2 domain.^{131,134}

Pure dimer and monomer of Grb2-SH2 can be isolated using gel filtration, and the dimer can be converted to monomer by heating, adding organic solvents, or by lowering the pH of the buffer.¹³¹ However, incubation of purified monomer or dimer (concentration <10 mg/mL, pH 7.0 and 4, 25 and 37 °C) did not result in interconversion of the two forms. Thus, the energy barrier for dimer-monomer conversion is rather high, and the monomer or dimer is stable under mild conditions. Importantly, ITC measurements using the monomer and dimer Grb2-SH2 resulted in equivalent binding measurements.¹³¹ Glutathion transferase (GST) fusion proteins are commonly employed to purify the Grb2-SH2 domain, and GST has a tendency to induce dimerization of the protein partner.¹³⁴ Hence, we will avoid using GST fusion proteins in our expression and purification of Grb2-SH2.

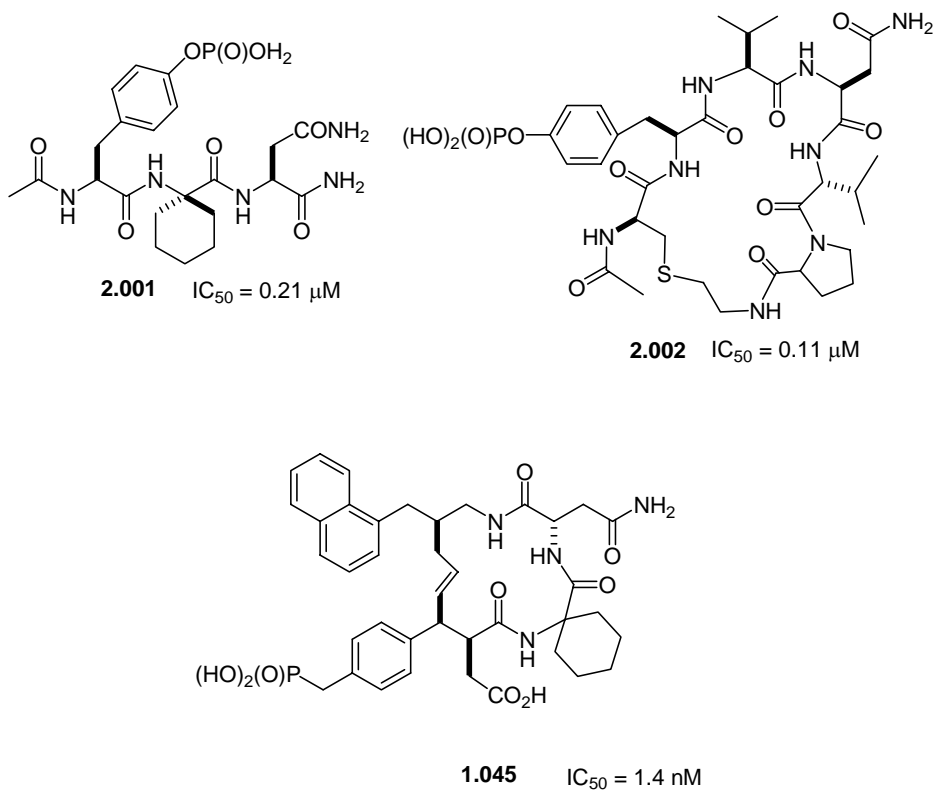
Figure 2.2: Cartoon of domain swapping.



2.1.2 Ligands for the Grb2-SH2 Domain

Several research groups have reported the synthesis of ligands for the Grb2-SH2 domain.¹²⁸ Their work suggests that there is considerable flexibility in the structure of the group at the pY+1 position. For example α,α -disubstituted cyclic α -amino acids were used to stabilize the β -turn conformation at pY+1, and the most potent ligand **2.001** had a cyclohexyl group at this site and exhibited an IC_{50} of 0.21 μ M (Figure 2.3).¹⁴¹ Many macrocycles have also been designed to stabilize the β -turn found in the ligand (see chapter 1). For example, in **2.002** a backbone to backbone macrocycle was prepared as a ligand for Grb2-SH2 domain with an IC_{50} of 0.11 μ M.¹²⁹ The crystal structure of the macrocycle bound to the Grb2-SH2 domain clearly showed the β -turn conformation at the pY+1 position in the ligand and the binding interaction for the pTyr-Val-Asn sequence was identical to that observed in the corresponding linear peptide (NH₂-Lys-Pro-Phe-pTyr-Val-Asn-Val-Glu-Phe). One of the most potent Grb2-SH2 antagonists **1.045** also contains a macrocycle. Some of the more potent Grb2-SH2 antagonists along with their biological data are shown in Figure 2.3.

Figure 2.3: Some of the most potent Grb2-SH2 domain antagonists to date.^{91,129,134,141,142}



In most studies on binding affinity of ligands to the Grb2-SH2 domain only IC_{50} values are reported. However, ITC can provide the complete thermodynamic profile, including entropy, for ligand and protein binding interactions. ITC has been used previously to determine the thermodynamic parameters for the binding of different Ala containing peptides to the Grb2-SH2.⁵³

2.2 DESIGN OF CYCLOPROPANE-CONTAINING LIGANDS FOR GRB2-SH2 DOMAIN

The Martin group has recently determined the energetic parameters for the binding of ligands with *trans*-cyclopropane phosphotyrosine replacements **1.086** and **1.088** binding to the Src-SH2 domain (see chapter 1). The flexible analogues **1.087** and

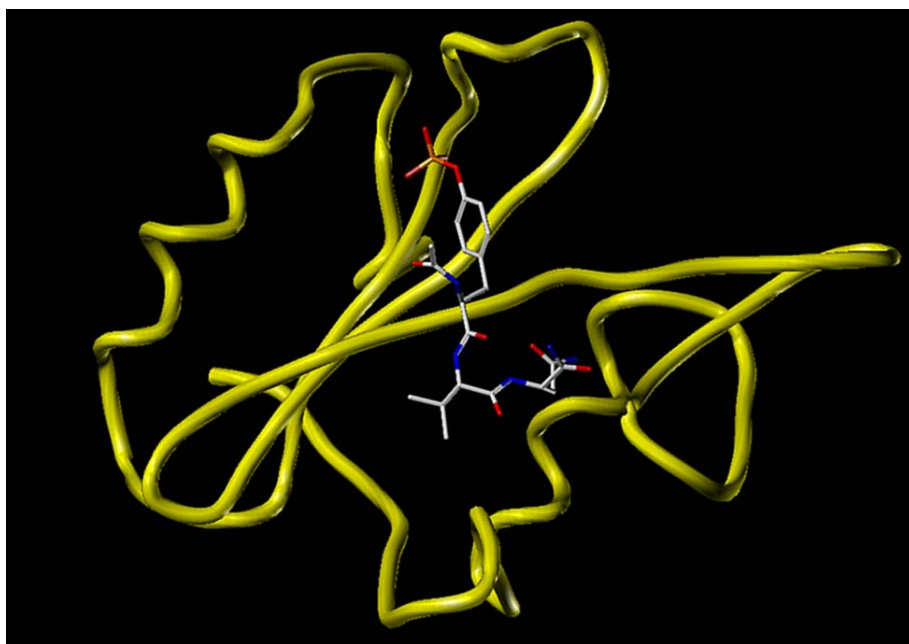
1.089 served as controls in order to determine the effect of introducing conformational constraints upon the binding energetics. The enthalpic and entropic consequences of using cyclopropane replacements at the pTyr residue of pTyr-Glu-Glu-Ile were evaluated employing ITC. In comparing the constrained cyclopropanes to the flexible control, there was an entropic advantage associated with introducing the cyclopropane but this entropic gain was accompanied by a loss in enthalpy resulting from enthalpy-entropy compensation. There was no net difference in the overall binding energy ($\Delta\Delta G_{\text{binding}}$) between the cyclopropane and control ligands. Further discussion about enthalpy-entropy compensation can be found in Section 1.1. Structural studies once again showed the ability of the *trans*-cyclopropane replacement to stabilize the extended backbone conformation.¹⁰⁵

While the data obtained in these studies supports the notion that incorporating a conformational constraint in a ligand can lead to an entropic advantage to the binding, whether or not this is a general phenomenon is still undetermined. In addition, the use of *cis*-cyclopropane replacements has not yet been established to stabilize a β -turn. We hypothesized that *cis*-cyclopropane replacements would conformationally stabilize reverse turns in pseudopeptides. We hoped to demonstrate a *cis*-cyclopropane's ability to stabilize a β -turn and use ITC to determine the thermodynamic parameters of binding (ΔH , ΔS , ΔG and K_d).

A crystal structure of Grb2-SH2 complexed with a ligand was recently solved that clearly shows the unique reverse turn at the pY+1 ligand H₂N-Lys-Pro-Phe-pTyr-Val-Asn-Val-NH₂ (Figure 2.4).¹³⁰ In the Grb2-SH2 domain, the extended conformation is sterically blocked by the Trp 121 side chain. In order to evaluate the viability of *cis*-cyclopropane replacements, Grb2-SH2 was chosen as a testing ground. Based on evaluating the crystal structure of ligands bound to both the Src-SH2 domain and the

Grb2-SH2 domain, the binding pocket for pTyr residue in the Grb-SH2 domain is virtually identical to the binding pocket in the Src-SH2 domain allowing us to use the same cyclopropane and flexible pTyr replacements that were used previously for the Src-SH2 domain.¹³⁰ Since we wanted to evaluate the pTyr cyclopropane replacements in a different system, we designed cyclopropane-containing pseudopeptide ligands for the Grb2-SH2 domain.

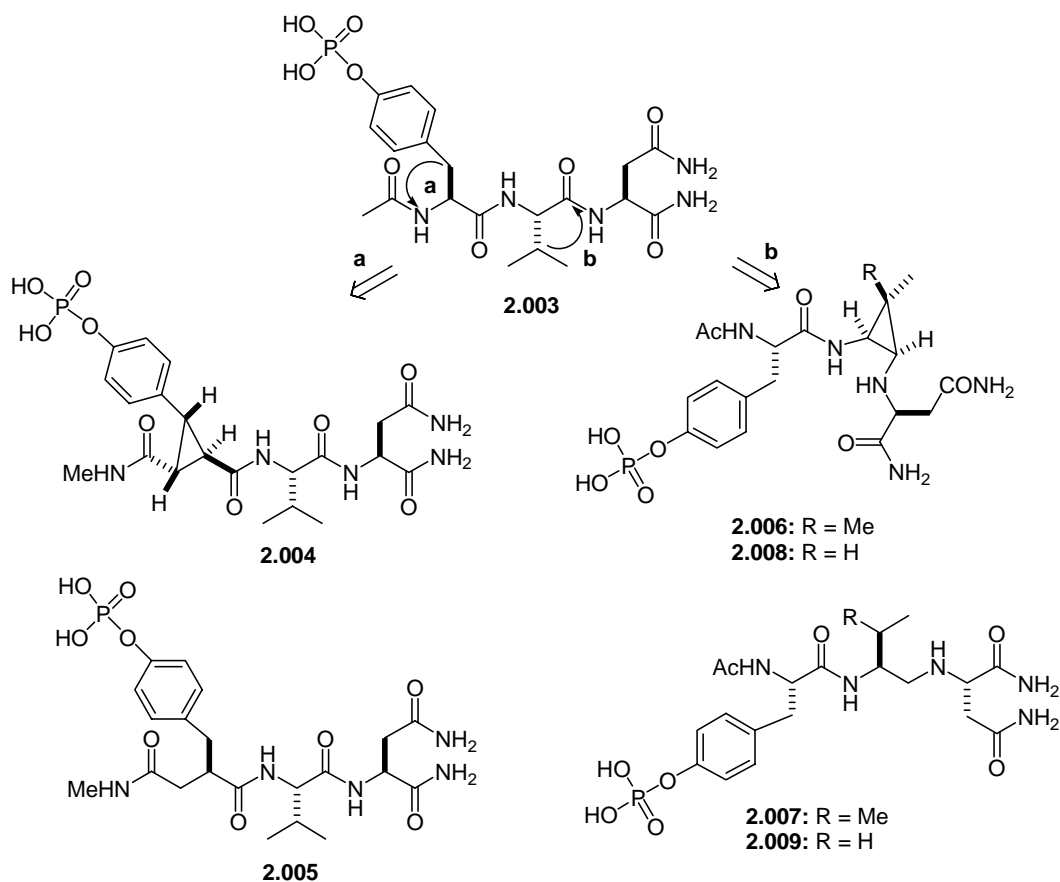
Figure 2.4: X-ray structure of peptide ligand H₂N-Lys-Pro-Phe-pTyr-Val-Asn-Val-NH₂ bound to Grb2-SH2 domain.¹³⁰



Compounds **2.004**, **2.005**, **2.006**, **2.007**, **2.008** and **2.009** were designed to enforce the structural features of the ligand **2.003** in the protein-ligand complex (Figure 2.5). The *trans*-cyclopropane in pseudopeptide **2.004** was derived from the native tripeptide **2.003** by replacing the nitrogen atom of the tyrosine residue in the native tripeptide with a

carbon atom and connecting this atom to the benzylic carbon of the Tyr side chain (mode **a**). The carbonyl carbon atom of the Val was similarly replaced giving *cis*-cyclopropane peptide mimics **2.006** and **2.008** (mode **b**). Flexible peptide replacements **2.005**, **2.007** and **2.009** containing the same number and type of heavy atoms (C, N, O and P) as their constrained counterparts, were synthesized as control molecules. Accordingly, these flexible replacements are excellent controls because they only differ from their cyclic analogues by an equivalent of H₂.

Figure 2.5: The design of the pYVN ligands.

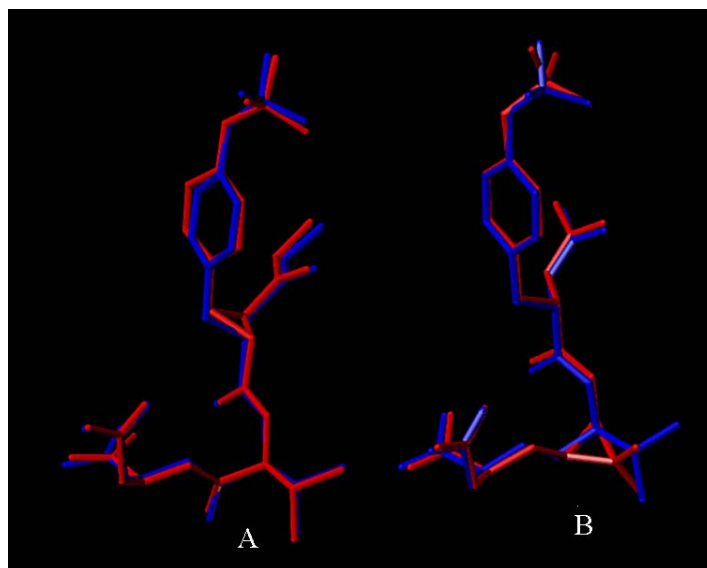


The tyrosine N-H that is removed in order to form **2.004** and **2.005** should not affect binding as the crystal structure of the Grb2-SH2 domain complexed with ligands reveals that there are no hydrogen bonds between the domain and this N-H of the ligand. Even so, the amide functionality can be maintained by moving the amide nitrogen over two carbons creating a reverse amide and helping to maintain any hydrogen bonds at this position. The tyrosine carbonyl carbon is within 3 Å of the side chain of Arg67 and is likely involved in a hydrogen bond interaction. In the mimics **2.006** and **2.008**, a basic amino residue replaces the amide bond at pY+1. The spatial geometry of the amino residue in the mimics is different than the geometry of the amide bond in the native peptide. Also, if protonated the amine replacement will have a different charge than the amide. Because neither the carbonyl oxygen nor the N-H of this mutated amide bond interact directly with the Grb2-SH2 domain, it seemed reasonable to assess the impact of an aminoethyl substitution in these systems, even though there was no literature precedent for an amino functional group at this residue of the ligand.

Modeling studies suggested that the cyclopropane ring in the pseudopeptides related to **2.004** and **2.006** can locally stabilize the extended and β -turn conformations, respectively. Energy minimization calculations of the cyclopropane-containing ligands were estimated using the Tripos Force field supplied by Sybyl 6.4 and overlaid with the crystal structure of **2.003** bound to the Grb2-SH2 domain (Figure 2.6).¹³⁰ In Figure 2.6A, **2.004** (shown in red) overlays nicely with the ligand bound to the SH2 domain (shown in blue). Examination of Figure 2.5B shows that the cyclopropane-containing mimic (shown in red) overlays well with the ligand bound to the protein (shown in blue). The *trans*-cyclopropane replacement **2.004** fixes an extended backbone conformation for the tyrosine residue similar to previous cyclopropane-containing ligands as shown in crystal structures of HIV-1 protease and Src-SH2 domain complexed with cyclopropane

derived pseudopeptides (see Chapter 1).^{104,105} We hypothesized that *cis*-cyclopropane replacement **2.006** would constrain the backbone in the desired β -turn conformation.

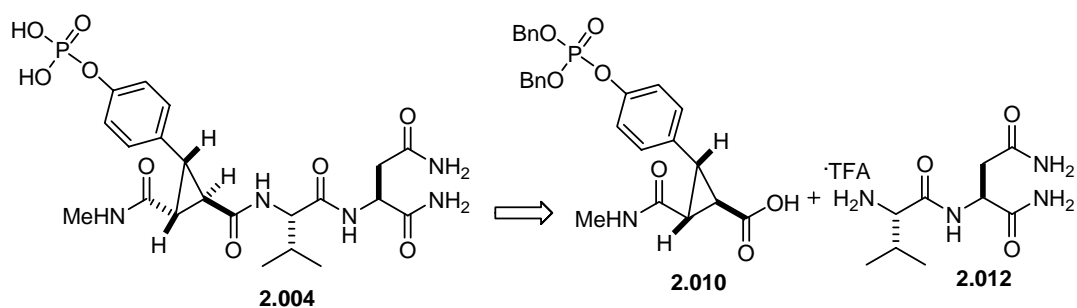
Figure 2.6: A: Overlay of mimics **2.004** (red) and **2.003** (blue) B: Overlay of mimics **2.006** (red) and **2.003** (blue).



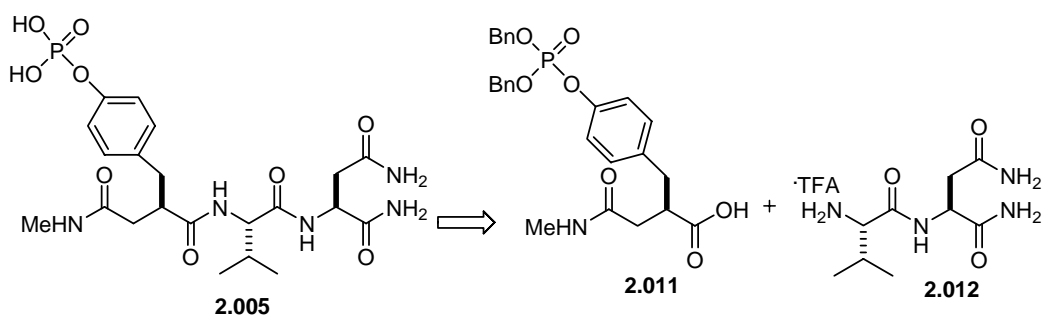
2.3 SYNTHESIS OF PY CYCLOPROPANE AND CONTROL LIGANDS

We envisioned that the pYVN mimics **2.004** and **2.005** could be readily prepared from coupling the tyrosine mimics **2.010** and **2.011** with the dipeptide **2.012** (Schemes 2.1 and 2.2), which had been previously synthesized in our laboratories.^{105,109,121} Since it was necessary to prepare these subunits, their synthesis will be briefly described.

Scheme 2.1



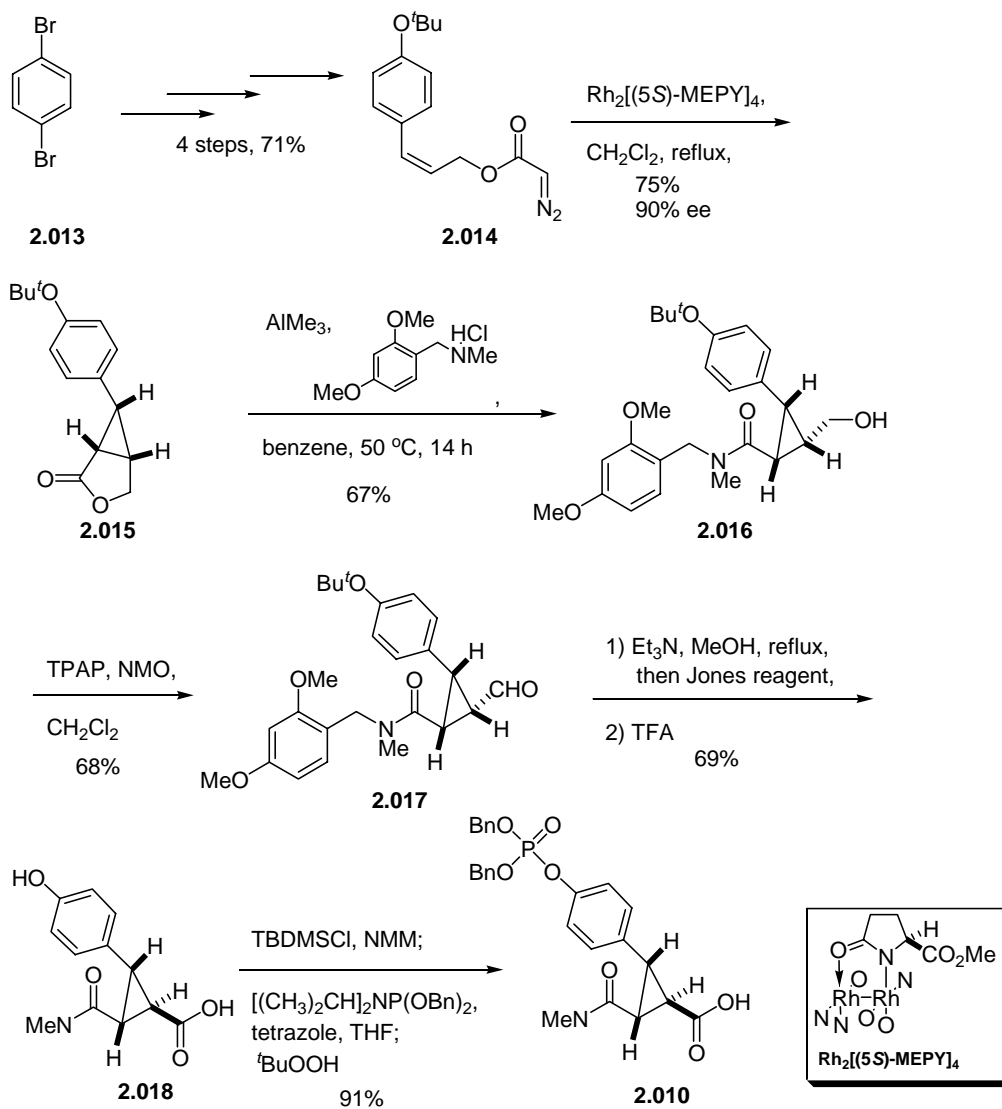
Scheme 2.2



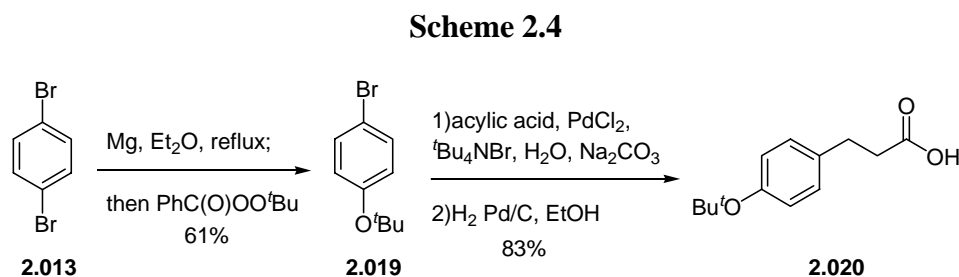
The synthesis of the cyclopropane carboxylic acid **2.010** began with the conversion of 1,4-dibromobenzene **2.013** into diazoester **2.014** in four steps using a previously described procedure (Scheme 2.3).¹⁰⁹ Asymmetric intramolecular cyclopropanation of the diazoester **2.014** using $\text{Rh}_2[(5S)\text{-MEPY}]_4$ as a catalyst gave the lactone **2.015** in 75% yield and 90% enantiomeric excess (ee). The lactone **2.015** was opened under Weinreb amidation conditions to provide the alcohol **2.016**. The alcohol **2.016** was then oxidized (TPAP, NMO), the resultant aldehyde was epimerized with Et_3N , and the *trans*-cyclopropane **2.017** was then oxidized to the acid. Acid catalyzed cleavage of the *tert*-butyl and dimethoxy benzyl protecting groups cleanly provided

2.018. Phosphorylation of **2.018** under standard conditions then gave the protected phosphotyrosine mimic **2.010** in 91% yield.¹⁴³

Scheme 2.3

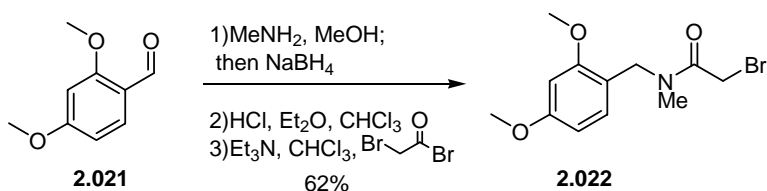


The synthesis of the phosphotyrosine flexible mimic acid **2.011** commenced with the conversion of 1,4-dibromobenzene (**2.013**) into the Grignard reagent and subsequent reaction with *tert*-butyl peroxybenzoic acid to give 4-*tert*-butoxybromobenzoate **2.018** in 61% overall yield (Scheme 2.4). Heck coupling of acrylic acid with **2.019** provided an α,β unsaturated acid that was reduced to give the propionic acid **2.020** in 83% yield over the two steps.¹⁴⁴ We experience problems reproducing this procedure. It was important to use pure H₂O for the Heck reaction, since using deionized H₂O from the tap resulted in poor yield, possibly due to some contamination in the deionized H₂O. The addition of the phase transfer catalyst Bu₄NBr improved both the yields and reaction times for this reaction (i.e. 65 to 83% and 30 h to 14 h).



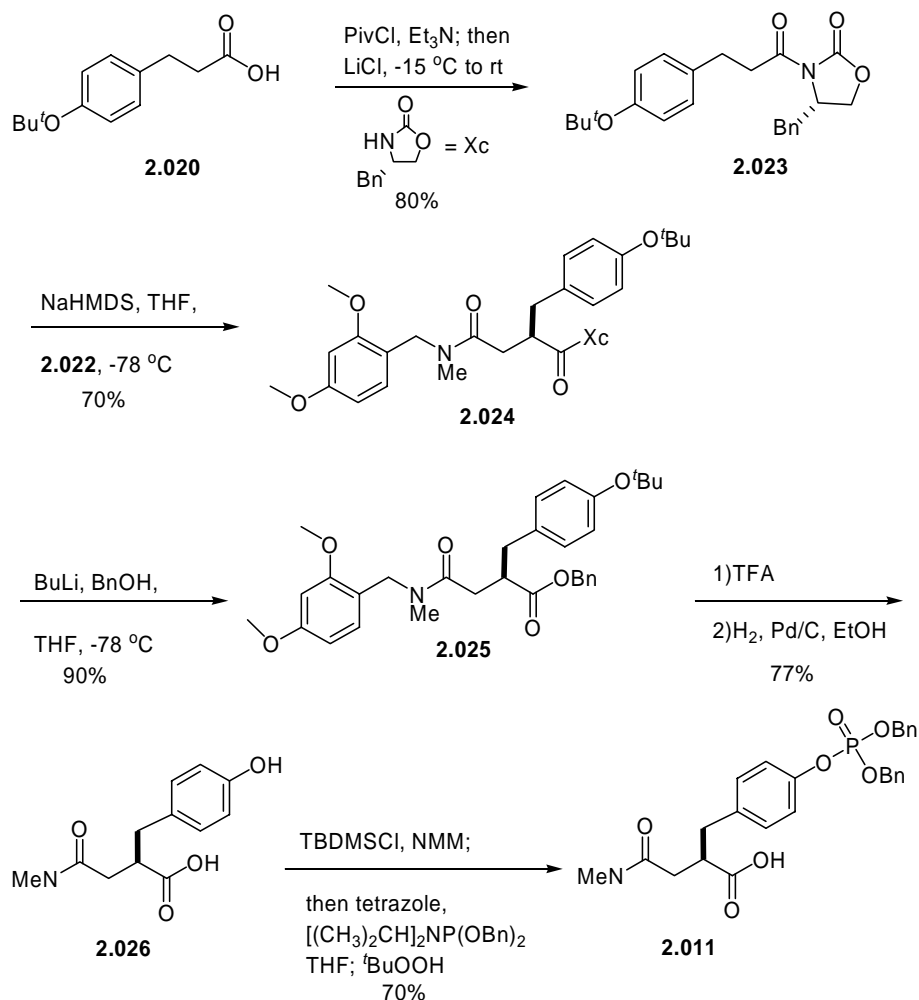
Bromoacetamide **2.022** was synthesized in 62% overall yield by reductive amination of 2,4-dimethoxybenzaldehyde **2.021** with methyl amine followed by acetylation with bromoacetyl bromide (Scheme 2.5).

Scheme 2.5



The oxazolidinone imide **2.023** was formed via the mixed anhydride of **2.020** (Scheme 2.6).¹⁴⁵ Deprotonation of **2.023** followed by treatment of the corresponding enolate with the bromoacetamide **2.022** gave **2.024** in 70% yield as a single enantiomer.¹²¹ When **2.024** was treated with the anion of benzyl alcohol, the benzyl ester **2.025** was isolated in 90% yield. Deprotection of **2.025** with TFA and hydrogenolysis produced **2.030** in 77% yield over the two steps. Finally, **2.030** was phosphorylated to provide the protected flexible phosphotyrosine mimic **2.011** (70% yield).

Scheme 2.6



With **2.010** and **2.011** in hand, attention was turned towards synthesizing the L-valinyl-L-asparaginyl-amide **2.012**. A number of amino acid coupling agents were examined to couple Boc-Val-OH **2.027** with Asn-NH₂ **2.028** (Scheme 2.7). The amine moieties in amino acids Ile and Val are somewhat hindered and thus racemization can be a side reaction from the coupling of these amines to activated carboxylic acids. When EDCI and HOBT were used to couple **2.027** and **2.028** the dipeptide **2.029** was obtained in 72% yield. Although use of HATU gave the best yield (82%) of **2.029**, its cost made

of the reaction (Figure 2.7).^{147,148} The clean protected tripeptide underwent hydrogenolysis in EtOH:H₂O (1:1) to give the native tripeptide **2.003** in 89% yield (Scheme 2.8).

Scheme 2.8

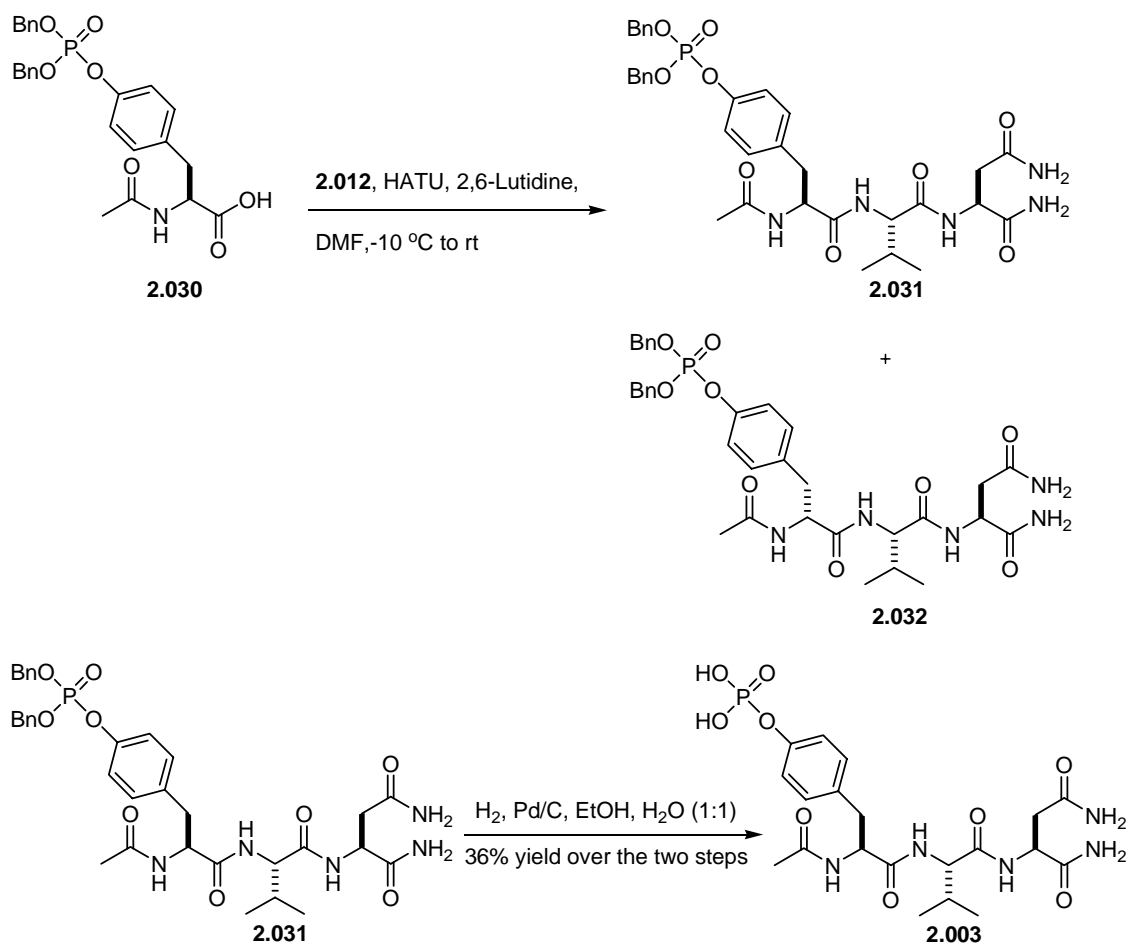
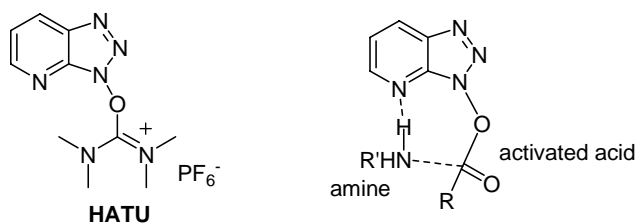
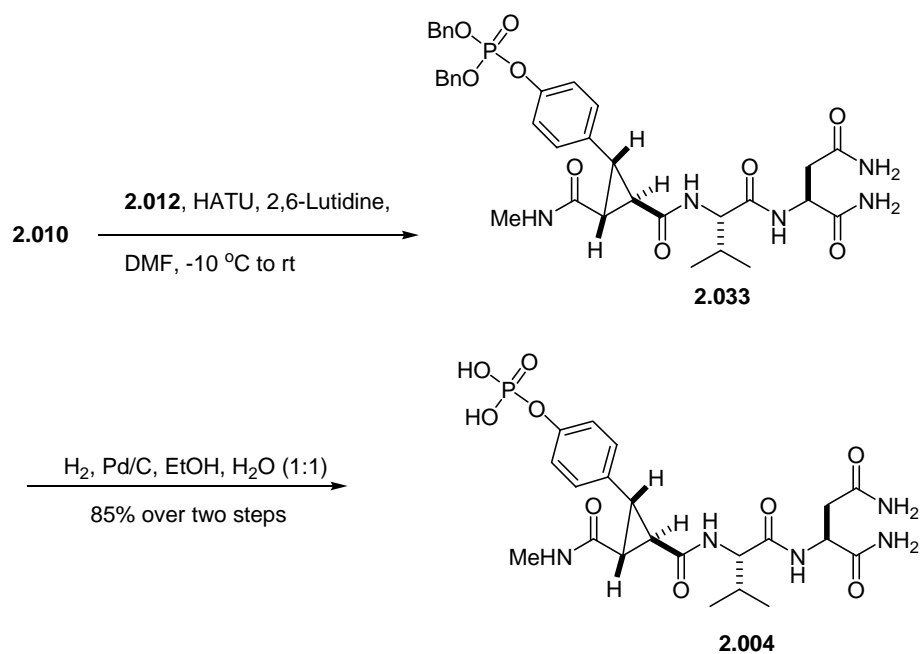


Figure 2.7: HATU can be used to increase the coupling reaction rate.

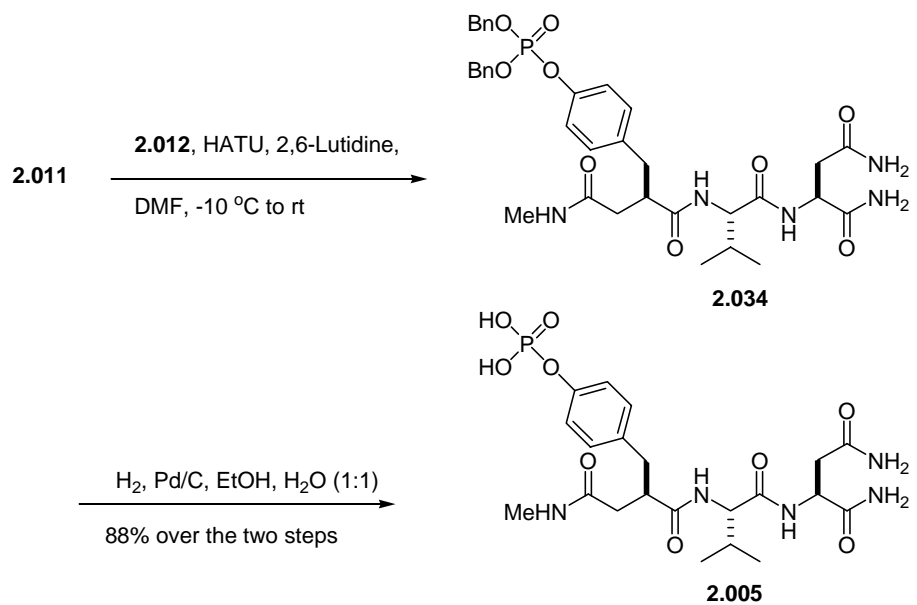


The pseudopeptides **2.004** and **2.005** were synthesized in good yields via coupling the flexible and constrained phosphotyrosine acid mimics **2.010** and **2.011** with the dipeptide **2.012** to provide the benzyl ester protected tripeptides **2.033** and **2.034** with no detectable epimerization (Scheme 2.9 and 2.10). The coupling reagent HATU was chosen over EDCI/HOBt because it worked well in the synthesis of the tripeptide **2.003**. Hydrogenolysis of the benzyl esters in **2.033** and **2.034** was plagued with problems due to their limited solubilities. Although the benzyl esters **2.033** and **2.034** were completely soluble in DMSO, the hydrogenolysis did not proceed in this solvent and starting material was recovered. The protected tripeptides **2.033** and **2.034** were partially soluble in acetonitrile:H₂O (1:1), but again the hydrogenolysis was not successful. Despite the limited solubility's of the protected tripeptides **2.033** and **2.034** in EtOH:H₂O (1:1), the hydrogenolysis proceeded in quantitative yield to give the desired tripeptides **2.004** and **2.005** after extended periods of time (12-18 h).

Scheme 2.9



Scheme 2.10



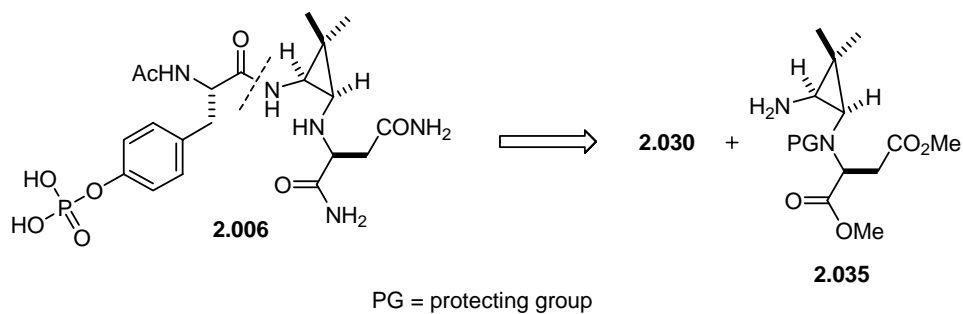
2.4 SYNTHESIS OF PY+1 CYCLOPROPANE AND CONTROL LIGANDS

With the pYVN-derived pseudopeptides **2.004** and **2.005** in hand, attention was turned toward the synthesis of **2.006** and **2.007**, which contain cyclopropane replacements at the pY+1 position.

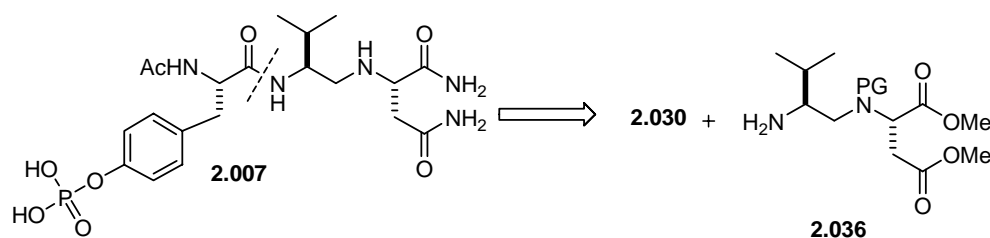
2.4.1 First Generation Synthesis of **2.006**

We envisioned the pseudopeptides **2.006** and **2.007** would arise from coupling **2.030** with the VN replacements **2.035** and **2.036** (Scheme 2.11 and 2.12). Conversion of the methyl ester functionalities to amides followed by hydrogenolysis would furnish the desired peptides **2.006** and **2.007**. Due to the limited solubilities of **2.033** and **2.034**, we decided to install the amide functionalities in **2.006** and **2.007** at a late stage in the synthesis.

Scheme 2.11

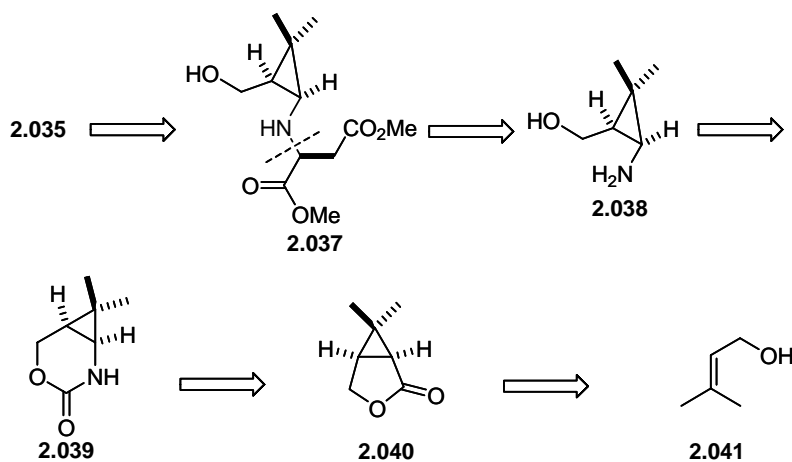


Scheme 2.12



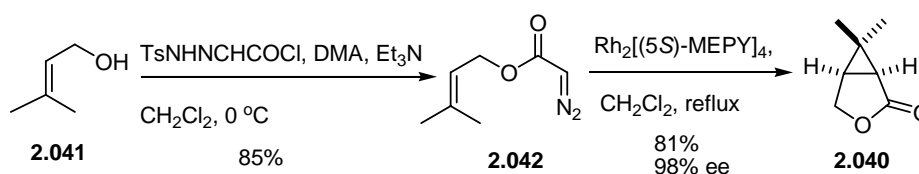
We envisioned that the amine **2.035** could be obtained through an oxidation of the alcohol moiety in **2.037** and subsequent Curtius rearrangement (Scheme 2.13). *N*-Alkylation of the amino alcohol **2.038**, which would arise from the cyclic urethane **2.039**, could provide **2.037**.^{149,150} Urethane **2.039** could come from the lactone **2.040** through a Curtius rearrangement following previous work done in our laboratories for the synthesis of MMP containing inhibitors.¹⁵⁰ The lactone **2.040** could be obtained through asymmetric cyclopropanation of the diazoester derived from 3-methyl-2-buten-1-ol **2.041**.

Scheme 2.13



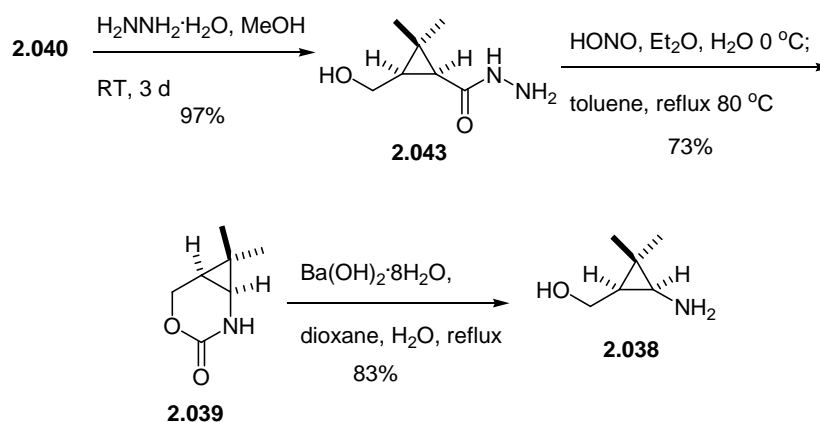
The synthesis of the constrained VN replacement **2.035** began with the $\text{Rh}_2[(5S)\text{-MEPY}]_4$ -catalyzed cyclopropanation of the diazoester **2.042** which was obtained in 85% yield from **2.041** in 85% yield, (Scheme 2.14).^{151,152} The asymmetric cyclopropanation proceeded in 81% yield to give the lactone **2.040** with 98% ee (determined by using ^1H NMR spectra with the chiral shift reagent $\text{Eu}(\text{hfc})_3$).^{104,113,153}

Scheme 2.14



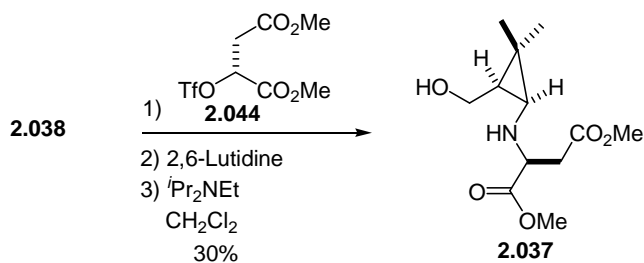
The lactone **2.040** was then opened using hydrazine to give the hydrazide **2.043** in 97% yield (Scheme 2.15). Treatment of **2.043** with nitrous acid gave an acyl azide that underwent a Curtius rearrangement that spontaneously cyclized to afford the cyclic urethane **2.039** in 73% overall yield. The amino alcohol **2.038** was then produced in 83% yield via base-induced hydrolysis of cyclic urethane **2.039**. $\text{Ba}(\text{OH})_2$ was determined to be the best reagent for this reaction based on previous work in our group.^{110,150,154}

Scheme 2.15



The L-asparaginyl-amide moiety was then introduced onto **2.038** by *N*-alkylation of the amino alcohol **2.038** with (*R*)-dimethylmalate triflate **2.044** in the presence of 2,6-lutidine and *i*Pr₂NEt to give the secondary amino alcohol **2.037** in 30% yield (Scheme 2.16).¹⁴⁹

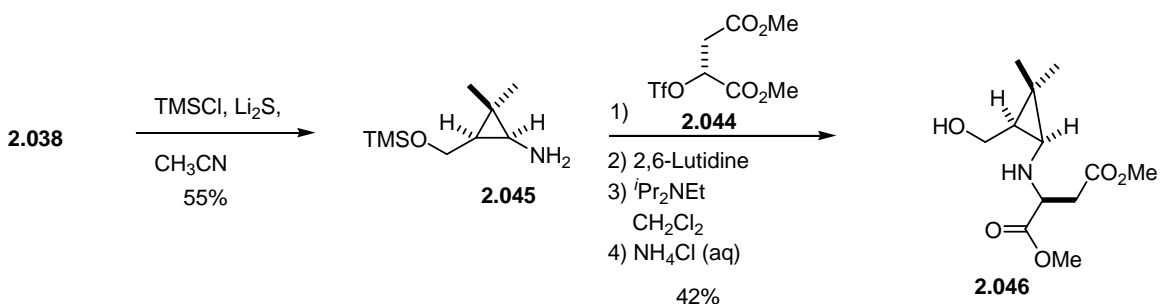
Scheme 2.16



Improving the yield of this *N*-alkylation step in the synthesis of the pseudopeptide **2.006** was crucial. It was hypothesized that protecting the seminucleophilic primary alcohol **2.038** might help the yield of the alkylation. Toward this end, the primary alcohol **2.038** was protected as its TMS ether using TMS-Cl and Li₂S to give ether **2.045** in 55%

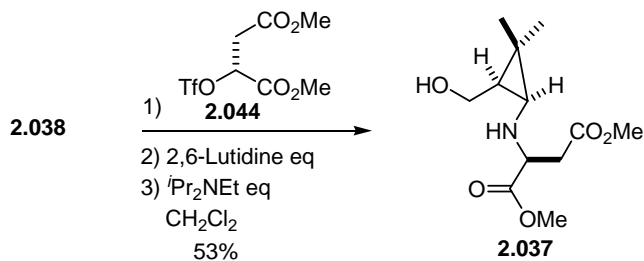
unoptimized yield (Scheme 2.17).¹⁵⁵ The amine **2.045** was alkylated with the triflate derivative of dimethylmalate **2.044** to give the secondary amine **2.037** in 42% yield. This yield is not a significant improvement over using the *N*-alkylation of free alcohol.

Scheme 2.17



Eventually, it was found that adding an extra equivalent of *i*Pr₂NEt to the amino alcohol **2.038** prior to reaction with the triflate **2.044** resulted in a reproducible yield of 53% for the secondary amine **2.037** (Scheme 2.18).¹⁵⁰

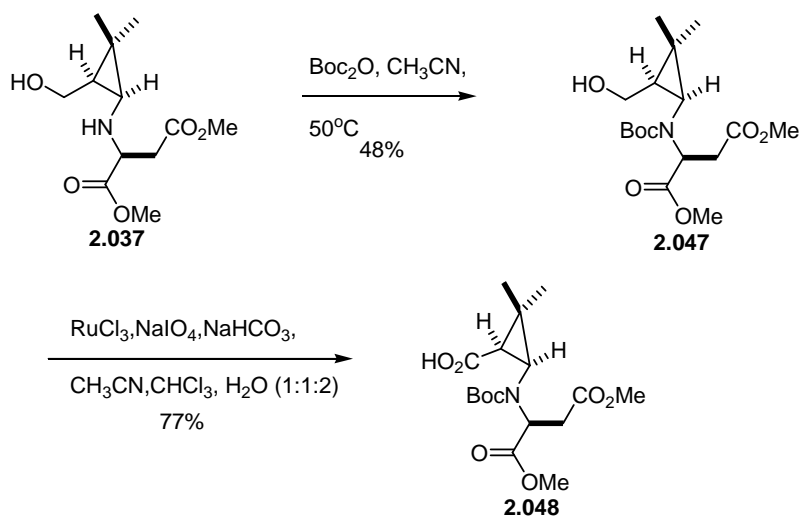
Scheme 2.18



The secondary amine moiety of **2.037** was then protected with di-*tert*-butyl dicarbonate to give **2.047** in 48% yield (Scheme 2.19). When a catalytic amount of DMAP was added to the reaction in an attempt to increase the yield, an unidentified product was obtained which had a ¹HNMR spectrum similar to starting material, but the hydroxy methyl peaks next to the cyclopropane ring moved downfield by 0.5 ppm. The

unidentified product also had a peak in the low resolution mass spectrum at 304 m/z corresponding that that of the product MS-56 (loss of t Bu group). I was not able to assign the structure of this product.

Scheme 2.19

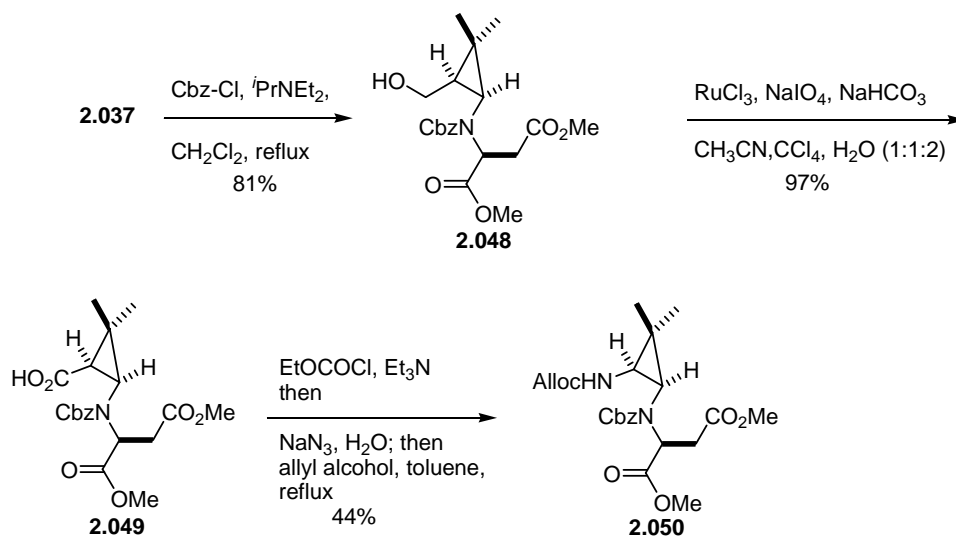


The next step involved the oxidation of alcohol **2.047**. Similar cyclopropane alcohols with Boc-protected amines have been reported to ring open under acid oxidation conditions.¹⁵⁴ Due to concern about the ring opening of the cyclopropane, non-acidic oxidation conditions were utilized. The valinyl-asparaginyl mimic acid **2.048** was produced in 77% yield by oxidation of **2.047** with $\text{RuCl}_3/\text{NaIO}_4$.

After discussion with fellow co-workers, the amine protecting group of **2.047** was changed from Boc to the benzyl carbamate (Cbz). The Cbz group can be removed in the same step as the deprotection of the phosphobenzyl esters required at the end of the synthesis. By switching amine protecting groups, we decrease the length of the synthesis by one step. We also hoped that the new protection step would be higher yielding. The

amino group of **2.037** was thus protected using Cbz-Cl and *i*Pr₂NEt to give **2.048** in 81% yield (Scheme 2.20). The alcohol moiety in **2.048** was then oxidized with RuCl₃/NaIO₄ providing the acid **2.049**. The yield of this oxidation was dramatically increased (from <5% to 97%) when CCl₄ was used as a co-solvent instead of CHCl₃.^{156,157} The acid group **2.049** was then converted to the Alloc-protected amine **2.050** in 44% yield using a modified Curtius reaction that proceeded via a mixed anhydride.

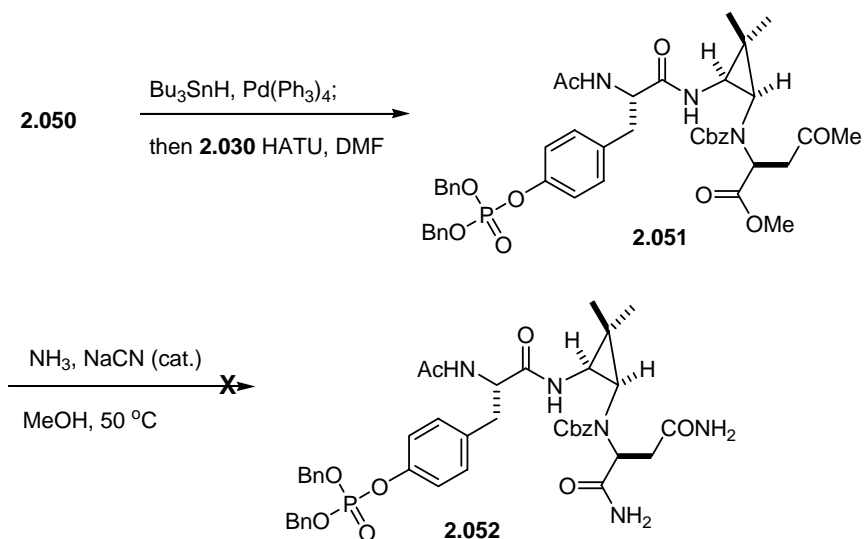
Scheme 2.20



The Alloc-carbamate of **2.050** was removed via exposure to Pd(PPh₃)₄ and Bu₃SnH, and the intermediate amine was coupled *in situ* with *N*-acetyl-p-Tyr **2.030** in the presence of HATU to give the protected tripeptide **2.051** (Scheme 2.21).^{110,158} Since we successfully used HATU in the amino acid couplings for pseudopeptides **2.031**, **2.033** and **2.034**, HATU was employed in this reaction to decrease any racemization that might occur during the reaction and increase the yield of the reaction. We then intended to

convert the methyl esters of **2.051** into amide groups using ammonia in MeOH to give **2.052**. However, reactions of **2.051** with ammonia in methanol with catalytic amount of NaCN were unsuccessful under a variety of conditions; mixtures of products were obtained, none of which had a signal in the ^{31}P NMR spectra.¹⁵⁹ It was difficult to determine the structure of any of these products due to the rotamers that were present in their ^1H NMR spectra. A hydrogenolysis was performed on this mixture to remove all protection groups with the intent of determining the components of the mixture, but this did not lead to identification of any of the products.

Scheme 2.21



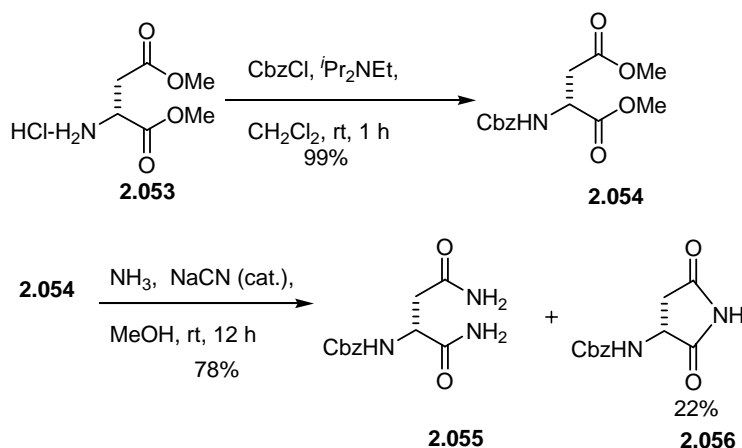
2.4.2 Second Generation Synthesis of the **2.006**

With **2.051** in hand only two steps would remain to complete the synthesis of **2.006**. However, it was necessary to address the problems associated with converting the methyl ester moieties into amides. A model system was examined in order to determine

the best reagents and conditions for converting the dimethyl ester array in **2.051** to the corresponding diamide.

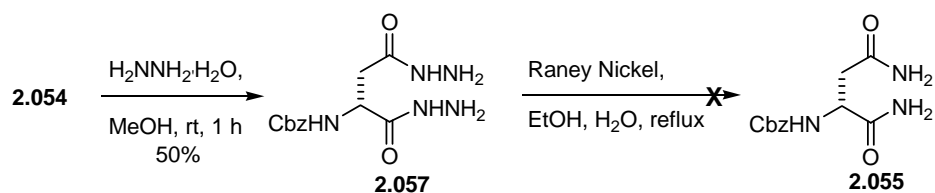
The amino group of L-aspartic acid dimethyl ester **2.053** was protected to give the carbamate **2.054** in 99% yield (Scheme 2.22). When **2.054** was exposed to NH_3 in MeOH in the presence of a catalytic amount of NaCN, the desired diamide **2.055** was obtained in 78% yield; the imide **2.056** was also isolated as a side product (22% yield). We suspected that it would not be easy to open this imide and form the desired diamide functionality.

Scheme 2.22

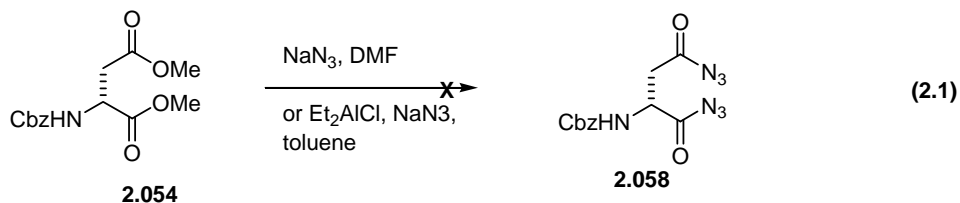


Hydrazine was also examined as a reagent for converting the ester group in **2.054** to an amide (Scheme 2.23). Although the dihydrazide **2.057** was obtained in 68% yield, attempts to cleave the dihydrazide N-N bond to give the desired **2.055** using Raney nickel were unsuccessful.¹⁶⁰ It was apparent by the ¹H NMR and mass spectra that the Cbz protecting group had been removed but the N-N bond was not reduced under these conditions.

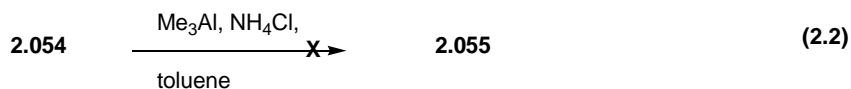
Scheme 2.23



We hoped that we could obtain the desired diamide groups by reduction of acid azides.^{161,162} However, attempts to convert the ester functionality of **2.054** to acid azides using NaN_3 or $\text{Et}_2\text{AlCl}/\text{NaN}_3$ were also unsuccessful (Equations 2.1).¹⁶³

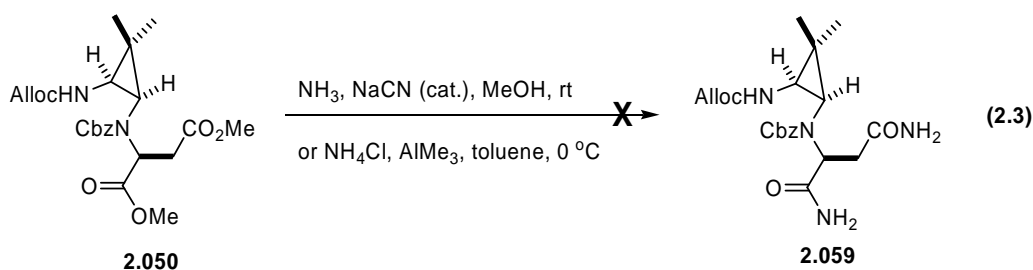


We also examined Weinreb's amidation conditions (Me_3Al , NH_4Cl) to convert methyl ester **2.054** to diamide **2.055** (Equation 2.2).^{164,165} However, these efforts led only to recovered starting material as evident from the ^1H NMR spectrum.

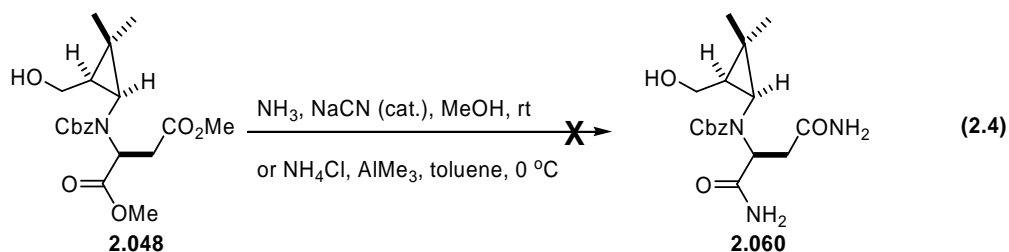


The preceding studies suggested that the conversion of esters into amides would best be accomplished with NH_3 in MeOH with cat. NaCN . However, as noted above, this did not work with the protected mimic **2.051**. We hypothesized that the

phosphobenzyl ester functionality might not be compatible with ammonia. So we decided to examine reaction of the Alloc amine **2.050** with NH_3 (Equation 2.3). However, treatment of **2.050** with NH_3 gave recovered starting material, a monoester-monoamide, and other unknown products; none of the desired **2.059** was obtained. Weinreb conditions were then employed on **2.050**, but this led only to the formation of a mixture of unidentifiable products and none of **2.059**.

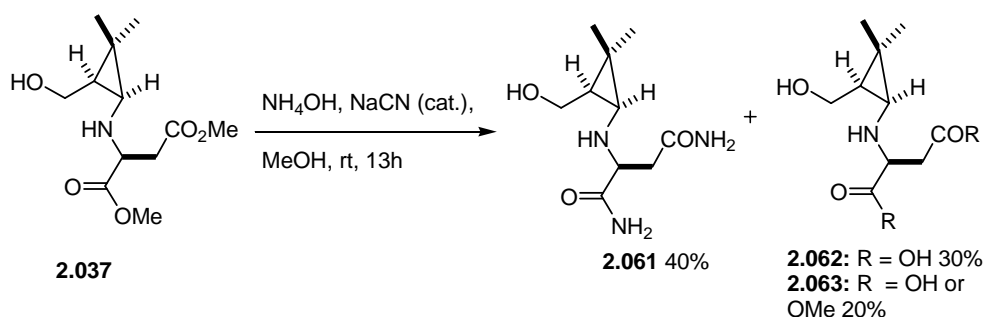


We then hypothesized that the alloc carbamate in **2.050** might not be compatible with NH_3 . Hence, we examined the reaction the *N*-Cbz carbamate **2.048** with NH_3 (Equation 2.4). When **2.048** was allowed to react with NH_3 in MeOH in the presence of catalytic NaCN, a product was recovered that showed no methyl esters in the ^1H NMR spectrum and a peak in the low resolution mass spectrum at 376 m/z (starting material MW = 393, product MW = 363). The same unidentified product was also formed when methyl ester **2.050** was exposed to Weinreb's conditions (Equation 2.4).



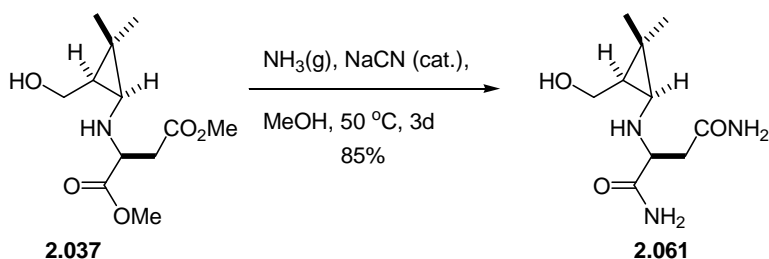
We suspected that the problems with our amidation attempts may have arisen from the presence of the Cbz moiety, since it has been reported that ammonia or ammonium hydroxide can react with this protecting group to give the unprotected amine.¹⁶⁶ As such, attention was then turned toward the free secondary amine **2.037** (Scheme 2.24). Gratifyingly, **2.037** was converted to the desired diamide **2.61** using ammonium hydroxide (NH₄OH) in MeOH in the presence of cat. NaCN to give the diamide **2.061** in 40% yield; the diacid **2.062** and mono acid **2.063** were also obtained as side products (30% and 20% yield, respectively).

Scheme 2.24



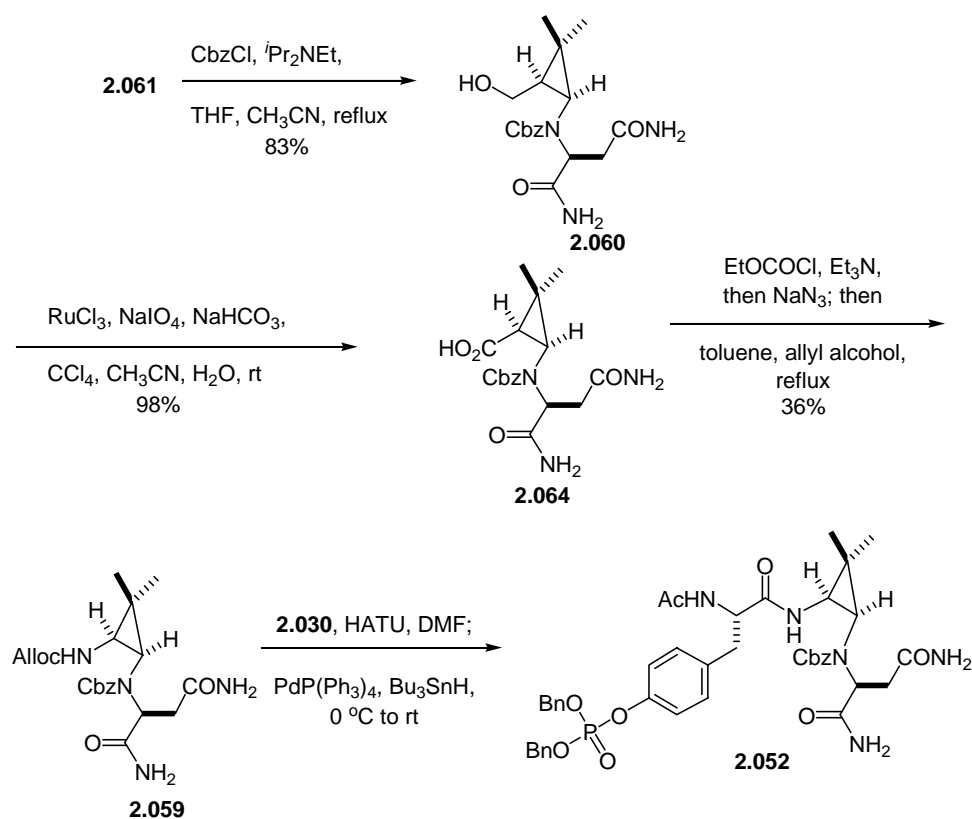
The yield of **2.061** was increased to 85% when **2.037** was treated with NH₃ in MeOH with a catalytic amount of NaCN (Scheme 2.25).

Scheme 2.25



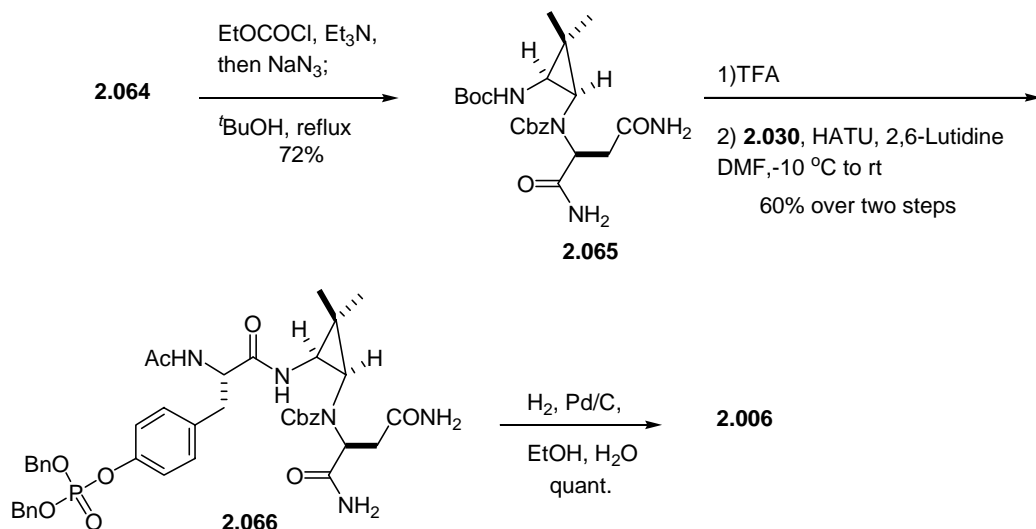
The amino group in **2.061** was then selectively protected using Cbz-Cl and $i\text{Pr}_2\text{NEt}$ to give the primary alcohol **2.060** in 83% yield (Scheme 2.26). Oxidation of the alcohol **2.060** with $\text{RuCl}_3/\text{NaIO}_4$ afforded the carboxylic acid **2.064** in 98% yield. The acid **2.064** was then subjected to a modified Curtius reaction as before to afford the Alloc-protected amine **2.059** (36% unoptimized yield). The Alloc-carbamate **2.059** was reacted with the *in situ* generated *N*-acetyl-p*Y **2.030** activated ester in the presence of $\text{Pd}(\text{PPh}_3)_4$ and Bu_3SnH to give **2.052**.¹⁵⁸ Unfortunately, it was not possible to obtain clean **2.052** by this procedure, and the yield of the reaction was poor (<10%). We therefore decided to pursue a different route.

Scheme 2.26



Due to the low yield in the coupling reaction, an analogue of **2.059** was pursued wherein the Alloc group was replaced with a Boc group, even though this would increase the length of the synthesis by one step. To this end, the Curtius rearrangement of acid **2.064** was performed as before to form an intermediate isocyanate that was trapped with t BuOH to provide **2.065** in 72% yield (Scheme 2.27). The cyclopropane **2.065** was deprotected with TFA to give the unstable free amine, that was immediately coupled with *N*-Ac-pTyr*-OH **2.030** in the presence of HATU to give a 60% yield of the desired protected tripeptide **2.066** as a single diastereomer. Global deprotection of **2.066** under hydrogenolysis conditions afforded the desired tripeptide **2.006** in quantitative yield.

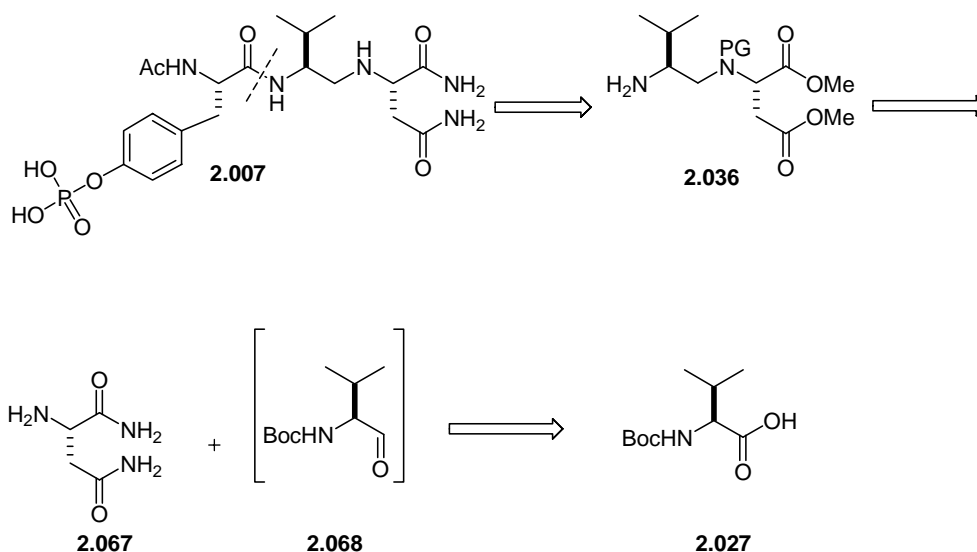
Scheme 2.27



2.4.3 First Generation Synthesis of 2.007

Attention was then turned toward the synthesis of the flexible control **2.007**. The dipeptide replacement **2.036** would be obtained by a reductive amination of **2.067** with aldehyde **2.068**, which would be obtained from Boc-N-Val-OH (**2.027**) (Scheme 2.28).

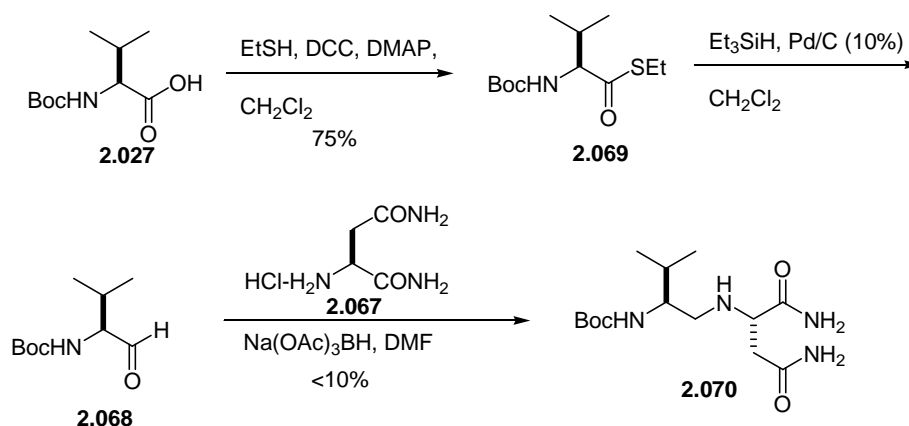
Scheme 2.28



PG = protecting group

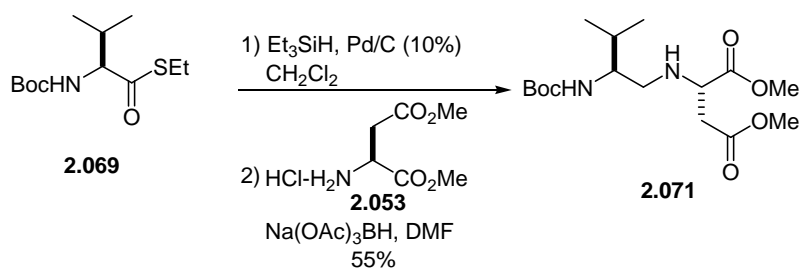
The synthesis of the flexible amine **2.036** was carried out by Thomas Sundberg and Angela Woodward, both undergraduate students under my direction. Boc-N-Val-OH **2.027** was first converted to the thioester **2.069** in 75% yield with DCC and EtSH (Scheme 2.29). The thioester **2.069** was then reduced to the aldehyde **2.068** according to the Fukuyama reduction protocol.^{167,168} Subsequent reductive amination of aldehyde **2.068** with asparagine amine hydrochloride (**2.067**) using Na(OAc)₃BH gave the secondary amine **2.070** in <10% yield.

Scheme 2.29



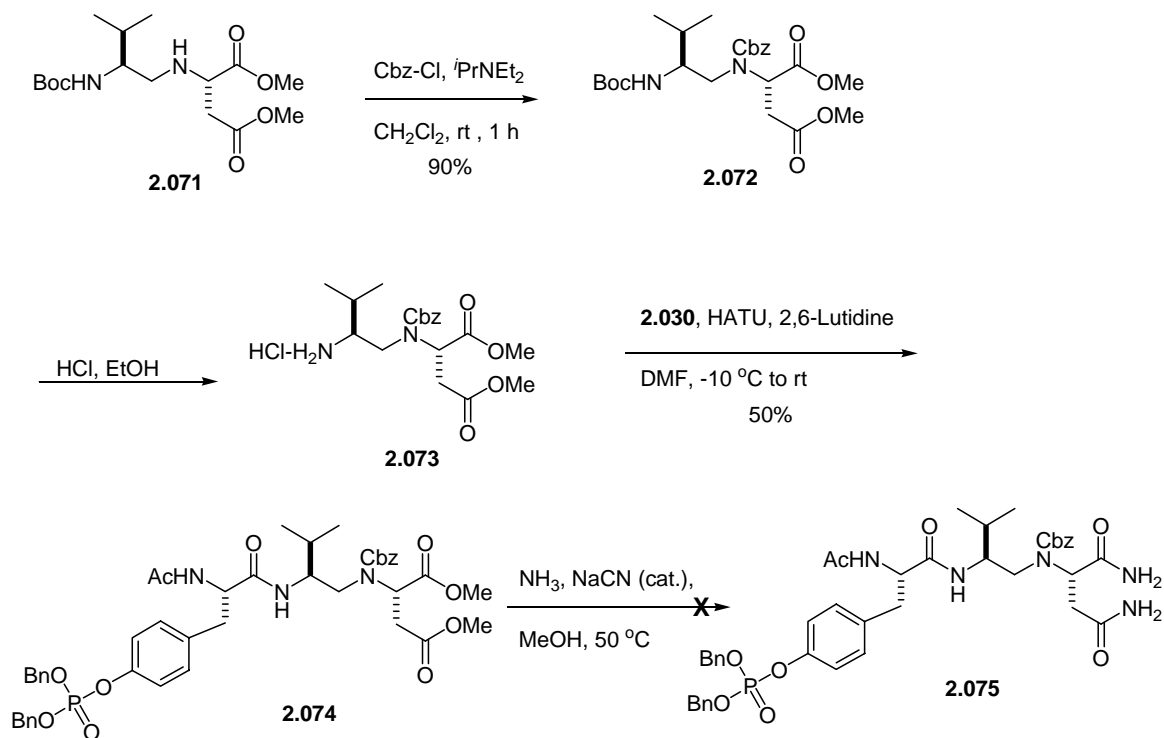
Because the low yield in this step was thought to arise from the limited solubility of **2.067**, L-aspartic acid dimethyl ester hydrochloride **2.053** was used instead of **2.067**. The reductive amination of thioester **2.069** with the L-aspartic acid dimethyl ester **2.053** gave the secondary amine **2.071** in 55% yield over two steps (Scheme 2.30). It has been reported that the reduction to the aldehyde and reductive amination can be done in the same pot,¹⁶⁸ but so far the one pot reaction gave only low yields (~20%) of product. Moreover, the aldehyde **2.068** is not stable and must to be treated immediately with the amine **2.053**. Attempts to isolate the aldehyde **2.068** using column chromatography resulted in partial racemization of the chiral center. Storage of the aldehyde **2.068** even for less than 1 h at $-20\text{ }^\circ\text{C}$ also resulted in partial racemization. This partial racemization was apparent from analysis of the ^1H NMR spectrum of the reductive amination product **2.071**. The peaks at δ 4.76 (*R*-H) and 4.52 (*S*-H) ppm represent the proton of each diastereomer on the carbon atom bearing the isopropyl group. The reaction sequence was performed on racemic **2.027** to establish that the two epimers could be distinguished in the ^1H NMR spectrum.

Scheme 2.30



The amine **2.071** was then protected using Cbz-Cl and *i*Pr₂NEt as the Cbz carbamate to give **2.072** in 90% yield. Finally, the Boc group was removed with HCl to give the free amine **2.073**. Amine **2.073** was coupled to N-Ac-pTyr*-OH **2.030** using HATU to give the protected pseudopeptide **2.074** (Scheme 2.31). Amidation of **2.074** with NH₃ and cat. NaCN was then examined. Analysis of the ¹H NMR for the crude reaction mixture showed loss of both dimethyl ester peaks, but low resolution mass spectrum analysis did not show peaks that corresponded to either starting material or the diamide product **2.075**. This same step also proved problematic in the synthesis of the cyclopropane-containing pseudopeptide **2.006**.

Scheme 2.31

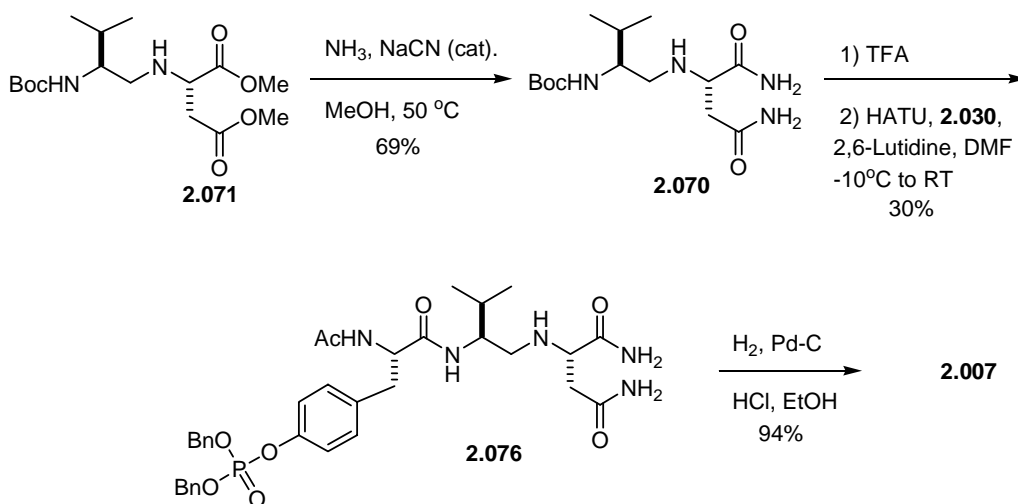


2.4.4 Second Generation Synthesis of **2.007**

The problems with the amination of **2.074** prevented the synthesis of the pY+1 mimic **2.007** according to the plan in Schemes 2.12 and 2.28. However, the solution that was developed for the synthesis of **2.006** could also be applied to solve the present problem. Dimethyl ester **2.071** was first treated with NH_3 and cat. amount of NaCN to give the desired diamide **2.070** in 80% yield (Scheme 2.32). We queried whether the protecting group for secondary amine in **2.070** was really essential, as this nitrogen seemed somewhat hindered and unlikely to react in the coupling reaction. In order to

evaluate this hypothesis, the *N*-Boc protected amine **2.070** was deprotected using TFA, and the resultant unstable free amine, which decomposed upon standing, was immediately coupled with *N*-Ac-pY*-OH **2.030** using HATU as the coupling reagent to give the desired protected tripeptide **2.076** in 30% overall yield. Global deprotection of **2.076** by hydrogenolysis proceeded in 94% yield with the addition of HCl. In the absence of HCl, the yield of **2.007** was only 18%. Most likely, the acid was needed to protonate the free amine and thus prevent the free amine from poisoning the Pd-catalyst.¹⁶⁹

Scheme 2.32

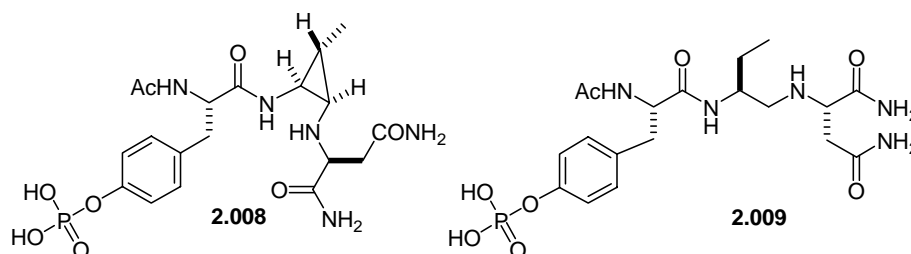


2.5 SYNTHESIS OF PY+1 SECOND GENERATION LIGANDS **2.008** AND **2.009**

As mentioned in Section 3.1, the ITC data indicated that the *cis*-cyclopropane mimic **2.006** interacts weakly ($K_a < 10^3$) with the Grb2-SH2 domain. On the other hand, the flexible control **2.007** does bind to the protein, albeit with approximately 10-fold lower affinity than pseudopeptides **2.003-2.005** (see Chapter 3). Because the control **2.007** does bind to the Grb2-SH2 domain, the amine functionality present in **2.006** and

2.007 is not the cause for the low affinity of **2.006**. The control **2.007** is flexible and can therefore readily adopt the conformation required for binding. We designed **2.006** predicting that it would be preorganized into the β -turn conformation. However, we presumed that the presence of the *gem*-dimethyl moiety on the cyclopropane ring of **2.006** might sterically prevent **2.006** from adopting the proper conformation for binding to the domain. To explore this possibility, we synthesized a *cis*-cyclopropane mimic containing only one methyl group **2.008** (Figure 2.8). The appropriate acyclic control of **2.008** is **2.009**.

Figure 2.8: Ligands **2.008** and **2.009**.

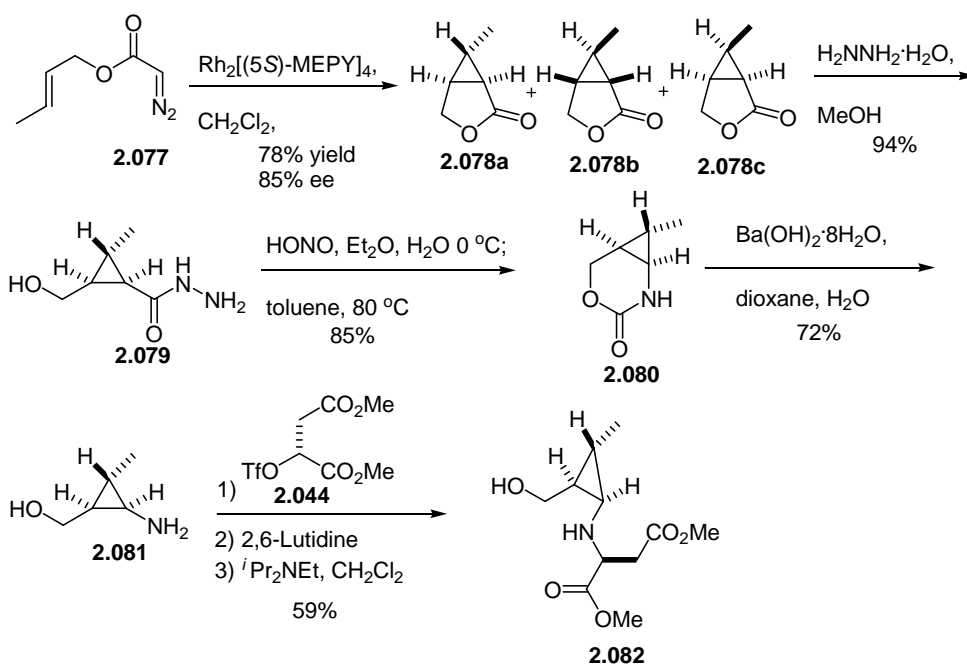


2.5.1 Synthesis of Mono-Methyl Cyclopropane **2.008**

The syntheses of **2.008** and **2.009** followed closely the syntheses of **2.006** and **2.007**. Crotyl alcohol was first transformed into the diazoester **2.077**, which was then subjected to an enantioselective cyclopropanation to give **2.078** (as a mixture of isomers **2.078a-c**) in 78% yield and 85% ee determined using ¹H NMR spectra with a chiral shift reagent in the (Scheme 2.33).^{104,113,153} Unfortunately the crotyl alcohol used to prepare **2.077** was only 90% *trans*, so **2.078c** was also produced in the reaction. In addition, the %ee for the cyclopropanation reaction was low and resulted in the formation of **2.078b**.

The major component of the mixture was the desired lactone **2.078a**. Using column chromatography, we were not able to separate **2.078a-c** at this time, so the mixture of isomers was carried on through the synthesis and separated at a later stage. For simplification only the desired isomer from the mixture is shown in the following schemes. The mixture of lactones **2.078** was converted to the hydrazides **2.079** (94% yield) upon reaction with H_2NNH_2 . Reaction of **2.079** with HONO gave an intermediate azide that underwent a Curtius rearrangement to give **2.080** in 85% yield. Base-induced hydrolysis of **2.080** in gave **2.081** in 72% yield. *N*-Alkylation of **2.081** with the triflate derived from dimethylmalate **2.044** gave the amino alcohol **2.082** in 59% yield.

Scheme 2.33

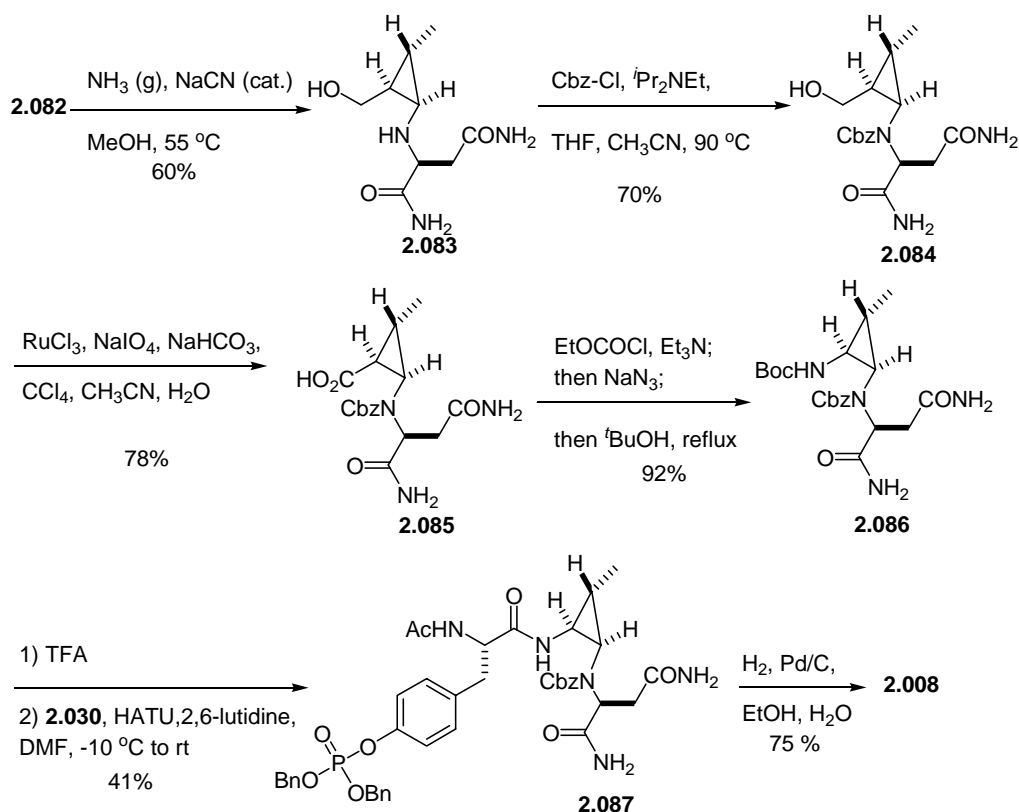


The diester groups of **2.082** was converted into the desired amide **2.083** in 60% yield using NH_3 in the presence of catalytic amounts of NaCN (Scheme 2.34). The

reaction was performed in a sealed tube at 55 °C and only took 24 h for completion. The secondary amine was then protected as its Cbz carbamate, providing **2.084** in 70% yield. Oxidation of the alcohol functionality in **2.084** gave an acid **2.085** as a mixture of isomers (7:3 ratio) in 78% yield. The isomers could now be separated using flash column chromatography. The mixture of isomers was not separable at any earlier stage as evident by TLC and HPLC analysis.

The pure acid **2.085** was transformed into the *N*-Boc carbamate **2.086** in 92% yield via Curtius rearrangement followed by trapping of the isocyanate intermediate. Removal of the carbamate protecting group with TFA gave an amine that was coupled with *N*-Ac-pY*-OH **2.030** under standard coupling conditions (HATU, 2,6-lutidine, DMF, -10 °C to rt) to provide the protected tripeptide **2.087** in 41% yield as a single diastereomer. Finally, the desired cyclopropane-containing ligand **2.008** was obtained in 75% yield by hydrogenolysis of the benzyl protecting groups of **2.087**.

Scheme 2.34



2.5.2 Synthesis of Reduced Abu Control Ligand 2.009

The flexible mimic **2.009** was designed as the control molecule of **2.008** for subsequent thermodynamic and structural evaluations. Under my direction Neda Nosrati, an undergraduate student, performed with the first two steps of the synthesis of ligand **2.009**. The synthesis of **2.009** began with converting 4-(*tert*-butoxycarbonylamino) butyric acid (**2.088**) into the thioester **2.089** in nearly quantitative yield (Scheme 2.35). The thioester was reduced to an aldehyde (Pd/C, Et₃SiH), which was immediately subjected to reductive amination in the presence of Na(OAc)₃BH to afford in 83% yield the desired amine **2.090** in 17:1 d.r. as determined by analysis of the

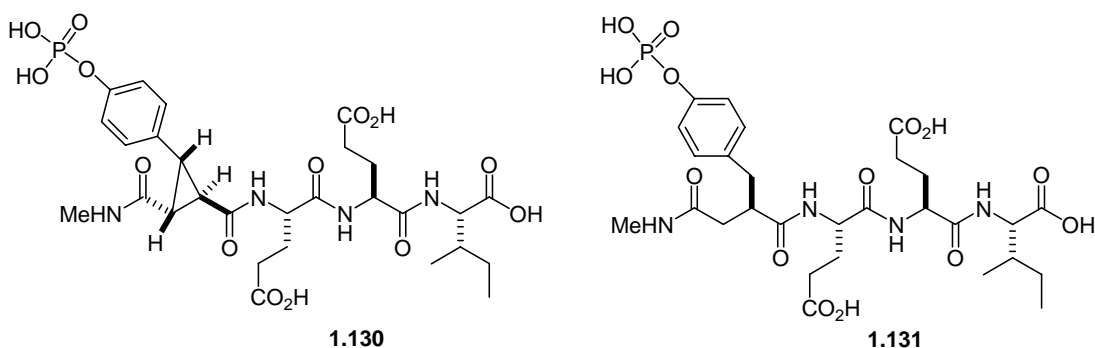
¹H NMR spectrum at 500 MHz (key ¹H NMR δ 4.56 and 4.52 ppm). When this reaction was carried out at room temperature, a mixture of diastereomers (7:1) was obtained resulting from epimerization of the intermediate aldehyde. However, if this reaction was carried out at 0 °C for 90 min, the ratio of diastereomers was improved to 17:1. At -78 °C the reaction was slow and did not proceed to completion. The reaction sequence was performed on racemic **2.088** to establish that the two epimers could be distinguished by analysis of the ¹H NMR spectrum. The ester groups of **2.090** were converted to amides using NH₃ with NaCN as before to provide **2.091** in 85% yield. The *N*-Boc-protecting group was removed, and the resultant amine was immediately coupled with N-Ac-pY*-OH **2.030** to furnish the flexible tripeptide **2.092** in 67% yield as a single diastereomer. Removal of the benzyl protecting groups on **2.092** via hydrogenolysis afforded the desired tripeptide mimic **2.009** in nearly quantitative yield.

reductive amination as the key step. The major obstacles in the syntheses of **2.006**, **2.007**, **2.008** and **2.009** were the conversion of the methyl esters to amides and the epimerization during the reductive amination and coupling reaction. In the synthetic route to these molecules, the amination step must precede further functionalization. Despite the length of the synthesis of pseudopeptide **2.006** and **2.008** enough material to carry out the ITC measurements was obtained. The next step is to evaluate the thermodynamic binding profile for these ligands. The energetics of binding of these ligands with the Grb2-SH2 domain were evaluated using ITC (Chapter 3). The synthetic steps explored in this chapter could be used to make future ligand for the Grb2-SH2 domain.

Chapter 3. The Thermodynamic and Structural Evaluation of Cyclopropane-Derived Pseudopeptides for Grb2-SH2 Domain

3.1 INTRODUCTION

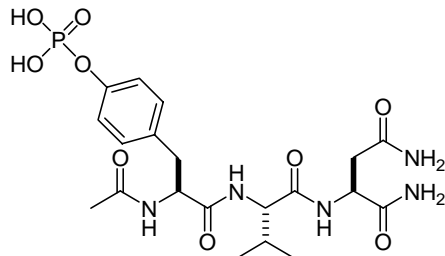
One area of research in the Martin group has been to examine the effect of introducing a cyclopropane ring into the phosphotyrosine (pY) moiety of ligands that bind to the Src-SH2 domain.^{105,121} The thermodynamic profiles of the cyclopropane-containing ligand **1.086** and its flexible analogue **1.087** binding to this protein domain were investigated using ITC (see Chapter 1 for more discussion). The ITC data established that the two molecules have similar binding affinities for the Src-SH2 domain. The cyclopropane-containing ligand **1.086** was found to have a greater entropic advantage over its flexible partner **1.087**. This entropic advantage was, however, accompanied by an enthalpic disadvantage, a ubiquitous phenomenon known as enthalpy-entropy compensation (see Chapter 1 for discussion). The balancing of entropy and enthalpy resulted in no net change in the overall binding affinity due to the introduction of a conformational constraint to the pY residue of the ligand. Structural data revealed that the cyclopropane-containing ligand **1.086** bound to the SH2 domain in a similar mode as a peptide ligand; however, obtaining an X-ray structure of the flexible control **1.087** bound to the Src-SH2 domain for comparison with the **1.086**/Src-SH2 complex has been elusive.



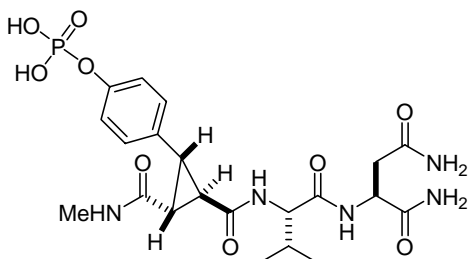
3.2 ISOTHERMAL MICROCALORIMETRY EVALUATIONS

We wanted to examine another system where we could introduce a cyclopropane ring into a peptide ligand in order to enforce the biologically active conformation of the ligand. Compounds **2.004** and **2.005** were thus prepared in order to examine the energetic consequences on binding caused by the introduction of a cyclopropane at the pY residue of ligands that bind to the Grb2-SH2 domain and to compare these results with the conclusions drawn from our Src-SH2 system (see Chapter 2 for syntheses of these ligands). In addition, we wanted to assess the effect of introducing a cyclopropane ring into a system that would allow us to evaluate the use of *cis*-cyclopropane constraints to stabilize peptide turned conformations. Pseudopeptides **2.006** and **2.007** were prepared in order to examine the energetic consequences on binding caused the introduction of a *cis*-cyclopropane at the pY+1 residue of the peptide that binds to the Grb2-SH2 domain. The thermodynamic profiles for binding of the cyclopropanes **2.004** and **2.006**, the flexible controls **2.005** and **2.007**, and peptide **2.003** to the Grb2-SH2 domain were determined using isothermal titration calorimetry (ITC). ITC provides an effective method to obtain K_d , and to determine stoichiometry and ΔH of binding in a single experiment. In a typical experiment, the ligand was titrated stepwise into a solution of protein at constant temperature. The heat generated during the ligand-protein complex

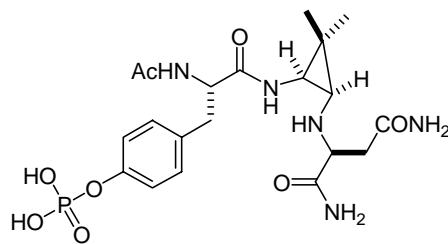
formation was recorded.^{11,53,54} K_a , stoichiometry and ΔH of binding were obtained from the binding curve, and these values were used to calculate ΔG and ΔS of binding. In order to diminish heat exchange due to the differences between the solutions of ligand and protein, the ligand was dissolved in final dialysate from the Grb2-SH2 sample purification. Each experiment was repeated at least three times, and the values were averaged. A blank of ligand titrated into buffer solution was also obtained. The values were subtracted from each ligand into protein titration to account for any heat of dilution during the experiment.



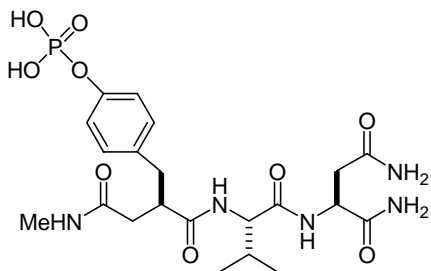
2.003



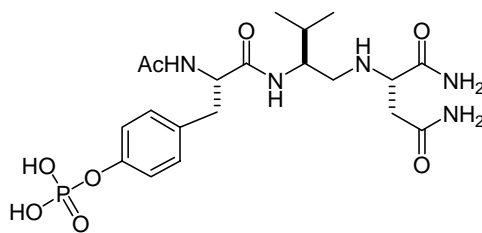
2.004



2.006



2.005



2.007

3.2.1 pY Pseudopeptides

The thermodynamic profiles for compounds **2.003**, **2.004** and **2.005** are summarized in Table 3.1. By examining the ΔG for each ligand, one can see that all three ligands bind with similar overall affinities to the Grb2-SH2 domain.

Table 3.1: Thermodynamic binding parameters of phosphotyrosine mimics **2.003**, **2.004** and **2.005**.

Compound	K_a (M^{-1})	ΔG (kcal mol ⁻¹)	ΔH (kcal mol ⁻¹)	ΔS (cal mol ⁻¹)
AcpYVN 2.003	$4.9 (\pm 0.4) \times 10^5$	-7.8 ± 0.05	-5.9 ± 0.08	6.3 ± 0.4
Cp[pY]VN 2.004	$5.2 (\pm 0.7) \times 10^5$	-7.8 ± 0.08	-6.5 ± 0.04	4.5 ± 0.4
Flex[pY]VN 2.005	$2.9 (\pm 0.7) \times 10^5$	-7.4 ± 0.2	-5.0 ± 0.2	8.1 ± 1

^aReported errors are the standard deviations of three experiments. Errors in $T\Delta S$ were calculated by propagation of error, as the standard deviations were often smaller than expected. Concentrations of ligands were 0.6-0.9 mM and protein was 0.052 mM.

The differences in the thermodynamic profiles for the binding of the ligands **2.004** and **2.005** to the Grb2-SH2 domain are listed in Table 3.2. There was little energetic difference between the binding of the cyclopropane mimic **2.004** and the flexible mimic **2.005** ($\Delta\Delta G = -0.4$ kcal mol⁻¹). However, examination of the data in Table 3.2 reveals the surprising result that cyclopropane-containing ligand **2.004** binds with *less favorable entropy of binding* ($\Delta\Delta S = -3.7$ cal mol⁻¹ K⁻¹) than its flexible analogue **2.005**. However, this entropic disadvantage was accompanied by an enthalpic gain, with **2.004** binding with more favorable enthalpy of binding ($\Delta\Delta H = -1.5$ kcal mol⁻¹) than **2.005**. This was completely the opposite of the results obtained in our Src-SH2 domain system where the cyclopropane-containing ligand was entropically favored and enthalpically disfavored. But like before, enthalpy-entropy compensation was evident in the binding of **2.003-2.005** to the Grb2-SH2 domain. To the best of our knowledge, this is the only example where in the introduction of a conformational constraint results in an entropic

disadvantage in the binding event. This unique observation may question to the validity of the hypothesis that introducing a conformational constraint into a peptide ligand should increase binding affinity by decreasing the conformational entropic penalty paid upon ligand binding (see Chapter 1). Additionally, Martin Teresk and Laura Milspaugh have examined pseudopeptide ligands similar to **2.004** and **2.005** that contain an Ile at the pY+1 position. Using ITC, they obtained the same trends for their ligands as observed for **2.004** and **2.005**; namely, the introduction of the cyclopropane at pY residue of the ligand was associated with an entropic disadvantage when binding to the Grb2-SH2 domain.

Table 3.2: Changes in energetics of binding.

Compound	$\Delta\Delta G^a$ (kcal mol ⁻¹)	$\Delta\Delta H$ (kcal mol ⁻¹)	$-T\Delta\Delta S$ (kcal mol ⁻¹)	$\Delta\Delta S$ (cal mol ⁻¹ K ⁻¹)
2.004/2.005	-0.4	-1.5	1.1	-3.6

^a $\Delta\Delta X$ is ΔX **2.004** - ΔX **2.005**.

In order to determine if the ligands have the same desolvation free energies, the octanol to water partition coefficients (P) for **2.004** and **2.005** were measured (see Chapter 5 for more details). For any of the phosphotyrosine ligands to move from the aqueous to organic phases, it was critical that the pH of the aqueous phase be less than 2. The pKa for phosphotyrosine ligands has been report to be around 2.0 and the ligands need to be fully protonated in order to be dissolved in the organic phase.^{170,171} P values of 1.0 for **2.004** and 0.89 for **2.005**. The mole-fraction partition coefficients were calculated from the P by multiplying the value by 0.114 (the ratio of the molar volumes of water and octanol). The values were then converted into free energy using $\Delta G = -RT \ln (P * 0.114)$.^{35,37} The difference in the free energy of desolvation for the two ligands was

less than 0.1 kcal mol⁻¹. This suggests that the two ligands have similar interactions with the solvent. However, we were unable to repeat this experiment more than once.

3.2.2 pY+1 Pseudopeptides

A *cis*-cyclopropane conformational constraint was introduced at the pY+1 residue of the peptide ligand with hope that the cyclopropane would enforce the desired β -turn present at the pY+1 and pY+2 positions when a ligand binds to the Grb2-SH2 domain (see Chapter 2). The binding data is summarized in Table 3.3. The flexible control **2.007** binds the Grb2-SH2 domain with 10-fold less affinity than the peptide **2.003**. This difference might arise from the presence of the amine functionality t in **2.007**. At physiological pH the amine moiety has different geometry and charge than the corresponding amide moiety present in **2.003**. The amide and amine groups could interact differently with the protein and/or the solvent and result in the affinity difference between the two ligands. However, examination of X-ray structures of Grb2-SH2 domain complexed with peptide ligands revealed that the pY+1 amide NH does not interact with the SH2 domain.^{130,134} On the other hand, the cyclopropane-containing ligand **2.006** binds very poorly to the Grb2-SH2 domain ($K_a < 1 \times 10^3 \text{ M}^{-1}$) suggesting that the *cis*-cyclopropane does not enforce the desired turned conformation for this residue of the ligand. The *gem* dimethyls on the cyclopropane ring might sterically prevent the conformation required for binding because one methyl is on the same side of the ring as the backbone groups. This steric crowding may force the backbone moieties to bend away from the desired turned conformation. Thus, we prepared **2.008** and **2.009** where this methyl group is replaced by a hydrogen atom.

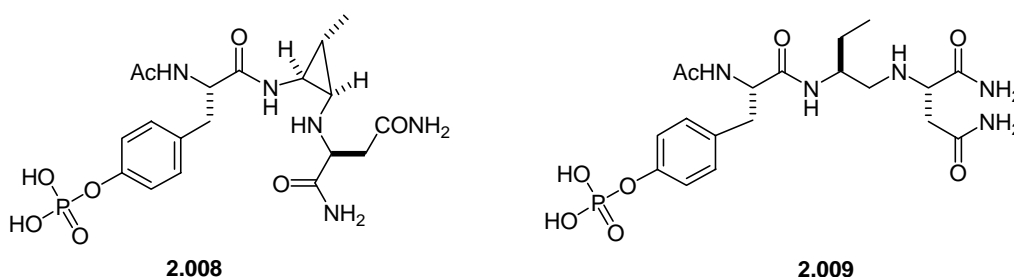


Table 3.3: Thermodynamic binding parameters of pY[V]N.

Compound	K_a (M^{-1})	ΔG ($kcal\ mol^{-1}$)	ΔH ($kcal\ mol^{-1}$)	ΔS ($cal\ mol^{-1}$)
Ac-pYVN 2.003	$4.9 (\pm 0.4) \times 10^5$	-7.8 ± 0.05	-5.9 ± 0.08	6.3 ± 0.4
pY-Cp[V]N 2.006	$<1 \times 10^3$			
pY-Flex[V]N 2.007	$2.0(\pm 0.5) \times 10^4$	-5.9 ± 0.1	-3.0 ± 0.2	9.5 ± 1.2

^aReported errors are the standard deviations of three experiments. Errors in $T\Delta S$ were calculated by propagation of error, as the standard deviations were often smaller than expected. Concentrations of ligands were 0.6 mM for **2.003**, 1.5 mM for **2.006**, and 1.7 mM for **2.007** and protein was 0.052-0.057 mM.

3.3 X-RAY STRUCTURES

In addition to the thermodynamic measurements, it is important to determine the structures of the complexes formed between the constrained and flexible ligands and the protein. One must ensure that the structures of the bound forms of constrained and flexible control ligands are similar. Otherwise, any differences in binding energetics between the two molecules could be associated with additional ligand-protein interactions and not to the conformational constraint itself. Without structural information, the true impact of introducing a conformational constraint cannot be evaluated.

3.3.1 Introduction

Aaron Benfield has been successful in obtaining crystals of the cyclopropane-derived ligand **2.004** bound to the Grb2-SH2 domain. Unfortunately, the complex between the peptide **2.003** and the Grb2-SH2 domain was obtained as a domain swapped

dimer at poor resolution ($> 3 \text{ \AA}$) making it difficult to use for structural comparisons. Efforts to crystallize the flexible ligand **2.005** complexed to the Grb2-SH2 domain are in progress.

3.3.2 X-ray Structures of **2.004** Bound to Grb2-SH2 Domain

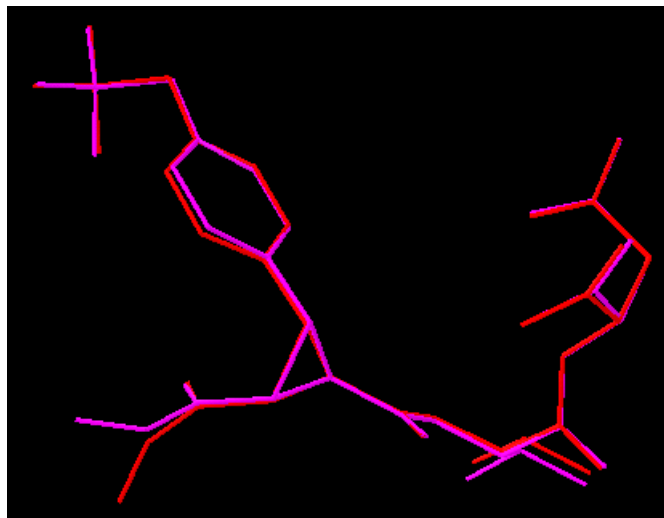
The X-ray structure of **2.004** bound to the Grb2-SH2 domain was solved to 1.9 \AA resolution. It had an R factor of 0.2005 and final free R of 0.2335. In the solved structure, there were two complexes in the asymmetric unit, a situation that provided two independent views of the **2.004**/Grb2-SH2 complex. The two complexes align with an r.m.s deviation of 0.69 \AA for all protein atoms (0.32 \AA for α -carbon atoms, 0.32 \AA for backbone atoms, and 0.91 \AA for side chain atoms) meaning the two complexes are superimposable within approximately 0.7 \AA (Figure 3.1).

Figure 3.1: Overlay of the protein backbone for the two **2.004**/Grb2-SH2 complexes in the asymmetric unit, one in pink and the other in red.



The only significant difference between the conformations of the ligands in the two complexes is the conformation of the *N*-terminal methylene (Me-N-C=O conformation) (Figure 3.2). The carbonyls in both conformations interact through hydrogen bonds with Arg 67 protein residue; the oxygen atom of the carbonyl is 2.73 Å from one guanidinium N-H and 3.10 Å away from the other guanidinium N-H. The carbonyl oxygen atom for both ligand conformations is in the same location but there are different positions for the *N*-methyl, indicating that there are two different conformations for this amide bond. In one structure the conformation about this amide is *cis* with the *N*-methyl and carbonyl almost co-planar (the dihedral angle for Me-N-C=O is -19°). In the other structure, this methyl amide is in a *pseudotrans*-conformation (the dihedral angle for Me-N-C=O is 60°). In either conformation, the methyl nitrogen is not interacting with the protein. For simplification, only one conformation, the *N*-methylene *pseudotrans*-conformation, will be used for the rest of the discussion.

Figure 3.2: Overlay of the two **2.004** ligands bound to Grb2-SH2 domain, one in pink the other in red.



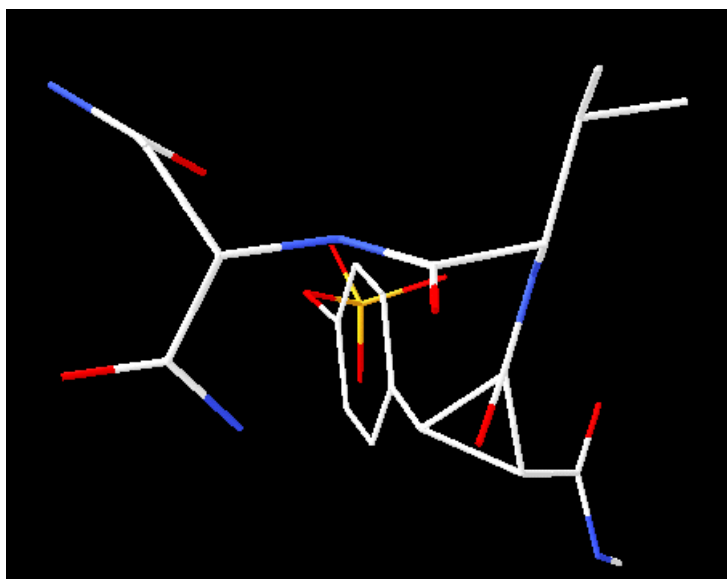
An X-ray structure of the cyclopropane-containing ligand **1.086** bound to the Src-SH2 domain was previously determined.^{105,121} An overlay of **1.086** and **2.004** bound to their respective domains shows the very similar conformation for the cyclopropane residue of these ligands (see Figure 3.3). There is only one *N*-methylamide conformations in **1.086**/Src-SH2 complex. There are also slight differences in the interactions found between the Grb2 and Src/cyclopropane-containing ligand complexes. For example, the *N*-methylamide carbonyl of **1.086** is 2.84 Å from one guanidinium N-H of Arg 155 and 3.10 Å away from the other guanidinium N-H. These distances are similar to the ones seen for this carbonyl of **2.004** interacting with Arg 67 of the Grb2-SH2 domain. In addition, the bridging phosphate oxygen of **2.004** is 3.02 Å from Ser 96 of Grb2 while this oxygen of **1.086** is 3.21 Å away from Cys 185 of Src. One of the non-bridging phosphate oxygens of **2.004** is closer to the Arg 86 residue of Grb2 while another non-bridging oxygen is near Arg 67, 2.75 Å and 2.73 Å, respectively. In the Src complex, two of the non-bridging phosphate oxygens are both close to Arg 175, 2.69 Å and 2.78 Å away, respectively. The third non-bridging phosphate oxygen of the cyclopropane-containing ligands is 2.55 Å away from Ser 90 in the Grb2 complex, while this oxygen atom is 2.69 Å from Thr 179 in the Src-SH2 domain complex. In addition, the Src complex contains an additional interaction between protein residue Glu 178 and a non-bridging phosphate oxygen of **1.086** (distance between the groups is 2.78 Å). Despite these slight differences, we conclude that the Src- and Grb2-SH2 domains bind the pY residue of the cyclopropane-containing ligands **2.004** and **1.086** in a similar manner.

Figure 3.3: Overlay of **2.004** bound to Grb2-SH2 domain (in pink) and a similar cyclopropane-containing ligand **1.086** bound to Src-SH2 domain (in yellow).^{105,121}



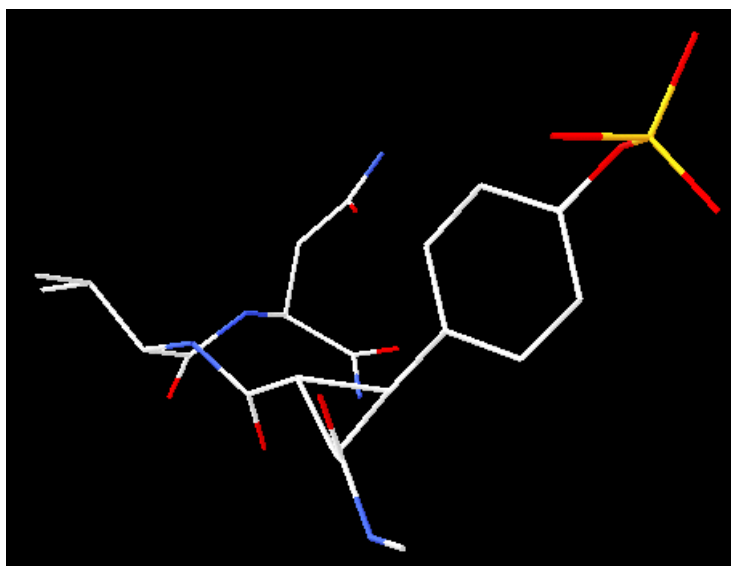
Further inspection of the cyclopropane conformation in the X-ray structure shows the carbonyls on either side of the cyclopropane have distinct orientations. The carbonyl (pY+1 amide) at the *C*-terminus clearly bisects the cyclopropane ring (Figure 3.4). The same conformation was seen in a simple X-ray structure of an unbound cyclopropane-carboxamide suggesting that it is the preferred conformation for the *C*-terminal carbonyl.¹⁰³ This bisecting conformation of **2.004** in our complex has been seen in similar cyclopropane-containing ligands bound to proteins.^{104,105,121} The fact that this bisecting conformation was seen in both uncomplexed and complexed molecules indicates that the ψ peptide torsional angle is being constrained by introducing the cyclopropane constraint.

Figure 3.4: Bisecting orientation of the pY to +1 Val carbonyl of **2.004**.



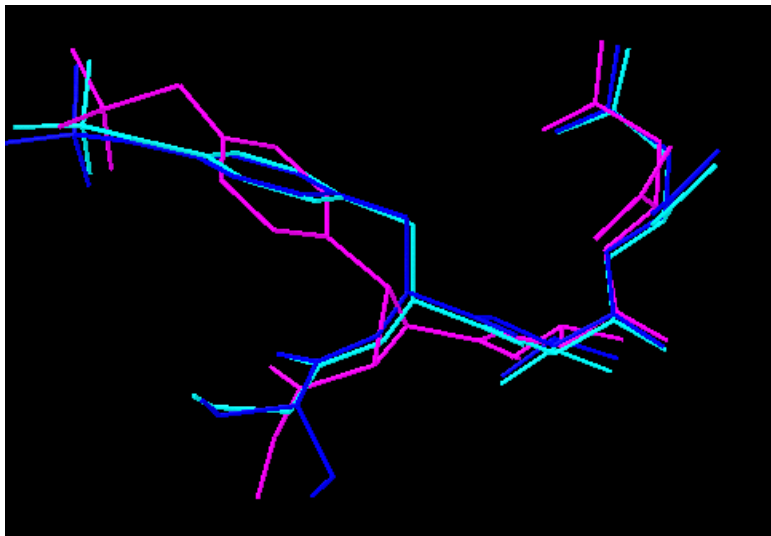
On the other hand, the *N*-terminal carbonyl *N*-methylamide deviates from the aforementioned preferred bisecting conformation (Figure 3.5). The conformation of this carbonyl in the unbound structure deviates from the bisecting orientation by approximately 47° . However, the conformation of this carbonyl in the **2.004** complex is about 18° different from the bisecting orientation. As mentioned before, this carbonyl is probably involved in hydrogen bond interactions with the Arg 67 residue of the Grb2 SH2-domain. This interaction may be responsible for the deviation of the carbonyl orientation from the bisecting conformation or the conformation seen in the unbound crystal structure. A similar conformation was seen in the X-ray structure of **1.086** bound to the Src-SH2 domain.^{105,121} Thus, it is not clear that the introduction of a cyclopropane conformational constraint restricts the ϕ peptide torsional angle conformation.

Figure 3.5: The orientation of the pY to methylamide carbonyl of **2.004**.



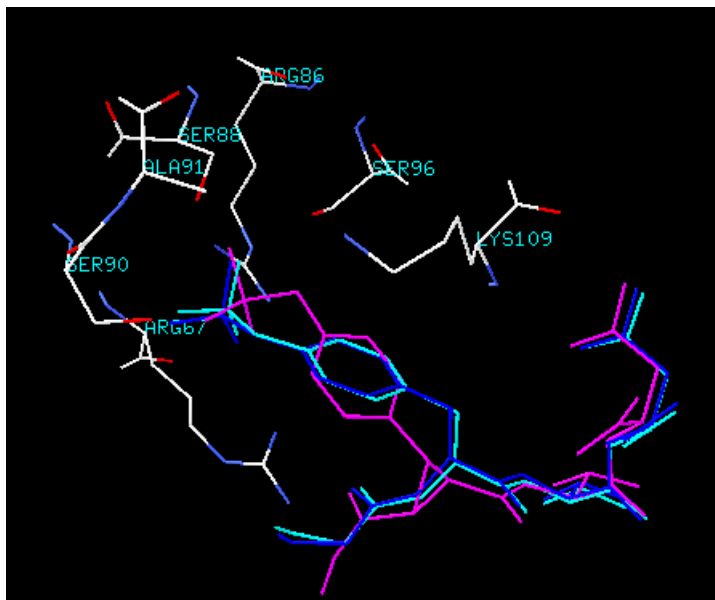
We have been unable to solve an X-ray structure of a flexible control **2.005** bound to the Grb2-SH2 domain. Thus, we can only compare our structure of the complex of **2.004** to the Grb2-SH2 with other structures reported in the literature. We choose two published structures 1TZE¹³⁰ and 1JYR¹³⁴ each having a peptide ligand similar to **2.003** bound to the SH2 domain that contain. 1TZE structure was solved to 2.1 Å resolution and contained a 7-peptide residue ligand with an IC₅₀ of 0.15 μM bound to the domain. Structure 1JYR was solved to 1.5 Å resolution and contained 9-peptide residue ligand with an IC₅₀ of 72 nM and a K_d of 18 nM bound to the domain. An overlay of the three structures is shown in Figure 3.6. It is clear that the bound conformation of the pY residue of **2.004** deviates from the pY residue of the peptides, especially at the bridging phosphate oxygen moiety.

Figure 3.6: Overlay of **2.004** (shown in pink) and other peptide ligands (shown in light and dark blue) bound to Grb2-SH2 domain.^{130,134}



The different binding modes of **2.004** and the peptide ligands can be illustrated by examining the X-ray structure of the complexes, specifically the residues of the Grb2-SH2 domain that are near the phosphotyrosine ring of the ligands (Figure 3.7). Some residues in the flexible loop are closer to the bridging phosphate oxygen of **2.004** than this oxygen moiety of the peptides. These differences could affect the interactions between the ligands and the protein. For example, the distance between hydroxyl of Ser 96 of the SH2 domain and this oxygen of **2.004** is 3.02 Å, which is within hydrogen bonding distance. However, in the structures of the peptide complexes the distance between these groups is 3.98 Å, which is too far to be considered a hydrogen bond interaction.

Figure 3.7: The Grb2-SH2 protein residues which are within 6 Å of pY moiety of the ligands.



In addition, two of the three non-bridging phosphate oxygens of the ligands could also have different interactions with the protein. For example, the hydroxyl residue of Ser 90 of the protein is 2.83 Å from one of the non-bridging oxygens of the peptide ligand, while this protein residue is 2.55 Å away from this oxygen in **2.004**. On the other hand, the distance between one of the other non-bridging oxygens of **2.004** and Ser 88 hydroxyl is longer than the distance between this oxygen moiety in the peptides and Ser 88 hydroxyl, 3.27 Å and 2.87 Å, respectively. Conversely, the distance between the third non-bridging phosphate oxygens of **2.004** and the peptides and a guanidinium N-H group of domain residue Arg 86 is almost identical.

Although the pY residue of **2.004** and the peptide ligands do not seem to bind to the Grb2-SH2 domain in precisely the same manner, the pY+1 Val and pY+2 Asn

positions of the ligands overlap nicely (Figure 3.8). Thus, introducing a cyclopropane at the pY residue of the ligand does not seem to affect the way the pY+1 Val and pY+2 Asn residues bind and the desired β -turn conformation is maintained.

Figure 3.8: Overlay of **2.004** (shown in pink) and other peptide ligands (shown in blue) bound to Grb2-SH2 domain, pY+1 Val clearly overlap.^{130,134}

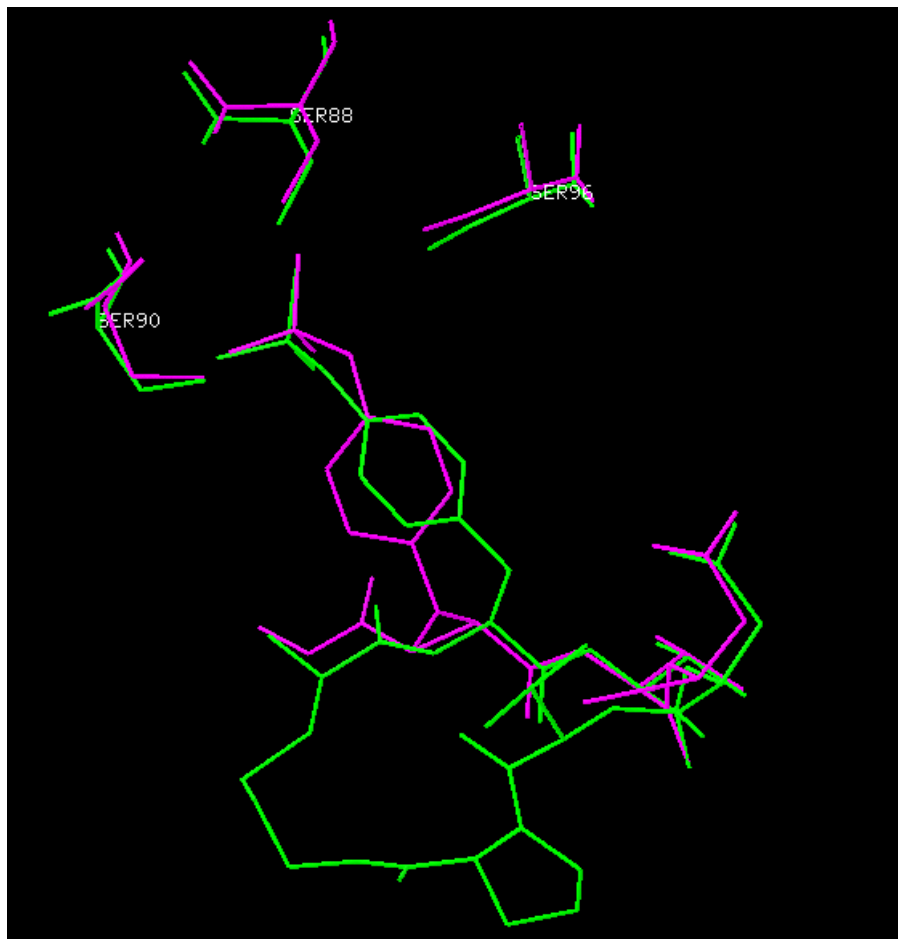


The difference in the distances between a functional group of the ligand and the protein residues that it is interacting with will affect the strength of the non-covalent interactions. The resulting differences in the non-covalent interactions between the protein and the ligand will affect the energetics of the ligand binding. These different interactions found in the **2.004** and peptide complexes make it difficult to compare the thermodynamic binding profiles between **2.004** and the peptide ligands. Additionally, from these different binding modes of **2.004** and the peptide ligands we can conclude anything about the effects of introducing a cyclopropane conformational constraint. Instead, we would need a complex of the flexible control **2.005** bound to the Grb2-SH2

domain in order to compare to the **2.004**/Grb2 complex. We are currently working to obtain this structure.

The crystal structure of another constrained peptide-like ligand bound to the Grb2-SH2 domain has been reported in the literature. Macrocycle **2.002** has IC_{50} of 0.11 μ M and the **2.002**/Grb2-SH2 domain complex (1BM2) was solved with 2.1 Å resolution.⁹² Macrocycle **2.002** binds to the Grb2-SH2 domain in a slightly similar manner as the cyclopropane containing **2.004** (Figure 3.9). The bridging oxygen in **2.002** and **2.004** are in a similar location compared to the bridging oxygen found in the ligands. The Ser 96 hydroxyl residue of the domain and the bridging oxygen in **2.002** and **2.004** are similar distance apart, 3.34 and 3.02 Å, respectively. On the other hand, the non-bridging oxygens are different distances from Ser 88 and Ser 90 residues of the Grb2-SH2 domain. For example, two of the three non-bridging oxygens of **2.002** are 2.93 and 3.04 Å away from Ser 88 and Ser 90 hydroxyl residue. However, these non-bridging oxygens of **2.004** are 3.27 and 2.55 Å away from those respective residues on the domain.

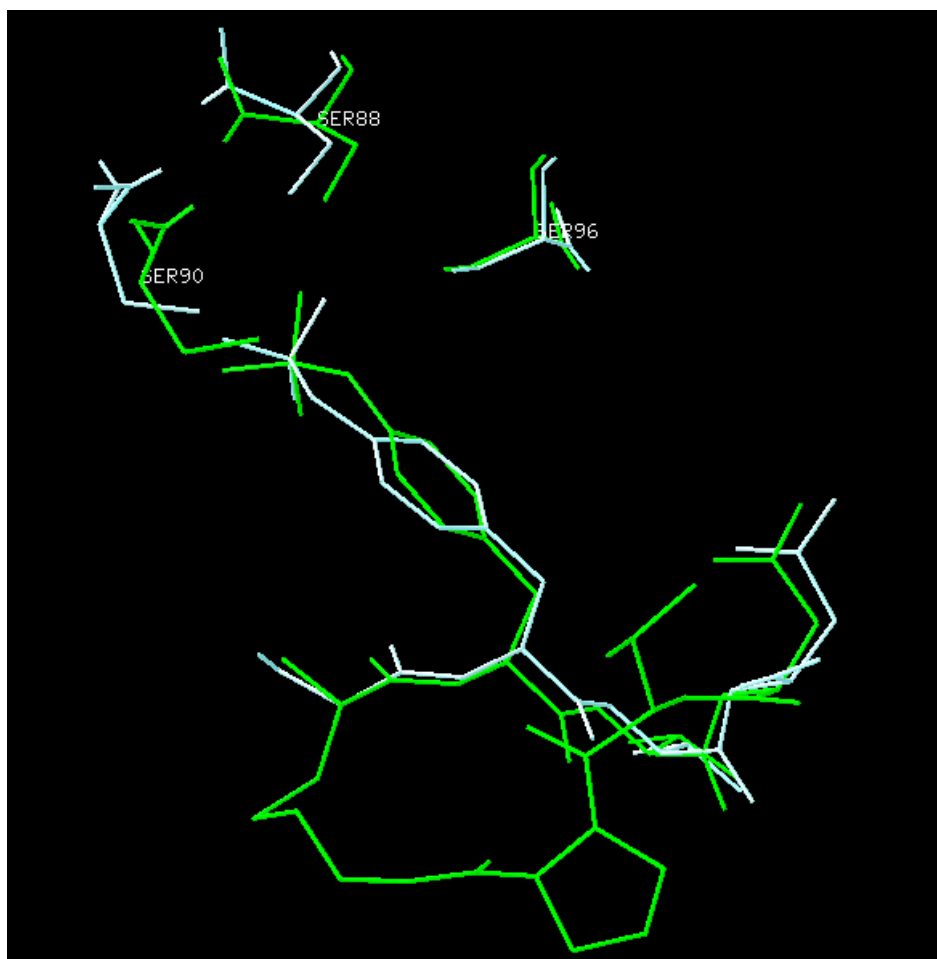
Figure 3.9: Overlay of **2.004** (shown in pink) and macrocyclic peptide **2.002** (shown in green)⁹² bound to Grb2-SH2 domain.



The orientation of **2.002** bound to the SH2 domain is also slightly different than the orientation of a peptide bound to the domain. This can be illustrated by the overlay of the two structures (1TZE¹³⁰ and 1BM2⁹², Figure 3.10). The non-bridging oxygens of **2.002** and the peptide ligand have similar contacts with Ser 88 and Ser 90. For example, two of the three non-bridging oxygens of the peptide ligand are 2.87 and 2.83 Å from Ser 88 and Ser 90 hydroxyl residues, respectively. These non-bridging oxygens of **2.002** are 2.93 and 3.04 Å apart from Ser 88 and Ser 90. On the other hand, the bridging oxygens

of the two ligands make very different contact with Ser 96. The bridging oxygen of **2.002** is only 3.34 Å apart from the hydroxyl of Ser 96 while this oxygen in the peptide ligand is 3.98 Å from the residue, which is out of the range for hydrogen bonding interactions with the domain. By comparing these structures, it appears that there is some flexibility in the Grb2-SH2 domain binding site.

Figure 3.10: Overlay of **2.002** (shown in green) ⁹² and peptide ligand (shown in blue) ¹³⁰ bound to Grb2-SH2 domain.



3.3.3 Conclusions from X-ray Structure

The complex of **2.004** bound to the Grb2-SH2 domain provides interesting insight into the energetics of binding. First, the pY residues of the cyclopropane-containing ligands **2.004** and **1.086** bind to their respective Grb2-SH2 and Src SH2 domains in a similar manner. However, it is clear that the pY residues of the peptide ligands and **2.004** bind to Grb2-SH2 domain in different modes. On the other hand, constrained macrocycle **2.002** and constrained cyclopropane-containing **2.004** bind to the domain in a somewhat similar manner. This suggests that there is some flexibility in the Grb2-SH2 domain binding pocket. In order to determine the structural consequences of introducing a cyclopropane ring, we need an X-ray structure of the flexible control **2.005** bound to the Grb2-SH2 domain. Comparing the bound structures of **2.004** and **2.005** will allow us to further understand the consequence of introducing a cyclopropane constraint and might confirm our recent finding that the introduction of a conformational constraint cannot be associated with an entropic advantage to binding.

3.4 SUMMARY AND CONCLUSIONS

Many scientists have believed that introducing a conformational constraint into a flexible ligand will enhance binding affinity provided the two ligands bind in the same manner making the same contacts with the protein. This prediction follows from the idea that the constrained molecule should pay a reduced entropic penalty upon binding to a protein. However, the present and related work reveals that introducing a cyclopropane conformational constraint generally does not seem to influence the net affinity of peptide-like ligands binding to SH2 domains (both Src and Grb2).

Comparing the ITC data for the binding of **2.004** and **2.005** to the Grb2-SH2 domain reveals that the introduction of a cyclopropane ring at the pY replacement in pYVN tripeptide actually results in entropic disadvantage. This disadvantage is

completely different than results we obtained for binding of similar peptide-like ligands to the Src-SH2 domain. In these cases the constrained ligand had an entropic advantage over its flexible partner. It is also the first time, to our knowledge, that introducing conformational constraint is associated with an entropic disadvantage for binding. The origin of the observed entropic disadvantage is perplexing. We must consider the total entropy of the binding even, both the ligand and the protein, before and after complexation. By pre-organizing the ligand into the biologically active conformation, the net conformational entropy required for the ligand to bind to the protein has been reduced. Thus, it seems likely that this disadvantage may be associated with the difference in the conformational entropy of the protein before and after complexation. For the Grb2-SH2 domain, binding a rigid compound may reduce the flexibility of the protein more than the binding of a flexible analogue. Namely, the conformational entropy of the protein in the complex may be dependent upon the flexibility of the bound ligand, and binding a less flexible ligand resulted in a complex that was more ordered and less entropically favored.

An X-ray structure of **2.004** bound to the Grb2-SH2 domain reveals that **2.004** binds in a different mode than native peptide ligands. There are additional interactions between the SH2 domain and **2.004** that are not present in the structures of the bound peptide ligands. These additional interactions could contribute to the enthalpic advantage seen for the binding of the constrained ligand. The additional interactions between the constrained ligand and the protein might be expected to then result in an entropic disadvantage associated with the binding of the constrained ligand. If the ligand and protein are held tightly together by enthalpic interactions, then the ligand and protein will have less freedom of motion and therefore less entropy. Additionally, regions of the protein may gain or lose conformational entropy upon binding a pre-organized ligand.

On the other hand, it appears that constrained ligands **2.002** and **2.004** bind to the Grb2-SH2 domain in a slightly similar manner, suggesting that there is some flexibility in the binding pocket. This comparison is not completely accurate since peptide ligands are not the ideal control partners for **2.004**. However, we have not been able to obtain an X-ray structure of **2.005** bound to the Grb2-SH2 domain. This structure is critical for determining whether **2.004** and **2.005** bind to the domain in a similar manner.

It has not yet been possible to demonstrate that the introduction of a *cis*-cyclopropane at the pY+1 residue in ligands that bind to the Grb2-SH2 domain can stabilize the β -turn conformation required for binding.

In general the theory of introducing a conformational constraint in order to obtain a ligand with higher binding affinity through an entropic advantage has been applied in an overly simplistic fashion (see Chapter 1 for more discussion). The conformational entropy of the ligand has been the focus. Unfortunately, this ignores the possibility that the protein could have different conformational entropy depending on the flexibility of the bound ligand and that this conformational entropy could impact the enthalpic interactions associated with complexation. We now have an example where the introduction of a conformational constraint does not enhance binding affinity, and an entropic disadvantage is associated with the binding of the pre-organized ligand. In addition, the theory does not account for the enthalpy-entropy compensation, a widely observed phenomenon.

There are many more experiments that should be conducted within this research area to further probe the validity of the theory of pre-organization. It is necessary to apply our conformational constraint to different biological systems. We have only evaluated the thermodynamic parameters of binding constrained and flexible molecules to SH2 domains. Extending this research to enthalpically or entropically driven systems

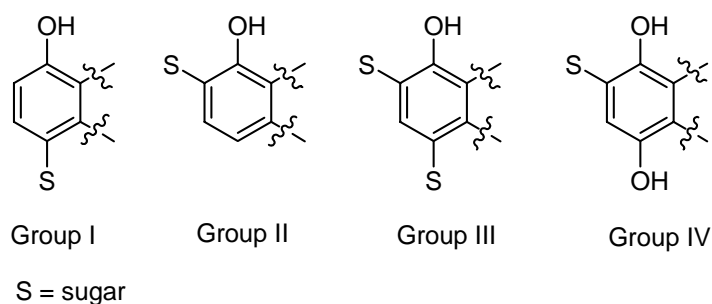
might provide intriguing insight into the energetics of binding. In addition, our cyclopropane constraints are backbone to side chain constraints. Evaluating other conformational constraints such as backbone to backbone or side chain to backbone cyclizations would also be interesting. In order to determine the flexibility of the protein in the complex, dynamic, time-resolved NMR experiments need to be conducted.¹⁷² These experiments will lead to a further understanding of the energetics associated with ligand-protein interactions and of the entropic disadvantage associated with binding our pre-organized ligands.

Chapter 4. Studies Toward the Synthesis of C-Aryl Glycosides

4.1 INTRODUCTION OF C-ARYL GLYCOSIDES

C-Aryl glycoside antibiotics are an important subclass of the C-glycoside family of natural products that have attracted considerable interest owing to their range of significant biological activities and resistance to enzymatic hydrolysis.¹⁷³⁻¹⁷⁵ C-Aryl glycosides are divided into four classes based on the substitution pattern of the phenolic hydroxy group(s) relative to the carbohydrate functionality(ies) (Figure 4.1).¹⁷⁶ In Group I C-aryl glycosides, the sugar is *para* to the phenolic hydroxyl group, while in Group II the sugar is *ortho* to this function. Group III C-aryl glycoside contain two carbohydrate moieties both *ortho* and *para* positions to the hydroxyl group, whereas group IV C-aryl glycosides is a 1,4-dihydroxy quinone with a sugar at the 2 position.

Figure 4.1: Different groups of C-aryl glycosides.

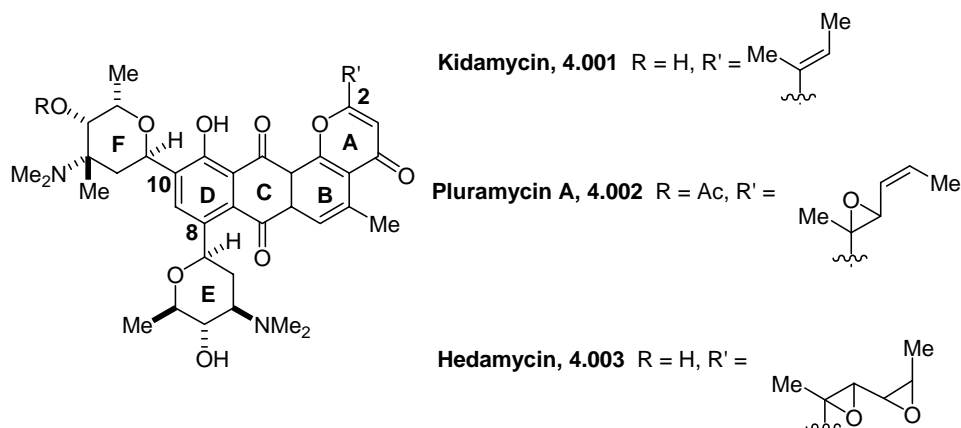


4.1.1 Kidamycin

One challenge to the synthesis of C-aryl glycoside natural products is their unsymmetrical substitution pattern. For example, the pluramycins are a family of

antibiotic natural products belonging to the Group III class of *C*-aryl glycosides that contain highly substituted 4*H*-anthra[1,2-*b*]pyran-4,7,12-triones with two sugars attached (Figure 4.2).¹⁷⁷ The sugar at position 8 is anglosamine and represents ring E. An *N,N*-dimethylvancosamine is positioned at carbon 10 and referred to as ring F. A few members of the pluramycin family differ in the functionality at position 2, including kidamycin (**4.001**), pluramycin A (**4.002**) and hedamycin (**4.003**). Kidamycin was isolated from a *Streptomyces* in 1956 and was found to possess antimicrobial and anticancer activity.¹⁷⁷ The mechanism of action for the biological activity involves the ability of kidamycin to bind strongly to DNA.¹⁷⁸ To date, no total synthesis has been reported for these *C*-aryl glycosides, although the synthesis of *O*-methylkidamycinone, an aglycone derivative of kidamycin, and *bis*-substituted *C*-aryl glycosides have been reported.^{176,179} In addition, Dr. David Kaelin, has explored several routes to prepare structures related to the kidamycin core and the synthesis of ring E and F sugars.¹⁸⁰

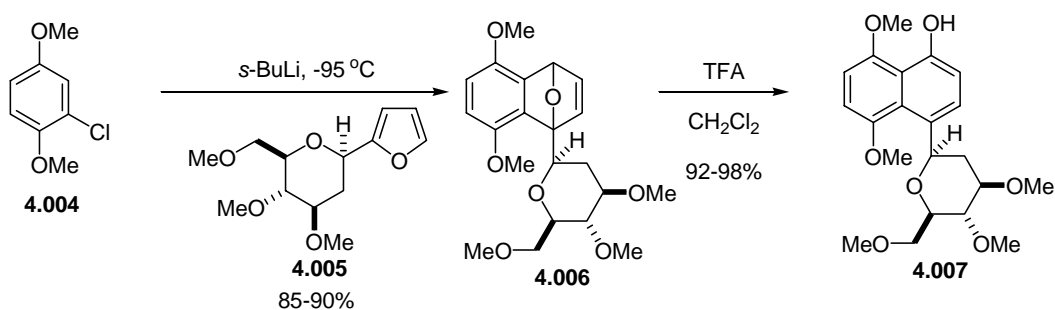
Figure 4.2: Members of the pluramycin class of natural products.



4.2 THE TETHERED BENZYNE CYCLOADDITION METHODOLOGY

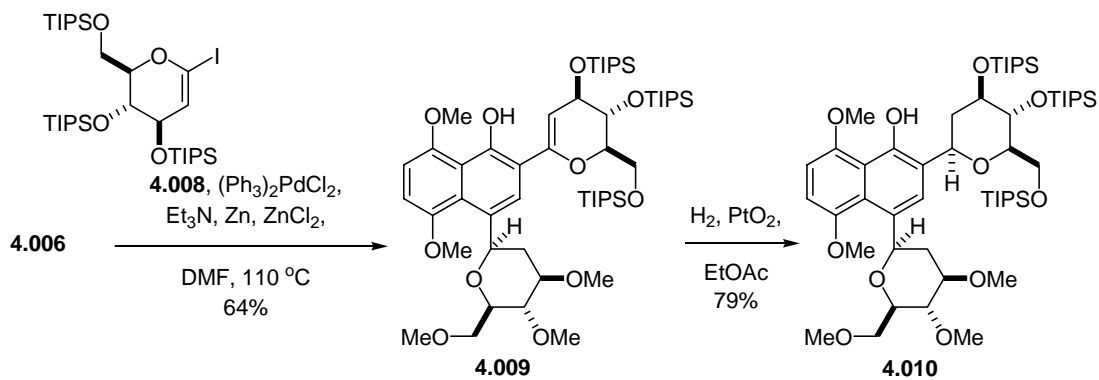
For some time the Martin group has been interested in synthesizing *C*-aryl glycoside natural products. Several methods were developed in our group; however, none provided access to the unsymmetric substitution pattern of the natural products. The Martin group recently disclosed two general approaches to prepare the major classes of *C*-aryl glycosides.¹⁸⁰⁻¹⁸² The first method involved an acid-catalyzed ring opening of a benzyne-furan cycloadduct. For example, deprotonation of **4.004** gave the benzyne that underwent cyclization with furan **4.005** to provide cycloadduct **4.006** in excellent yield (Scheme 4.1). Acid-catalyzed ring opening of **4.006** provided the model Group I *C*-aryl glycoside **4.007**.

Scheme 4.1



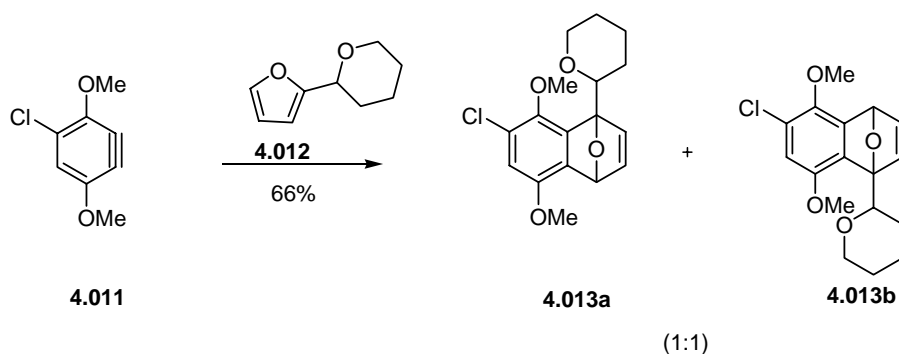
In the second developed approach to *C*-aryl glycosides, a palladium-catalyzed S_N2'-type ring opening of a benzyne-furan cycloadduct with an iodoglycal, followed by appropriate adjustment of oxidation states provided *C*-aryl glycosides. This route allowed for a later stage introduction of carbohydrate residues, which was especially useful for the synthesis of Group III *C*-aryl glycosides. For example, palladium-catalyzed ring opening of cycloadduct **4.006** with **4.008** provided the naphthol **4.009** in 64% yield. Reduction of **4.009** afforded **4.010**, an example of a Group III *C*-aryl glycoside (Scheme 4.2).¹⁸⁰⁻¹⁸²

Scheme 4.2



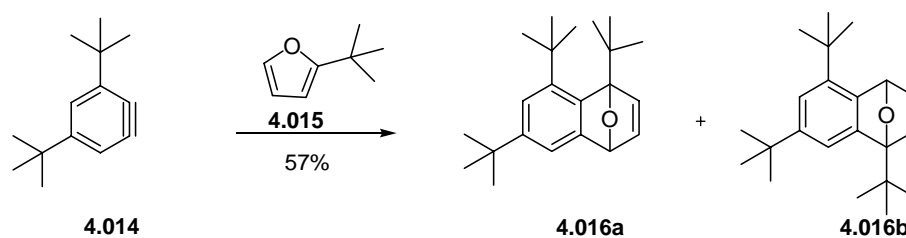
In these initial studies symmetrical benzyne were universally employed as reaction partners, so the regioselectivity of the cycloaddition was not an issue. Although unsymmetrical benzyne can undergo regioselective Diels-Alder reactions,¹⁸³ such cycloadditions typically proceed with poor regioselectivity.^{184,185} For example, in our labs Dr. David Kaelin studied the Diels-Alder reaction between furan **4.011** and the benzyne **4.012** (Scheme 4.3),¹⁸⁰ obtaining a mixture (1:1) of products **4.013a** and **4.013b**.

Scheme 4.3



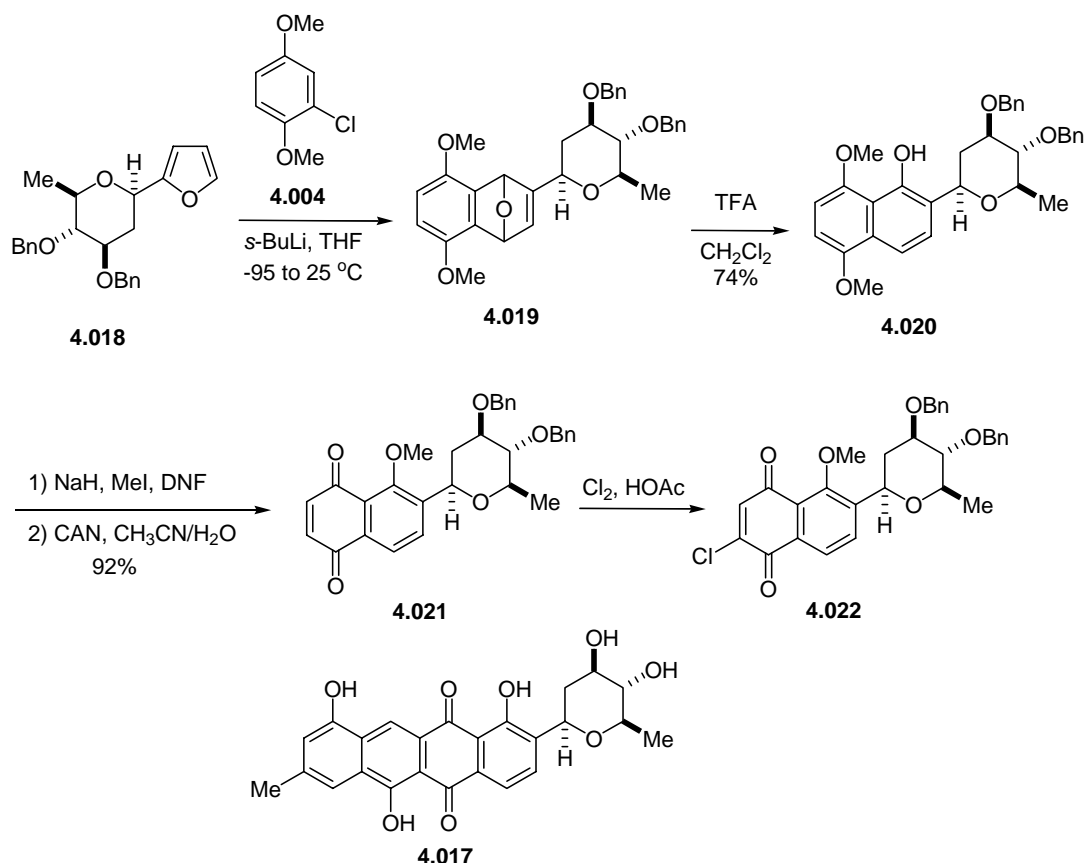
There are reports in the literature using steric bulk to direct regioselectivity in benzyne cycloadditions, but these were unsuccessful. This can be illustrated by the cycloaddition between di-*tert*-butyl benzyne **4.014** and *tert*-butylfuran **4.015** produced a mixture (1.3:1) of the two regioisomers **4.016a** and **4.016b** in 57% yield (Scheme 4.4).^{186,187}

Scheme 4.4



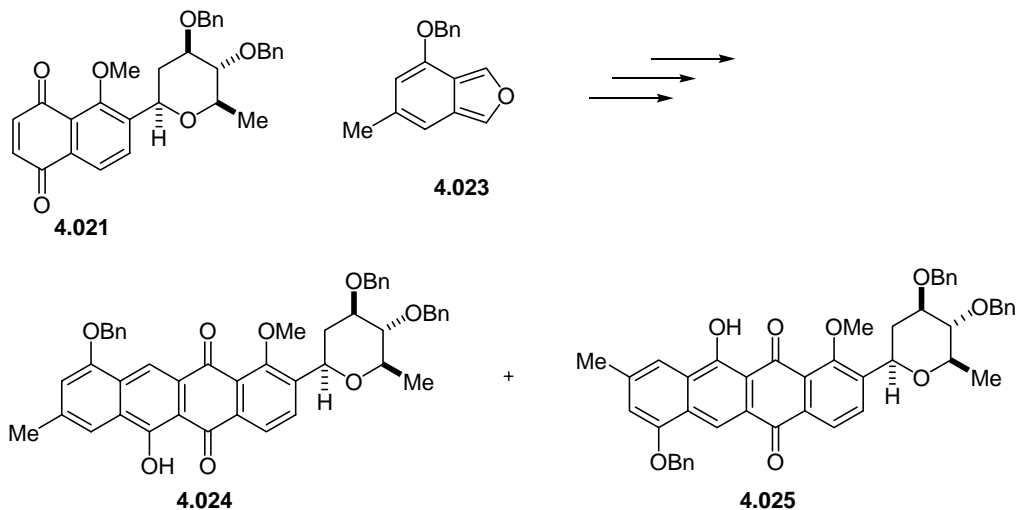
In addition, the lack of regiocontrol in the cycloaddition became manifest during recent work that culminated in a formal synthesis of the *C*-aryl glycoside galtamycinone (**4.017**).¹⁸⁸ Furyl glycoside **4.018** was reacted with the benzyne generated from **4.004** providing a mixture of diastereomeric Diels-Alder adducts **4.019** (Scheme 4.5). Acid-catalyzed ring opening furnished the naphthol **4.020**, which underwent *O*-methylation and oxidation to give juglone **4.021**. Chlorination of **4.021** proceeded with complete regioselectivity to give chlorojuglone **4.022** as a single diastereomer and its preparation constitutes a formal synthesis of **4.017**.

Scheme 4.5



Next, members of the Martin group investigated whether glycosyl juglones like **4.021** would undergo a regioselective Diels-Alder reaction with isobenzofuran **4.023** to provide access to galtamycinone (Scheme 4.6). An exploratory study in which juglone **4.021** was allowed to react with isobenzofuran was conducted, but this reaction gave an uncharacterized mixture of regio- and stereoisomeric products. Due to this limitation, benzyne Diels-Alder reactions alone cannot be used to access unsymmetrical *C*-aryl glycosides. Nevertheless, the mixture was carried on to provide a separable mixture (1.1:1) of the regiomers **4.024** and **4.025**. The preparation of the *C*-aryl glycoside **4.024** represented a formal synthesis of galtamycinone (**4.017**).

Scheme 4.6

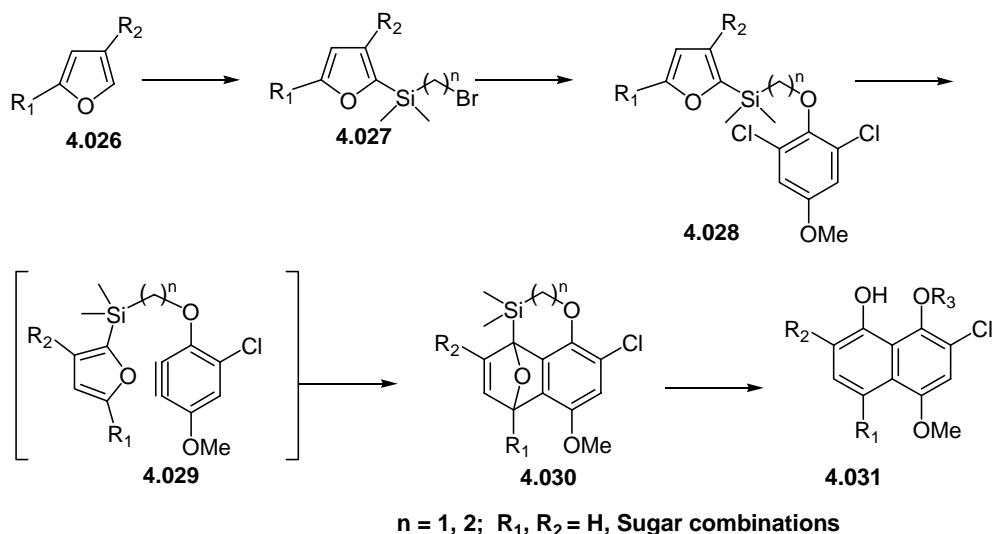


In order to apply our benzyne Diels-Alder methodology to the synthesis of naturally occurring *C*-aryl glycosides, which are all unsymmetrically substituted, it is essential to control the regiochemistry of the pivotal benzyne-furan cycloadditions. It was discovered that a disposable silicon tether could be exploited to control the regiochemistry of benzyne-furan cycloadditions that led to the major groups of *C*-aryl glycosides.^{180,189}

Two protocols, differing only in the number of carbon atoms in the tether, were envisioned (Scheme 4.7). In the first method, the regioselective metallation of glycosyl furan derivatives **4.026** followed by trapping the carbanions with an appropriate chlorosilane, followed by refunctionalization as needed would lead to the silanes **4.027** which would be coupled with halophenols to give **4.028**. Selective deprotonation of **4.028** followed by expulsion of the *ortho* chloride would generate the benzyne **4.029**, and a subsequent intramolecular Diels-Alder reaction would furnish the cycloadducts

4.030. Based upon the prior art of Rickborn and Stork,¹⁹⁰⁻¹⁹² it was anticipated that fluoride ion would induce the cleavage of the silicon–carbon bonds in the tethers of **4.030** to give intermediates that could undergo acid-catalyzed opening of the oxabicyclic ring to deliver either glycosyl naphthol **4.031** ($R_3 = \text{H}$ or Me), depending on the nature of the tether and the precise tactics used to effect its removal.

Scheme 4.7

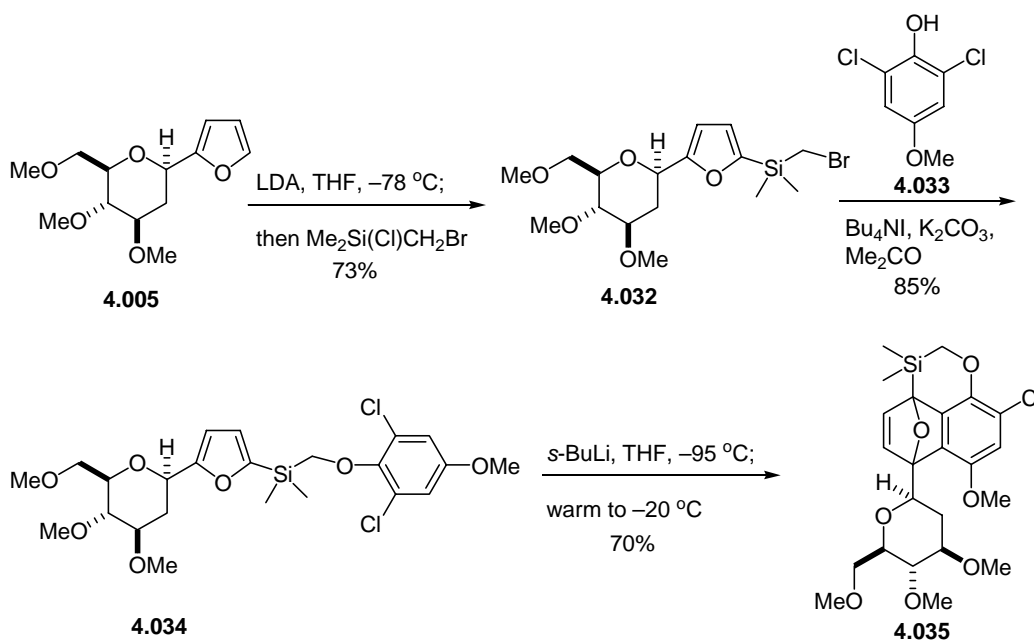


4.2.1 Application to Group I C-Aryl Glycosides

The use of silicon tethers to access Group I C-aryl glycosides is illustrated by two related strategies. In the first of these, Dr. David Kaelin converted the known glycosyl furan **4.005**¹⁸¹ into the furylsilane **4.032** by sequential metallation (LDA, THF, $-78\text{ }^\circ\text{C}$) and reaction with bromomethylchlorodimethylsilane to afford the furylsilane **4.032** in 73% yield (Scheme 4.8).¹⁸⁰ *O*-Alkylation of 2,6-dichloro-4-methoxyphenol (**4.033**)¹⁹³ with **4.032** provided the Diels-Alder precursor **4.034** in 85% yield. When **4.034** was treated with *s*-BuLi in THF at $-95\text{ }^\circ\text{C}$, facile deprotonation *ortho* to methoxy group

ensued. The resultant anion underwent elimination upon warming to generate an intermediate benzyne that cyclized with the pendant glycosyl furan to provide cycloadduct **4.035** as a diastereomeric mixture in 70% yield.

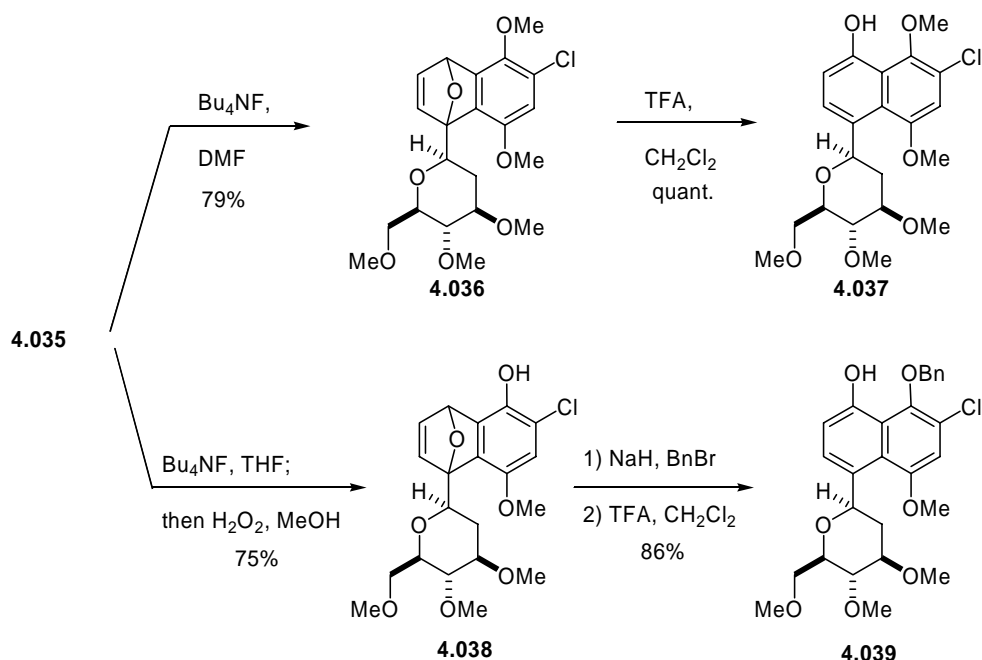
Scheme 4.8



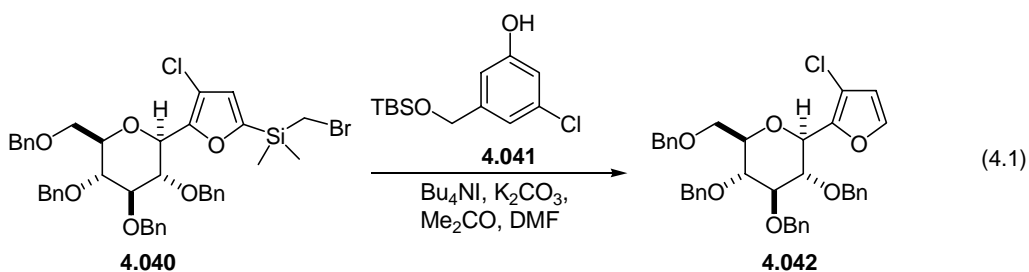
Two tactics were developed for converting the cycloadduct **4.035** into substituted naphthols. In the event, reaction of **4.035** with excess Bu_4NF (TBAF) in DMF cleaved both carbon-silicon bonds to afford **4.036** (79% yield), which underwent acid-catalyzed ring opening to furnish quantitatively **4.037**, a representative Group I C-aryl glycoside (Scheme 4.9). Alternatively, when **4.035** was treated with TBAF in THF, only the bridgehead carbon-silicon bond was cleaved. Subsequent Tamao oxidation (H_2O_2 , KHCO_3 , CH_3OH) furnished the phenol **4.038** in 75% yield.¹⁹⁴⁻¹⁹⁶ Dr. Steve Sparks found that *O*-alkylation of **4.038** followed by acid-catalyzed ring opening gave **4.039**

(86% overall yield) in which each of the phenolic hydroxyls is nicely differentiated for subsequent transformations.

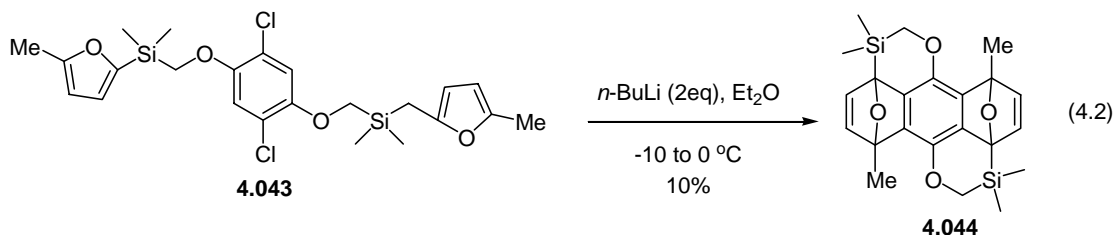
Scheme 4.9



It was found that *O*-alkylations of other phenols with bromomethyl silanes like **4.028** may be problematic due to competing nucleophilic attack on silicon.¹⁹⁷ For example, when bromosilane **4.040** is reacted with phenol **4.041**, furan **4.042** is formed (Equation 4.1).¹⁹⁸

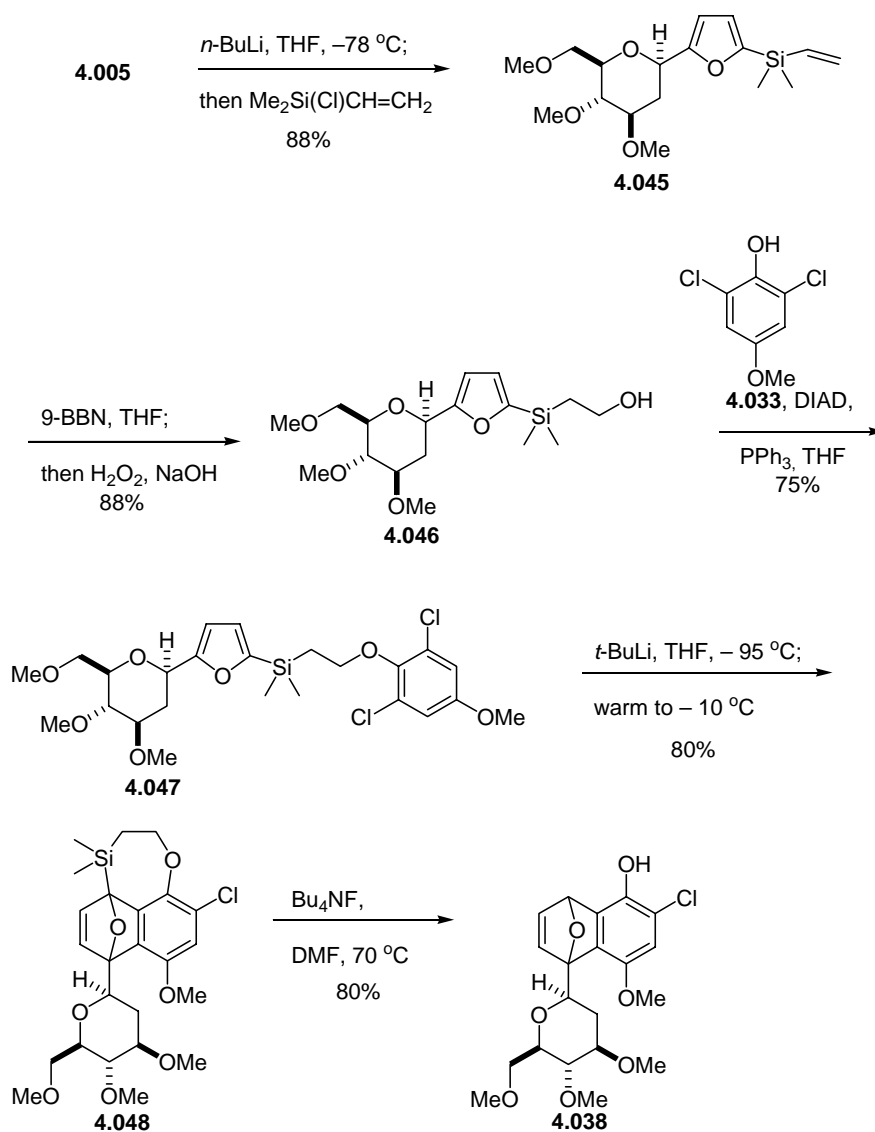


In addition, Dr. Steve Sparks discovered a problem in the cycloaddition of **4.043**. When **4.043** was treated with *n*-BuLi low yields of cycloadduct **4.044** were obtained and the ¹H NMR spectra of the crude reaction mixture contained multiple peaks at δ 5.7 to 6.0 ppm, which were in indication of the presence of bridge head protons (Equation 4.2). He felt the formation of these protons were the result of C-Si bond cleavage.¹⁹⁹



Dr. Steve Sparks hypothesized that ring strain might be the reason for the low yield of this reaction and developed a solution to this problem that featured the use of a tether containing an additional carbon atom.^{189,199} Thus, **4.005** was converted into the vinylsilane **4.045** through metallation and trapping the resultant anion with chlorodimethylvinyl silane (Scheme 4.10). Regioselective hydroboration and oxidation of **4.045** afforded the alcohol **4.046** in 77% yield.²⁰⁰ Mitsunobu coupling (DIAD, PPh₃, THF) of alcohol **4.046** with phenol **4.033** then afforded **4.047** in 75% yield.²⁰¹ Deprotonation of **4.047** with *t*-BuLi led to the formation of an intermediate benzyne that underwent cycloaddition to deliver **4.048** in 80% yield. When **4.048** was treated with TBAF in DMF at 70 °C, the tether, which resembles a SEM protecting group, was cleaved, and **4.038** was obtained in 80% yield. Our group is currently applying this two-carbon silicon tether strategy to the synthesis of vineomycinone B₂ methyl ester, a member of the Group I class of *C*-aryl glycosides.

Scheme 4.10

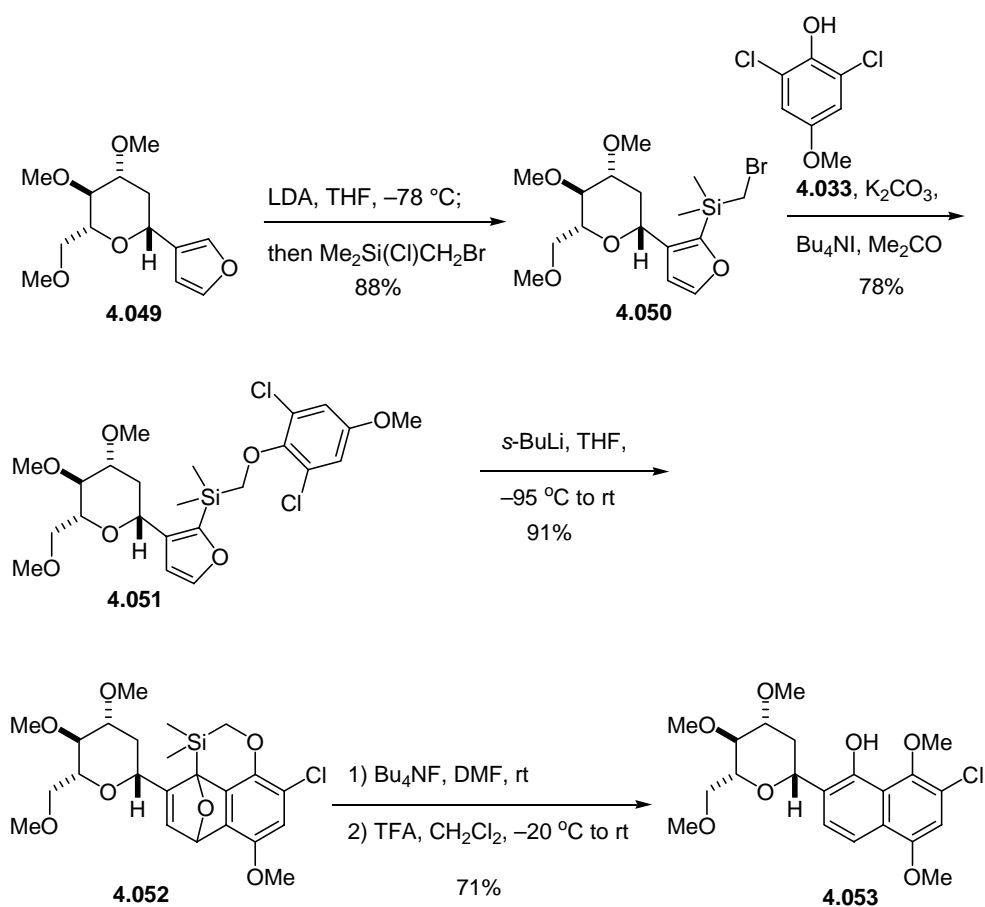


4.2.2 Application to Group II C-Aryl Glycosides

Having developed an effective strategy for the regioselective preparation of Group I C-aryl glycosides, it remained to extend this approach to representative glycosides of Groups II and III. Toward this goal Dr. David Kaelin converted the known

glycosyl furan **4.049**¹⁸¹ into **4.050** by directed metallation (LDA, THF, $-78\text{ }^{\circ}\text{C}$) and reaction with bromomethylchlorodimethylsilane to provide **4.043** in 88% yield (Scheme 4.11). *O*-Alkylation of phenol **4.033** with **4.050** afforded **4.051** in 78% yield. The benzyne generated *in situ* cyclized from **4.051** as before to provide cycloadduct **4.052** in 91% yield as a mixture of diastereomers. Cleavage of both carbon-silicon bonds using TBAF in DMF provided intermediate dimethyl ether that underwent ring opening upon exposure to TFA to afford naphthol **4.053** as a single isomer in 71% yield over the two steps.

Scheme 4.11



4.2.3 Conclusions

Drs. David Kaelin and Steve Sparks were able to apply the tether methodology to the synthesis of Group I and Group II *C*-aryl glycosides. This method could now be used to access unsymmetric *C*-aryl glycoside natural products. However, it was imperative to extend this method to Group III *C*-aryl glycosides of which kidamycin is a member of.

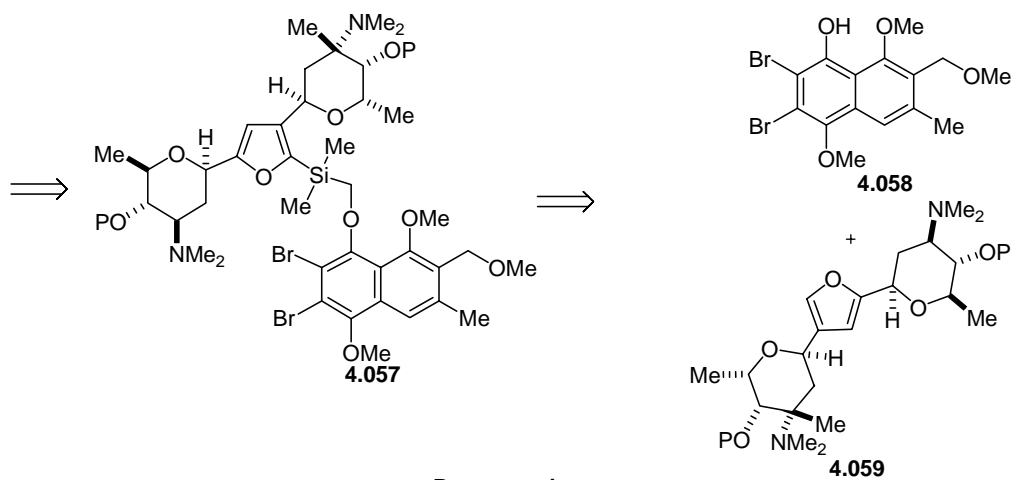
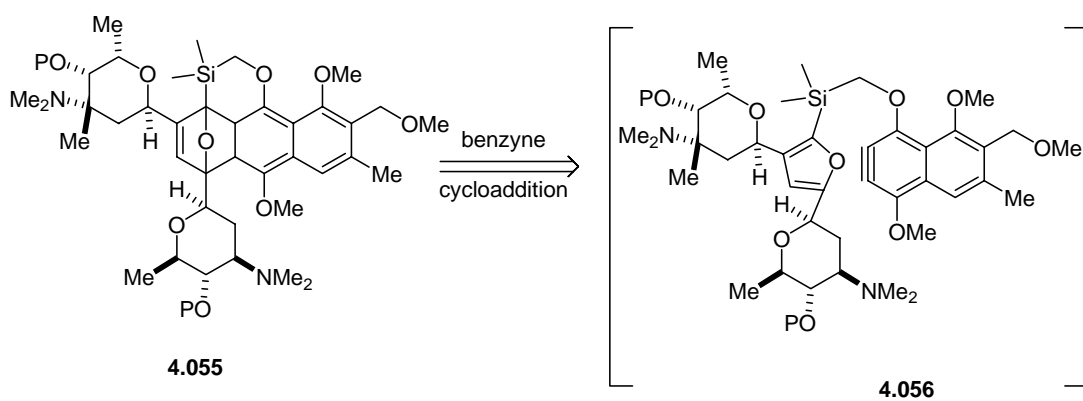
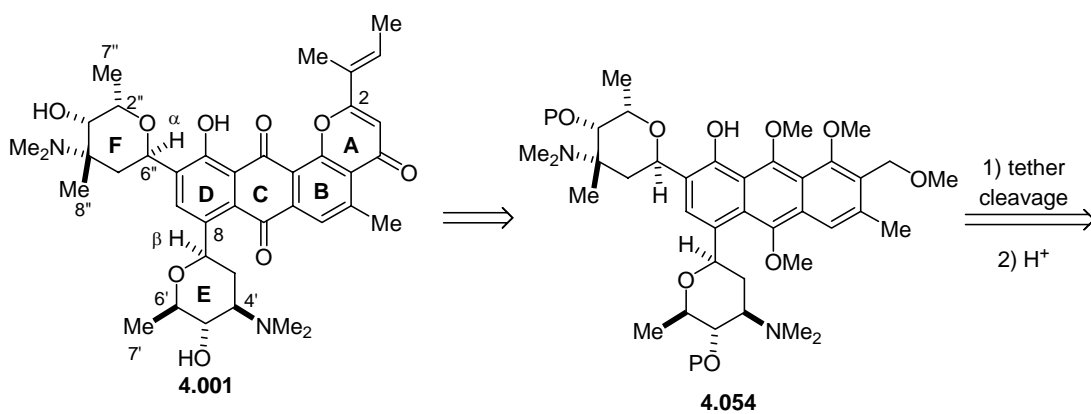
4.3 STUDIES TOWARD THE SYNTHESIS OF KIDAMYCIN

It was previously demonstrated that a disposable tether can be used to produce Group I and II *C*-aryl glycosides in a regioselective manner (see Sections 4.2.1 and 4.2.2). A primary objective of research in the group is to apply this methodology to the synthesis of natural products. This novel tether strategy could be applied to the total synthesis of kidamycin.

4.3.1 Retrosynthesis

Due to instability of the side chain olefin, which was shown to easily isomerize, we planned to install ring 2 at a late stage in the synthesis.¹⁸⁰ Thus, kidamycin (**4.001**) could arise from **4.054** (Scheme 4.12). We envisioned that a benzyne-glycosylfuran cycloaddition using a tether linkage to enforce the correct regiochemistry could afford **4.055**. Cleavage of the tether followed by ring opening would provide phenol **4.054**. The cycloaddition precursor **4.056** can be accessed by coupling 3,5-*bis*-sugar furan **4.059** with **4.058**. The benzyne will be generated from the dibromide array in **4.058**.¹⁸⁰

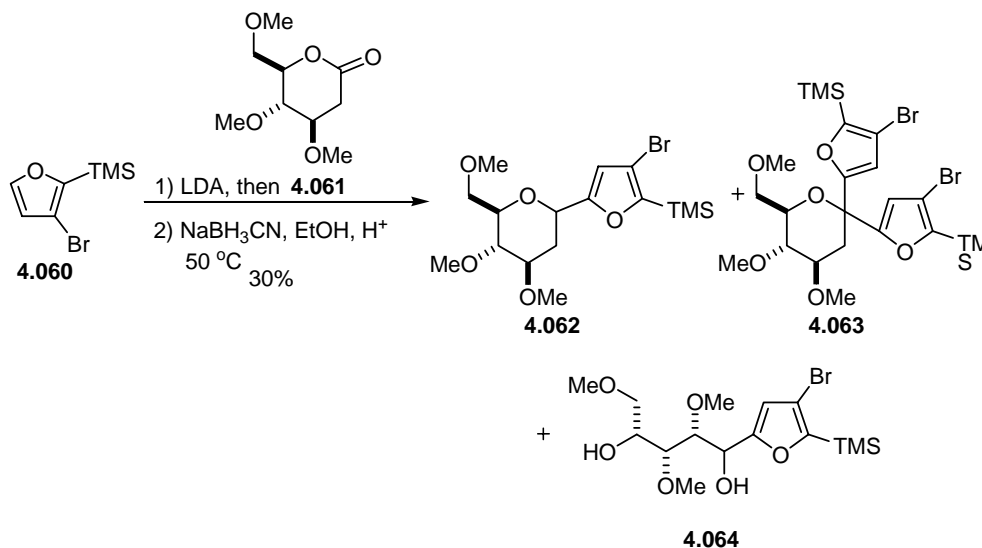
Scheme 4.12



4.3.2 Application of the Tether Methodology to Group III C-Aryl Glycosides

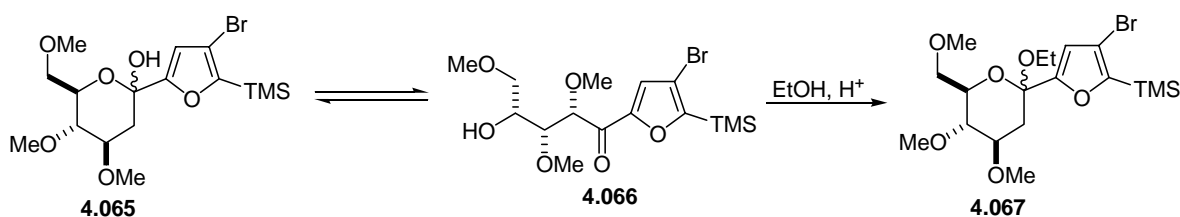
Before undertaking the total synthesis of kidamycin, we wanted to extend our tether methodology previously used to control the regioselectivity in the benzyne cycloadditions to Group III C-aryl glycosides. A *bis*-substituted furan with sugars in the 3- and 5- positions was needed to apply this strategy. The known bromofuran **4.060**²⁰² was deprotonated with LDA, and the anion was treated with sugar lactone **4.061**²⁰³ (Scheme 4.13).¹⁸⁰ The mixture of lactols obtained was reduced with NaBH₃CN in ethanolic HCl at 50 °C. This reaction yielded a mixture of the desired sugar furan **4.062** along with the *bis*-furan **4.063** and the diol **4.064**, which were identified by analysis of the ¹H NMR spectra and low resolution mass spectra. In order to prevent formation of the *bis*-furan sugar **4.063**, the order of addition was modified so that the anion derived from furan **4.060** was added dropwise to a solution of the lactone **4.061** at –78 °C.

Scheme 4.13

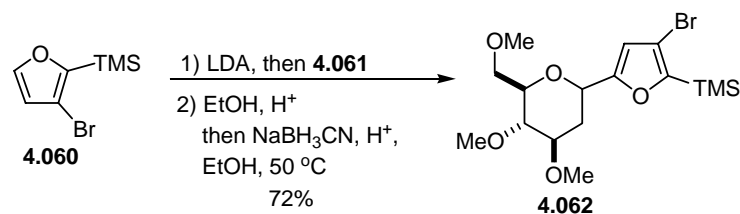


The diol **4.064**, presumably arose from reduction of the open-form of hydroxyketone **4.066** that was in equilibrium with the lactols **4.065** (Scheme 4.14). To prevent the formation of **4.064**, this mixture of **4.065** and **4.066** was treated with ethanolic HCl (cat.), forming the ethyl glycoside. At this point, the reaction was worked up and the ethyl acetals **4.067** were characterized by ^1H NMR spectra and peaks in the low resolution mass spectrum. A one pot procedure was also devised that avoided the problems encountered in the previous experiment. It was discovered that the ethyl acetal can be formed *in situ* by stirring the lactol mixture in acidic EtOH. Thus, deprotonated bromofuran **4.060** was reacted with **4.061**. The products were dissolved in acidic EtOH and reduced with NaBH_3CN in the same pot to afford **4.062** (Scheme 4.15). These modifications improved the yield of **4.062** from 30% to 72%.

Scheme 4.14

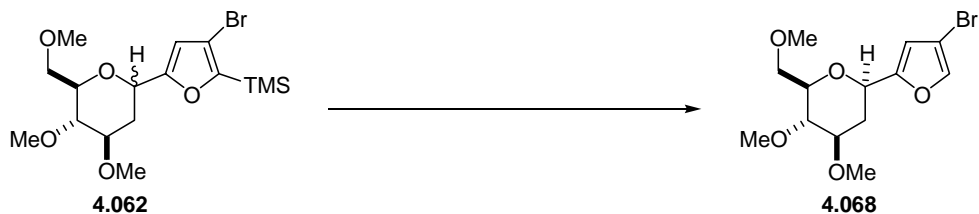


Scheme 4.15



The 2-position of furan **4.062** is blocked by a TMS group and this group needed to be removed. However, cleaving the TMS blocking group at the 2-position of **4.062** to produce the desired bromofuran **4.068** proved problematic (Scheme 4.16). Exposure of **4.062** to TBAF resulted in recovered starting material.²⁰⁴ Treatment of **4.062** with ethanolic HCl also provided no reaction after 12 h as apparent by TLC and ¹H NMR spectra of the crude material. Decomposition of starting material was observed upon prolonged exposure to HCl and TFA. Interestingly, the desired product **4.068** was once isolated in 47% yield after treatment with TFA for 2 days, but this result could not be reproduced. Reaction of **4.062** with TfOH at rt or at 0 °C also resulted in decomposition. Eventually it was found that reaction of **4.062** with TfOH at -78 °C with slow warming to rt formed the desired bromofuran **4.068** in a reproducible 90% yield.

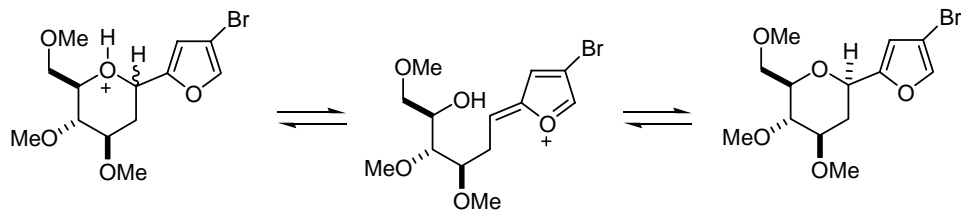
Scheme 4.16



<u>Conditions:</u>	<u>Result:</u>
TBAF, THF, rt	no reaction
H ⁺ , EtOH, rt	no reaction or decomposition
TFA, DCM, 0 °C or rt	no reaction or decomposition
TfOH, DCM, 0 °C or rt	only decomposition
TfOH, DCM, -78 °C	90% yield

A single diastereomer of **4.068** was obtained that likely resulted from epimerization under the acidic conditions to form the more thermodynamically stable product (Scheme 4.17). The ¹H NMR spectra of **4.068** clearly shows only one diastereomer with spectra similar to those reported for other β-glycosides (δ 4.38 ppm as a dd, *J* = 12.0, 1.6 Hz)

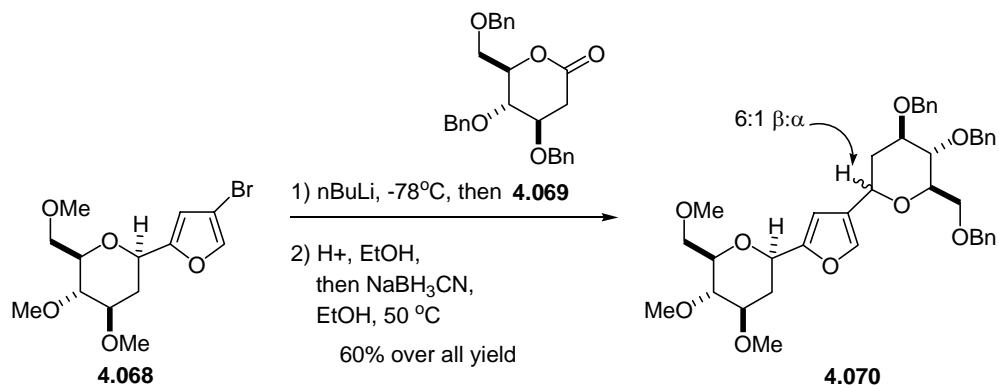
Scheme 4.17



Addition of the anion derived from **4.068** by treating with *n*-BuLi to the lactone **4.069**²⁰⁵ gave a mixture of anomeric lactols. These were converted *in situ* to the ethyl

acetals that were reduced with acidic NaBH_3CN to provide the *bis*-sugar furan **4.070** in 60% overall yield (Scheme 4.18). David Kaelin previously reported the synthesis glycosyl furan **4.070**.^{180,181} Even though he reported that **4.070** was found as a single isomer, closer inspection of the ^1H NMR spectra indicated that **4.070** was actually a 6:1 mixture of epimers (β : α). The mixture could not be separated using column chromatography, but is easily distinguishable by peaks in the ^1H NMR spectra. Namely, the β -anomeric proton in **4.070** is a doublet at 4.6 ppm while the α -anomeric proton is a broad doublet at 5.4 ppm. The ratio of this mixture of anomers could also be determined using HPLC, which gave approximately the same 6:1 ratio. It was of no consequence that **4.070** is an anomeric mixture of compounds because the mixture was expected to equilibrate in the acid-catalyzed ring opening of the oxabicyclic ring to afford only the β -anomer.

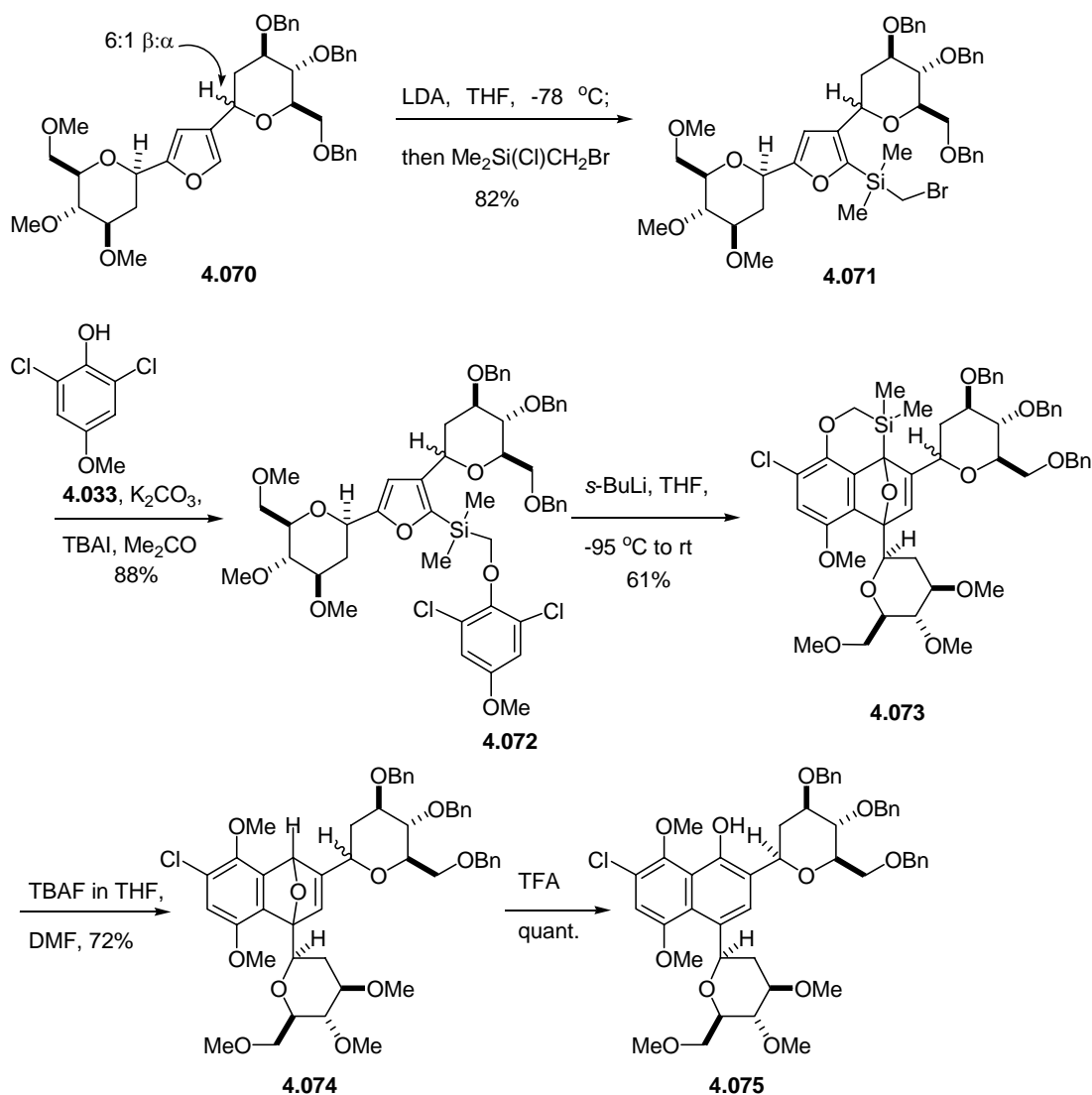
Scheme 4.18



With the *bis*-sugar furan **4.070** in hand, work was directed toward installation of the silyl tether. The mixture of anomers of **4.070** was converted in 82% yield to the furysilanes **4.071** by metallation and silylation as before (Scheme 4.19). The epimeric

mixture could be separated at this stage using column chromatography; however, the mixture was carried forward to demonstrate that the acid-catalyzed ring opening would be accompanied by epimerization to afford a single isomer. Thus, *O*-alkylation of **4.071** in the presence of TBAI and K₂CO₃ with phenol **4.033** provided **4.072** in 88% yield. Deprotonation of **4.072** with *s*-BuLi at -95 °C followed by warming furnished cycloadduct **4.073** as a complex mixture of diastereomers in 61% yield. All carbon-silicon bonds were cleaved with TBAF in DMF to afford **4.074** in 72% yield. Acid-catalyzed ring opening of **4.074** quantitatively furnished the Group III *C*-aryl glycoside **4.075** as a *single* isomer based on ¹H NMR spectra. Thus, the 6:1 ratio of β:α anomers of **4.070** was epimerized to afford the β-*C*-aryl glycoside **4.075**. Chemical shifts and coupling constants in the ¹H NMR are indicative of a β-anomer for both sugars, one anomeric proton is a broad doublet at 5.21 ppm (*J* = 10.2 Hz) while the other is a doublet of doublets at 5.01 ppm (*J* = 11.2, 1.8 Hz). The resonance of the anomeric proton on a α-glycoside is further downfield than the anomeric proton on a β-glycoside due to overlap with the ring oxygen's lone pairs of electrons. In addition, the anomeric proton of a β-glycoside should have two coupling constants, one big (*J* = 10 – 13 Hz) and one small; where as the anomeric proton of a α-glycoside should have only small coupling constant(s). Due to the resolution of the NMR, one of the doublet of doublets is an apparent broad doublet because the second coupling constant is too small to be seen. Now that we have applied the tether methodology to the synthesis of Group III *C*-aryl glycosides, we can approach the synthesis of kidamycin.

Scheme 4.19

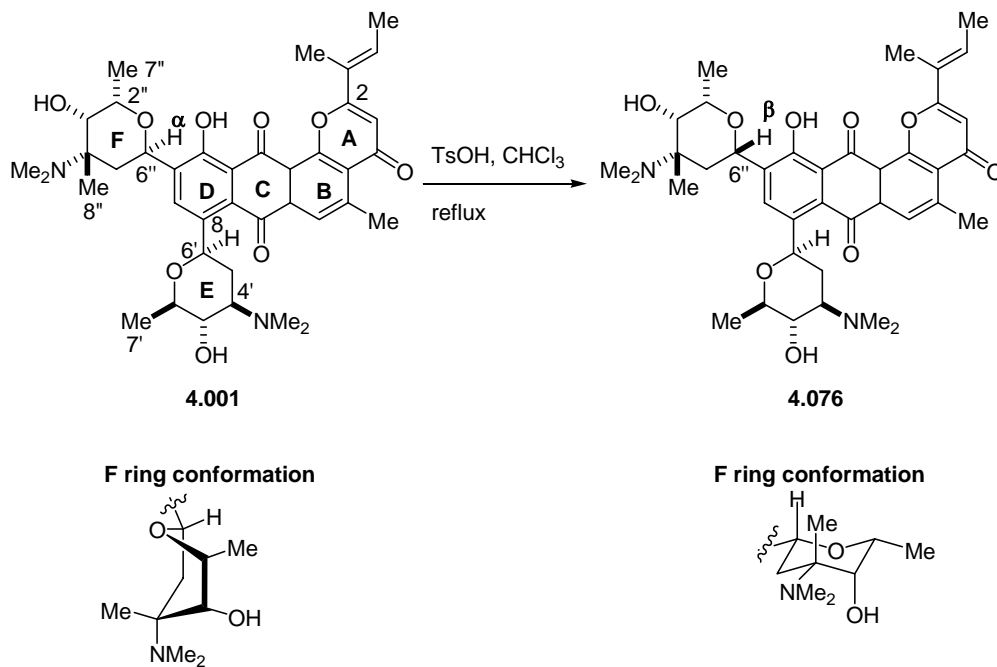


4.3.3 Problem with Tether Methodology

One major hurdle in the proposed synthesis of kidamycin (**4.001**) will be controlling the stereochemistry of the α -anomeric center on the *N,N*-dimethyl vancosamine sugar position 6'' (Figure 4.3). Analysis of an X-ray structure of triacetyl methoxykidamycin reveals that the F ring is in a twist boat conformation (Figure 4.3).²⁰⁶

However, heating kidamycin in the presence of acid causes epimerization at position 6'' to form the more stable β -anomer of ring F and gives isokidamycin **4.076**, which has reduced biological activity. An X-ray structure of a derivative of isokidamycin (isokidamycin bis(*m*-bromobenzoate) confirms this conformation (Figure 4.3).²⁰⁷ The conformation of the E ring sugar is not effected by these acidic conditions because it is already in a stable conformation.

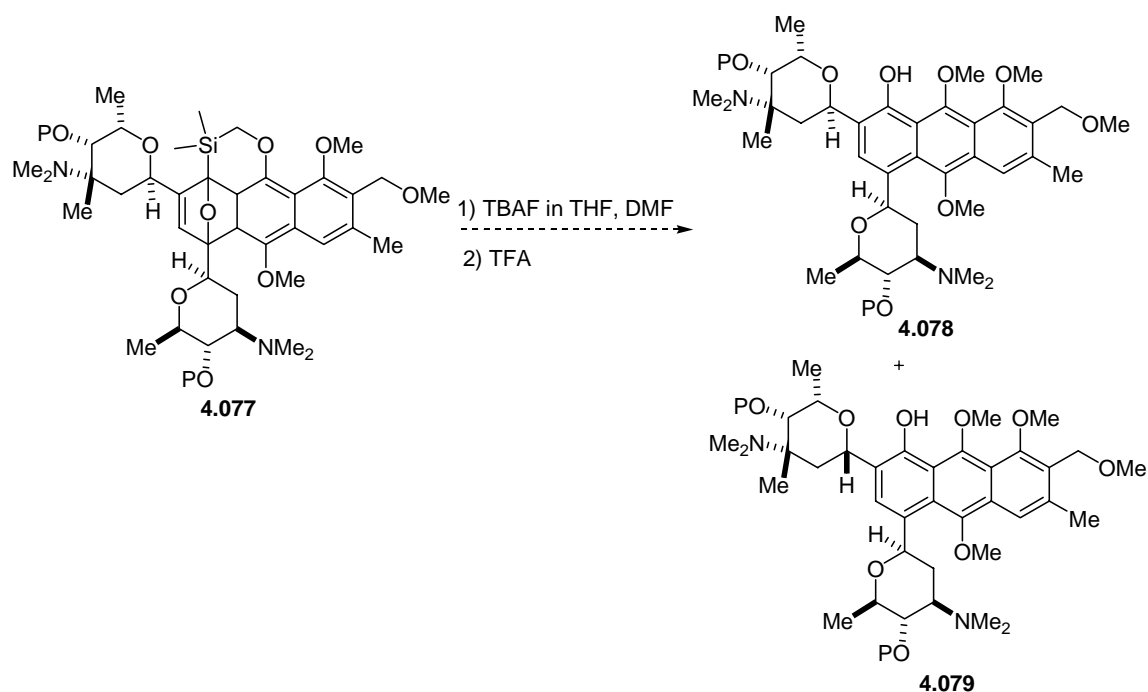
Figure 4.3: A cartoon of the conformations of kidamycin (**4.001**) and isokidamycin (**4.076**).



Since the less thermodynamically stable form of ring F is present in the final product, we were concerned that the acid-catalyzed opening of the oxobicycloheptadiene ring to furnish the glycosyl naphthol in our benzyne-cycloaddition tether methodology might result in the epimerization of C6'' on ring F and form the undesired and unnatural

derivative, even though the condition for our ring opening are milder than the conditions reported for epimerization of **4.001**. For example, reacting cycloadduct **4.077** with TBAF followed by TFA might produce either **4.078** or **4.079** (Scheme 4.20). As we continued to explore our tether strategy toward the synthesis of **4.001** we also began to look at other methods to install the ring F sugar; however, procedures yielding only α -C-aryl glycosides, the thermodynamically less stable epimer, are very rare in the literature.²⁰⁸⁻
210

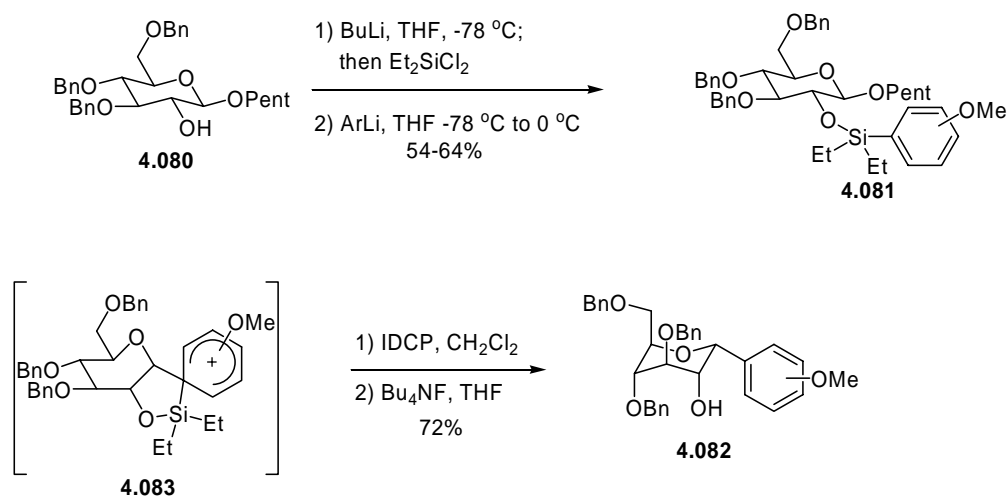
Scheme 4.20



One recent approach to the less stable α -C-aryl glycosides involves intramolecular delivery of an aromatic ring to the anomeric center in the presence of a mild Lewis acid.²¹¹ For example, glucopyranoside **4.080** was converted to the arylsilyl

derivative **4.081** via deprotonation, silylation with Et_2SiCl_2 and treatment with a suitable aryl lithium derivative (Scheme 4.21). When silyl ether **4.081** was reacted sequentially with iodonium dicollidine perchlorate (IDCP), and then Bu_4NF , the α -C-aryl glycoside **4.082** was obtained in 72% yield; no β -anomer was isolated. The authors suggested that the glycosylation reaction occurred by internal substitution of the Ar-Si bond by the electrophilic anomeric carbon atom generated from activation of the pentenyl group with IDCP, thus providing intermediate **4.083**. While this is a useful procedure for the synthesis of gluco derivatives, it cannot be applied to the synthesis of kidamycin without a deoxygenation step since the required substitution on the C2-position of the pyranose ring of both sugars in kidamycin are deoxy; therefore, a different method to install the ring F with the correct stereochemistry would be required.

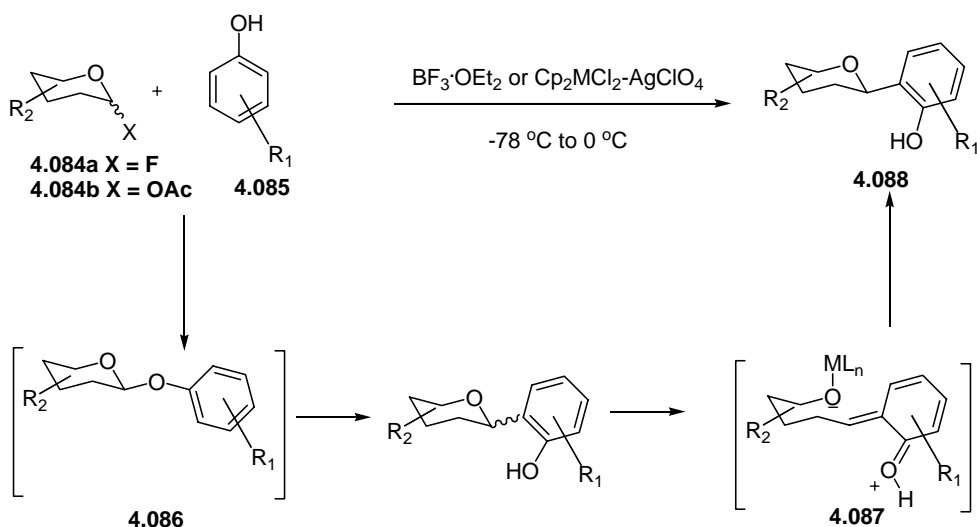
Scheme 4.21



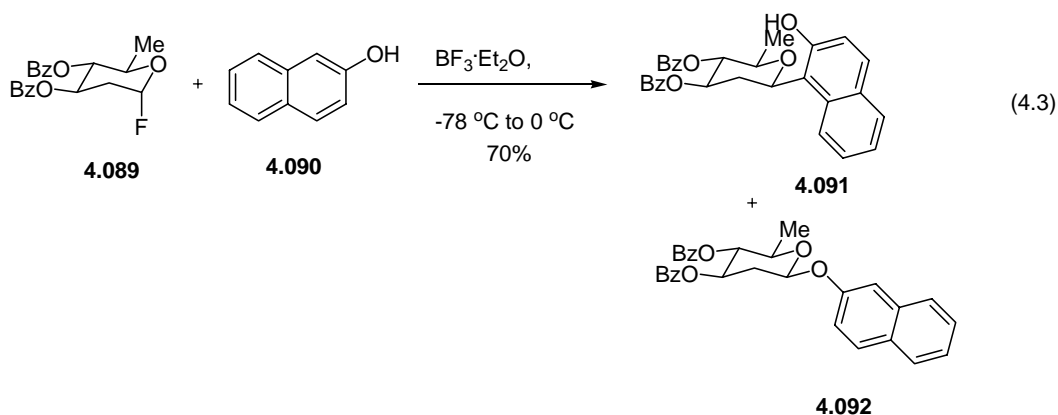
Suzuki has also developed a nice method for preparing C-aryl glycosides via an $O \rightarrow C$ glycoside rearrangement. This process involves a two-step reaction that proceeds in one pot in the presence of a Lewis acid, such as $\text{Cp}_2\text{HfCl}_2\text{—AgClO}_4$ or $\text{BF}_3\cdot\text{OEt}_2$.

The first step features *O*-glycosidation of a sugar derivative like **4.084a** or **b** with phenol **4.084** at low temperature to give the *O*-glycoside **4.086** (Scheme 4.22).^{212,213} **4.086** was then converted *in situ* into *ortho* *C*-aryl glycoside **4.088** by raising the reaction temperature. Warming can allow the reaction to equilibrate, and the $\alpha:\beta$ ratio of **4.088** could be determined not only by kinetics but also by possible contribution of the *ortho*-quinone methide **4.087** and could provide a thermodynamic $\alpha:\beta$ ratio of **4.088**.

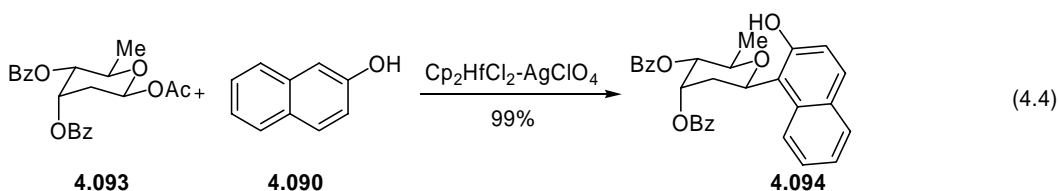
Scheme 4.22



For example, coupling sugar **4.089** with naphthol **4.090** provided the *C*-glycoside **4.090**. When Cp₂HfCl₂-AgClO₄ was used as the promoter, the β anomer **4.091** was isolated in 98% yield (Equation 4.3). However, when BF₃·OEt₂ was used as the promoter, **4.091** was obtained in 70% yield as a 3.4:1 ($\alpha:\beta$) ratio; 28% of the *O*-glycoside **4.092** was also isolated.²¹⁴ 1-Acetyl sugars may also be used as glycosyl donors.²¹⁵



Although acetyl protected sugars are less reactive than fluoro sugars, 1-*O*-acetyl sugars **4.084b** are shelf stable, readily available, and nicely serve as efficient glycosyl donors in the *O* → *C* glycoside rearrangement. For example, **4.93** and **4.090** were coupled to provide the *C*-aryl glycoside **4.094** in 99% yield (Equation 4.4).²¹⁵ The product could be enriched in the α -anomer if the reaction was quenched at low-temperature. Amino sugars have also been shown to work well in the *O* → *C* rearrangement under specific conditions (1:3 molar ration of amino sugar to naphthol and 3:6 ratio of Cp_2HfCl_2 to AgClO_4).²¹⁵

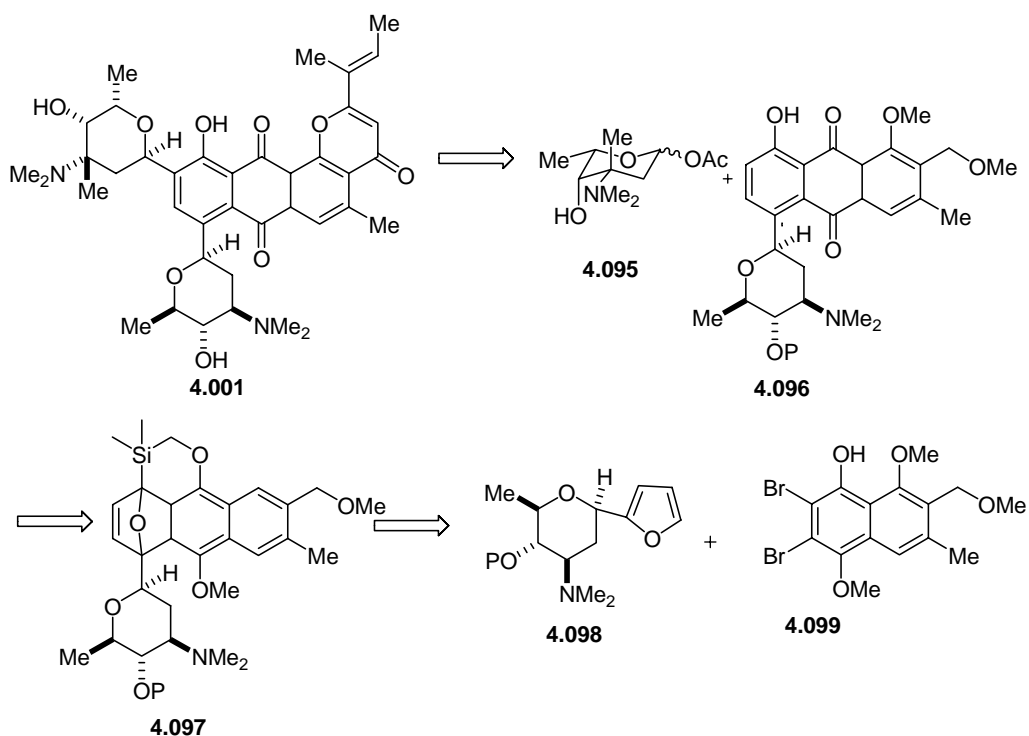


4.3.4 Synthetic Studies of Ring E: Anglosamine

We felt that *O* → *C* glycoside rearrangement could be utilized to install the α -glycoside ring F if we encounter problem with epimerization in our tether approach. Using Suzuki's method could provide an alternative route to kidamycin. Namely,

kidamycin (**4.001**) would arise from the coupling of sugar **4.095** and phenol **4.096** using Suzuki's $O \rightarrow C$ rearrangement procedure (Scheme 4.23). Phenol **4.097** could be obtained from cycloadduct **4.097** though tether cleavage and ring opening. Cycloadduct **4.097** could come from a benzyne Diels-Alder reaction using our newly developed tether protocol to control the regiochemistry of the cycloaddition. Thus, it remained to synthesize the furyl amino glycoside **4.098** and phenol **4.099**.

Scheme 4.23

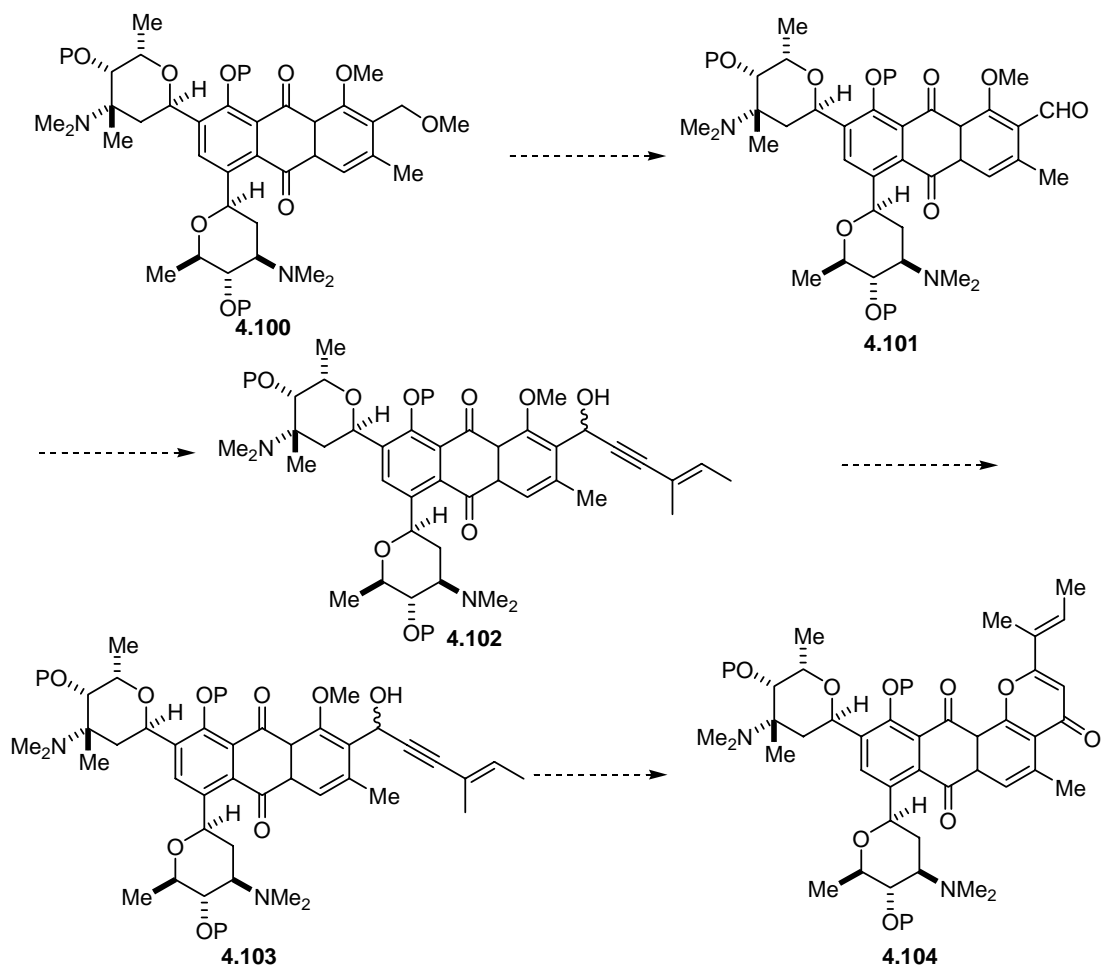


P = protecting group

The methyl ether **4.100** can be converted into ring A in a few steps (Scheme 2.24). Deprotection and oxidation should provide aldehyde **4.101**. Next, alkylation of the aldehyde will install the ene-ynone functionality in **4.102**. Oxidation to the ketone

followed by deprotection of the methyl ether should allow for the intramolecular cyclization to provide **4.104**.

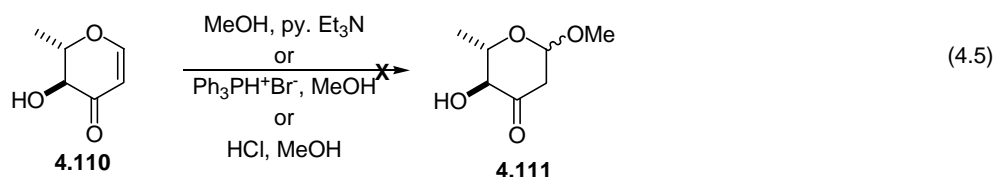
Scheme 2.24



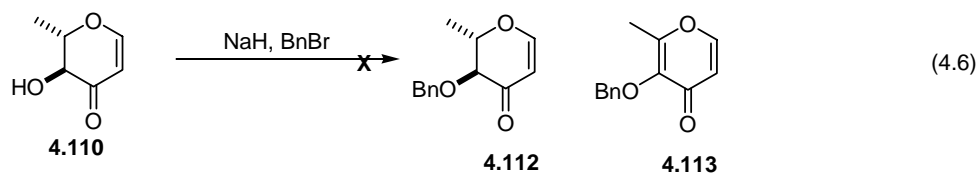
P = protecting group

No one has shown that benzyne chemistry is incompatible with the *N,N*-dimethylamine functionality in ring E of kidamycin. In 2000, Suzuki stated “benzyne chemistry...*might* be precluded by the presence of a dimethylamine function” in his synthesis of ravidomycin with no reference or reason given.²¹⁶ However, this has not

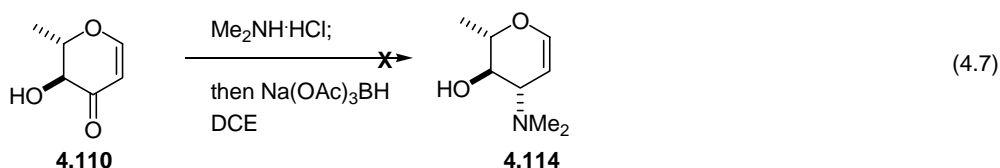
The next step was the installation of an oxygen functionality at the anomeric position of **4.110**. A Michael-type addition was envisioned to achieve this conversion as such reactions had been reported in the literature using both acidic and basic conditions.²¹⁸⁻²²⁰ However, attempts to prepare **4.111** from **4.110** via Michael addition failed under all conditions (Equation 4.5). The most promising experiment involved stirring **4.110** with Ph₃PHBr in MeOH until all starting material disappeared (3 days). An unidentified product was isolated that contained the desired C2 protons, anomeric proton(s) and methoxy peaks in the ¹H NMR, but the peaks in the low resolution mass spectrum did not correspond to **4.110** or **4.111**.



Attempts to protect the C4 hydroxy moiety of **4.110** to provide **4.112** failed under standard conditions (BnBr, NaH) (Equation 4.6). We recovered a compound that was missing signals for the C4 and C5 protons, and the olefinic protons for C1 and C2 were shifted downfield in the ¹H NMR. In the low resolution mass spectrum there was a peak corresponding to product minus 2 protons. The structure of this product has tentatively been assigned as the dienone **4.113**. We suspect that hydroxy ketones are difficult to alkylate due to their low nucleophilicity. In the future, the protection under acidic conditions (BnOC(NH)CCl₃) should be attempted.

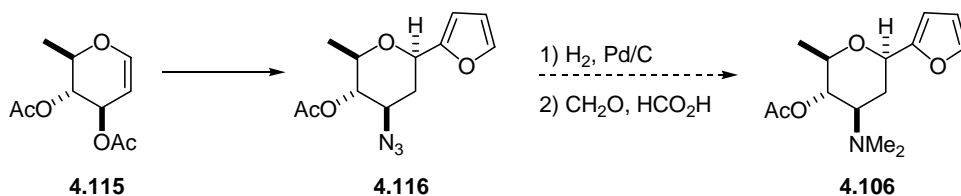


We also tried to effect the reductive amination condition of the enone **4.110** to produce the desired *N,N*-dimethylamine **4.114** using Na(OAc)₃BH; however, nothing useful was recovered (Equation 4.7).²²¹ There are no reported examples of vinylogous esters undergoing reductive aminations in the literature.



In the face these obstacles, this route to furylanglosamine **4.106** was abandoned. In the future it might be possible to convert the azide **4.116**, which was previously obtained in 3 steps from **4.115** in 60% yield,¹⁸⁰ to the desired *N,N*-dimethylamine **4.106** using reductive conditions (Scheme 4.27).²²²

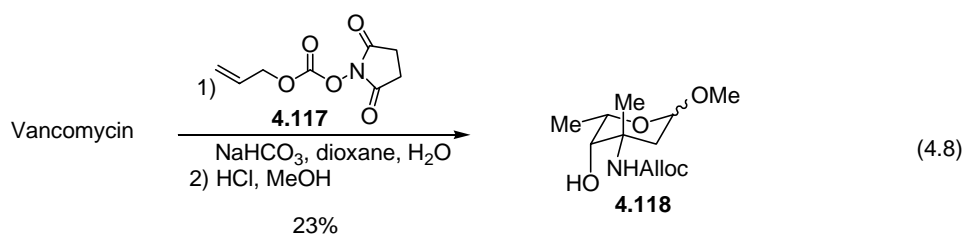
Scheme 4.27



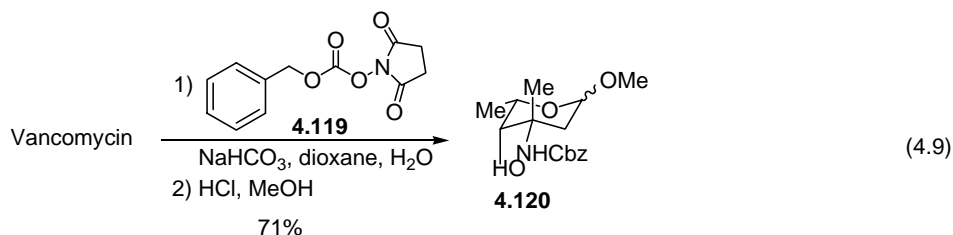
4.3.5 Synthetic Studies of Ring F: *N,N*-Dimethylvancosamine

We planned to obtain the 1-*O*-acetyl-vancosamine (**4.095**) required to apply Suzuki's method to the synthesis of kidamycin through degradation of vancomycin. 1-*O*-Methoxy-*N*-alloc carbamate vancosamine (**4.118**) has been previously obtained by

degradation of vancomycin (Equation 4.8).²²³ Thus, vancomycin hydrochloride was reacted with *N*-allyloxy(carboxyloxy) succinimide (**4.117**) under basic conditions, the product was precipitated from solution by adding acetone, and collected by filtration to give *N,N'*-dialloc vancomycin. The crude material was then subjected to aqueous methanolysis under acidic conditions, and the byproducts were precipitated by adding acetone. The filtrate was further purified using chromatography to give **4.118** together with a number of side products that remained on the baseline. In the literature, the yield reported for this sequence is 115%.²²³ Further purification of the product using flash column chromatography afforded clean **4.118**, albeit in only 30% yield.

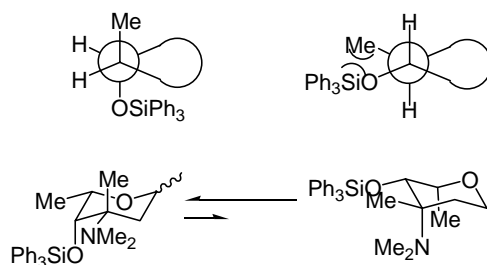


After contacting the Kahne research group, which reported the *N*-alloc vancosamine work, they informed us that they now employ *N*-Cbz derivative in order to obtain the vancosamine sugar from vancomycin. We, therefore, investigated the *N*-Cbz derivative.²²⁴ Thus, vancomycin hydrochloride was allowed to react with *N*-Cbz succinimide (**4.119**) under basic conditions. Adding acetone precipitated the *N,N'*-diCbz vancomycin. The solid then was subjected to acid methanolysis under anhydrous conditions. Once the reaction was complete, the mixture was neutralized with bicarbonate, and the byproducts were precipitated with acetone. The filtrate was purified using flash column chromatography to afford **4.120** in 71% yield as a mixture (1:1.5) of α : β anomers (Equation 4.9).

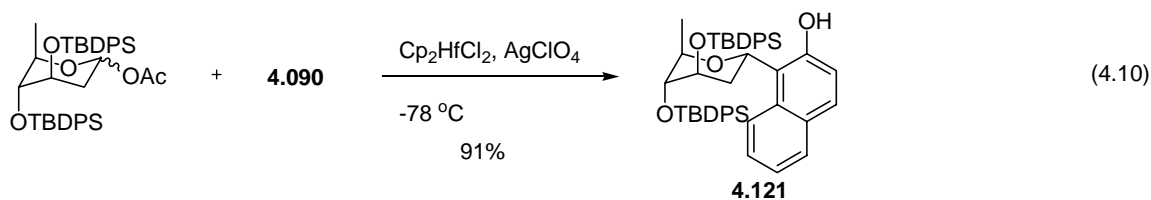


We then decided to install a large silyl protecting group on the 4-hydroxy group because it is reported that large silylethers on pyranosides favor an axial disposition due to the gauche interaction when in the equatorial position (Figure 4.4). In fact a triphenylsilylether has a surprisingly small A value (OSiMe₃: A = 1.31 kcal mol⁻¹ and OSiPh₃: A = 0.71 kcal mol⁻¹).²²⁵

Figure 4.4: The preferred conformation for large silyl ethers.

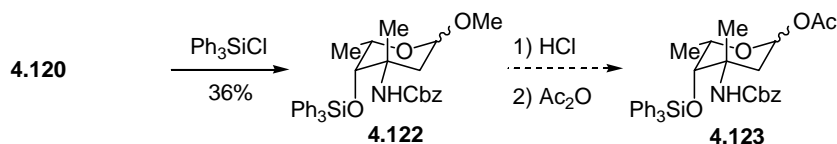


The propensity for bulky silyl-protected hydroxyl groups to prefer axial orientation is exemplified by Suzuki's use a large silyl protecting group to make the α -C-aryl glycoside **4.121** as the sole detectable product in 91% yield; an X-ray structure confirmed the conformation and structure of **4.121** (Equation 4.10).²²⁶



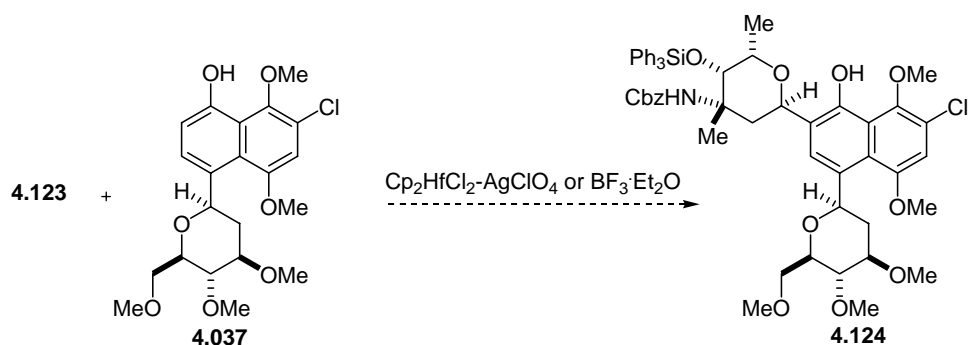
We thus set out to convert **4.120** to **4.122**. However, under varied reaction conditions (Ph_3SiCl , pyridine or Ph_3SiCl , imidazole, DMAP²²⁷), substantial quantities of unreacted starting material were recovered (at least 34% recovered) as shown in Scheme 4.28. In the future, the 1-methoxy group of **4.122** will be converted to the acetate **4.123**. The yield of the silylation may also be improved by heating the reaction or modification of reaction conditions.

Scheme 4.28



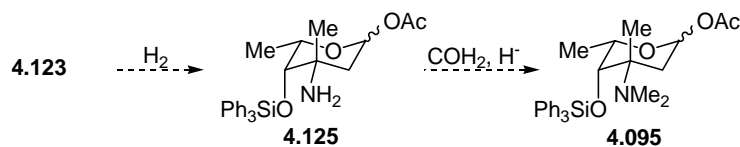
Someone may be able to apply Suzuki's method in order to couple acetate **4.123** with the naphthol **4.037** and may obtain the desired **4.124** in the future (Scheme 4.29).

Scheme 4.29



The α/β ratio for this reaction could be obtained at this point. Additional steps for the synthesis of **4.095** include removal of the *N*-Cbz carbamate with hydrogenolysis giving amine **4.125** and conversion to the *N,N*-dimethyl derivative **4.095** (Scheme 4.30).

Scheme 4.30



Hopefully in the future, we will attempt the $O \rightarrow C$ glycoside rearrangement to provide **4.109** and hope for enrichment in the α -anomer (Scheme 4.31).

Scheme 4.31



4.4 CONCLUSIONS AND FUTURE DIRECTIONS

The Martin group has developed a facile approach to *C*-aryl glycosides using a disposable tether to control the regiochemistry of a benzyne cycloaddition that allows access to unsymmetrically substituted Group I and II *C*-aryl glycoside natural products. In the present work, this methodology was applied to the synthesis of Group III *C*-aryl glycosides. The synthesis of the *bis*-sugar furan **4.070** was improved, and **4.070** was found to be a mixture of anomers. The application of this method to the synthesis of kidamycin is underway. Toward that end, some potential precursors for the ring E anglosamine and ring F *N,N'*-dimethylvancosamine were prepared. In the future, Suzuki's *O* → *C* glycoside rearrangement may be used to obtain the desired stereochemistry of the ring F sugar. In addition, an unprecedented benzyne Diels-Alder cycloaddition in the presence of an amine might be used to install ring E. It is still unknown if novel tether methodology can be applied to the synthesis of this interesting natural product, but with some work in the future we may have success to report.

Chapter 5. Experimentals

5.1 BIOLOGICAL MATERIALS AND METHODS

5.1.1 Materials

Escherichia coli cells, (SG13009, lon⁻) containing the GE-60 plasmid, were obtained from Schering-Plough Research Institute (Kenilworth, NJ). Isopropyl- β -D-thiogalactopyranoside (IPTG), was obtained from Acros/Fischer Scientific (Houston, TX). Ethylenediaminetetraacetic acid (EDTA) was obtained from Fischer Scientific (Houston, TX). Kanamycin was purchased from SIGMA (St. Louis, MO). The phosphotyrosine affinity column was synthesized using NHS-activated Sepharose 4 Fast Flow (Pharmacia Biotech, Piscataway, NJ) as described in the instruction manual (NHS-activated Sepharose 4 Fast Flow INSTRUCTIONS). The MCS isothermal titration calorimeter was obtained from MicroCal Corp. (Northampton, MA)

5.1.2 Methods

Bacterial Expression. *E coli* cells, (SG13009, lon⁻) containing the GE-60 plasmid with a T5 promoter and the grb2-sh2 domain gene (primary amino acid sequence 53-163) were spread onto LB plates with kanamycin at 50 μ g/mL and ampicillin at 100 μ g/mL (LB^{kan50/amp100}) and incubated at 37 °C for 24 h. One colony from the plate was selected and grown in 30 mL LB^{kan50/amp100} at 30 °C overnight (18 h) to make a starter culture that was poured into 1 L LB^{kan50/amp100} and grown at 30 °C at 225 rpm until an OD₆₀₀ of 0.5 - 0.8 was obtained (approximately 3 - 4 h). The cultures were induced with 1 mM IPTG (234 mg) and grown at 30 °C and 225 rpm for 7 - 18 h. The cells were centrifuged, and the pellet was stored at -78 °C.

*Purification of the Isolated Grb2-SH2 domain from E coli.*⁵³ The pellet was resuspended in buffer A (25 mM Tris, pH 7.5) (22 mL) containing 1 mM EDTA. A French Press (2 passages with 1,000 pressure each time) was used to lyse the cells (Sonication was an irreproducible method for lysing the cells). Following centrifugation of the cell lysate, the supernatant containing soluble Grb2-SH2 protein was applied to a Q-Sepharose column using FPLC. The column was washed with 10 mL buffer A, and sample containing Grb2-SH2 protein was recovered from unbound fractions. These fractions were directly applied to the phosphotyrosine affinity column using FPLC. This column was washed with buffer A, and the protein was eluted with buffer B (25 mM Tris, 200 mM NaCl, pH 7.5). The Grb2-SH2 fractions were > 98% pure, based on SDS-PAGE Coomassie-stained gels. The fractions were pooled, concentrated and dialyzed against 50 mM HEPES, 150 mM NaCl, pH 7.5. ($\epsilon = 15600 \text{ M}^{-1} \text{ mL}^{-1}$ or $1.2 \text{ mg}^{-1} \text{ mL}^{-1}$). In a typical experiment, purification would yield approximately 15 – 30 mg of protein per L of LB broth.

5.1.3 Isothermal Titration Calorimetry:

Calorimetry experiments were performed with an MCS titration calorimeter (Microcal Inc., Northampton, MA) as described.^{53,54,105,121} Grb2-SH2 was dialyzed for 48 h with two exchanges of buffer (50 mM HEPES, 150 mM NaCl, pH 7.5) (1/1000 v/v). To reduce errors arising from heats of dilution due to buffer differences between samples in the syringe and the stirred vessel, lyophilized peptide ligands were suspended in the final dialysate from the Grb2-SH2 sample. Protein and ligand solutions were degassed with stirring under reduced pressure for 15 min. For a typical titration, Grb2-SH2 domain (50 μM) was placed in the 1.4 mL reaction cell, and the ligand (0.7 mM) was loaded into the 250 μL injection syringe. The solutions of ligands were injected in 4-

6 μL increments. At least five injections were typically performed after saturation was observed. All values are the result of at least three independent titration experiments. The data for each titration were collected and processed with the ORIGIN software provided with the calorimeter. The titration curves were fit using the same software to give ΔH and K_a (see Appendix for examples). For each ligand, at each experimental temperature, a blank was run where the ligand was injected into buffer alone to establish the nonzero heat of dilution for the ligand. This heat was subtracted from the raw titration data prior to fitting. The integrated data from all experiments fits the single-site binding model with the stoichiometry of binding being between 0.95 and 1.12 for all titrations. The estimated experimental error associated with each titration experiment is approximately 5 – 10%.²²⁸⁻²³⁰

5.1.4 In P:

Volume fraction octanol to water partition coefficients were measured. Pseudopeptides were dissolved dialysate buffer from the Grb2-SH2 samples (See Section 5.1.3). Due to the pKa of phosphotyrosine, the pH of the buffer was changed from 7.5 to 2.0 by adding HCl.^{170,171} At pH 7.5, no pseudopeptide was present in the octanol phase. The final concentration of the buffer solutions was 0.7 mM. The buffer ligand solution was saturated with octanol by adding 10 μL of octanol to the solution to provide the pseudopeptide stock solution. Octanol was also saturated with buffer by adding 10 μL of the buffer to the octanol to provide the octanol solution. Solutions of pseudopeptide stock (1 mL) and octanol (1 mL) were placed in a screw cap vial mixed for 12 h at 225 rpm and 25 °C. After equilibration, the concentrations of the pseudopeptide in the buffer phase and in the pseudopeptide stock solution were measured using a UV/vis spectrometer. The A_{280} was recorded in triplicate and averaged. The volume formation partition coefficients are defined by $P = P_b/P_o$ where P_b and P_o are the pseudopeptide

concentrations in the buffer and octanol phases, respectively. The pseudopeptide concentration in the octanol phase was determined indirectly by comparing the concentration in the buffer phase with that of the pseudopeptide stock solution so that $P = P_b / (P_s - P_b)$ where P_s is the relative concentration of the pseudopeptide in the stock solution. The mole-fraction partition coefficients were calculated from the P by multiplying the value by 0.114 (the ratio of the molar volumes of water and octanol). The values were then converted into free energy using $\Delta G = -RT \ln (P * 0.114)$ and shown in Table 5.1.^{35,37}

Table 5.1: Partition Coefficients for pseudopeptides.

compound	P	ΔG kcal mol ⁻¹
2.004	1.03	1.28
2.005	0.886	1.37
	difference	-0.09

5.2 ORGANIC SYNTHESIS

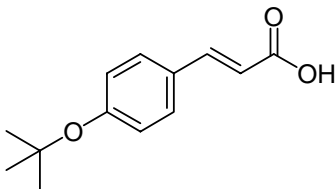
5.2.1 General

Solvents and reagents were reagent grade and were used without purification unless noted otherwise. Tetrahydrofuran (THF) and ether (Et₂O) were dried by passage through two columns of activated neutral alumina. Methanol (MeOH), acetonitrile (CH₃CN) and *N, N*-dimethylformamide (DMF) were dried by passage through two columns of activated molecular sieves. Triethylamine (Et₃N), *N*-methylmorpholine (NMM), 2,6-lutidine and diisopropylethylamine (*i*Pr₂NEt) were distilled from calcium hydride. Trifluoromethanesulfonic anhydride (Tf₂O) was distilled from phosphorus

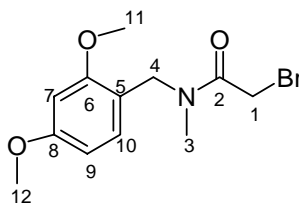
pentoxide. Trifluoroacetic acid (TFA) was distilled prior to use. Toluene was dried by sequential passage through a column of activated neutral alumina followed by a column of Q5 reactant. Reactions involving air- or moisture-sensitive reagents or intermediates were performed under argon in glassware that had been flame-dried. Solvents were removed under reduced pressure with rotary evaporation at 15 mm Hg (30 °C bath temp). Flash chromatography was performed following the Still²³¹ protocol with the indicated solvents and Merck 250-400 mesh silica gel. Analytical TLC was performed with Merck-60 TLC plates and the indicated solvents.

Melting points were determined on a Thomas-Hoover melting point apparatus and are uncorrected. Infrared (IR) spectra were obtained using a Perkin-Elmer FTIR 1600 series spectrometer as solutions in CHCl₃ or CDCl₃. Proton (¹H) and Carbon 13 (¹³C) nuclear magnetic resonance (NMR) were obtained using a Varian Unity Plus (300 MHz) or Varian Unity Plus (500 MHz) spectrometer as solutions in CDCl₃, unless otherwise indicated. Chemical shifts are reported in parts per million (ppm, δ) and are referenced relative to the 7.26 ppm resonance of CDCl₃ for ¹H and center of the triplet resonance of CDCl₃ at 77.0 ppm unless otherwise indicated. Coupling constants are reported in hertz (Hz). Splitting patterns are designated as s, singlet; d, doublet; t, triplet; q, quartet; p, pentuplet; hep, heptet; m, multiplet; comp, complex multiplet; br, broad; app, apparent. Low-resolution chemical ionization mass (CI) or fragment atomic bombardment (FAB) spectra were obtained on a Finnigan TSQ-70 instrument. High-resolution chemical ionization mass spectra (HR) were obtained on a VG Analytical ZAB-2E instrument.

5.2.2 Compounds



3-(4-*tert*-Butoxyphenyl)acrylic acid. (hrp1-045). A mixture of Na₂CO₃ (3.22 g, 30.4 mmol), acrylic acid (1.03 mL, 15 mmol), *tert*-butylammonium bromide (161.19 mg, 0.5 mmol), palladium (II) chloride (18 mg, 0.1 mmol) and 4-*tert*-butoxyphenyl bromide (**2.019**) (2.29 g, 10 mmol) in freshly distilled H₂O (59 mL) under argon was stirred vigorously at rt for 15 min and then heated under reflux for 14.5 h. The reaction mixture was then cooled to rt and filtered through a pad of Celite. The pad was washed with sat. NaHCO₃ (2 x 25 mL). The filtrate and washings were washed with Et₂O (1 x 25 mL) and then acidified with 1 M HCl to pH 1.0. The aqueous layer was extracted with Et₂O (3 x 25 mL). The organic layers were combined, washed with brine (1 x 25 mL), dried (NaSO₄) and concentrated under reduced pressure to yield 1.89 g of 3-(4-*tert*-Butoxyphenyl)acrylic acid as a white solid (85.5%).¹²¹



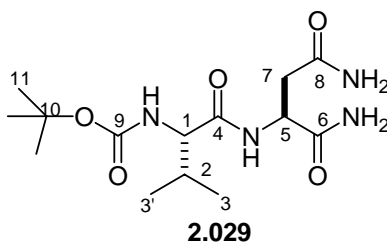
2.022

2-Bromo-*N*-(2,4-dimethoxybenzyl)-*N*-methyl acetamide (2.022). Et₃N (20 mL, 150 mmol) and bromoacetyl bromide (2.18 mL, 25 mmol) were added to **2.021**¹²¹ (5.4 g, 25 mmol) in CHCl₃ (200 mL) at -78 °C. The reaction was stirred at -78 °C for 30 min and then the cold bath was removed and the reaction slowly warmed to rt over 1 h. H₂O (50 mL) was then added and the layers were separated. The organic layer was washed with 2 M HCl (1 x 50 mL), sat. NaHCO₃ (1 x 50 mL), brine (1 x 50 mL), dried (MgSO₄) and then concentrated under reduced pressure to yield 4.65 g of **2.022** as a yellow oil (62%). Compound exists as a mixture (40:60) of 2 rotamers at rt; ¹H NMR (500 MHz) δ 7.15, (d, *J* = 8.9 Hz, 0.4 H), 7.00 (d, *J* = 8.7 Hz, 0.6 H), 6.47- 6.44 (comp, 2 H), 4.54 (s, 0.8 H), 4.46 (s, 1.2 H), 4.03 (s, 1.2 H), 3.89 (s, 0.8 H), 3.80-3.78 (comp, 6 H), 3.00 (s, 0.8 H), 2.88 (s, 1.2 H); ¹³C NMR (125 MHz) δ 166.8, 166.4, 160.7, 160.2, 158.3, 158.4, 130.1, 129.0, 116.8, 115.8, 104.1, 103.9, 98.5, 98.1, 55.1, 49.6, 45.3, 41.4, 35.4, 33.3, 26.6, 26.4; IR (CHCl₃) 3003, 1645, 1614, 1507, 1464, 1158 cm⁻¹; mass spectrum (CI) *m/z* 302.0396 [C₁₂H₁₇NO₃Br (M+1) requires 302.0392], 302, 222.

NMR Assignments. Rotamer 1 (40%) ¹H NMR (500 MHz) δ 7.15, (d, *J* = 8.9 Hz, 0.4 H, C7-H), 6.47-6.44 (comp, 2 H, C9-H & C10-H), 4.54 (s, 0.8 H, C4-H), 3.89 (s, 0.8 H, C1-H), 3.80-3.78 (comp, 6 H, C11-H & C12-H), 3.00 (s, 0.8 H, C3-H); ¹³C NMR (125 MHz) δ 166.4 (C2), 160.2 (C8, C6 or C5), 158.3 (C8, C6 or C5), 130.1

(C7), 116.8 (C8, C6 or C5), 103.9 (C9 or C10), 98.1 (C9 or C10), 55.1 (C11 & C12), 45.3 (C4), 35.4 (C3), 26.6 (C1).

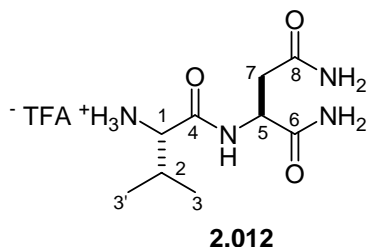
NMR Assignments. Rotamer 2 (60%) ^1H NMR (500 MHz) δ 7.00 (d, $J = 8.7$ Hz, 0.6 H, C7-H), 6.47- 6.44 (comp, 2 H, C9-H & C10-H), 4.46 (s, 1.2 H, C4-H), 4.03 (s, 1.2 H, C1-H), 3.80-3.78 (comp, 6 H, C11-H & C12-H), 2.88 (s, 1.2 H, C3-H); ^{13}C NMR (125 MHz) δ 166.8 (C2), 160.7 (C8, C6 or C5), 158.4 (C8, C6 or C5), 129.0 (C7), 115.8 (C8, C6 or C5), 104.1 (C9 or C10), 98.5 (C9 or C10), 49.6 (C11 & C12), 41.4 (C4), 33.3 (C3), 26.4 (C1).



(1S, 1'S)-[1-(1, 2)-Dicarbamoylethylcarbamoylethyl]-2-methylpropyl carbamic acid *tert*-butyl ester (2.029). (hrp1-084). *N*-Methylmorpholine (NMM) (0.3 mL, 3.0 mmol), 1-(3-(dimethylamino)propyl]-3-ethylcarbodiimide hydrochloride (EDC) (210 mg, 1.1 mmol) and 1-hydroxybenzotriazole hydrate (HOBT) (270 mg, 2 mmol) were added to a solution of Boc-Valine (217 mg, 1.0 mmol) in DMF (30 mL) at -10 °C (ice-salt bath). The mixture was stirred at -10 °C for 1 h, and then asparagine-amide-HCl salt (218 mg, 1.3 mmol) was added. The mixture was stirred at -10 °C for 30 min and then at rt for 16 h. The mixture was concentrated under reduced pressure, and the yellow residue was triturated with sat. NaHCO_3 (2 x 15 mL), 0.5 M HCl (2 x 15 mL), and H_2O (1 x 10 mL) to yield 237 mg of **2.029** (72%) as a white solid: mp 200-205 °C, dec; ^1H NMR (300 MHz, CD_3OD) δ 4.70 (t, $J = 5.7$ Hz, 1 H), 3.80 (d, $J = 6.0$ Hz, 1 H), 2.81-2.66 (comp, 2

H), 2.10-2.01 (comp, 1 H), 1.45 (s, 9 H), 0.95 (dd, $J = 9.0, 6.9$ Hz, 6 H); ^{13}C NMR (75 MHz, DMSO- d_6) δ 172.8, 171.8, 171.0, 155.9, 78.4, 60.3, 49.4, 36.6, 29.9, 28.2, 19.1, 18.0; mass spectrum (CI) m/z 331.1975 [$\text{C}_{14}\text{H}_{27}\text{N}_4\text{O}_5$ (M+1) requires 331.1981], 275 (base), 231.

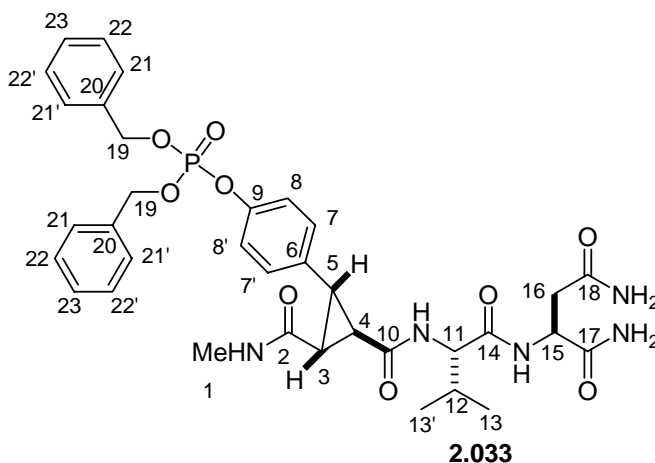
NMR Assignments. ^1H NMR (300 MHz, CD_3OD) δ 4.70 (t, $J = 5.7$ Hz, 1 H, C5-H), 3.80 (d, $J = 6.0$ Hz, 1 H, C1-H), 2.81-2.66 (comp, 2 H, C7-H), 2.10-2.01 (comp, 1 H, C2-H), 1.45 (s, 9 H, C11-H), 0.95 (dd, $J = 7.0, 9.0$ Hz, 6 H, C3-H & C3'-H); ^{13}C NMR (75 MHz, DMSO) δ 172.8 (C6, C8 or C4), 171.8 (C6, C8 or C4), 171.0 (C6, C8 or C4), 155.9 (C9), 78.4 (C10), 60.3 (C1), 49.4 (C5), 36.6 (C7), 29.9 (C2), 28.2 (C11), 19.1 (C3), 18.0 (C3').



(1S, 1'S)-1-(1, 2)-Dicarbamoylethylcarbamol)-2-methylpropyl ammonium trifluoroacetate salt (2.012). (hrp1-157). A solution of **2.029** (94 mg, 0.285 mmol) in neat TFA (1 mL) was stirred for 2 h at rt. The reaction mixture was concentrated under reduced pressure. The white foam residue was recrystallized in hot isopropyl alcohol (3 mL) to yield 94 mg of **2.012** (96%) as a white powder: mp 125-127 °C; ^1H NMR (300 MHz, CD_3OD) δ 4.77 (dd, $J = 8.2, 5.8$ Hz, 1 H), 3.70 (d, $J = 6.8$ Hz, 1 H), 2.78 (dd, $J = 15.9, 5.8$ Hz, 1 H), 2.67 (d, $J = 15.9, 8.2$ Hz, 1 H), 2.21 (app hep, $J = 6.9$ Hz, 1 H), 1.04 (t, $J = 6.9$ Hz, 6 H); ^{13}C NMR (75 MHz, CD_3OD) δ 175.0, 174.6, 169.5, 59.7, 51.4, 37.8,

31.5, 18.9, 17.9; IR 3407, 1668, 1208, 1138 cm^{-1} , mass spectrum (CI) m/z 231.1457 [$\text{C}_9\text{H}_{19}\text{N}_4\text{O}_3$ (M+1) requires 231.1457], 232, 246, 214, 115.

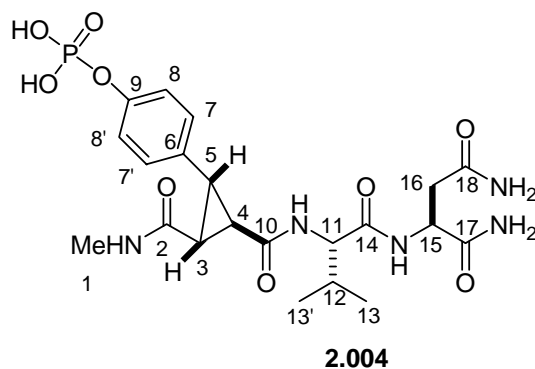
NMR Assignments. ^1H NMR (300 MHz, CD_3OD) δ 4.77 (dd, $J = 8.2, 5.8$ Hz, 1 H, C5), 3.70 (d, $J = 6.8$ Hz, 1 H, C1), 2.78 (dd, $J = 15.9, 5.8$ Hz, 1 H, C7-H), 2.67 (d, $J = 15.9, 8.2$ Hz, 1 H, C7'-H), 2.21 (app hep, $J = 6.9$ Hz, 1 H, C2), 1.04 (t, $J = 6.9$ Hz, C3 & C3'); ^{13}C NMR (75 MHz, CD_3OD) δ 175.0 (C6, C8 or C4), 174.6 (C6, C8 or C4), 169.5 (C6, C8 or C4), 59.7 (C1), 51.4 (C5), 37.8 (C7), 31.5 (C2), 18.9 (C3), 17.9 (C3').



(1R, 2S, 3R, 1S', 1S'') Phosphoric acid dibenzyl ester 4-{2-[1-(1,2-dicarbamoylethylcarbamoyl)-2-methylpropylcarbamoyl]-3-methylcarbamoyl cyclopropyl}phenyl ester (**2.033**). (hrp1-187). 2,6-Lutidine (14 mg, 15 μL , 0.13 mmol) and then HATU (16 mg, 0.042 mmol) were added to a solution of **2.012** (15 mg, 0.042 mmol) and **2.012** (21 mg, 0.042 mmol) in DMF (1 mL) at -10 $^{\circ}\text{C}$ (ice-salt bath). The mixture was stirred at -10 $^{\circ}\text{C}$ for 1 h and then stirred at rt for 12 h. The mixture was concentrated under reduced pressure, and the yellow residue was triturated with sat. NaHCO_3 (2 x 15 mL), 0.5 M HCl (2 x 15 mL), and H_2O (1 x 10 mL) to yield 26 mg of # (87%) as a white solid: mp 226-227 $^{\circ}\text{C}$, dec; ^1H NMR (300 MHz, DMSO-d_6) δ 8.53 (d,

$J = 7.6$ Hz, 1 H), 8.11 (d, $J = 8.0$ Hz, 1 H), 8.09-8.06 (m, 1 H), 7.41-7.35 (comp, 10 H), 7.29-7.28 (comp, 3 H), 7.06-7.00 (comp, 4 H) 6.82 (br s, 1 H), 5.12 (d, $J = 8.2$ Hz, 4 H), 4.44 (dd, $J = 14.0, 6.0$ Hz, 1 H), 4.07 (t, $J = 6.6$ Hz, 1 H), 3.02-2.99 (m, 1 H), 2.59 (dd, $J = 9.6, 6.0$ Hz, 1 H), 2.61-2.43 (comp, 5 H), 2.38-2.35 (m, 1 H), 2.00 (app hep, $J = 6.6$ Hz, 1 H), 0.88 (d, $J = 6.6$ Hz, 6 H); ^{13}C NMR (75 MHz, DMSO- d_6) δ 172.8, 171.7, 171.0, 170.6, 167.3, 148.6, 135.7, 135.6, 133.2, 130.4, 128.5, 128.0, 119.0, 69.3, 58.8, 49.5, 36.6, 30.1, 29.9, 25.7, 25.6, 19.1, 18.1; mass spectrum (CI) m/z 708.2789 [$\text{C}_{35}\text{H}_{43}\text{N}_5\text{O}_9\text{P}$ (M+1) requires 708.2798], 273 (base), 545.

NMR Assignments. ^1H NMR (300 MHz, DMSO) δ 8.53 (d, $J = 7.6$ Hz, 1 H, N-H), 8.11 (d, $J = 8.0$ Hz, 1 H, N-H), 8.09-8.06 (m, 1 H, N-H), 7.41-7.35 (comp, 10 H, C21-H & C21'-H, C22-H & C22'-H & C23-H), 7.29-7.28 (comp, 3 H, C7-H, C7'-H or C8-H, C8'-H & N-H), 7.06-7.00 (comp, 4 H, C7-H, C7'-H or C8-H, C8'-H & N-H) 6.82 (br, 1 H, N-H), 5.12 (d, $J = 8.2$ Hz, 4 H, C19-H), 4.44 (dd, $J = 6.0, 14.0$ Hz, C15-H), 4.07 (t, $J = 6.6$ Hz, 1 H, C11-H), 3.02-2.99 (m, 1 H, C4-H) 2.59 (dd, $J = 9.6, 6.0$ Hz, 1 H, C5-H), 2.61-2.43 (comp, 5 H, C16-H & C1-H), 2.38-2.35 (m, 1 H, C3-H), 2.00, (app hep, $J = 6.6$ 1 H, C12-H), 0.88 (d, $J = 6.8$ Hz, 6 H, C13-H & C13'-H); ^{13}C NMR (75 MHz, DMSO) δ 172.8 (C2, C10, C14, C17 or C18), 171.7 (C2, C10, C14, C17 or C18), 171.0 (C2, C10, C14, C17 or C18), 170.6 (C2, C10, C14, C17 or C18), 167.3 (C2, C10, C14, C17 or C18), 148.6 (C6, C9, C21, C21', C22, C22' or C23), 135.7 (C6, C9, C21, C21', C22, C22' or C23), 135.6 (C6, C9, C21, C21', C22, C22' or C23), 133.2 (C6, C9, C21, C21', C22, C22' or C23), 130.4 (C8 & C8'), 128.5 (C21, C21', C22, C22' or C23), 128.0 (C21, C21', C22, C22' or C23), 119.0 (C7 & C7'), 69.3 (C19), 58.8 (C11), 49.5 (C15), 36.6 (C16), 30.1 (C5 & C12), 29.9 (C3), 25.7 (C4), 25.6 (C1), 19.1 (C13), 18.1 (C13').



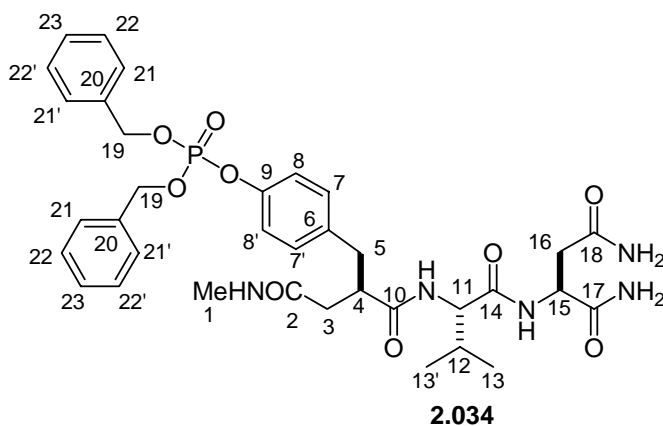
(1R, 2S, 3R, 1S', 1S'') Phosphoric acid mono-(4-{2-[1-(1,2-dicarbamoyl ethylcarbamoyl)-2-methylpropylcarbamoyl]-3-methylcarbamoylcyclopropyl}

phenyl) ester (2.004). (hrp1-191) A solution of **2.033** (5 mg, 0.007 mmol) in EtOH and H₂O (1:1, 2 mL) containing 10 % Pd/C (5 mg) was stirred under H₂ (1 atm) for 13 h.

The catalyst was removed by filtration through a pad of celite, and the filtrate was concentrated under reduced pressure to yield 4 mg of **2.004** (100%) as a white solid: mp 262-265 °C, dec; ¹H NMR (500 MHz, D₂O) δ 7.27 (d, *J* = 8.7 Hz, 2 H), 7.12 (d, *J* = 7.4 Hz, 2 H), 4.73-4.70 (m, 1 H), 4.13 (d, *J* = 6.9 Hz, 1 H), 2.96-2.94 (m, 1 H), 2.87-2.84 (comp, 2 H), 2.76-2.74 (m, 1 H), 2.60 (s, 3 H), 2.54 (dd, *J* = 10.0, 4.8 Hz, 1 H), 2.17-2.08 (m, 1 H), 0.99 (d, *J* = 8.1 Hz, 3 H), 0.97 (d, *J* = 8.1 Hz, 3 H); ¹³C NMR (125 MHz, D₂O) δ 174.7, 174.4, 173.6, 173.4, 170.3, 150.8, 130.5, 129.8, 120.2, 60.3, 50.0, 36.0, 30.0, 29.9, 29.5, 25.7, 25.6, 18.0, 17.4; mass spectrum (FAB +) *m/z* 528.1867 [C₂₁H₃₁N₅O₉P (M+1) requires 528.1859], 275 (base), 526.

NMR Assignments. ¹H NMR (300 MHz, D₂O) δ 7.27 (d, *J* = 8.7 Hz, 2 H, C7-H, C7'-H or C8-H, C8'-H), 7.12 (d, *J* = 7.4 Hz, 2 H, C7-H, C7'-H or C8-H, C8'-H), 4.73-4.70 (m, 1 H, C15-H), 4.13 (d, *J* = 6.9 Hz, 1 H, C11-H), 2.96-2.94 (m, 1 H, C4-H), 2.87-2.84 (comp, 2 H, C5-H & C16-H), 2.76-2.74 (m, 1 H, C16-H), 2.60 (s, 3 H, C1-H), 2.54 (dd, *J* = 10.0, 4.8 Hz, 1 H, C3-H), 2.17-2.08 (m, 1 H, C12-H), 0.99 (d, *J* = 8.1 Hz, 3 H,

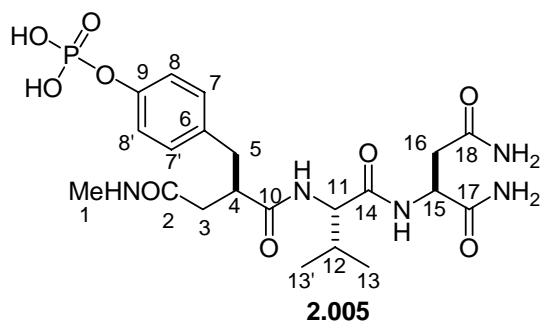
C13-H), 0.97 (d, $J = 8.1$ Hz, 3 H, C13'-H); ^{13}C NMR (75 MHz, D_2O) δ 174.7 (C2, C10, C14, C17 or C18), 174.4 (C2, C10, C14, C17 or C18), 173.6 (C2, C10, C14, C17 or C18), 173.4 (C2, C10, C14, C17 or C18), 170.3 (C2, C10, C14, C17 or C18), 150.8 (C6 or C9), 130.5 (C6 or C9), 129.8 (C7, C7' or C8, C8'), 120.2 (C7, C7' or C8, C8'), 60.3 (C11), 50.0 (C15), 36.0 (C16), 30.0 (C3), 29.9 (C5), 29.5 (C12), 25.7 (C4), 25.6 (C11), 18.0 (C13), 17.4 (C13').



(2*S*, 1*S'*, 1*S''*) Phosphoric acid dibenzyl ester 4-[2-[1-(1,2-dicarbamoyl ethylcarbamoyl)-2-methylpropylcarbamoyl]-3-methylcarbamoylpropyl]phenyl ester (2.034**). (**hrp2-188**) 2,6-Lutidine (12 mg, 13 μL , 0.11 mmol) and HATU (14 mg, 0.036 mmol) were added to a solution of **2.012** (12 mg, 0.036 mmol) and **2.011** (18 mg, 0.036 mmol) in DMF (1 mL) at -10 $^{\circ}\text{C}$ (ice-salt bath). The mixture was stirred at -10 $^{\circ}\text{C}$ for 1 h and then at rt for 12 h. The mixture was concentrated under reduced pressure, and the yellow residue was triturated with sat. NaHCO_3 (2 x 15 mL), 0.5 M HCl (2 x 15 mL), and H_2O (1 x 10 mL) to yield 20 mg of **2.034** (77%) as a white solid: mp 119-201 $^{\circ}\text{C}$; ^1H NMR (500 MHz, DMSO-d_6) δ 7.99 (d, $J = 7.9$ Hz, 1 H), 7.91 (d, $J = 8.0$ Hz, 1 H), 7.67-7.65 (m, 1 H), 7.38-7.31 (comp, 10 H), 7.30-7.29 (m, 1 H), 7.18 (d, $J = 8.5$ Hz, 2**

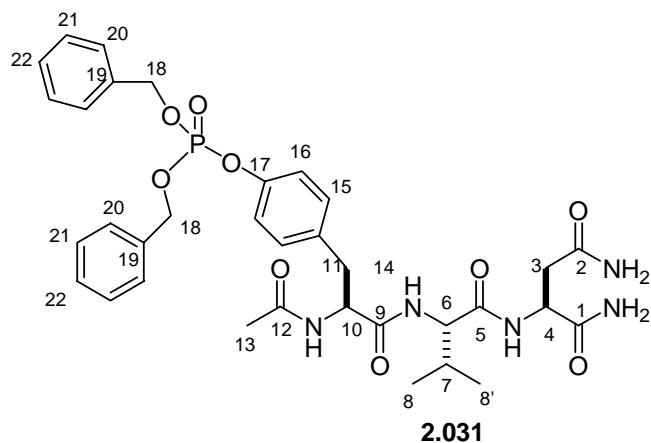
H), 7.07 (d, $J = 8.3$ Hz, 2 H), 6.86 (br s, 1 H), 5.13 (d, $J = 8.2$ Hz, 4 H), 4.43 (dd, $J = 14.0, 7.0$ Hz, 1 H), 4.03 (dd, $J = 7.8, 6.4$ Hz, 1 H), 3.07-3.05 (m, 1 H), 2.94-2.90 (m, 1 H), 2.50-2.47 (comp, 5 H), 2.33 (dd, $J = 14.5, 9.6$ Hz, 1 H), 2.00-1.94 (comp, 1 H), 0.83 (t, $J = 6.0$ Hz, 6 H); ^{13}C NMR (125 MHz, DMSO- d_6) δ 174.2, 172.7, 171.7, 170.9, 170.6, 148.5, 148.4, , 136.4, 135.7, 135.6, 130.3, 128.5, 127.9, 119.6, 69.3, 58.3, 49.4, 42.9, 36.8, 36.6, 36.55, 30.1, 25.4, 19.0, 17.9; mass spectrum (CI) m/z 710.2942 [$\text{C}_{35}\text{H}_{45}\text{N}_5\text{O}_9\text{P}$ (M+1) requires 710.2955], 570 (base), 693, 710.

NMR Assignments. ^1H NMR (300 MHz, DMSO- d_6) 7.99 (d, $J = 7.9$ Hz, 1 H, N-H), 7.91 (d, $J = 8.0$ Hz, 1 H, N-H), 7.67-7.65 (m, 1 H, N-H), 7.38-7.31 (comp, 10 H, C21-H & C21'-H, C22-H & C22'-H & C23-H), 7.30-7.29 (m, 1 H, N-H), 7.18 (d, $J = 8.5$ Hz, 2 H, C7-H, C7'-H or C8-H, C8'-H), 7.07 (d, $J = 8.3$ Hz, 2 H, C7-H, C7'-H or C8-H, C8'-H), 6.86 (br, 1 H, N-H), 5.13 (d, $J = 8.2$ Hz, 4 H, C19-H), 4.43 (dd, $J = 7.0, 14.0$ Hz, C15-H), 4.03 (dd, $J = 7.8, 6.4$ Hz, 1 H, 11-H), 3.07-3.05 (m, 1 H, C4-H), 2.94-2.90 (m, 1 H, C5-H), 2.50-2.47 (comp, 5 H, C16-H & C1-H), 2.33 (dd, $J = 14.5, 9.6$ Hz, 1 H, C3-H), 2.00-1.94, (comp, 3 H, C3-H, C5-H & C12-H), 0.83 (t, $J = 6.0$ Hz, 6 H, C13-H & C13'-H); ^{13}C NMR (75 MHz, DMSO) δ 174.2 (C2, C10, C14, C17 or C18), 172.7(C2, C10, C14, C17 or C18), 171.7(C2, C10, C14, C17 or C18), 170.9(C2, C10, C14, C17 or C18), 170.6 (C2, C10, C14, C17 or C18), 148.5 (C6, C9, C21, C21', C22, C22' or C23), 148.4 (C6, C9, C21, C21', C22, C22' or C23), 136.4 (C6, C9, C21, C21', C22, C22' or C23), 135.7 (C6, C9, C21, C21', C22, C22' or C23), 135.6 (C6, C9, C21, C21', C22, C22' or C23), 130.3 (C8 & C8'), 128.5 (C21, C21', C22, C22' or C23), 127.9 (C21, C21', C22, C22' or C23), 119.6 (C7 & C7'), 69.3 (C19), 58.3 (C11), 49.4 (C15), 42.9 (C4), 36.8 (C5), 36.6 (C16), 36.6 (C3), 30.1 (C12), 25.4 (C1), 19.0 (C13), 17.9 (C13').



(2*S*, 1*S'*, 1*S''*) Phosphoric acid mono-(4-{2-[1-(1,2-dicarbamoyl)ethylcarbamoyl]-2-methylpropylcarbamoyl]-3-methylcarbamoylpropyl}phenyl) ester (**2.005**). (**hrp1-196**). A solution of **2.034** (29 mg, 0.041 mmol) in EtOH and H₂O (1:1, 10 mL) containing 10 % Pd/C (10 mg) was stirred under H₂ (1 atm) for 13 h. The catalyst was removed by filtration through a pad of celite, and the filtrate was concentrated under reduced pressure to yield 22 mg of **2.005** (100%) as a white solid: mp 179-181 °C, dec; ¹H NMR (500 MHz, D₂O) δ 7.17-7.09 (comp, 4 H), 4.57 (dd, *J* = 7.7, 6.1 Hz, 1 H), 3.96 (d, *J* = 7.8 Hz, 1 H), 3.13-3.08 (m, 1 H), 2.81-2.77 (comp, 3 H), 2.68-2.65 (m, 1 H), 2.64 (s, 3 H), 2.53-2.41 (comp, 2 H), 1.93 (app hep, *J* = 6.8 Hz, 1 H), 0.85 (d, *J* = 6.8 Hz, 6 H); ¹³C NMR (125 MHz, D₂O) δ 179.1, 177.4, 177.1, 176.7, 175.5, 136.2, 133.0, 132.8, 123.1, 62.2, 52.9, 47.8, 40.8, 39.9, 38.9, 32.8, 28.6, 20.9, 20.4; mass spectrum (FAB +) *m/z* 530.2009 [C₂₁H₃₃N₅O₉P (M+1) requires 530.2000], 531 (base).

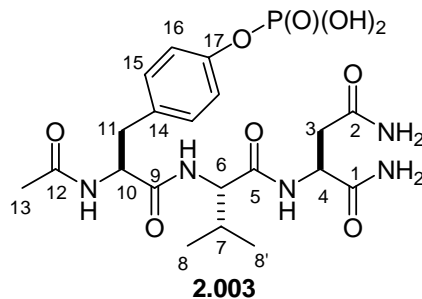
NMR Assignments. ¹H NMR (500 MHz, D₂O) δ 7.17-7.09 (comp, 4 H, C7-H & C8-H) 4.57 (dd, *J* = 7.7, 6.1 Hz, 1 H, C15-H), 3.96 (d, *J* = 7.8 Hz, 1 H, C11-H), 3.13-3.08 (m, 1 H, C4-H), 2.81-2.77 (comp, 3 H, C1-H & C16-H), 2.68-2.65 (m, 1 H, C16'-H), 2.64 (s, 3 H, C1-H), 2.53-2.41 (comp, 2 H, C3-H), 1.93 (app hep, *J* = 6.8 Hz, 1 H, C12-H), 0.85 (d, *J* = 6.8 Hz, 6 H, C13-H); ¹³C NMR (125 MHz, D₂O) δ 179.1, 177.4, 177.1, 176.7, 175.5, 136.2, 133.0, 132.8, 123.1, 62.2, 52.9, 47.8, 40.8, 39.9, 38.9, 32.8, 28.6, 20.9, 20.4



(2*S*, 1*S'*, 1*S''*) **Phosphoric acid 4-{acetylamino-[1-[(1,2-dicarbamoylethylcarbamoyl)-2-methylpropylcarbamoyl]methyl]phenyl}ester benzyl ester methyl ester (2.031).** (**hrp1-228**) 2,6-Lutidine (40 μ L, 0.36 mmol) and HATU (46 mg, 0.12 mmol) were added to a solution of **2.012** (58 mg, 0.12 mmol) and **2.030** (41 mg, 0.12 mmol) in DMF (1 mL) at -10 $^{\circ}$ C (ice-salt bath). The mixture was stirred at -10 $^{\circ}$ C for 1 h and then rt for 12 h. The mixture was concentrated under reduced pressure to yield a yellow solid that was triturated with CHCl_3 (1 x 5 mL), 0.5 M HCl (1 x 5 mL), and H_2O (1 x 5 mL) to give a white solid. The crude material was purified by flash column chromatography eluting with $\text{CH}_3\text{Cl}/\text{MeOH}$ (7:1) to yield 33 mg (40%) of **2.031** as a white solid: mp 208-211 $^{\circ}$ C; ^1H NMR (500 MHz, DMSO-d_6) δ 8.10 (d, $J = 8.3$ Hz, 1 H), 8.06 (d, $J = 7.8$ Hz, 1 H), 8.00 (d, $J = 8.1$ Hz, 1 H) 7.39-7.32 (comp, 11 H), 7.26 (d, $J = 8.6$ Hz, 2 H), 7.07 (d, $J = 7.8$ Hz, 2 H), 7.02 (d, $J = 17.3$ Hz, 2 H), 6.87 (br s, 1 H), 5.14 (d, $J = 8.3$ Hz, 2 H), 5.12 (d, $J = 8.3$ Hz, 2 H), 4.57, (ddd, $J = 10.5, 8.3, 3.7$ Hz, 1 H), 4.45 (dd, $J = 14.0, 6.4$ Hz, 1 H), 4.10 (dd, $J = 8.1, 6.6$ Hz, 1 H) 3.01 (dd, $J = 14.1, 3.7$ Hz, 1 H), 2.70 (dd, $J = 14.1, 10.5$ Hz, 1 H), 2.53-2.43 (m, 2 H), 2.00 (ap hep, $J = 6.6$ Hz, 1 H), 1.73 (s, 3 H), 0.86 (d, $J = 6.6$ Hz, 3 H), 0.84 (d, $J = 6.6$ Hz, 3 H); ^{13}C NMR (125 MHz, DMSO-d_6) δ 172.7, 171.8, 171.6, 170.4, 169.2, 135.7, 135.6, 135.2, 130.5, 128.5,

127.9, 119.4, 69.3, 58.0, 53.7, 49.5, 36.7, 36.4, 30.3, 22.3, 19.1, 17.9; mass spectrum (CI) m/z 696.2801 [$C_{34}H_{42}N_5O_9P$ (M+1) requires 696.2798], 574 (base), 484, 466.

NMR Assignments. 1H NMR (500 MHz, DMSO- d_6) δ 8.10 (d, $J = 8.3$ Hz, 1 H, N-H), 8.06 (d, $J = 7.8$ Hz, 1 H, N-H), 8.00 (d, $J = 8.1$ Hz, 1 H, N-H) 7.39-7.32 (comp, 11 H, C20-H, C20'-H, C21-H, C21'-H, C22-H, & N-H), 7.26 (d, $J = 8.6$ Hz, 2 H, C15-H & C15'-H or C16-H & C16'-H), 7.07 (d, $J = 7.8$ Hz, 2 H, C15-H & C15'-H or C16-H & C16'-H), 7.02 (d, $J = 17.3$ Hz, 2 H, N-H), 6.87 (br s, 1 H, N-H), 5.14 (d, $J = 8.3$ Hz, 2 H, C18-H), 5.12 (d, $J = 8.3$ Hz, 2 H, C18'-H), 4.57, (ddd, $J = 10.5, 8.3, 3.7$ Hz, 1 H, C10-H), 4.45 (dd, $J = 14.0, 6.4$ Hz, 1 H, C4-H), 4.10 (dd, $J = 8.1, 6.6$ Hz, 1 H, C6-H) 3.01 (dd, $J = 14.1, 3.7$ Hz, 1 H, C11-H), 2.70 (dd, $J = 14.1, 10.5$ Hz, 1 H, C11-H), 2.53-2.43 (m, 2 H, C3-H), 2.00 (ap hep, $J = 6.6$ Hz, 1 H, C7-H), 1.73 (s, 3 H, C13-H), 0.86 (d, $J = 6.6$ Hz, 3 H, C8-H), 0.84 (d, $J = 6.6$ Hz, 3 H, C8'-H); ^{13}C NMR (125 MHz, DMSO- d_6) δ 172.7 (C1, C2, C5, C9, or C12), 171.8 (C1, C2, C5, C9, or C12), 171.6 (C1, C2, C5, C9, or C12), 170.4 (C1, C2, C5, C9, or C12), 169.2 (C1, C2, C5, C9, or C12), 135.7 (C14, C17 or C19), 135.6 (C14, C17 or C19), 135.2 (C14, C17 or C19), 130.5 (C15 or C16), 128.5 (C20 & C21 or C22), 127.9 (C20 & C21 or C22), 119.4 (C15 or C16), 69.3 (C18), 58.0 (C6), 53.7 (C10), 49.5 (C4), 36.7 (C3), 36.4 (C11), 30.3 (C7), 22.3 (C13), 19.1 (C8), 17.9 (C8').

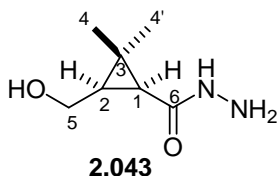


(2*S*, 1*S'*, 1*S''*) Phosphoric acid mono-(4-{acetylamino-[1-[(1,2-dicarbamoylethylcarbamoyl)-2-methylpropylcarbamoyl]methyl]phenyl)ester

(2.003). (hrp1-238) A mixture of **2.031** (20 mg, 0.029 mmol) in EtOH and H₂O (1:1, 4 mL total) containing 10% Pd/C (10 mg) was stirred under H₂ (1 atm) for 13 h. The mixture was then filtered through a pad of celite. The filtrate was concentrated under reduced pressure to yield 23 mg (89%) of **2.003** as a white solid: mp 208-211 °C; ¹H NMR (500 MHz, D₂O) δ 7.20 (d, *J* = 8.6 Hz, 2 H), 7.14-7.12 (comp, 2 H), 4.63 (dd, *J* = 8.0, 6.0 Hz, 1 H), 4.58 (dd, *J* = 8.0, 7.0 Hz, 1 H), 4.06 (d, *J* = 7.6 Hz, 1 H), 3.05 (dd, *J* = 13.9, 7.0 Hz, 1 H), 2.96 (dd, *J* = 13.9, 8.0 Hz, 1 H), 2.81 (dd, *J* = 15.5, 6.0 Hz, 1 H), 2.75-2.71 (m, 1 H), 2.00 (ap hep, *J* = 6.8 Hz, 1 H), 1.95 (s, 3 H), 0.90 (d, *J* = 6.8 Hz, 3 H), 0.89 (d, *J* = 6.8 Hz, 3 H); ¹³C NMR (125 MHz, D₂O) δ 177.4, 177.1, 176.8, 176.2, 175.4, 153.7, 134.7, 133.0, 123.2, 62.1, 57.8, 53.0, 39.0, 38.9, 33.0, 24.3, 20.9, 20.3; mass spectrum (FAB -) *m/z* 515.1776 [C₂₀H₃₀N₅O₉P (M-1) requires 515.1781], 245 (base) 275.

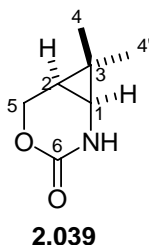
NMR Assignments. ¹H NMR (500 MHz, D₂O) δ 7.20 (d, *J* = 8.6 Hz, 2 H, C15-H & C15'-H or C16-H & C16'-H), 7.14-7.12 (comp, 2 H, C15-H & C15'-H or C16-H & C16'-H), 4.63 (dd, *J* = 8.0, 6.0 Hz, 1 H, C4-H), 4.58 (dd, *J* = 8.0, 7.0 Hz, 1 H, C10-H), 4.06 (d, *J* = 7.6 Hz, 1 H, C6-H), 3.05 (dd, *J* = 13.9, 7.0 Hz, 1 H, C11-H), 2.96 (dd, *J* = 13.9, 8.0 Hz, 1 H, C11-H), 2.81 (dd, *J* = 15.5, 6.0 Hz, 1 H, C3-H), 2.75-2.71 (m, 1 H,

C3-H), 2.00 (ap hep, $J = 6.8$ Hz, 1 H, C7-H), 1.95 (s, 3 H, C13-H), 0.90 (d, $J = 6.8$ Hz, 3 H, C8-H), 0.89 (d, $J = 6.8$ Hz, 3 H, C8'-H); ^{13}C NMR (125 MHz, D_2O) δ 177.4 (C1, C2, C5, C9, or C12), 177.1 (C1, C2, C5, C9, or C12), 176.8 (C1, C2, C5, C9, or C12), 176.2 (C1, C2, C5, C9, or C12), 175.4 (C1, C2, C5, C9, or C12), 153.7 (C14 or C17), 134.7 (C14 or C17), 133.0 (C15 or C16), 123.2 (C15 or C16), 62.1 (C6), 57.8 (C10), 53.0 (C4), 39.0 (C3), 38.9 (C11), 33.0 (C7), 24.3 (C13), 20.9 (C8), 20.3 (C8').



(1S, 3R)-3-Hydroxymethyl-2,2-dimethyl-1-cyclopropane carboxylic acid hydrazide (2.043). (hrp1-110). Hydrazine monohydrate (1.5 mL, 30.2 mmol) was added over 15 min to a solution of lactone **2.040** (646 mg, 5.12 mmol) in MeOH (18 mL) at rt. The reaction was stirred at rt for 3 d and then concentrated under reduced pressure. Residual solvent was removed using azeotropic distillation with toluene (2 x 10 mL) to yield 786 mg of **2.043** (97%) as an off-white solid: mp 71-72°C; ^1H NMR (500 MHz, CD_3OD) δ 3.95 (dd, $J = 11.7, 7.7$ Hz, 1 H), 3.84 (dd, $J = 11.7, 7.2$ Hz, 1 H), 1.40 (d, $J = 8.8$ Hz, 1 H), 1.30-1.26 (comp, 1 H), 1.22 (s, 3 H), 1.16 (s, 3 H); ^{13}C NMR (125 MHz, CD_3OD) δ 175.2, 58.8, 43.0, 29.7, 29.1, 24.6, 14.8; mass spectrum (CI) m/z 159.1133 [$\text{C}_7\text{H}_{15}\text{N}_2\text{O}_2$ (M+1) requires 159.1134], 141 (base), 127, 83.

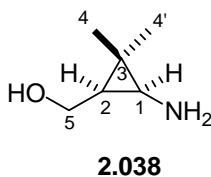
NMR Assignments. ^1H NMR (500 MHz, CD_3OD) δ 3.95 (dd, $J = 7.7, 11.7$ Hz, 1 H, C5-H), 3.84 (dd, $J = 7.2, 11.7$ Hz, 1 H, C5-H), 1.40 (d, $J = 8.8$ Hz, 1 H, C1-H), 1.30-1.26 (comp, 1 H, C2-H), 1.22 (s, 3 H, C4-H), 1.16 (s, 3 H, C4'-H); ^{13}C NMR (125 MHz, CD_3OD) δ 175.2 (C6), 58.8 (C5), 34.0 (C2), 29.7 (C1), 29.1 (C4), 24.6 (C3), 14.8 (C4').



(1R, 6S)-7,7 Dimethyl-4-oxa-2-azabicyclo[4.1.0]heptane-3-one (2.039). (hrp2-117) 6 N aqueous HCl (2.2 mL, 13.3 mmol) was added dropwise to a vigorously stirred mixture of NaNO₂ (916 mg, 13.3 mmol) and hydrazide **2.043** (1.4 g, 8.9 mmol) in Et₂O and H₂O (1:1, 40 mL) at 0 °C. The yellow mixture was stirred vigorously at 0 °C for 45 min and then cold toluene (20 mL) was added. The layers were separated and the aqueous layer was extracted with toluene (3 x 20 mL). The organic layers were combined, washed with brine (1 x 20 mL), dried (Na₂SO₄) and concentrated under reduced pressure to approximately 30 mL. A stir bar was added and the mixture was heated at 80 °C for 1.5 h. After cooling to rt, the solvent was removed under reduced pressure and the residue purified with flash column chromatography eluting with EtOAc/hexanes (2:1) to yield 1.17 g of **2.039** (94%) as an off-yellow solid: mp 95-97 °C; ¹H NMR (500 MHz) δ 6.75 (br s, 1 H), 4.26 (dd, *J* = 12.6, 8.7 Hz, 1 H), 4.05 (dd, *J* = 12.6, 5.5 Hz, 1 H), 2.58 (dd, *J* = 8.7, 2.0 Hz, 1 H), 1.20 (app dt, *J* = 8.7, 5.5 Hz, 1 H), 1.04 (s, 3 H), 1.00 (s, 3 H); ¹³C NMR (125 MHz) δ 155.3, 65.6, 37.3, 24.3, 22.1, 16.0, 13.0; IR (CHCl₃) 2253, 1710, 1465, 1074, 910, 649 cm⁻¹; mass spectrum (CI) *m/z* 142.0866 [C₇H₁₂NO₂ (M+1) requires 142.0867], 143, 98.

NMR Assignments. ¹H NMR (500 MHz) δ 6.75 (br s, 1 H, N-H), 4.26 (dd, *J* = 8.7, 12.6 Hz, 1 H, C5-H), 4.05 (dd, *J* = 5.5, 12.6 Hz, 1 H, C5-H), 2.58 (dd, *J* = 2.0, 8.7 Hz, 1 H, C1-H), 1.20 (ap dt, *J* = 5.5, 8.7 Hz, 1 H, C2-H), 1.04 (s, 3 H, C4-H), 1.00 (s, 3

H, C4'-H); ^{13}C NMR (125 MHz) δ 155.3 (C6), 65.6 (C5), 37.3 (C1), 24.3 (C4), 22.1 (C3), 16.0 (C2), 13.0 (C4').

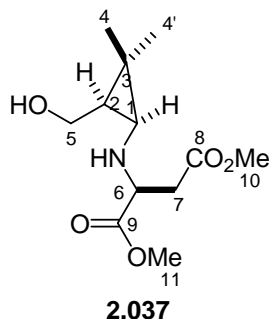


(1R, 3S)-(3-Amino-2,2-dimethylcyclopropyl)-1-methanol (2.038). (hrp1-107)

A mixture of $\text{Ba}(\text{OH})_2 \cdot 8 \text{H}_2\text{O}$ (2.73 g, 8.67 mmol) and urethane **2.039** (612 mg, 4.33 mmol) in dioxane and H_2O (2:1, 30 mL) was heated under reflux for 90 min with vigorous stirring. After cooling to rt, the reaction mixture was filtered through a pad of celite. The celite pad was washed with CH_2Cl_2 (2 x 10 mL) and the combined filtrate and washes were washed with brine (30 mL). The aqueous layer was extracted with CH_2Cl_2 (5 x 30 mL). The organic layers were combined, dried (Na_2SO_4), and concentrated under reduced pressure to yield 414 mg of **2.038** (83%) as a yellow oil. This material was shown to be > 95% pure by ^1H NMR and was used without further purification; ^1H NMR (300 MHz) δ 3.87 (dd, $J = 11.3, 6.4$ Hz, 1 H), 3.81 (dd, $J = 11.3, 7.7$ Hz, 1 H), 3.70 (s, 1 H), 2.23 (d, $J = 7.2$ Hz, 1 H), 1.70 (br s, 2 H), 1.10 (s, 3 H), 1.00 (s, 3 H), 0.77-0.70 (m, 1 H); ^{13}C NMR (65 MHz,) δ 58.0, 37.6, 28.8, 27.1, 18.9, 13.3; IR (CHCl_3) 3552, 3020, 2254, 1469, 1385, 1215, 908, 734, 647 cm^{-1} ; mass spectrum (CI) m/z 116.1078 [$\text{C}_6\text{H}_{14}\text{NO}$ (M+1) requires 116.1075], 114, 98 (base).

NMR Assignments. ^1H (300 MHz) δ 3.87 (dd, $J = 6.4, 11.3$ Hz, 1 H, C5-H), 3.81 (dd, $J = 7.7, 11.3$ Hz, 1 H, C5-H), 3.70 (s, 1 H, O-H), 2.23 (d, $J = 7.2$ Hz, 1 H, C1-H), 1.70 (br s, 2 H, N-H), 1.10 (s, 3 H, C4-H), 1.00 (s, 3 H, C4'-H), 0.77-0.70 (m, 1 H,

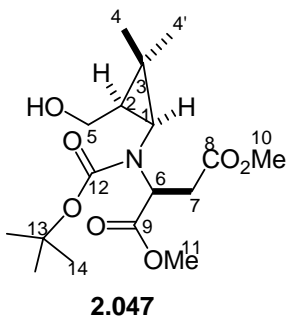
C2-H); ^{13}C NMR (65 MHz,) δ 58.0 (C5), 37.6 (C1), 28.8 (C4), 27.1 (C3), 18.9 (C2), 13.3 (C4').



2S, 1'S, 3'R)-2-(3-Hydroxymethyl-2,2-dimethyl-1-cyclopropanylamino)succinic acid dimethyl ester (2.037). (**hrp2-152**) Freshly distilled Tf_2O (1.92 g, 1.15 mL, 6.82 mmol) was added dropwise to a solution of (*R*)-dimethylmalate (1.23 g, 1.0 mL, 7.58 mmol) in CH_2Cl_2 (11 mL) at 0 °C. This mixture was stirred at 0 °C for 5 min, and 2,6-lutidine (739 mg, 0.794 mL, 6.82 mmol) was added. This mixture was stirred at 0 °C for an additional 10 min, and then $i\text{Pr}_2\text{NEt}$ (928 mg, 1.25 mL, 7.20 mmol) was added. Then, a mixture of amino alcohol **2.038** (436 mg, 3.79 mmol) and $i\text{Pr}_2\text{NEt}$ (490 mg, 0.660 mL, 3.79 mmol) in CH_2Cl_2 (6 mL) was then added dropwise. The reaction was stirred at 0 °C for 1 h and then warmed to rt for 30 min. CH_2Cl_2 (20 mL) was added, and the mixture was washed with brine (20 mL). The aqueous layer was extracted with CH_2Cl_2 (1 x 20 mL). The combined organic layers were washed with sat. NaHCO_3 (1 x 20 mL), dried (Na_2SO_4) and concentrated under reduced pressure. The residue was purified by flash column chromatography eluting with EtOAc/hexanes (1:1) to yield 524 mg **2.037** (54%) as a yellow oil; ^1H NMR (300 MHz) δ 3.79-3.65 (comp, 8 H), 3.53 (dd, $J = 7.2, 5.9$ Hz, 1 H), 2.67 (dd, $J = 15.8, 5.9$ Hz, 1 H), 2.58 (dd, $J = 15.8, 7.2$ Hz, 1 H), 2.02 (br s, 2 H), 1.97 (d, $J = 7.4$ Hz, 1 H), 1.04 (s, 3 H), 0.98 (s, 3 H), 0.78 (dd, $J = 14.1, 7.4$ Hz, 1 H); ^{13}C NMR (75 MHz,) δ 174.2, 171.2, 58.9, 58.3, 52.1, 51.8, 42.6, 38.0, 29.9,

27.2, 20.0, 13.7; IR 3448, 2954, 2254, 1738, 1459, 1438, 1374, 1282, 1222, 1170, 1096, 1013, 992, 908, 774, 738, 669, 650 cm⁻¹; mass spectrum (CI) *m/z* 260.1506 [C₁₂H₂₂NO₅ (M+1) requires 260.1498], 242, 228, 163

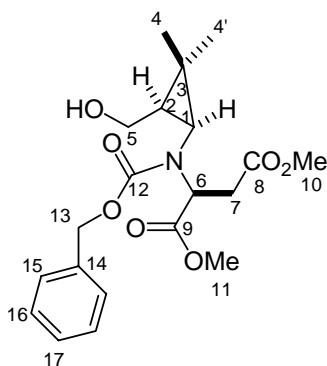
NMR Assignments. ¹H NMR (300 MHz) δ 3.79-3.65 (comp, 8 H, C5-H, C10-H & C11-H), 3.53 (dd, *J* = 5.9, 7.2 Hz, 1 H, C6-H), 2.67 (dd, *J* = 15.8, 5.9 Hz, 1 H, C7-H), 2.58 (dd, *J* = 15.8, 7.2 Hz, 1 H, C7-H), 2.02 (br s, 2 H, O-H & N-H), 1.97 (d, *J* = 7.4 Hz, 1 H, C1-H), 1.04 (s, 3 H, C4-H), 0.98 (s, 3 H, C4'-H), 0.78 (dd, *J* = 14.1, 7.4 Hz, 1 H, C2-H); ¹³C NMR (75 MHz,) δ 174.2 (C9 or C8), 171.2 (C8 or C9), 58.9 (C6), 58.3 (C5), 52.1 (C11 or C10), 51.8 (C10 or C11), 42.6 (C1), 38.0 (C7), 29.9 (C2), 27.2 (C4), 20.0 (C3), 13.7 (C4').



(2*S*, 1'*S*, 3'*R*)-2-[*tert*-Butoxycarbonyl-(3-hydroxymethyl-2,2-dimethyl-1-cyclopropanyl)amino]succinic acid dimethyl ester (2.047). (hrp1-112). Boc₂O (128 mg, 0.590 mmol) was added to a solution of **2.037** (51 mg, 0.196 mmol) in CH₃CN (2 mL) at rt, and the reaction mixture was stirred at rt for 90 min. The mixture was then heated at 50 °C for 1 d, whereupon more Boc₂O (128 mg, 0.567 mmol) was added, and the heating continued for 3 d. The crude reaction mixture was concentrated under reduced pressure, and the residue was purified by flash column chromatography eluting with EtOAc/hexanes (1:1) to yield **2.037** as a clear oil (34 mg, 48%); ¹H NMR (500

MHz, DMSO-d₆) δ 4.46 (dd, $J = 5.5, 8.2$ Hz, 1 H), 3.65-3.58 (comp, 7 H), 3.55-3.51 (m, 1 H), 3.31 (br s, 1 H), 2.97 (dd, $J = 8.2, 15.8$ Hz, 1 H), 2.73 (dd, $J = 5.5, 15.8$ Hz, 1 H), 2.35, (d, $J = 7.0$ Hz, 1 H), 1.37 (s, 9 H), 1.04 (s, 3 H), 1.00 (s, 3 H), 0.86 (dd, $J = 7.0, 14.6$ Hz, 1 H); ¹³C NMR (125 MHz, DMSO) δ 171, 156, 79.7, 58.8, 56.4, 52.0, 51.4, 44.5, 33.4, 29.8, 27.7, 26.5, 20.9, 14.4; IR (CHCl₃) 3398, 2980, 2955, 1741, 1609, 1154, 1025 cm⁻¹; mass spectrum (CI) m/z 360.2005 [C₁₇H₃₀NO₇ (M+1) requires 360.2022], 286, 260 (base), 242, 228.

NMR Assignments. ¹H NMR (500 MHz, DMSO-d₆) δ 4.46 (dd, $J = 5.5, 8.2$ Hz, 1 H, C6-H), 3.65-3.58 (comp, 7 H, C5-H, C10-H & C11-H), 3.55-3.51 (m, 1 H, C5'-H), 3.31 (br s, 1 H, O-H), 2.97 (dd, $J = 8.2, 15.8$ Hz, 1 H, C7-H), 2.73 (dd, $J = 5.5, 15.8$ Hz, 1 H, C7'-H), 2.35, (d, $J = 7.0$ Hz, 1 H, C1-H), 1.37 (s, 9 H, C14-H), 1.04 (s, 3 H, C4-H), 1.00 (s, 3 H, C4'-H), 0.86 (dd, $J = 7.0, 14.6$ Hz, 1 H, C2-H); ¹³C NMR (125 MHz, DMSO) δ 171.0 (C9 or C8), 170.7 (C8 or C9), 156 (C12), 79.7 (C13), 58.8 (C6), 56.4 (C5), 52.0 (C11 or C10), 51.4 (C10 or C11), 44.5 (C1), 33.4 (C7), 29.8 (C2), 27.7 (C14), 26.5 (C4), 20.9 (C3), 14.4 (C4').

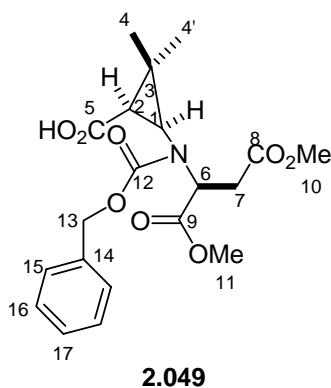


2.048

(2*S*, 1'*S*, 3'*R*)-2-[Benzyloxycarbonyl-(3-hydroxymethyl-2,2-dimethylcyclopropylamino)]succinic acid dimethyl ester (2.048). (hrp1-255). *i*Pr₂NEt (197 μ L, 1.13 mmol) and then Cbz-Cl (135 μ L, 0.94 mmol) were added to a stirred solution of **2.037** (163 mg, 0.63 mmol) in CH₂Cl₂ (7 mL) at rt. The reaction mixture was heated under reflux for 40 h. The reaction was cooled to rt, and the crude reaction mixture was concentrated under reduced pressure. The light yellow residue was purified by flash column chromatography eluting with hexanes/EtOAc (2:1) to yield 200 mg (81%) of **2.048** as a yellow oil; ¹H NMR (500 MHz, DMSO-d₆, 383K) δ 7.38-7.30 (comp, 5 H), 5.09 (d, *J* = 12.3 Hz, 1 H), 5.03 (d, *J* = 12.3 Hz, 1 H), 4.49 (dd, *J* = 7.4, 6.0 Hz, 1 H), 3.63-3.54 (comp, 8 H) 3.05 (dd, *J* = 15.9, 7.4 Hz, 1 H), 2.77 (dd, *J* = 15.9, 6.0 Hz, 1 H), 2.47 (d, *J* = 7.6 Hz, 1H), 1.0 (s, 3 H), 0.98 (s, 3 H), 0.96-0.93 (m, 1 H); ¹³C NMR (125 MHz, DMSO-d₆, 383K) δ 170.2, 169.2, 159.3, 135.7, 127.6, 127.3, 78.4, 66.5, 58.9, 56.2, 51.2, 50.6, 45.2, 34.0, 30.1, 25.9, 20.4, 13.6; IR (CHCl₃) 2253, 1740, 1699, 1458, 1378, 1351, 1149, 1098, 904, 650 cm⁻¹; mass spectrum (CI) *m/z* 394.1860 [C₂₀H₂₇NO₇ (M+1) requires 394.1866], 376 (base), 332.

NMR Assignments. ¹H NMR (500 MHz, DMSO-d₆, 383K) δ 7.38-7.30 (comp, 5 H, C15-H, C15'-H, C16-H, C16'-H & C17-H), 5.09 (d, *J* = 12.3 Hz, 1 H, C13-H), 5.03

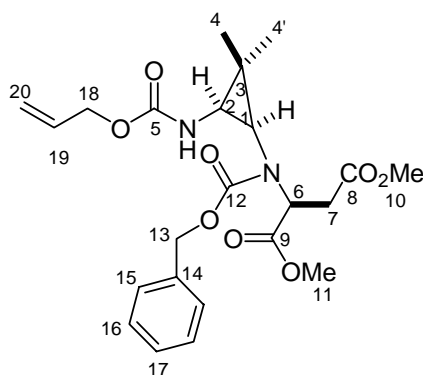
(d, $J = 12.3$ Hz, 1 H, C13-H), 4.49 (dd, $J = 7.4, 6.0$ Hz, 1 H, C6-H), 3.63-3.54 (comp, 8 H, C5-H, C10-H & C11-H), 3.05 (dd, $J = 15.9, 7.4$ Hz, 1 H, C7-H), 2.77 (dd, $J = 15.9, 6.0$ Hz, 1 H, C7-H), 2.47 (d, $J = 7.6$ Hz, 1 H, C1-H), 1.0 (s, 3 H, C4-H), 0.98 (s, 3 H, C4'-H), 0.96-0.93 (m, 1 H, C2-H); ^{13}C NMR (125 MHz, DMSO- d_6 , 383K) δ 170.2 (C8, C9 or C12), 169.2 (C8, C9 or C12), 159.3 (C8, C9 or C12), 135.7 (C15, C16 or C17), 127.6 (C15, C16 or C17), 127.3 (C15, C16 or C17), 78.4 (C14), 66.5 (C13), 58.9 (C6), 56.2 (C5), 51.2 (C10 or C11), 50.6 (C10 or C11), 45.2 (C1), 34.0 (C7), 30.1 (C2), 25.9 (C4), 20.4 (C3), 13.6 (C4).



(2*S*,1'*S*,3'*R*)-2-[Benzyloxycarbonyl-(3-carboxy-2,2-dimethylcyclopropylamino)] succinic acid dimethyl ester (2.049). (hrp1-236). NaHCO₃ (34 mg, 0.41 mmol), NaIO₄ (74 mg, 0.35 mmol), and RuCl₃ (1 mg, 0.0062 mmol) were added to a solution of **2.048** (24 mg, 0.062 mmol) in CH₃CN, CCl₄, H₂O (1:1:2, 3 mL total) at rt. The orange emulsion reaction mixture was stirred vigorously for 30 min, whereupon an additional 0.1 equivalent of RuCl₃ was added. The reaction mixture was vigorously stirred for 1 h at rt. The reaction mixture was diluted with EtOAc (5 mL), and 3 M HCl sat. with NaCl was added until aqueous layer was pH = 1.0. The layers were separated, and the aqueous layer was back extracted EtOAc (1 x 5 mL).

The organic layers were combined and dried (Na_2SO_4) and concentrated under reduced pressure. The orange residue was purified by filtering through a pad of silica eluting with EtOAc to yield 24 mg (94%) of **2.049** as a orange oil; ^1H NMR (500 MHz, DMSO-d_6 , 383K) δ 7.37-7.29 (comp, 5 H), 5.11 (d, $J = 12.6$ Hz, 1 H), 4.94 (d, $J = 12.6$ Hz, 1 H), 4.29 (dd, $J = 8.9, 3.6$ Hz, 1 H), 3.65 (s, 3 H), 3.58 (s, 3 H), 3.24 (dd, $J = 16.8, 8.9$ Hz, 1 H), 2.92 (d, $J = 7.6$ Hz, 1 H), 2.76 (dd, $J = 16.8, 3.6$ Hz, 1 H), 1.70 (d, $J = 7.6$ Hz, 1 H), 1.29 (s, 3 H), 1.15 (s, 3 H); ^{13}C NMR (125 MHz, DMSO-d_6 , 383K) δ 170.3, 169.9, 169.1, 155.9, 135.7, 127.6, 127.1, 127.0, 66.3, 58.9, 51.3, 50.8, 48.0, 35.5, 30.9, 25.9, 25.8, 14.0; IR (CHCl_3) 3001, 2956, 1734, 1455, 1438, 1328, 1306, 1240, 1026, 1012 cm^{-1} ; mass spectrum (CI) m/z 408.1660 [$\text{C}_{20}\text{H}_{25}\text{NO}_8$ (M+1) requires 408.1658], 390, 364.

NMR Assignments. ^1H NMR (500 MHz, DMSO-d_6 , 383K) δ 7.37-7.29 (comp, 5 H, C15-H, C15'-H, C16-H, C16'-H & C17-H), 5.11 (d, $J = 12.6$ Hz, 1 H, C13-H), 4.94 (d, $J = 12.6$ Hz, 1 H, C13-H), 4.29 (dd, $J = 8.9, 3.6$ Hz, 1 H, C6-H), 3.65 (s, 3 H, C10-H or C11-H), 3.58 (s, 3 H, C10-H or C11-H), 3.24 (dd, $J = 16.8, 8.9$ Hz, 1 H, C7-H), 2.92 (d, $J = 7.6$ Hz, 1 H, C1-H), 2.76 (dd, $J = 16.8, 3.6$ Hz, 1 H, C7-H), 1.70 (d, $J = 7.6$ Hz, 1 H, C2-H), 1.29 (s, 3 H, C4-H), 1.15 (s, 3 H, C4'-H); ^{13}C NMR (125 MHz, DMSO-d_6 , 383K) δ 170.3 (C8, C9 or C12), 169.9 (C5), 169.1 (C8, C9 or C12), 155.9 (C8, C9 or C12), 135.7 (C15, C16 or C17), 127.6 (C15, C16 or C17), 127.1(C15, C16 or C17), 127.0 (C14) 66.3 (C13), 58.9 (C6) , 51.3 (C10 or C11), 50.8 (C10 or C11), 48.0 (C1), 35.5 (C7), 30.9 (C2), 25.9 (C4), 25.8 (C3), 14.0 (C4).



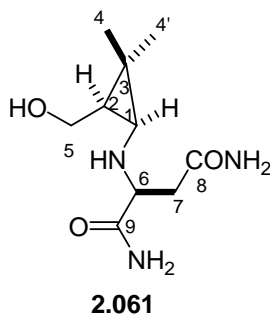
2.050

(2*S*,1'*S*,3'*R*)-2-[(3-Allyloxycarbonylamino-2,2-dimethylcyclopropyl)

benzyloxycarbonylamino] succinic acid dimethyl ester (2.050). (hrp1-257). Ethyl chloroformate (51 μ L, 0.53 mmol) and Et₃N (68 μ L, 0.49 mmol) were added to a solution of **2.049** (166 mg, 0.41 mmol) in acetone:H₂O (10:1, 4 mL total) at rt. The mixture was stirred at rt for 1 h, and NaN₃ was added (40 mg, 0.61 mmol). The mixture was stirred at rt for 1 h, and cold toluene (20 mL) was then added. The mixture was washed with brine (1 x 20 mL), and the aqueous layer was back extracted with toluene (1 x 20 mL). The organic phases were combined, dried (Na₂SO₄) and concentrated to ca. 3 mL under reduced pressure. Allyl alcohol (1 mL) was added, and the reaction was heated under reflux for 22 h. The reaction was then concentrated under reduced pressure, and the yellow residue was purified by flash column chromatography eluting with hexanes/EtOAc (2:1) to yield 84 mg (44%) of **12** as a yellow oil; ¹H NMR (500 MHz, DMSO-d₆, 383K) δ 7.38-7.30 (comp, 5 H), 5.93 (br s, 1 H), 5.90 (ddt, *J* = 17.2, 10.5, 5.5 Hz, 1 H), 5.27 (dq, *J* = 17.2, 1.6 Hz, 1 H) 5.17 (dq, *J* = 10.5, 1.6 Hz, 1 H), 5.10 (d, *J* = 12.4 Hz, 1 H), 5.05 (d, *J* = 12.4 Hz, 1 H), 4.50 (dq, *J* = 5.5, 1.6 Hz, 2 H), 4.23 (dd, *J* = 7.9, 5.3 Hz, 1 H), 3.63 (s, 3 H), 3.59 (s, 3 H), 3.10 (dd, *J* = 7.9, 16.4 Hz, 1 H), 2.84-2.83 (m, 1 H), 2.67 (dd, *J* = 6.8, 5.7 Hz, 1 H), 2.56 (d, *J* = 6.8 Hz, 1 H), 1.04 (s, 3 H), 0.98 (s,

3 H); ^{13}C NMR (125 MHz, DMSO- d_6 , 383K) δ 170.2, 169.9, 156.2, 155.9, 135.5, 132.9, 127.7, 127.3, 127.2, 116.3, 66.7, 64.1, 58.6, 51.5, 50.8, 43.7, 38.4, 28.2, 23.9, 20.5, 13.3; IR (CHCl₃) 3404, 2992, 2956, 1732, 1490, 1456, 1439, 1411, 1311, 1269, 1154 cm⁻¹; mass spectrum (CI) m/z 463.2068 [C₂₃H₃₀N₂O₈ (M+1) requires 463.2080].

NMR Assignments. ^1H NMR (500 MHz, DMSO- d_6 , 383K) δ 7.38-7.30 (comp, 5 H, C15-H, C16-H, C15'-H, C16'-H & C17-H), 5.93 (br s, 1 H, N-H), 5.90 (ddt, $J = 17.2, 10.5, 5.5$ Hz, 1 H, C19-H), 5.27 (dq, $J = 17.2, 1.6$ Hz, 1 H, C20-H) 5.17 (dq, $J = 10.5, 1.6$ Hz, 1 H, C20-H), 5.10 (d, $J = 12.4$ Hz, 1 H, C13-H), 5.05 (d, $J = 12.4$ Hz, 1 H, C13-H), 4.50 (dq, $J = 5.5, 1.6$ Hz, 2 H, C18-H), 4.23 (dd, $J = 7.9, 5.3$ Hz, 1 H, C6-H), 3.63 (s, 3 H, C10-H or C11-H), 3.59 (s, 3 H, C10-H or C11-H), 3.10 (dd, $J = 16.4, 7.9$ Hz, 1 H, C7-H), 2.84-2.83 (m, 1 H, C7-H), 2.67 (dd, $J = 6.8, 5.7$ Hz, 1 H, C2-H), 2.56 (d, $J = 6.8$ Hz, 1 H, C1-H), 1.04 (s, 3 H, C4-H), 0.98 (s, 3 H, C4'-H); ^{13}C NMR (125 MHz, DMSO- d_6 , 383K) δ 170.2 (C8, C9, or C12), 169.92 (C8, C9, or C12), 156.22 (C5), 155.92 (C8, C9, or C12), 135.5 (C15, C16, or C17), 132.9 (C20), 127.7 (C15, C16, or C17), 127.3 (C14), 127.2 (C15, C16, or C17), 116.3 (C19), 66.7 (C13), 64.1 (C18), 58.6 (C6), 51.5 (C10 or C11), 50.8 (C10 or C11), 43.7 (C1), 38.4 (C2), 28.2 (C7), 23.9 (C4), 20.5 (C3), 13.3 (C4').

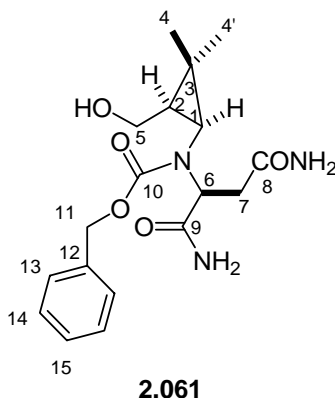


(2*S*,1'*S*,3'*R*)-2-(3-Hydroxymethyl-2,2-dimethyl-1-cyclopropanylamino)

succinic amide (2.061). (hrp2-108). A mixture of **2.037** (311 mg, 1.2 mmol) in MeOH (12 mL) containing NaCN (6 mg, 0.12 mmol) at rt was saturated with NH₃ by bubbling the gas into solution for 20 min at rt. The mixture was stirred at 50 °C for 3 d, during which time it was resaturated with NH₃ every 12 h. The mixture was then concentrated under reduced pressure, and the residue was recrystallized from minimal amounts of hot MeOH, EtOAc (1:50, 10 mL total) to yield 239 mg of **2.061** (85%) as an off white solid: mp 134-136 °C; ¹H NMR (500 MHz, CD₃OD) δ 3.70-3.64 (comp, 2 H), 3.42 (dd, *J* = 7.9, 5.4 Hz, 1 H), 2.48 (dd, *J* = 14.7, 5.4, 1 H), 2.44 (dd, *J* = 14.7, 7.9 Hz, 1 H), 1.94 (d, *J* = 7.4 Hz, 1 H), 1.09 (s, 3 H), 1.01 (s, 3 H), 0.75 (dd, *J* = 14.5, 7.4, 1 H); ¹³C NMR (125 MHz, CD₃OD) δ 179.1, 176.1, 60.5, 59.1, 43.3, 39.8, 31.0, 27.7, 20.8, 14.1; IR 3430, 1713 cm⁻¹, mass spectrum (CI) *m/z* 230.1510 [C₁₀H₁₉N₃O₃ (M+1) requires 230.1505], 198, 212 (base), 230.

NMR Assignments. ¹H NMR (500 MHz, CD₃OD) δ 3.70-3.64 (comp, 2 H, C5-H), 3.42 (dd, *J* = 7.9, 5.4 Hz, 1 H, C6-H), 2.48 (dd, *J* = 14.7, 5.4, 1 H, C7-H), 2.44 (dd, *J* = 14.7, 7.9 Hz, 1 H, C7'-H), 1.94 (d, *J* = 7.4 Hz, 1 H, C1-H), 1.09 (s, 3 H, C4-H), 1.01 (s, 3 H, C4'-H), 0.75 (dd, *J* = 14.5, 7.4, 1 H, C2-H); ¹³C NMR (125 MHz, CD₃OD) δ 179.1

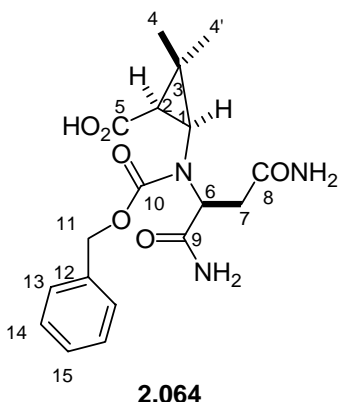
(C8 or C9), 176.1 (C8 or C9), 60.5 (C6), 59.1 (C5), 43.3 (C1), 39.8 (C7), 31.0 (C2), 27.7 (C4), 20.8 (C3), 14.1 (C4).



(2'S,1'S,3'R)-(1,2-Dicarbamoylethyl)-(3-hydroxymethyl-2,2-dimethylcyclopropyl) carbamic acid benzyl ester (2.061). (hrp2-194). *i*Pr₂NEt (14 mg, 19 μ L, 0.11 mmol) and Cbz-Cl (16 mg, 13 μ L, 0.09 mmol) were added to a stirred solution of **2.061** (23 mg, 0.1 mmol) in THF, CH₃CN (1:1, 2 mL total) at rt. The reaction was sonicated at rt for 1 h and then heated under reflux for 3 h. The mixture was cooled to rt, and EtOAc (5 mL) was added. The mixture was washed with 1 M HCl sat. with NaCl (1 x 5 mL), and the aqueous layer was back extracted with EtOAc (2 x 5 mL). The organic layers were combined and washed with sat. Na₂CO₃ (2 x 5 mL), and the aqueous layer was back extracted with EtOAc (2 x 5mL). The organic layers were combined, dried (Na₂SO₄) and concentrated under reduced pressure to yield 30 mg of **2.061** (83%) as a yellow oil; ¹H NMR (500 MHz, DMSO-d₆, 383K) δ 7.39-7.28 (comp, 5 H), 6.79-6.67 (comp, 3 H), 5.63 (s, 1 H), 5.06 (d, *J* = 12.5 Hz, 2 H), 4.10 (dd, *J* = 7.0, 5.6 Hz, 1 H), 3.60 (dd, *J* = 11.5, 7.0 Hz, 1 H), 3.44 (dd, *J* = 11.5, 5.6 Hz, 1 H), 2.96 (dd, *J* = 15.8, 7.0 Hz, 1 H), 2.87 (br s, 1 H), 2.66 (dd, *J* = 15.8, 7.0 Hz, 1 H), 2.51 (d, *J* = 7.8 Hz, 1 H), 1.02 (s, 3 H), 0.99 (s, 3 H), 0.93-0.90 (m, 1 H); ¹³C NMR (125 MHz, DMSO-

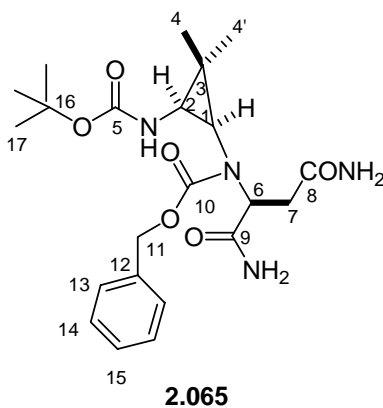
d₆, 383K) δ 172.2, 171.3, 157.3, 136.0, 127.5, 127.1, 66.2, 60.7, 56.8, 53.9, 46.0, 36.5, 30.4, 26.2, 19.8, 14.0; IR 3475, 3408, 3350, 2956, 1682, 1592, 1403, 1296, 1150, 1023, 909 cm⁻¹; mass spectrum (CI) m/z 364.1875 [C₁₈H₂₅N₃O₅ (M+1) requires 364.1872], 329, 346, 365.

NMR Assignments. ¹H NMR (500 MHz, DMSO-d₆, 383K) δ 7.39-7.28 (comp, 5 H, C13-H, C13'-H, C14-H, C14'-H & C15-H), 6.79-6.67 (comp, 3 H, N-H), 5.63 (s, 1 H, N-H), 5.06 (d, $J = 12.5$ Hz, 2 H, C11-H), 4.10 (dd, $J = 7.0, 5.6$ Hz, 1 H, C6-H), 3.60 (dd, $J = 11.5, 7.0$ Hz, 1 H, C5-H), 3.44 (dd, $J = 11.5, 7.5$ Hz, 1 H, C5'-H), 2.96 (dd, $J = 15.8, 7.0$ Hz, 1 H, C7-H), 2.87 (br, 1 H, O-H), 2.66 (dd, $J = 15.8, 7.0$ Hz, 1 H, C7'-H), 2.51 (d, $J = 7.8$ Hz, 1 H, C1-H), 1.02 (s, 3 H, C4-H), 0.99 (s, 3 H, C4'-H), 0.93-0.90 (m, 1 H, C2-H); ¹³C NMR (125 MHz, DMSO-d₆, 383K) δ 172.2 (C8, C9 or C10), 171.3 (C8, C9 or C10), 157.3 (C8, C9 or C10), 136.0 (C13, C14 or C15), 127.5 (C13, C14 or C15), 127.1 (C13, C14 or C15), 66.2 (C11), 60.7 (C6), 56.8 (C5), 53.9 (C12), 46.0 (C1), 36.5 (C7), 30.4 (C2), 26.2 (C4), 19.8 (C3), 14.0 (C4').



(3R,1'S,1S)-3-[Benzyloxycarbonyl-(1,2-dicarbamoylethyl)amino]-2,2-dimethyl cyclopropanecarboxylic acid (2.064). (hrp2-156). A mixture of NaHCO₃ (144 mg, 1.72 mmol), NaIO₄ (311 mg, 1.46 mmol), RuCl₃ (5 mg, 0.26 mmol) and **2.060** (95 mg, 0.260 mmol) in CH₃CN, CCl₄, H₂O (1:1:2, 20 mL total) was stirred vigorously for 30 min at rt. An additional 0.1 equivalent of RuCl₃ was then added, and the reaction mixture was stirred vigorously for 1 h at rt. The reaction mixture was diluted with CH₂Cl₂ (20 mL), and the layers were separated. The aqueous layer was washed with CH₂Cl₂ (3 x 20 mL). The aqueous layer was acidified with 1 M HCl sat. with NaCl. The aqueous layer was then extracted with EtOAc (3 x 20 mL). The organic layers were combined, dried (Na₂SO₄) and concentrated under reduced pressure to yield 93 mg of **2.064** (95%) as a white solid: 124 – 126 °C; ¹H NMR (500 MHz, DMSO-d₆, 383K) δ 7.38-7.28 (comp, 6 H), 6.79, (br s, 2 H), 5.10-5.08 (comp, 2 H), 5.00-4.98 (m, 1 H), 4.12 (dd, *J* = 6.9, 5.7 Hz, 1 H), 3.06 (dd, *J* = 16.1, 6.9 Hz, 1 H), 2.82 (d, *J* = 7.6 Hz, 1 H), 2.47 (dd, *J* = 17.3, 5.7 Hz, 1 H), 1.64 (d, *J* = 7.6 Hz, 1 H), 1.21 (s, 3 H), 1.11 (s, 3 H); ¹³C NMR (125 MHz, DMSO-d₆, 383K) δ 172.1, 171.2, 170.6, 156.3, 135.9, 127.6, 127.1, 127.0, 66.4, 59.4, 47.6, 34.6, 29.9, 27.4, 26.1, 14.2; mass spectrum (CI) *m/z* 378.1664 [C₁₈H₂₅N₃O₆ (M+1) requires 378.1665], 361, 378 (base), 468.

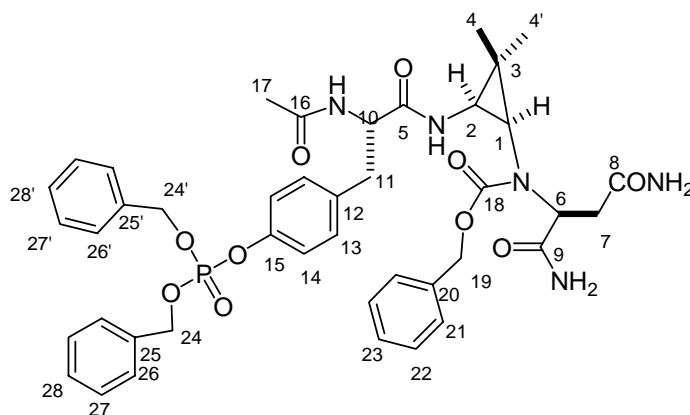
NMR Assignments. ^1H NMR (500 MHz, DMSO- d_6 , 383K) δ 7.38-7.28 (comp, 6 H, N-H, C13-H, C13'-H, C14-H, C14'-H & C15-H), 6.79, (br s, 2 H, N-H), 5.1-5.08 (comp, 2 H, C11-H & N-H), 5.00-4.98 (m, 1 H, C11'-H), 4.12 (dd, $J = 6.9, 5.7$ Hz, 1 H, C6-H), 3.06 (dd, $J = 16.1, 6.9$ Hz, 1 H, C7-H), 2.82 (d, $J = 7.6$ Hz, 1 H, C1-H), 2.47 (dd, $J = 17.3, 5.7$ Hz, 1 H, C7'-H), 1.64 (d, $J = 7.6$ Hz, 1 H, C2-H), 1.21 (s, 3 H, C4-H), 1.11 (s, 3 H, C4'-H); ^{13}C NMR (125 MHz, DMSO- d_6 , 383K) δ 172.1 (C5, C8, C9 or C10), 171.2 (C5, C8, C9 or C10), 170.6 (C5, C8, C9 or C10), 156.3 (C5, C8, C9 or C10), 135.9 (C12), 127.6 (C13, C14 or C15), 127.1 (C13, C14 or C15), 127.0 (C13, C14 or C15), 66.4 (C11), 59.4 (C6), 47.6 (C1), 34.6 (C7), 29.9 (C2), 27.4 (C3), 26.1 (C4), 14.2 (C4').



(1'S,2'S,3'S)-(3-*tert*-Butoxycarbonylamino-2,2-dimethylcyclopropyl)-(1,2-dicarbamoylethyl)carbamic acid benzyl ester (2.065). (hrp2-127). Ethyl chloroformate (12 mg, 11 μL , 0.114 mmol) and Et_3N (11 mg, 15 μL , 0.104 mmol) were added to a solution of **2.064** (33 mg, 0.087 mmol) in aqueous acetone (10:1, 2 mL total) at 0 $^\circ\text{C}$, and the mixture was stirred at 0 $^\circ\text{C}$ for 30 min. A solution of NaN_3 (8 mg, 0.131 mmol) dissolved in H_2O (200 μL) was then added, and the mixture was stirred at 0 $^\circ\text{C}$ for 30 min. Cold H_2O (2 mL) was added, and the mixture was extracted with CH_2Cl_2 (3 x 5 mL). The organic layers were combined, dried (Na_2SO_4) and concentrated to ca. 2 mL

under reduced pressure, *tert*-Butyl alcohol (2 mL) was added, and the reaction was heated under reflux for 13 h. The reaction was then concentrated under reduced pressure to yield 27 mg of **2.065** (70%) as a yellow oil; ^1H NMR (500 MHz, DMSO- d_6 , 373K) δ 7.39-7.30 (comp, 5 H), 6.90 (br s, 1 H), 6.15 (br s, 1 H), 5.10 (d, $J = 12.5$ Hz, 1 H), 5.03 (d, $J = 12.5$ Hz, 1 H), 4.07 (dd, $J = 6.9, 6.1$ Hz, 1 H), 3.48-3.45 (m, 1 H), 2.97-2.92, (m, 1 H), 2.66 (dd, $J = 15.6, 6.1$ Hz, 1 H), 2.51-2.49 (m, 1 H), 1.39 (s, 9 H), 0.98 (s, 3 H), 0.93 (s, 3 H); ^{13}C NMR (125 MHz, DMSO- d_6 , 373K) δ 171.9 171.8, 156.7, 155.8, 135.9, 127.7, 127.2, 127.1, 78.5, 66.4, 60.0, 43.8, 38.0, 35.8, 27.6, 24.0, 20.6, 13.6; IR 3476, 3408, 2960, 1720, 1687, 1592, 1367, 1161 cm^{-1} ; mass spectrum (CI) m/z 449.2403 [$\text{C}_{22}\text{H}_{33}\text{N}_4\text{O}_6$ (M+1) requires 499.2400], 393 (base), 349.

NMR Assignments. ^1H NMR (500 MHz, DMSO- d_6 , 373K) δ 7.39-7.30 (comp, 5 H, C13-H, C13'-H, C14-H C14'-H, C15-H), 6.90 (br s, 1 H, N-H), 6.15 (br s, 1 H, N-H), 5.10 (d, $J = 12.5$ Hz, 1 H, C11-H), 5.03 (d, $J = 12.5$ Hz, 1 H, C11-H), 4.07 (dd, $J = 6.9, 6.1$ Hz, 1 H, C6-H), 3.48-3.45 (m, 1 H, C1-H), 2.97-2.92, (m, 1 H, C7-H), 2.66 (dd, $J = 15.6, 6.1$ Hz, 1 H, C7'-H), 2.51-2.49 (m, 1 H, C2-H), 1.39 (s, 9 H, C17-H), 0.98 (s, 3 H, C4-H), 0.93 (s, 3 H, C4'-H); ^{13}C NMR (125 MHz, DMSO- d_6 , 373K) δ 171.9 (C10 or C9 or C8, or C5), 171.8 (C10 or C9 or C8, or C5), 156.7 (C10 or C9 or C8, or C5), 155.8 (C10 or C9 or C8, or C5), 135.9 (C12), 127.7 (C13 or C14 or C15), 127.2 (C13 or C14 or C15), 127.1 (C13 or C14 or C15), 78.5 (C16), 66.4 (C11), 60.0 (C6), 43.8 (C1), 38.0 (C7), 35.8 (C2), 27.6 (C17), 24.0 (C4), 20.6 (C3), 13.6 (C4).

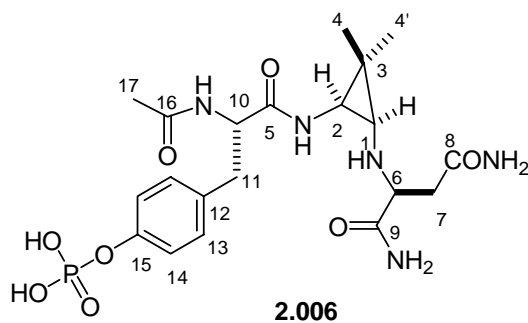


2.066

(1'S,2''S,3S)-3-{2-Acetylamino-3-[4-bisbenzyloxyphosphorloxyphenyl]propionylamino}-2,2-dimethylcyclopropyl-1,2-dicarbamoylethyl) carbamic acid benzyl ester (2.066). (hrp2-158 & 159). A solution of **2.065** (76 mg, 0.169 mmol) in neat TFA (1.5 mL) was stirred for 90 min. The reaction mixture was concentrated under reduced pressure, and the residue was triturated with Et₂O (3 x 2 mL) to give an off white solid.(62 mg) This crude amine was dissolved in DMF (2 mL) containing **2.030** (65 mg, 0.134 mmol) at -10 °C, and 2,6-lutidine (43 mg, 47 μL, 0.402 mmol) and HATU (51 mg, 0.134 mmol) were added. The mixture was stirred at -10 °C for 1 h and then at rt for 1h. EtOAc (10 mL) was added, and the organic layer was washed with sat. NaHCO₃ (10 mL), 1 M HCl sat. with NaCl (10 mL) and brine (10 mL). The organic layer was dried (Na₂SO₄) and concentrated under reduced pressure. The crude residue was purified by flash chromatography, eluting with CH₂Cl₂/MeOH (15:1) to yield 65 mg of **2.066** (60%) as a yellow oil: ¹H NMR (500 MHz, DMSO-d₆, 373K) δ 8.10 (br s, 1 H), 7.91 (d, *J* = 8.3, 1 H) 7.38-7.28 (comp, 16 H), 7.19 (d, *J* = 11.5, 4 H), 7.06-7.04 (m, 2 H), 6.83 (br s, 1 H), 5.12-5.01 (comp, 6 H), 4.44-4.39 (m, 1 H), 3.98 (t, *J* = 6.7, 1 H), 2.91-2.87 (m, 2 H), 2.79 (t, *J* = 7.0, 1 H), 2.72-2.68 (m, 2 H), 2.52 (d, *J* = 7.0, 1 H), 1.74 (s, 3 H), 0.95 (s, 3 H), 0.84 (s, 3 H); ¹³C NMR (125 MHz, DMSO-d₆, 373K) δ 173.0, 172.2, 171.9, 169.3,

156.7, 148.6, 136.2, 135.6, 134.9, 130.4, 128.4, 128.2, 128.1, 127.9, 127.8, 126.6, 127.2, 119.3, 72.1, 66.8, 60.0, 54.0, 36.8, 36.6, 24.2, 22.2, 21.4, 14.1; IR 3476, 3408, 2960, 1720, 1687, 1592, 1367, 1161 cm^{-1} ; mass spectrum (CI) m/z 814.3217 [$\text{C}_{42}\text{H}_{49}\text{N}_5\text{O}_{10}\text{P}$ (M+1) requires 814.3246].

NMR Assignments. ^1H NMR (500 MHz, DMSO-d_6 , 373K) δ 8.10 (br s, 1 H, N-H), 7.91 (d, $J = 8.3$, 1 H, N-H) 7.38-7.28 (comp, 16 H, C21-H, C22-H, C23-H, C24-H, C24'-H, C25-H, C25'-H, C26-H), 7.19 (d, $J = 11.5$, 4 H, C13-H or C14-H, N-H), 7.06-7.04 (m, 2 H, C13-H or C14-H), 6.83 (br s, 1 H, N-H), 5.12-5.01 (comp, 6 H, C24-H, C24'-H, C19-H), 4.44-4.39 (m, 1 H, C10-H), 3.98 (t, $J = 6.7$, 1 H, C6-H), 2.91-2.87 (m, 2 H, C7-H), 2.79 (t, $J = 7.0$, 1 H, C2-H), 2.72-2.68 (m, 2 H, C11-H), 2.52 (d, $J = 7.0$, 1 H, C1-H), 1.74 (s, 3 H, C17-H), 0.95 (s, 3 H, C4-H), 0.84 (s, 3 H, C4'-H); ^{13}C NMR (125 MHz, DMSO-d_6 , 373K) δ 173.0 (C5 or C8 or C9 or C16 or C18), 172.2 (C5 or C8 or C9 or C16 or C18), 171.9 (C5 or C8 or C9 or C16 or C18), 169.3 (C5 or C8 or C9 or C16 or C18), 156.7 (C5 or C8 or C9 or C16 or C18), 148.6 (C12 or C15 or C20 or C25), 136.2 (C12 or C15 or C20 or C25), 135.6 (C12 or C15 or C20 or C25), 134.9 (C12 or C15 or C20 or C25), 130.4 (C13 or C14), 128.4 (C26, C26', C27 C27', C21, C22), 128.2 (C26, C26', C27 C27', C21, C22), 128.1 (C26, C26', C27 C27', C21, C22), 127.9 (C26, C26', C27 C27', C21, C22), 127.8 (C26, C26', C27 C27', C21, C22), 126.6 (C26, C26', C27 C27', C21, C22), 127.2 (C26, C26', C27 C27', C21, C22), 119.3 (C13 or C14), 72.1 (C19 or C24), 66.8 (C19 or C24), 60.0 (C6), 54.0 (C10), 36.8 (C7, C2, C11), 36.6 (C7, C2, C11), 24.2 (C4), 22.2 (C17), 21.4 (C3), 14.1 (C4').

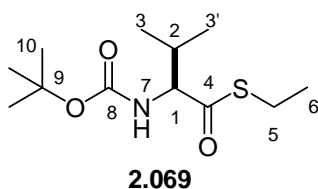


(1''S,2S,2'S,3'S)-Phosphoric Acid mono 4-{2-acetylamino-2-[3-(1,2-dicarbamoylethylamino-2,2-dimethylcyclopropylcarbamoyl)ethyl]phenyl}ester

(2.006). (hrp2-211). A solution of **2.066** (4 mg, 0.0172 mmol) in EtOH (2 mL) containing 10% Pd/C (10 mg) was stirred under H₂ (1 atm) for 12 h. The catalyst was removed by filtration through a pad of celite, and the filtrate was concentrated under reduced pressure to yield 10 mg of **3** (100%) as a white solid: mp 88 - 90 °C; ¹H NMR (500 MHz, D₂O) δ 7.22 (d, *J* = 8.5 Hz, 2 H), 7.19 (d, *J* = 8.5 Hz, 2 H), 4.52-4.49 (m, 1 H), 3.52-3.49 (m, 1 H), 3.14-2.89 (comp, 2 H), 2.62 (dd, *J* = 15.0, 5.7, 1 H), 2.53 (dd, *J* = 15.0, 8.0 Hz, 1 H), 2.30 (d, *J* = 6.0 Hz, 1 H), 2.00 (d, *J* = 6.0 Hz, 1 H), 1.95 (s, 3 H), 1.03 (s, 3 H), 0.93 (s, 3 H); ¹³C NMR (125 MHz, D₂O) δ 181.6, 178.1, 177.7, 176.7, 134.7, 133.1, 132.9, 123.2, 61.2, 58.0, 43.7, 40.5, 39.2, 38.3, 26.6, 24.3, 23.1, 15.0; mass spectrum (FAB +) *m/z* 500.1903 [C₂₀H₃₁N₅O₉P (M+1) requires 500.1910], 461, 369, 277 (base).

NMR Assignments. ¹H NMR (500 MHz, D₂O) δ 7.22 (d, *J* = 8.5 Hz, 2 H, C 15-H or C16-H), 7.19 (d, *J* = 8.5 Hz, 2 H, C15-H or C16-H), 4.52-4.49 (m, 1 H, C12-H), 3.52-3.49 (m, 1 H, C6-H), 3.14-2.89 (comp, 2 H, C13-H), 2.62 (dd, *J* = 15.0, 5.7, 1 H, C7-H), 2.53 (dd, *J* = 15.0, 8.0 Hz, 1 H, C7'-H), 2.30 (d, *J* = 6.0 Hz, 1 H, C1-H or C2-H), 2.00 (d, *J* = 6.0 Hz, 1 H, C1-H or C2-H), 1.95 (s, 3 H, C4-H), 1.03 (s, 3 H, C4'-H), 0.93 (s, 3 H); ¹³C NMR (125 MHz, D₂O) δ 181.6 (C5 or C8 or C9 or C10), 178.1 (C5 or C8 or C9 or

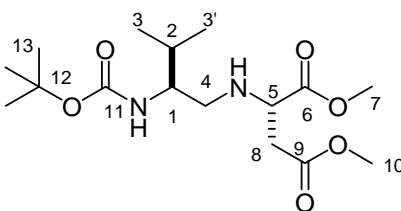
C10), 177.7 (C5 or C8 or C9 or C10), 176.7 (C5 or C8 or C9 or C10), 134.7 (C14 or C17), 133.1 (C14 or C17), 132.9 (C15 or C16), 123.2 (C15 or C16), 61.2 (C6), 58.0 (C12), 43.7 (C1 or C2), 40.5 (C7), 39.2 (C13), 38.3 (C1 or C2), 26.6 (C4), 24.3 (C11), 23.1 (C3), 15.0 (C4).



(2S)-2-tert-Butylthiobutyric acid S-ethyl ether (2.069). (tbs112). 4-Dimethylaminopyridine (DMAP) (40 mg, 0.3 mmol), ethanethiol (0.25 mL, 3.3 mmol), and dicyclohexylcarbodiimide (DCC) (681 mg, 3.3 mmol) were added to a solution of **2.027** (651 mg, 3.0 mmol) in CH₂Cl₂ (5 mL) at rt. The mixture was stirred at rt for 0.5 h and then filtered through a cotton plug. The filtrate was concentrated under reduced pressure to yield a white residue. The residue was purified by flash chromatography eluting with hexanes/EtOAc (5:1) to yield 582 mg of **2.069** (75%) as a white solid: mp 62-64 °C; ¹H NMR (125 MHz, CDCl₃) δ 4.95 (d, *J* = 8.9 Hz, 1 H), 4.23 (dd, *J* = 8.9 Hz, 5.0 Hz, 1 H), 2.85 (q, *J* = 7.4 Hz, 2 H), 2.27-2.20 (m, 1 H), 1.43 (s, 9 H), 1.21 (t, *J* = 7.4 Hz, 3 H), 0.95 (d, *J* = 6.8 Hz, 3 H), 0.83 (d, *J* = 6.8 Hz, 3 H); ¹³C NMR (75 MHz, CDCl₃) δ 201.1, 155.5, 80.1, 65.3, 31.1, 28.3, 23.2, 19.4, 16.7, 14.5; IR (CDCl₃) 2253, 1714, 1681, 1493, 1369 cm⁻¹; mass spectrum (CI) *m/z* 261.1470 [C₁₂H₂₄NO₃S (M+1) requires 262.1477], 206 (base), 144.

NMR Assignments. ¹H NMR (500 MHz, CDCl₃) δ 4.95 (d, *J* = 8.9 Hz, 1 H, N-H), 4.23 (dd, *J* = 8.9 Hz, 5.0 Hz, 1 H, C1-H), 2.85 (q, *J* = 7.4, 2 H, C5-H), 2.27-2.20 (m,

1 H, C2-H), 1.43 (s, 9 H, C10-H), 1.21 (t, $J = 7.4$ Hz, 3 H, C6-H), 0.95 (d, $J = 6.8$ Hz, 3 H, C3-H), 0.83 (d, $J = 6.8$ Hz, 3 H, C3'-H); ^{13}C NMR (125 MHz, CDCl_3) δ 201.1 (C8), 155.5 (C4), 80.1 (C9), 65.3 (C1), 31.1 (C10), 28.3 (C5), 23.2 (C4), 19.4 (C3), 16.7 (C3'), 14.5 (C6)

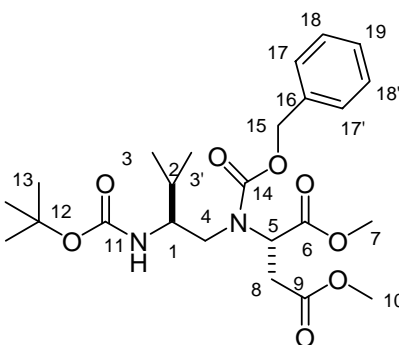


2.071

(2S, 2S')-2-(2-tert-butoxycarbonylamino-3-methylbutylamino)succinic acid dimethyl ester (2.071). (tbs153 & 154) Triethylsilane (Et_3SiH) (0.61 mL, 3.8 mmol) was added quickly to a solution of **2.069** (200 mg, 0.76 mmol) and 10% Pd/C (ca 10 mg) in CH_2Cl_2 (2 mL) at rt. The mixture was stirred at rt for 0.5 h and then filtered through a pad of celite. The filtrate was concentrated under reduced pressure, and the residue was diluted with DMF (1.5 mL). L-Aspartic acid dimethyl ester hydrochloride (180 mg, 0.91 mmol) and sodium triacetoxyborohydride ($\text{Na}(\text{OAc})_3\text{BH}$) (322 mg, 1.52) were added, and the mixture was stirred for 0.5 h at rt. Et_2O (8 mL) was added, and the organic layer was washed with saturated aqueous NaHCO_3 (3 x 5 mL) and brine (2 x 5 mL). The combined organic layers were dried (Na_2SO_4) and concentrated under reduced pressure to give a dark yellow oil. The residue was purified by flash chromatography eluting with hexanes/ EtOAc (1.5:1) to give 224 mg of **2.071** (85%) as a pale yellow oil; ^1H NMR (500 MHz, CDCl_3) δ 4.60-4.54 (br s, 1 H), 3.71 (s, 3 H), 3.68-3.64 (m, 1 H), 3.66 (s, 3 H), 3.46-3.38 (br s, 1 H), 2.79-2.74 (comp, 2 H), 2.63 (dd, $J = 16.1$ Hz, 7.2 Hz, 1 H), 2.54-2.50 (br s, 1 H), 1.81-1.74 (m, 1 H), 1.41 (s, 9 H), 0.87 (d, $J = 6.9$ Hz, 3 H), 0.84 (d,

$J = 6.9$ Hz, 3 H); ^{13}C NMR (125 MHz) δ 173.4, 171.2, 156.2, 79.1, 57.7, 55.5, 52.2, 51.9, 49.2, 37.3, 30.0, 28.4, 19.3, 18.0; IR 3378, 2959, 1738, 1504, 1360, 1247, 1171, 1003, 866, 733 cm^{-1} ; mass spectrum (CI) m/z 347.2182 (base) [$\text{C}_{16}\text{H}_{30}\text{N}_2\text{O}_6$ (M+1) requires 347.2104], 291, 247.

NMR Assignments: ^1H NMR (500 MHz, CDCl_3) δ 4.60-4.54 (br s, 1 H, N-H), 3.71 (s, 3 H, C10-H or C7-H), 3.68-3.64 (m, 1 H, C5-H), 3.66 (s, 3 H, C10-H or C7-H), 3.46-3.38 (br s, 1 H, C1-H), 2.79-2.74 (comp, 2 H, C8-H & C4-H), 2.63 (dd, $J = 16.1$ Hz, 7.2 Hz, 1 H, C8-H), 2.54-2.50 (br s, 1 H, C4-H), 1.81-1.74 (m, 1 H, C2-H), 1.41 (s, 9 H, C13-H), 0.87 (d, $J = 6.9$ Hz, 3 H, C3-H), 0.84 (d, $J = 6.9$ Hz, 3 H, C3'-H); ^{13}C NMR (75 MHz) δ 173.4 (C11), 171.2 (C9), 156.2 (C6), 79.1 (C12), 57.7 (C5), 55.5 (C1), 52.2 (C10 or C7), 51.9 (C10 or C7), 49.2 (C4), 37.3 (C8), 30.0 (C2), 28.4 (C13), 19.3 (C3), 18.0 (C3').

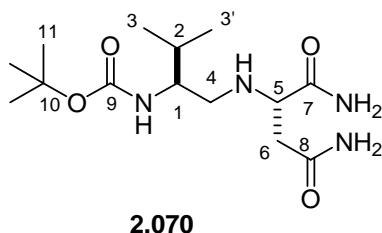


2.072

(2*S*, 2*S'*)-2-[Benzyloxycarbonyl-(2-*tert*-butoxycarbonylamino-3-methylbutylamino)succinic acid dimethyl ester (**2.072**). (tbs132) $i\text{Pr}_2\text{NEt}$ (46 μL , 0.32 mmol) and benzyl chloroformate (51 μL , 0.29 mmol) were added to a solution of **2.071** (56 mg, 0.16 mmol) in CH_2Cl_2 (2.0 mL) at rt. After stirring 2 h at rt, the reaction mixture was concentrated under reduced pressure. The residue was purified by flash

chromatography eluting with hexanes/EtOAc (2:1) to give 70 mg (90%) of **2.072** as a pale yellow oil; ^1H NMR (500 MHz, DMSO- d_6 , 373K) δ 7.37-7.29 (comp, 5 H), 5.95-5.92 (br s, 1 H), 5.08 (s, 2 H), 4.50 (qt, $J = 4.0$ Hz, 1 H), 3.63 (s, 3 H), 3.58-3.56 (m, 1 H), 3.57-3.54 (m, 1 H), 3.56 (s, 1 H), 3.17 (dd, $J = 17.2, 5.8$ Hz, 1 H), 3.16 (d, $J = 9.1$ Hz, 1 H), 2.69 (dd, $J = 17.2, 5.8$ Hz, 1 H), 1.69 (hept, $J = 5.0$ Hz, 1 H), 1.37 (s, 9 H), 0.85 (d, $J = 6.8$ Hz, 3 H), 0.82 (d, $J = 6.8$ Hz, 3 H); ^{13}C NMR (125 MHz, DMSO, 100 °C) δ 169.9, 169.6, 154.9, 154.7, 135.8, 127.5, 127.1, 126.9, 77.1, 66.3, 58.0, 55.0, 51.3, 50.9, 50.6, 34.6, 29.7, 27.54, 18.4, 16.9; mass spectrum (CI) m/z 480.2550 [$\text{C}_{24}\text{H}_{36}\text{N}_2\text{O}_8$ (M+1) requires 481.2548], 425, 381 (base).

NMR Assignments: ^1H NMR (500 MHz, DMSO- d_6 , 373K) δ 7.37-7.29 (comp, 5 H, C17-H, C18-H, & C19-H), 5.95-5.92 (br s, 1 H, N-H), 5.08 (s, 2 H, C15-H), 4.50 (qt, $J = 4.0$ Hz, 1 H, C5-H), 3.63 (s, 3 H, C10-H or C7-H), 3.58-3.56 (m, 1 H, C1-H), 3.57-3.54 (m, 1 H, C4-H), 3.56 (s, 1 H, C10-H or C7-H), 3.17 (dd, $J = 17.2, 5.8$ Hz, 1 H, C8-H), 3.16 (d, 1 H, $J = 9.1$ Hz, C4'-H), 2.69 (dd, $J = 17.2, 5.8$ Hz, 1 H, C8'-H), 1.69 (hept, $J = 5.0$ Hz, 1 H, C2-H), 1.37 (s, 9 H, C13-H), 0.85 (d, $J = 6.8$ Hz, 3 H, C3-H), 0.82 (d, $J = 6.8$ Hz, 3 H, C3'-H); ^{13}C NMR (125 MHz, DMSO, 100 °C) δ 169.9 (C9 or C6), 169.6 (C9 or C6), 154.9 (C14 or C11), 154.7 (C14 or C11), 135.8 (C16), 127.5 (C17, C18, or C19), 127.1 (C17, C18, or C19), 126.9 (C17, C18, or C19), 77.1 (C12), 66.3 (C15), 58.0 (C5), 55.0 (C1), 51.3 (C4), 50.9 (C10 or C7), 50.6 (C10 or C7), 34.6 (C8), 29.7 (C2), 27.5 (C13), 18.4 (C3), 16.9 (C3').

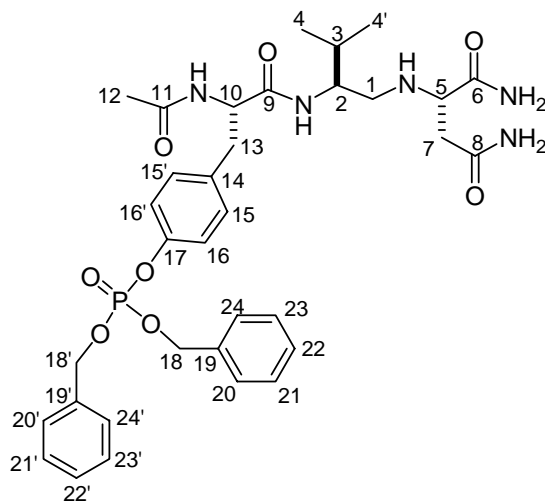


(2*S*, 2*S'*)-2-[(*tert*-butoxycarbonyl)amino]-3-methylbutyl]aspartamide (2.070).

(aw1-81). NaCN (5 mg, 0.09 mmol) was added to a stirred solution of **2.071** (290 mg, 0.92 mmol) in MeOH (10 mL) at rt. The reaction mixture was saturated with NH₃ by bubbling the gas into solution for 20 min at rt. The reaction was stirred at 50 °C for 3 d, during which time it was resaturated with NH₃ every 12 h. The mixture was then concentrated under reduced pressure, and the residue was recrystallized from minimal amounts of hot CH₃CN (ca. 7 mL) to yield 200 mg of **2.070** (69%) as a off white solid: mp 175-177 °C; ¹H NMR (500 MHz, CD₃OD) δ 3.39-3.37 (comp, 2 H), 2.64 (dd, *J* = 11.8, 4.2 Hz, 1 H), 2.57 (dd, *J* = 15.3, 4.2 Hz, 1 H), 2.54 (dd, *J* = 11.7, 4.1 Hz, 1 H), 2.45 (dd, *J* = 15.3, 4.2 Hz, 1 H), 1.73 (app hep, *J* = 6.8 Hz, 1 H), 1.44 (s, 9 H), 0.90 (d, *J* = 6.8 Hz, 3 H), 0.88 (d, *J* = 6.8 Hz, 3 H); ¹³C NMR (125 MHz, CD₃OD) δ 178.9, 176.0, 158.8, 79.9, 60.8, 57.6, 50.8, 38.8, 31.8, 28.8, 19.9, 18.7; IR 3292, 2361, 1664 cm⁻¹, mass spectrum (CI) *m/z* 317.2194 [C₁₄H₂₉N₄O₄ (M+1) requires 317.2189], 200 (base), 182.

NMR Assignments: ¹H NMR (500 MHz, CD₃OD) δ 3.39-3.37 (comp, 2 H, C1-H & C5-H), 2.64 (dd, *J* = 11.8, 4.2 Hz, 1 H, C6-H), 2.57 (dd, *J* = 15.3, 4.2 Hz, 1 H, C4-H), 2.54 (dd, *J* = 11.7, 4.1 Hz, 1 H, C6'-H), 2.45 (dd, *J* = 15.3, 4.2 Hz, 1 H, C4'-H), 1.73 (app hep, *J* = 6.8 Hz, 1 H, C2-H), 1.44 (s, 9 H, C11-H), 0.90 (d, *J* = 6.8 Hz, 3 H, C3-H), 0.88 (d, *J* = 6.8 Hz, 3 H, C3'-H); ¹³C NMR (125 MHz, CD₃OD) δ 178.9 (C7 or C8),

176.0 (C7 or C8), 158.8 (C9), 79.9 (C10), 60.8 (C1 or C5), 57.6 (C1 or C5), 50.8 (C6), 38.8 (C4), 31.8 (C2), 28.8 (C11), 19.9 (C3), 18.7 (C3').



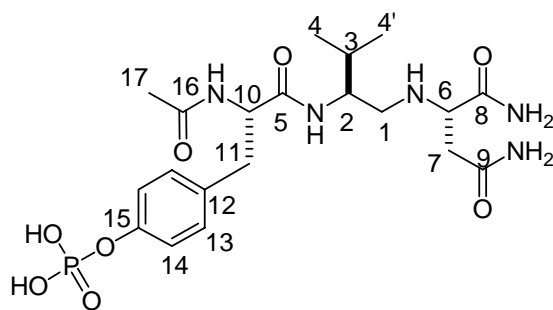
2.076

(2S,2S',1S'') **Phosphoric acid 4-(2-acetylamino-2-1{[1,2-dicarbamoylethylamino)methyl]-2-methylpropylcarbamoyl}ethyl)phenyl ester dibenzyl ester (2.076). (aw1-73).** A solution of **2.070** (85 mg, 0.20 mmol) neat in TFA (1 mL) was stirred for 90 min. The reaction mixture was concentrated under reduced pressure, and the residue was triturated with Et₂O (3 x 2 mL) to give an off-white solid. This crude amine was dissolved in DMF (2 mL) containing **2.030** (97 mg, 0.20 mmol) at -10 °C, and 2,6-lutidine (70 μL, 0.60 mmol), and HATU (76 mg, 0.20 mmol) were added. The cooling bath was removed, and the mixture was slowly warmed to rt over 1 h and stirred at rt for 15 h. The mixture was concentrated under reduced pressure, and the residue was dissolved in EtOAc (10 mL). The mixture was washed with saturated NaHCO₃ (3 x 10 mL) and brine (10 mL), dried (Na₂SO₄), and concentrated under reduced pressure. The crude residue was purified by flash chromatography, eluting with CH₂Cl₂/MeOH (19:1) to yield 40 mg of **2.076** (30%) as a clear solid: mp 69 – 74 °C; ¹H

NMR (500 MHz, DMSO- d_6) δ 8.04-8.03 (d, $J = 8.5$ Hz, 1 H), 7.50 (br d, $J = 9.0$ Hz, 1 H), 7.39-7.34 (comp, 12 H), 7.26 (d, $J = 8.5$ Hz, 2 H), 7.07-7.04 (comp, 3 H), 6.81 (s br, 1 H), 5.13 (s, 2 H), 5.12 (s, 2 H), 4.48 (ddd, $J = 10.3, 8.5, 4.0$ Hz, 1 H), 3.62-3.57 (m, 1 H), 3.19 (br s, 1 H), 2.95 (dd, $J = 13.9, 4.0$ Hz, 1 H), 2.71 (dd, $J = 13.9, 10.3$ Hz, 1 H), 2.47-2.44 (m, 2 H), 2.36 (dd, $J = 14.9, 4.0$ Hz, 1 H), 2.22 (dd, $J = 14.9, 8.6$ Hz, 1 H), 1.77-1.70 (comp, 4 H), 0.81 (dd, $J = 9.8, 6.8$ Hz, 6 H); ^{13}C NMR (125 MHz, DMSO- d_6) δ 172.6, 171.3, 169.0, 166.3, 148.6, 135.7, 135.6, 135.3, 130.5, 128.5, 127.9, 119.4, 119.3, 69.3, 69.2, 59.2, 54.0, 53.7, 48.9, 37.7, 36.9, 29.2, 22.4, 19.4, 18.3; IR 3010, 2395, 1217, 777. 666 cm^{-1} ; mass spectrum (FAB) m/z 682.3031 [$\text{C}_{34}\text{H}_{44}\text{N}_5\text{O}_8\text{P}$ (M+1) requires 682.3001], 289, 307, 682 (base).

NMR Assignments. ^1H NMR (500 MHz, DMSO- d_6) δ 8.04–8.03 (d, $J = 8.5$ Hz, 1 H, N-H), 7.50 (br d, $J = 9.0$ Hz, 1 H, N-H), 7.39–7.34 (comp, 12 H, C20-H & C20'-H, C21-H & C21'-H, C22-H & C22'-H, C23-H & C23'-H, C24-H & C24'-H, N-H), 7.26 (d, $J = 8.5$ Hz, 2 H, C15-H & C15'-H or C16-H & C16'-H), 7.07–7.04 (comp, 3 H, C15-H & C15'-H or C16-H & C16'-H, N-H), 6.81 (s br, 1 H, N-H), 5.13 (s, 2 H, C18-H or C18'-H), 5.12 (s, 2 H, C18-H or C18'-H), 4.48 (ddd, $J = 4.0, 8.5, 10.3$ Hz, 1 H, C10-H), 3.62–3.57 (m, 1 H, C2-H), 3.19 (s br, 1 H, C5-H), 2.95 (dd, $J = 4.0, 13.9$ Hz, 1 H, C13-H or C13'-H), 2.71 (dd, $J = 10.3, 13.9$ Hz, 1 H, C13-H or C13'-H), 2.45 (m, 2 H, C1-H), 2.36 (dd, $J = 14.8, 15.1$ Hz, 1 H, C7-H or C7'-H), 2.22 (dd, $J = 14.8, 15.1$ Hz, 1 H, C7-H or C7'-H), 1.77–1.70 (comp, 4 H, C3-H and C12-H), 0.81 (dd, $J = 9.8, 6.8$ Hz, 6 H, C4-H); ^{13}C NMR (125 MHz, DMSO) δ 172.6 (C8), 171.3 (C9), 169.0 (C11), 166.3 (C6), 148.6 (C14 or C17), 135.7 (C19, C19', C20, C20', C21, C21', C22, C22', C23, C23', C24, or C24'), 135.6 (C19, C19', C20, C20', C21, C21', C22, C22', C23, C23', C24, or C24'), 135.3 (C14 or C17), 130.5 (C19, C19', C20, C20', C21, C21', C22, C22', C23, C23', C24, or C24'), 128.5 (C19, C19', C20, C20', C21, C21', C22, C22', C23, C23', C24, or C24'),

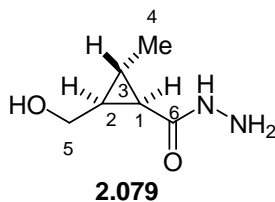
C24'), 127.9 (C19, C19', C20, C20', C21, C21', C22, C22', C23, C23', C24, or C24'), 119.4 (C15 & C15' or C16 & C16'), 119.3 (C15 & C15' or C16 & C16'), 69.3 (C18 or C18'), 69.2 (C18 or C18'), 59.2 (C5), 54.0 (C10), 53.7 (C2), 48.9 (C1), 37.7 (C7), 36.9 (C13), 29.2 (C3 or C12), 22.4 (C3 or C12), 19.4 (C4 or C4'), 18.3(C4 or C4').



2.007

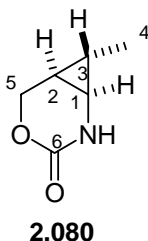
(2*S*, 2*S'*, 1*S''*) Phosphoric acid mono-[4-(2-acetylamino-2-{1-[(1,2-dicarbamoyl ethylamino) methyl]-2-methyl propylcarbamoyl} ethyl) phenyl] ester (2.007). (aw2-45). A solution of **2.076 (25 mg, 0.04 mmol) in EtOH and H₂O (1:1, 2 mL) containing 10 % Pd/C (10 mg) and 0.5 M HCl (37 μL) was stirred under H₂ (1 atm) at rt for 2 h. The catalyst was removed by filtration through a pad of celite, and the filtrate was concentrated to yield 17 mg (94%) of **5** as a white solid: mp 204-206 dec °C; ¹H NMR (500 MHz, D₂O) δ 7.27 (d, *J* = 8.2 Hz, 2 H), 7.17 (d, *J* = 8.2 Hz, 2 H), 4.57 (dd, *J* = 8.4, 7.0 Hz, 1 H), 4.26 (dd, *J* = 7.7, 4.9 Hz, 1 H), 3.98–3.94 (m, 1 H), 3.21 (dd, *J* = 12.9, 4.3 Hz, 1 H), 3.13 (dd, *J* = 13.9, 7.0 Hz, 1 H), 3.05–2.97 (comp, 2 H), 2.95–2.87 (comp, 2 H), 1.96 (s, 3 H), 1.90–1.84 (m, 1 H), 0.88 (dd, *J* = 16.9, 6.8 Hz, 6 H); ¹³C NMR (125 MHz, D₂O) δ 177.0, 176.9, 175.7, 172.3, 133.1, 123.2, 60.0, 58.1, 55.0, 51.1, 38.7, 36.4, 32.5, 24.3, 21.0, 19.4; mass spectrum (FAB) *m/z* 500.1930 [C₂₀H₃₂N₅O₈P (M-1) requires 500.1910], 275, 386, 500 (base).**

NMR Assignments. ^1H NMR (500 MHz, D_2O) δ 7.27 (d, $J = 8.2$ Hz, 2 H, C13-H or C14-H), 7.17 (d, $J = 8.2$ Hz, 2 H, C13-H or C14-H), 4.57 (dd, $J = 8.4, 7.0$ Hz, 1 H, C10-H), 4.26 (dd, $J = 7.7, 4.9$ Hz, 1 H, C6-H), 3.98-3.94 (m, 1 H, C2-H), 3.21 (dd, $J = 12.9, 4.3$ Hz, 1 H, C1-H), 3.13 (dd, $J = 13.9, 7.0$ Hz, 1 H, C11-H), 3.05-2.97 (comp, 2 H, C7-H & C11'-H), 2.95-2.87 (comp, 2 H, C1'-H & C7'-H), 1.96 (s, 3 H, C17-H), 1.90-1.84 (m, 1 H, C3-H), 0.88 (dd, $J = 16.9, 6.8$ Hz, 6 H, C4-H); ^{13}C NMR (125 MHz, D_2O) δ 177.0 (C5 or C8 or C9 or C16), 176.9 (C5 or C8 or C9 or C16), 175.7 (C5 or C8 or C9 or C16), 172.3 (C5 or C8 or C9 or C16), 153.8 (C12 or C15), 153.7 (C12 or C15), 133.1 (C13 or C14), 123.2 (C13 or C14), 60.0 (C6), 58.1 (C10), 55.0 (C2), 51.1 (C1), 38.7 (C11), 36.4 (C7), 32.5 (C3), 24.3 (C17), 21.0 (C4), 19.4 (C4').



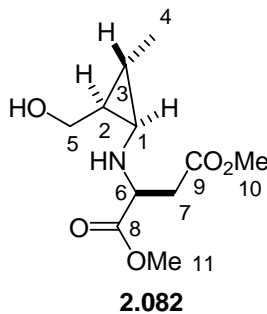
(1S,2R,3S)-2-Hydroxymethyl-3-methyl-cyclopropanecarboxylic acid hydrazide (2.079). (**hrp3-168**) Hydrazine monohydrate (1.33 mL, 27.5 mmol) was added over 15 min to a solution of lactone **2.078** (522 mg, 4.66 mmol) in MeOH (50 mL) at rt. The reaction was stirred at rt for 1 d and then concentrated under reduced pressure to give a white solid that was recrystallized from hot isopropanol to yield 631 mg (94%) of **2.079** as a white solid: mp 92-95 °C; ^1H NMR (500 MHz, CD_3OD) δ 3.78 (dd, $J = 11.4, 6.2$ Hz, 1 H), 3.36 (dd, $J = 11.4, 7.6$ Hz, 1 H), 1.42-1.36 (comp, 2 H), 1.27-1.21 (m, 1 H), 1.1 (d, $J = 5.8$ Hz, 3 H); ^{13}C NMR (125 MHz, CD_3OD) δ 173.9, 60.6, 32.0, 26.6, 19.5, 17.8; IR 1608, 1518, 1435, 1260, 1014 cm^{-1} , mass spectrum (CI) m/z 145.0975 [$\text{C}_6\text{H}_{12}\text{N}_2\text{O}_2$ (M+1) requires 145.0977], 127.

NMR Assignments. ^1H NMR (500 MHz, CD_3OD) δ 3.78 (dd, $J = 11.4, 6.2$ Hz, 1 H, C5-H), 3.36 (dd, $J = 11.4, 7.6$ Hz, 1 H, C5'-H), 1.42-1.36 (comp, 2 H, 1-H & C3-H), 1.27-1.21 (m, 1 H, C2-H), 1.1 (d, $J = 5.8$ Hz, 3 H, C4-H); ^{13}C NMR (125 MHz, CD_3OD) δ 173.9 (C6), 60.6 (C5), 32.0 (C2), 26.6 (C1 or C3), 19.5 (C1 or C3), 17.8 (C4).



(1R,6S,7S)-7-Methyl-4-oxa-2-azabicyclo[4.1.0]heptan-3-one (2.080). (**hrp4-052**). 6 N aqueous HCl (2.0 mL, 12.0 mmol) was added dropwise to a vigorously stirred mixture of NaNO_2 (833 mg, 12.0 mmol) and hydrazide **2.079** (1.16 g, 8.05 mmol) in a mixture of Et_2O (20 mL) and H_2O (20 mL) at 0 °C. The yellow mixture was stirred vigorously at 0 °C for 45 min, and then cold toluene (20 mL) was added. The layers were separated, and the aqueous layer was extracted with toluene (3 x 20 mL). The organic layers were combined, washed with brine (1 x 20 mL), dried (Na_2SO_4) and concentrated under reduced pressure to approximately 50 mL. A stirbar was added, and the mixture was heated at 80 °C for 2 h. After cooling to rt, the solvent was removed under reduced pressure to yield 867 mg (85%) of **2.080** as an orange-yellow oil. This material was shown to be >95% pure by ^1H NMR and was used without further purification: ^1H NMR (500 MHz, CDCl_3) δ 6.00 (br s, 1 H), 4.68 (dd, $J = 11.9, 6.8$ Hz, 1 H), 4.05 (dd, $J = 11.9, 5.4$ Hz, 1 H), 2.54 (dt, $J = 8.7, 2.4$ Hz, 1 H), 1.29-1.24 (m, 1 H), 1.04-0.98 (comp, 4 H); ^{13}C NMR (125 MHz, CDCl_3) δ 155.19, 69.3, 34.24, 23.9, 15.8, 15.2; IR (CDCl_3) 3019, 2253, 1715, 1469, 1213, 908, 789, 734, 651 cm^{-1} ; mass spectrum (CI) m/z 128.0718 [$\text{C}_6\text{H}_9\text{NO}_2$ (M+1) requires 128.0711], 110, 84.

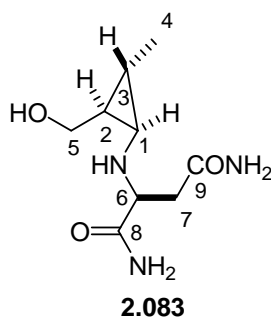
NMR Assignments. ^1H NMR (500 MHz, CDCl_3) δ 6.00 (br s, 1 H, N-H), 4.68 (dd, $J = 11.9, 6.8$ Hz, 1 H, C5-H), 4.05 (dd, $J = 11.9, 5.4$ Hz, 1 H, C5-H), 2.54 (dt, $J = 8.7, 2.4$ Hz, 1 H, C3-H), 1.29-1.24 (m, 1 H, C2-H), 1.04-0.98 (comp, 4 H, C1-H & C4-H); ^{13}C NMR (125 MHz, CDCl_3) δ 155.19 (C6), 69.3 (C5), 34.2 (C3), 23.9 (C1), 15.8 (C2), 15.2 (C4).



(2S, 1'S, 2'R, 3'S)-2-(2-Hydroxymethyl-3-methyl-1-cyclopropylamino)succinic acid dimethyl ester (2.082). (hrp4-53 & hrp4-54). $\text{Ba}(\text{OH})_2 \cdot 8 \text{H}_2\text{O}$ (4.30 g, 13.64 mmol) was added to a mixture of urethane **2.080** (867 mg, 6.82 mmol) in dioxane and H_2O (2:1, 37 mL). The mixture was heated under reflux for 90 min with vigorous stirring. The mixture was cooled and filtered through a pad of celite. The pad was then washed with CH_2Cl_2 (2 x 40 mL) washes, and the combined filtrate and washing were concentrated to ~ 5 mL and CH_2Cl_2 (100 mL) was added. The solution was dried (Na_2SO_4) and concentrated under reduced pressure to yield 498 mg of crude **2.081** (72%) as a yellow oil. Freshly distilled Tf_2O (2.50 g, 1.5 mL, 8.86 mmol) was added dropwise to a solution of (*R*)-dimethylmalate (1.710 g, 1.4 mL, 10.6 mmol) in CH_2Cl_2 (30 mL) at 0°C . This mixture was stirred at 0°C for 5 min, and 2,6-lutidine (948 mg, 1.03 mL, 8.86 mmol) was added. This mixture was stirred at 0°C for an additional 10 min, and then *i*-Pr₂NEt (1.21 g, 1.63 mL, 9.35 mmol) was added. A mixture of amino alcohol **2.081** (498 mg, 4.92 mmol) and *i*-Pr₂NEt (769 mg, 0.857 mL, 4.92 mmol) in CH_2Cl_2 (10 mL)

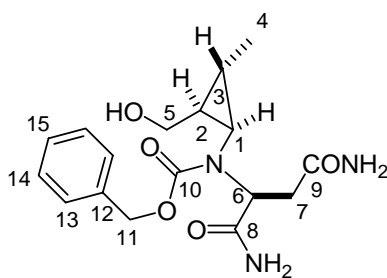
was added dropwise. The mixture was stirred at 0 °C for 1 h and then stirred to rt for 30 min. CH₂Cl₂ (20 mL) was added, and the mixture was washed with brine (20 mL). The aqueous layer was extracted with CH₂Cl₂ (1 x 20 mL), and the combined organic layers were dried (Na₂SO₄) and concentrated under reduced pressure. The residue was purified by flash column chromatography eluting with EtOAc/hexanes (1:1 to 2:1) to yield 712 mg **2.082** (59%) as a yellow oil; ¹H NMR (500 MHz) δ 3.94 (dd, *J* = 11.3, 3.1 Hz, 1 H) 3.80 (dd, *J* = 11.3, 5.3 Hz, 1 H), 3.77 (s, 3 H), 3.72 (dd, *J* = 7.9, 5.2 Hz, 1 H) 3.68 (s, 3 H), 2.71 (d, *J* = 15.9, 5.2 Hz, 1 H), 2.68-2.57 (br s, 1 H), 2.60 (dd, *J* = 15.9, 7.9 Hz, 1 H), 2.11 (dd, *J* = 6.9, 3.2 Hz, 1 H), 1.02 (d, *J* = 6.1, 3 H), 0.99-0.95 (m, 1 H), 0.77-0.73 (m, 1 H); ¹³C NMR (125 MHz,) δ 173.8, 171.1, 59.9, 58.1, 52.2, 51.9, 40.6, 37.8, 27.6, 16.8, 15.2; IR 3019, 2400, 2253, 1735, 1522, 1475, 1436, 1216, 908 cm⁻¹; mass spectrum (CI) *m/z* 246.1348 [C₁₁H₁₉NO₅ (M+1) requires 246.1341], 228, 214.

NMR Assignments. ¹H NMR (500 MHz) δ 3.94 (dd, *J* = 11.3, 3.1 Hz, 1 H, C5-H) 3.80 (dd, *J* = 11.3, 5.3 Hz, 1 H, C5-H), 3.77 (s, 3 H, C10-H or C11-H), 3.72 (dd, *J* = 7.9, 5.2 Hz, 1 H, C6-H) 3.68 (s, 3 H, C10-H or C11-H), 2.71 (d, *J* = 15.9, 5.2 Hz, 1 H, C7-H), 2.68-2.57 (br s, 1 H, N-H), 2.60 (dd, *J* = 15.9, 7.9 Hz, 1 H, C7-H), 2.11 (dd, *J* = 6.9, 3.2 Hz, 1 H, C2-H), 1.02 (d, *J* = 6.1, 3 H, C4-H), 0.99-0.95 (m, 1 H, C3-H), 0.77-0.73 (m, 1 H, C1-H); ¹³C NMR (125 MHz,) δ 173.8 (C8 or C9), 171.1 (C8 or C9), 59.9 (C5), 58.1 (C6), 52.2 (C10 or C11), 51.9 (C10 or C11), 40.6 (C2), 37.8 (C7), 27.6 (C1), 16.8 (C4), 15.2 (C3).



(*2S*, *1'S*, *2'R*, *3'S*)-2-(2-Hydroxymethyl-3-methylcyclopropylamino)succinamide (**2.083**). (**hrp4-055**). NaCN (9 mg, 0.188 mmol) was added to a stirred solution of **14** (461 mg, 1.88 mmol) in MeOH (19 mL) at rt. The reaction mixture was saturated with NH₃ by bubbling the gas into the solution for 20 min at rt. The reaction was stirred at 55 °C for 3 d during which time it was resaturated with NH₃ every 12 h. The mixture was concentrated under reduced pressure, and the residue was recrystallized from minimal amounts of hot CH₃CN (10 mL total) to yield 242 mg of **2.083** (60%) as an off white solid: mp 153-156 °C; ¹H NMR (500 MHz, CD₃OD) δ 3.76 (dd, *J* = 11.2, 5.2 Hz, 1 H), 3.61 (dd, *J* = 11.2, 8.0 Hz, 1 H), 3.55 (dd, *J* = 8.6, 5.0 Hz, 1 H), 2.48 (dd, *J* = 15.0, 5.0 Hz, 1 H), 2.42 (dd, *J* = 15.0, 8.6 Hz, 1 H), 2.00 (dd, *J* = 7.1, 3.4 Hz, 1 H), 1.03 (d, *J* = 6.2 Hz, 1 H), 0.82-0.76 (m, 1 H), 0.67-0.62 (m, 1 H); ¹³C NMR (125 MHz, CD₃OD) δ 178.9, 176.1, 61.5, 60.2, 41.9, 35.5, 30.0, 18.8, 17.3; IR 2361, 1655, 1408 cm⁻¹, mass spectrum (CI) *m/z* 216.1341 [C₉H₁₈N₃O₃ (M+1) requires 216.1348], 198, 133.

NMR Assignments. ¹H NMR (500 MHz, CD₃OD) δ 3.76 (dd, *J* = 11.2, 5.2 Hz, 1 H, C5-H), 3.61 (dd, *J* = 11.2, 8.0 Hz, 1 H, C5-H), 3.55 (dd, *J* = 8.6, 5.0 Hz, 1 H, C6-H), 2.48 (dd, *J* = 15.0, 5.0 Hz, 1 H, C7-H), 2.42 (dd, *J* = 15.0, 8.6 Hz, 1 H, C7-H), 2.00 (dd, *J* = 7.1, 3.4 Hz, 1 H, C1-H), 1.03 (d, *J* = 6.2 Hz, 1 H, C4-H), 0.82-0.76 (m, 1 H, C2-H), 0.67-0.62 (m, 1 H, C3-H); ¹³C NMR (125 MHz, CD₃OD) δ 178.9 (C8 or C9), 176.1 (C8 or C9), 61.5 (C5), 60.2 (C6), 41.9 (C1), 35.5 (C7), 30.0 (C2), 18.8 (C3), 17.3 (C4).

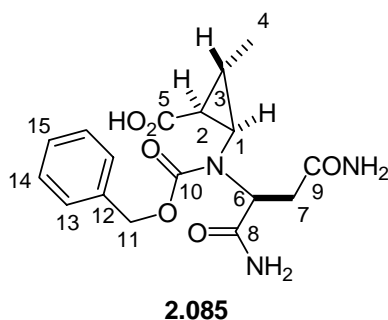


2.084

(*2S*, *1'S*, *2'R*, *3'S*)-(1,2-Dicarbamoylethyl)-(2-hydroxymethyl-3-methylcyclopropyl) carbamic acid benzyl ester (**2.084**). (hrp4-108). *i*Pr₂NEt (209 mg, 282 μ L, 1.62 mmol) and Cbz-Cl (184 mg, 154 μ L, 1.08 mmol) were added to a stirred solution of **2.083** (233 mg, 1.08 mmol) in a mixture of THF and CH₃CN (1:1, 10 mL total), and then the reaction was heated under reflux for 24 h. The mixture was cooled to rt, and EtOAc (10 mL) was added. The mixture was washed with 1 M HCl sat. with NaCl (1 x 10 mL), and the aqueous layer was back extracted with EtOAc (2 x 10 mL). The combined organic layers were washed with sat. Na₂CO₃ (2 x 10 mL), and the aqueous layer was back extracted with EtOAc (2 x 10 mL). The organic layers were combined and dried (Na₂SO₄). The solvent was removed under reduced pressure, and the residue was purified by flash column chromatography eluting with CHCl₃/MeOH (6:1) to give 236 mg (62%) of **2.084** as a clear oil; ¹H NMR (500 MHz, DMSO-d₆, 383 K) δ 7.40-7.12 (comp, 5 H), 6.75 (br s, 4 H), 5.12 (d, *J* = 12.8 Hz, 1 H), 5.05 (d, *J* = 12.8 Hz, 1 H), 4.58 (dd, *J* = 7.5, 6.2 Hz, 1 H), 3.80 (br s, 1 H), 3.57-3.52 (m, 1 H), 3.38-3.33 (m, 1 H), 2.89 (dd, *J* = 15.8, 6.2 Hz, 1 H), 2.63 (dd, *J* = 15.8, 7.5 Hz, 1 H), 2.45 (dd, *J* = 7.8, 4.0 Hz, 1 H), 1.12-1.08 (m, 1 H), 1.04 (d, *J* = 5.9 Hz, 3 H), 0.94-0.90 (m, 1 H); ¹³C NMR (125 MHz, DMSO-d₆, 383K) δ 171.9, 171.6, 156.9, 136.8, 128.2, 127.6, 127.5, 127.0, 126.8, 66.1, 58.9, 58.6, 41.2, 35.0, 29.8, 16.4, 16.2; IR 3480, 3408, 2960,

1690, 1590, 1400, 1309, 908 cm^{-1} ; mass spectrum (CI) m/z 350.1725 [$\text{C}_{17}\text{H}_{24}\text{N}_3\text{O}_5$ (M+1) requires 350.1420], 169.

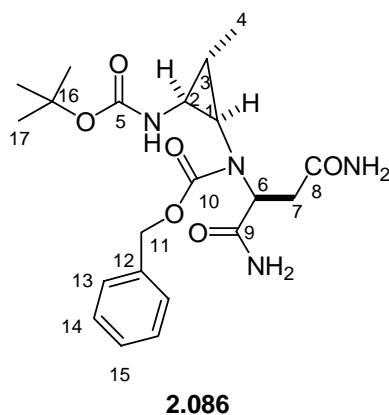
NMR Assignments. ^1H NMR (500 MHz, DMSO-d_6 , 383 K) δ 7.40-7.12 (comp, 5 H, C13-H, C14-H & C15-H), 6.75 (br s, 4 H, N-H), 5.12 (d, , $J = 12.8$ Hz, 1 H, C11-H), 5.05 (d, $J = 12.8$ Hz, 1 H, C11-H) , 4.58 (dd, $J = 7.5, 6.2$ Hz, 1 H, C6-H), 3.80 (br s, 1 H, O-H), 3.57-3.52 (m, 1 H, C5-H), 3.38-3.33 (m, 1 H, C5-H), 2.89 (dd, $J = 15.8, 6.2$ Hz, 1 H, C7-H), 2.63 (dd, $J = 15.8, 7.5$ Hz, 1 H, C7-H), 2.45 (dd, $J = 7.8, 4.0$ Hz, 1 H, C2-H), 1.12-1.08 (m, 1 H, C1-H), 1.04 (d, $J = 5.9$ Hz, 3 H, C4-H), 0.94-0.90 (m, 1 H, C3-H); ^{13}C NMR (125 MHz, DMSO-d_6 , 383K) δ 171.9 (C8 or C9), 171.6 (C8 or C9), 156.9 (C10), 136.8 (C12), 128.2 (C13, C14 or C15), 127.6 (C13, C14 or C15), 127.5 (C13, C14 or C15), 127.0 (C13, C14 or C15), 126.8 (C13, C14 or C15), 66.1 (C11), 58.9 (C5), 58.6 (C6), 41.2 (C2), 35.0 (C7), 29.8 (C3), 16.4 (C1), 16.2 (C4).



(1''S, 2R, 3S, 1S)-2-[Benzyloxycarbonyl-(1,2-dicarbamoylethyl) amino]-3-methylcyclopropanecarboxylic acid (2.085). (hrp4-112). A mixture of NaHCO_3 (375 mg, 4.46 mmol), NaIO_4 (808 mg, 3.78 mmol), RuCl_3 (14 mg, 0.0675 mmol) and **2.084** (236 mg, 0.675 mmol) in $\text{CH}_3\text{CN}/\text{CCl}_4/\text{H}_2\text{O}$ (1:1:2, 28 mL total) was stirred vigorously for 30 min at rt. An additional 0.1 mole equivalent of RuCl_3 was then added, and the reaction mixture was stirred vigorously for 1 h at rt. The reaction mixture was diluted

with CH₂Cl₂ (30 mL), and the layers were separated. The aqueous layer was washed with CH₂Cl₂ (2 x 30 mL). The aqueous layer was acidified with 1 M HCl sat. with NaCl. The aqueous layer was then extracted with EtOAc (3 x 30 mL). The organic layers were combined and dried (Na₂SO₄). The solvent was removed under reduced pressure, and the residue was purified by flash column chromatography eluting with CH₂Cl₂/EtOH (4:1) containing 1% CH₃CO₂H to give 110 mg of the major diastereomer and 24 mg of the other diastereomers of **22** (54%) as a clear oil: ¹H NMR (500 MHz, DMSO-d₆, 383K) δ 7.38-7.28 (comp, 5 H), 5.16 (d, *J* = 12.9 Hz, 1 H), 4.91 (d, *J* = 12.9 Hz, 1 H), 4.74 (dd, *J* = 8.8, 5.4 Hz, 1 H), 3.00 (dd, *J* = 16.2, 5.4 Hz, 1 H), 2.74 (t, *J* = 6.0 Hz, 1 H), 2.57 (dd, *J* = 16.2, 8.8 Hz, 1 H), 1.76-1.72 (m, 2 H), 1.14 (d, *J* = 5.6 Hz, 3 H); ¹³C NMR (125 MHz, DMSO-d₆, 383K) δ 172.4, 172.0, 171.4, 156.0, 136.0, 127.6, 127.0, 126.7, 66.3, 57.9, 41.6, 34.0, 28.7, 22.0, 15.0; mass spectrum (CI) *m/z* 364.1449 [C₁₇H₂₂N₃O₆ (M+1) requires 364.1509], 347.

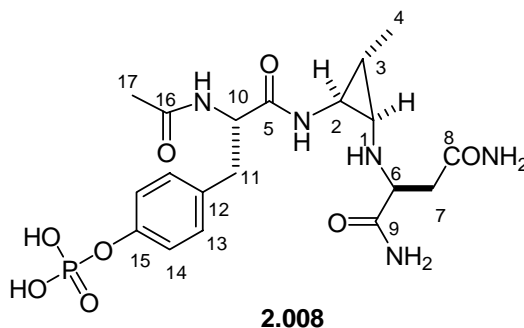
NMR Assignments. ¹H NMR (500 MHz, DMSO-d₆, 383K) δ 7.38-7.28 (comp, 5 H, C13-H, C14-H & C15-H), 5.16 (d, *J* = 12.9 Hz, 1 H, C11-H), 4.91 (d, *J* = 12.9 Hz, 1 H, C11-H), 4.74 (dd, *J* = 8.8, 5.4 Hz, 1 H, C6-H), 3.00 (dd, *J* = 16.2, 5.4 Hz, 1 H, C7-H), 2.74 (t, *J* = 6.0 Hz, 1 H, C2-H), 2.57 (dd, *J* = 16.2, 8.8 Hz, 1 H, C7-H), 1.76-1.72 (m, 2 H, C1-H & C3-H), 1.14 (d, *J* = 5.6 Hz, 3 H, C4-H); ¹³C NMR (125 MHz, DMSO-d₆, 383K) δ 172.4 (C8 or C9), 172.0 (C8 or C9), 171.4 (C5), 156.0 (C10), 136.0 (C12), 127.6 (C13, C14 or C15), 127.0 (C13, C14 or C15), 126.7 (C13, C14 or C15), 66.3 (C11), 57.9 (C6), 41.6 (C2), 34.0 (C7), 28.7 (C1 or C3), 22.0 (C1 or C3), 15.0 (C4).



(1''''S, 2'R, 3'S, 1S)-{2-[Benzyloxycarbonyl-(1,2-dicarbamoyl)ethyl] amino}-3-methylcyclopropyl} carbamic acid tert butyl ester (**2.086**). (hrp4-109). Ethyl chloroformate (27 mg, 24 μ L, 0.250 mmol) and Et₃N (23 mg, 32 μ L, 0.232 mmol) were added to a solution of **2.085** (70 mg, 0.193 mmol) in aqueous acetone (10:1, 2 mL total) at 0 $^{\circ}$ C, and the mixture was stirred at 0 $^{\circ}$ C for 30 min. A solution of NaN₃ (19 mg, 0.290 mmol) dissolved in H₂O (200 μ L) was then added, and the mixture was stirred at 0 $^{\circ}$ C for 30 min. Cold H₂O (2 mL) was added, and the mixture was extracted with CH₂Cl₂ (3 x 5 mL). The organic layers were combined, dried (Na₂SO₄) and concentrated to ca. 2 mL under reduced pressure. *tert*-Butyl alcohol (2 mL) was added, and the reaction was heated under reflux for 13 h. The reaction was then concentrated under reduced pressure to yield 44 mg of **2.086** (59%) as a yellow oil; ¹H NMR (500 MHz, DMSO-d₆, 373K) δ 7.38-7.28 (m, 5 H), 6.85 (br s, 4 H), 6.18 (br s, 1 H), 5.15 (d, *J* = 12.7 Hz, 1 H), 5.00 (d, *J* = 12.7 Hz, 1 H), 4.60 (dd, *J* = 7.8, 6.1, Hz, 1 H), 2.88 (dd, *J* = 15.8, 6.1 Hz, 1 H), 2.64 (dd, *J* = 15.8, 7.8 Hz, 1 H) 2.61-2.59 (m, 1 H), 2.39-2.37, (m, 1 H), 1.38 (s, 9 H), 1.25-1.18 (m, 1 H) 1.05 (d, *J* = 6.4 Hz, 1 H); ¹³C NMR (125 MHz, DMSO-d₆, 373K) δ 172.5, 171.5, 156.2, 155.2, 136.2, 127.6, 127.0, 126.7, 77.4, 66.1, 57.9, 39.8, 36.7, 34.8, 27.7,

19.0, 14.7; IR 2624, 2253, 1794, 1689, 1462, 1382, 1096, 945, 902 cm^{-1} ; mass spectrum (CI) m/z 435.2248 [$\text{C}_{21}\text{H}_{30}\text{N}_4\text{O}_6$ (M+1) requires 435.2244], 421, 379, 162.

NMR Assignments. ^1H NMR (500 MHz, DMSO-d_6 , 373K) δ 7.38-7.28 (m, 5 H, C12-H, C13-H, C14-H), 6.85 (br s, 4 H, N-H), 6.18 (br s, 1 H, N-H), 5.15 (d, $J = 12.7$ Hz, 1 H, C10-H), 5.00 (d, $J = 12.7$ Hz, 1 H, C10'-H), 4.60 (dd, $J = 7.8, 6.1$, Hz, 1 H, C5-H), 2.88 (dd, $J = 15.8, 6.1$ Hz, 1 H, C6-H), 2.64 (dd, $J = 15.8, 7.8$ Hz, 1 H, C6-H) 2.61-2.59 (m, 1 H, C1-H or C2-H), 2.39-2.37, (m, 1 H, C1-H or C2-H), 1.38 (s, 9 H, C17-H), 1.25-1.18 (m, 1 H, C3-H) 1.05 (d, $J = 6.4$ Hz, 1 H, C4-H); ^{13}C NMR (125 MHz, DMSO-d_6 , 373K) δ 172.5 (C7 or C8 or C9 or C15), 171.5 (C7 or C8 or C9 or C15), 156.2 (C7 or C8 or C9 or C15), 155.2 (C7 or C8 or C9 or C15), 136.2 (C11), 127.6 (C12 or C13 or C14), 127.0 (C12 or C13 or C14), 126.7 (C12 or C13 or C14), 77.4 (C16), 66.1 (C10), 57.9 (C5), 39.8 (C2 or C1), 36.7 (C2 or C1), 34.8 (C7), 27.7 (C17), 19.0 (C3), 14.7 C4).

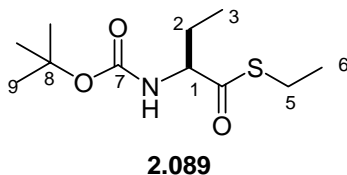


(2''S, 1'S, 3'S, 4''S)-Phosphoric acid mono-(4-{2-acetylamino-2-[2-(1,2-dicarbamoylethylamino)-3-methylcyclopropylcarbamoyl]ethyl}phenyl) ester (2.008). (hrp4-110, 111 and 119). A solution of 2.087 (44 mg, 0.101 mmol) in neat TFA (0.2 mL) was stirred for 90 min. The reaction mixture was concentrated under reduced pressure, and the residue was triturated with Et_2O (3 x 2 mL) to give an off white solid.(33 mg) This crude amine was dissolved in DMF (1 mL) containing 2.030 (36 mg,

0.0737 mmol) at $-10\text{ }^{\circ}\text{C}$, and 2,6-lutidine (24 mg, 26 μL , 0.221 mmol) and HATU (28 mg, 0.0773 mmol) were added. The mixture was stirred at $-10\text{ }^{\circ}\text{C}$ for 1 h and then at rt for 12 h. EtOAc (10 mL) was added, and the organic layer was washed with sat. NaHCO_3 (10 mL), 1 M HCl sat. with NaCl (10 mL) and brine (10 mL). The organic layer was dried (Na_2SO_4) and concentrated under reduced pressure. The crude residue was purified by flash chromatography, eluting with $\text{CH}_2\text{Cl}_2/\text{MeOH}$ (9:1) to yield 22 mg of 2.087 (37%) as a yellow oil. A solution of the product (4 mg, 0.006 mmol) in EtOH (2 mL) containing 10 % Pd/C (10 mg) was stirred under H_2 (1 atm) for 12 h. The catalyst was removed by filtration through a pad of celite, and the filtrate was concentrated under reduced pressure to yield 3 mg of 2.008 (100%) as a white solid: mp $^{\circ}\text{C}$; ^1H NMR (500 MHz, D_2O) δ 7.22 (d, $J = 8.3$ Hz, 2 H), 7.14 (d, $J = 8.3$ Hz, 2 H), 4.74 (dd, $J = 8.3, 6.5$ Hz, 1 H), 3.65 (br s, 1 H), 3.06 (dd, $J = 13.9, 6.5$ Hz, 1 H), 2.95 (dd, $J = 13.9, 8.3$ Hz, 1 H), 2.67 (dd, $J = 15.4, 5.8$ Hz, 1 H), 2.58 (dd, $J = 15.4, 8.0$ Hz, 1 H), 2.46-2.43 (m, 1 H), 2.16 (br s, 1 H), 1.95 (s, 3 H), 1.30-1.25 (m, 1 H), 1.05 (d, $J = 6.4$ Hz, 3 H); ^{13}C NMR (125 MHz, D_2O) δ 177.8, 177.6, 176.8, 176.8, 134.7, 133.0, 123.3, 58.0, 57.1, 42.4, 39.8, 39.2, 33.2, 24.3, 17.2, 13.5; mass spectrum (FAB $-$) m/z 484.1600 [$\text{C}_{19}\text{H}_{28}\text{N}_5\text{O}_9\text{P}$ (M-1) requires 484.1597].

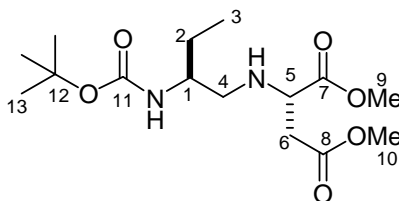
NMR Assignments. ^1H NMR (500 MHz, D_2O) δ 7.22 (d, $J = 8.3$ Hz, 2 H, C13-H or C14-H), 7.14 (d, $J = 8.3$ Hz, 2 H, C13'-H or C14'-H), 4.74 (dd, $J = 8.3, 6.5$ Hz, 1 H, C10-H), 3.65 (br s, 1 H, C6-H), 3.06 (dd, $J = 13.9, 6.5$ Hz, 1 H, C11-H), 2.95 (dd, $J = 13.9, 8.3$ Hz, 1 H, C11'-H), 2.67 (dd, $J = 15.4, 5.8$ Hz, 1 H, C7-H), 2.58 (dd, $J = 15.4, 8.0$ Hz, 1 H, C7'-H), 2.46-2.43 (m, 1 H, C1-H or C2-H), 2.16 (br s, 1 H, C1-H or C2-H), 1.95 (s, 3 H, 17-H), 1.30-1.25 (m, 1 H, C3-H), 1.05 (d, $J = 6.4$ Hz, 3 H, C4-H); ^{13}C NMR (125 MHz, D_2O) δ 177.8 (C5, C8, C9 or C16), 177.6 (C5, C8, C9 or C16), 176.8 (C5, C8, C9 or C16), 176.8 (C5, C8, C9 or C16),

134.7 (C12 & C15), 133.0 (C13 or C14), 123.3 (C13 or C14), 58.0 (C6), 57.1 (C10), 42.4 (C1 or C2), 39.8 (C7), 39.2 (C11), 33.2 (C1 or C2), 24.3 (C17), 17.2 (C4), 13.5 (C3).



(2S)-2-tert-Butoxycarbonylaminothiobutyric acid S-ethyl ester (2.089). (nn-015). DMAP (12 mg, 0.1 mmol) and EtSH (82 μ L, 1.1 mmol) were added to 4-(tert-butoxycarbonylamino) butyric acid (**2.088**) (203 mg, 1 mmol) in CH_2Cl_2 (10 mL). DCC (227 mg, 1.1 mmol) was added to the mixture, and the reaction was stirred for 30 mins at rt. The solution was filtered through cotton and concentrated under reduced pressure. The crude product was purified by column chromatography eluting with hexanes/EtOAc (6:1) to yield 245.2 mg (99%) of **2.089** as a colorless oil: ^1H NMR (300 MHz, CDCl_3) δ 4.94 (br s, 1 H), 4.26 (br d, $J = 5.0$ Hz, 1 H), 2.85 (q, $J = 7.4$ Hz, 2 H), 1.90-1.85 (m, 1 H), 1.65-1.55 (m, 1H), 1.43 (s, 9 H), 1.22 (t, $J = 7.4$ Hz, 3 H), 0.92 (t, $J = 7.4$ Hz, 3 H); ^{13}C NMR (75 MHz, CDCl_3) δ 201.3, 155.2, 80.1, 61.6, 28.3, 26.1, 23.1, 14.5, 9.6; IR (CDCl_3) 3439, 2972, 2932, 2252, 1714, 1494, 1368, 1163, 907, 730, 647 cm^{-1} ; mass spectrum (CI) m/z 248.1323 [$\text{C}_{11}\text{H}_{22}\text{NO}_3\text{S}$ requires 248.1320], 495, 248, 192 (base).

NMR Assignments. ^1H NMR (300 MHz, CDCl_3) δ 4.94 (br s, 1 H, N-H), 4.26 (br d, $J = 5.0$ Hz, 1 H, C1-H), 2.85 (q, $J = 7.4$ Hz, 2 H, C5-H), 1.90-1.85 (m, 1 H, C2-H), 1.65-1.55 (m, 1H, C2'-H), 1.43 (s, 9 H, C9-H), 1.22 (t, $J = 7.4$ Hz, 3 H, C6-H), 0.92 (t, $J = 7.4$ Hz, 3 H, C3-H); ^{13}C NMR (75 MHz, CDCl_3) δ 201.3 (C7 or C4), 155.2 (C7 or C4), 80.1 (C8), 61.6 (C1), 28.3 (C9), 26.1 (C2), 23.1 (C5), 14.5 (C6), 9.6 (C3).

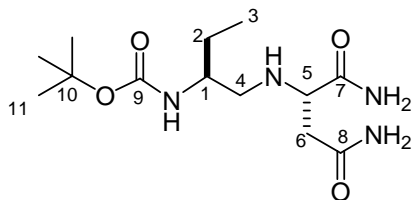


2.090

(2*S*, 2*S'*)-2-(2-*tert*-Butoxycarbonylamino)butylamino)succinic acid dimethyl ester (2.090). (hrp4-042). Et₃SiH (162 mg, 223 μL, 3.8 mmol) was added rapidly to a solution containing **2.089** (69 mg, 0.28 mmol) and 10% Pd/C (10 mg) in CH₂Cl₂ (2 mL) at 0 °C. The reaction mixture was stirred for 90 min at 0 °C, and the catalyst was removed by filtrations. DMF (1.0 mL) was added to the filtrate, and L-aspartic acid dimethyl ester hydrochloride (**2.036**) (57 mg, 0.288 mmol) was added at 0 °C. A solution of Na(OAc)₃BH (101 mg, 0.477 mmol) in DMF (0.5 mL) was then added, and the reaction mixture was stirred at 0 °C for 1 h and then at rt for 30 min. The solvent was removed under reduced pressure, and the residue was purified by flash column chromatography eluting with EtOAc/hexanes (1:2 to 1:1) to give 77 mg (83%) of **2.090** as a clear oil: ¹H NMR (500 MHz, CDCl₃) δ 4.58 (br s, 1 H), 3.72 (s, 3 H), 3.71-3.65 (comp, 4 H), 3.52 (br s, 1 H), 2.79-2.76 (comp, 2 H), 2.67-2.62 (m, 1 H), 2.53 (br s, 1 H), 1.57-1.47 (comp, 2 H), 1.42 (s, 9 H), 0.89 (t, *J* = 7.4 Hz, 3 H); ¹³C NMR (125 MHz, CDCl₃) δ 171.3, 79.1, 57.9, 52.3, 51.9, 50.9, 37.4, 28.4, 25.8, 10.2 ;IR (CDCl₃) 3157, 2254, 1794, 1736, 1707, 1466, 1380, 1167, 1095, 907 cm⁻¹; mass spectrum (CI) *m/z* 333.2024 [C₁₅H₂₉N₂O₆ requires 333.2026], 277 (base).

NMR Assignments. ¹H NMR (300 MHz, CDCl₃) δ 4.58 (br s, 1 H, N-H), 3.72 (s, 3 H, C10-H or C7-H), 3.71-3.65 (comp, 4 H, C10-H or C7-H, C5-H), 3.52 (br s, 1 H, C1-H), 2.79-2.76 (comp, 2 H, C4-H or C8-H), 2.67-2.62 (m, 1 H, C8-H), 2.53 (br s, 1 H, C4-H), 1.57-1.47 (comp, 2 H, C2-H), 1.42 (s, 9 H, C13-H), 0.89 (t, *J* = 7.4 Hz, 3 H, C3-H); ¹³C NMR (125 MHz, CDCl₃) δ 171.3 (C6, C9, & C11), 79.1 (C12), 57.9 (C5), 52.3

(C10 or C7), 51.9 (C10 or C7 & C1), 50.9 (C4), 37.4 (C8), 28.4 (C13), 25.8 (C2), 10.2 (C3).

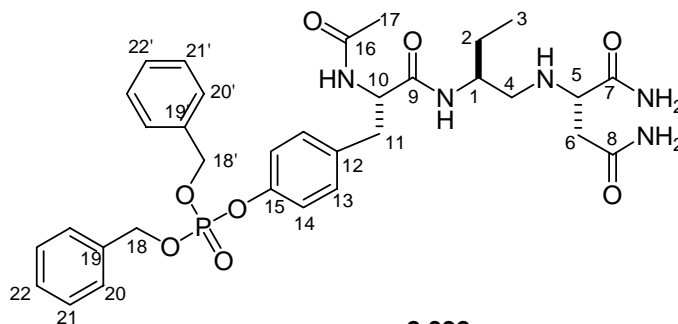


2.091

({1-[(1,2-Dicarbamoylethylamino)methyl]propyl}carbamic acid *tert*-butyl ester (2.091). (hrp3-284). Solid NaCN (6 mg, 0.128 mmol) was added to a solution of **2.090** (332 mg, 1.28 mmol) in MeOH (13 mL) at room temperature. The solution was saturated with ammonia gas for 30 min, and then heated at 55 °C for 3 d, during which time the mixture was resaturated with ammonia gas every 12 h. The mixture was then concentrated under reduced pressure, and the residue was recrystallized from minimal amounts of hot CH₃CN (10 mL total) to yield 328 mg of **2.091** (85%) as an off white solid: mp 177-180 °C; ¹H NMR (500 MHz, CD₃OD) δ 3.46 (br s, 1 H), 3.44 (dd, *J* = 8.5, 4.9 Hz, 1 H), 3.40 (dd, *J* = 7.1, 3.0 Hz, 1 H), 2.62-2.51 (comp, 3 H), 2.44 (dd, *J* = 15.4, 8.7 Hz, 1 H), 1.58-1.49 (m, 1 H), 1.43 (s, 9 H), 1.40-1.30 (m, 1 H), 0.91 (t, *J* = 7.4 Hz, 3 H); ¹³C NMR (125 MHz, CD₃OD) δ 178.7, 175.9, 158.6, 79.9, 60.4, 53.7, 52.6, 39.1, 28.8, 27.0, 10.8; IR 2100, 1684, 1639, 1528, 1390, 1291, 1247, 1173 cm⁻¹, mass spectrum (CI) *m/z* 303.2034 [C₁₂H₂₆N₄O₃ requires 303.2032], 286, 247.

NMR Assignments. ¹H NMR (500 MHz, CD₃OD) δ 3.46 (br s, 1 H, N-H), 3.44 (dd, *J* = 8.5, 4.9 Hz, 1 H, C5-H), 3.40 (dd, *J* = 7.1, 3.0 Hz, 1 H, C1-H), 2.62-2.51 (comp, 3 H, C4-H & C6-H), 2.44 (dd, *J* = 15.4, 8.7 Hz, 1 H, C6-H), 1.58-1.49 (m, 1 H, C2-H), 1.43 (s, 9 H, C11-H), 1.40-1.30 (m, 1 H, C2'-H), 0.91 (t, *J* = 7.4 Hz, 3 H, C3-H); ¹³C NMR

(125 MHz, CD₃OD) δ 178.7 (C7, C8 or C9), 175.9 (C7, C8 or C9), 158.6 (C7, C8 or C9), 79.9 (C10), 60.4 (C1), 53.7 (C5), 52.6 (C4), 39.1 (C6), 28.8 (C11), 27.0 (C2), 10.8 (C3).-

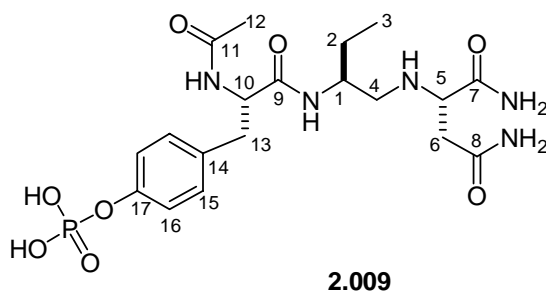


2.092

Phosphoric acid 4-(2-acetylamino-2-((1,2-dicarbamoylethylamino)methyl)propylcarbamoyl)ethyl)phenyl ester diphenyl ester (2.092). (hrp3-290 & hrp3-291). A solution of **2.091** (46 mg, 0.152 mmol) in TFA (0.4 mL) was stirred for 2 h at room temperature. The solution was concentrated and triturated with Et₂O (3 x 4 mL). The residual solid was dissolved in DMF (0.6 mL), and **2.030** (79 mg, 0.152 mmol) and 2,6-lutidine (49 mg, 53 μ L, 0.456 mmol) were added. The mixture was cooled to -10 °C and HATU (58 mg, 0.152 mmol) was added. The mixture was then stirred at -10 °C for 1 h and at rt for 14 h. The solution was concentrated under reduced pressure, and the residue was purified by flash column chromatography eluting with CHCl₃/MeOH (7:1) 68 mg (67%) of **2.092** as a yellow oil. ¹H NMR (500 MHz) δ 7.34 (br s, 1 H), 7.18-7.17 (comp, 11 H), 7.06 (d, *J* = 7.9 Hz, 1 H), 7.02 (d, *J* = 8.2 Hz, 2 H), 6.95 (br s, 1 H), 6.89 (d, *J* = 8.2 Hz, 2 H), 6.01 (br s, 1 H), 5.79 (br s, 1 H), 4.95 (d, *J* = 5.3 Hz, 2 H), 4.93 (d, *J* = 3.5 Hz, 2 H), 4.51-4.48 (m, 1 H), 3.65 (br s, 1 H), 3.22 (br s, 1 H), 2.92, (dd, *J* = 13.7, 6.4 Hz, 1 H), 2.77 (dd, *J* = 13.7, 7.5 Hz, 1 H), 2.51-2.42 (comp, 2 H), 2.36-2.32 (comp, 2 H), 1.73 (s, 3 H), 1.36-1.24, (comp, 2 H), 1.10 (br s, 1 H), 0.70 (t,

$J = 7.3$ Hz, 3 H); ^{13}C NMR (125 MHz, CD_3OD) δ 173.3, 173.2, 170.9, 170.0, 148.8, 135.0, 134.0, 130.3, 128.3, 128.2, 127.6, 119.3, 69.6, 69.5, 59.2, 54.2, 50.7, 50.5, 36.9, 36.7, 25.0, 22.6, 10.0; mass spectrum (CI +) m/z 668.2868 [$\text{C}_{33}\text{H}_{43}\text{N}_5\text{O}_8\text{P}$ (M+1) requires 668.2849.

NMR Assignments. ^1H NMR (500 MHz) δ 7.34 (br s, 1 H, N-H), 7.18-7.17 (comp, 11 H, C20-H, C21-H, C22-H), 7.06 (d, $J = 7.9$ Hz, 1 H, N-H), 7.02 (d, $J = 8.2$ Hz, 2 H, C15-H or C16-H), 6.95 (br s, 1 H, N-H), 6.89 (d, $J = 8.2$ Hz, 2 H, C15-H or C16-H), 6.01 (br s, 1 H, N-H), 5.79 (br s, 1 H, N-H), 4.95 (d, $J = 5.3$ Hz, 2 H, C18-H), 4.93 (d, $J = 3.5$ Hz, 2 H, C18'-H), 4.51-4.48 (m, 1 H, C10-H), 3.65 (br s, 1 H, C1-H), 3.22 (br s, 1 H, C5-H), 2.92, (dd, $J = 13.7, 6.4$ Hz, 1 H, C13-H), 2.77 (dd, $J = 13.7, 7.5$ Hz, 1 H, C13'-H), 2.51-2.42 (comp, 2 H, C4-H and C6-H), 2.36-2.32 (comp, 2 H, C4'-H and C6'-H), 1.73 (s, 3 H, C12-H), 1.36-1.24, (comp, 2 H, C2-H), 1.10 (br s, 1 H, N-H), 0.70 (t, $J = 7.3$ Hz, 3 H, C3-H); ^{13}C NMR (125 MHz, CD_3OD) δ 173.3 (C7 or C8 or C9 or C11), 173.2 (C7 or C8 or C9 or C11), 170.9 (C7 or C8 or C9 or C11), 170.0 (C7 or C8 or C9 or C11), 148.8 (C14 or C17 or C19), 135.0 (C14 or C17 or C19), 134.0 (C14 or C17 or C19), 130.3 (C15 or C16), 128.3 (C20 or C21 or C22), 128.2 (C20 or C21 or C22), 127.6 (C20 or C21 or C22), 119.3 (C15 or C16), 69.6 (C18), 69.5 (C18'), 59.2 (C5), 54.2 (C10), 50.7 (C4), 50.5 (C1), 36.9 (C13), 36.7 (C6), 25.0 (C2), 22.6 (C12), 10.0 (C3).

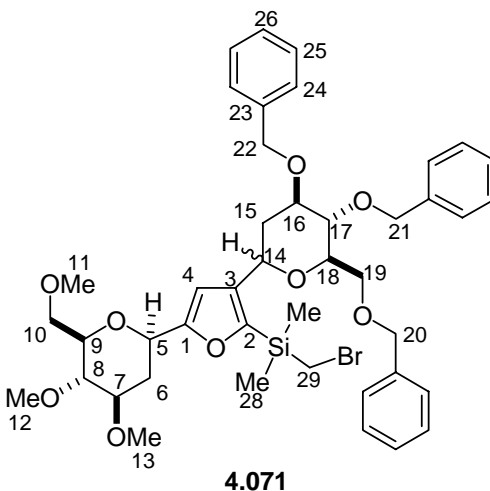


(2*S*, 1*S'*, 1*S''*) Phosphoric acid mono-(4-{acetylamino-[1-[(1,2-dicarbamoylethylcarbamoyl)-2-methylpropylcarbamoyl]methyl]phenyl)ester

(2.009). (hrp-038). A mixture of **2.092** (20 mg, 0.030 mmol) and HCl (0.5 M, 0.12 mL, 0.6 mmol) in EtOH and H₂O (1:1, 1 mL total) containing 10% Pd/C (10 mg) was stirred under H₂ (1 atm) for 13 h. The catalyst was removed by filtration and the filtrate was concentrated under reduced pressure to yield 10 mg (100%) of **2.009** as a white solid: mp 195-197 °C dec; ¹H NMR (500 MHz, D₂O) δ 7.27 (d, *J* = 8.1 Hz, 2 H), 7.16 (d, *J* = 8.1 Hz, 2 H), 4.52 (t, *J* = 7.8 Hz, 1 H), 4.27 (dd, *J* = 7.3, 5.0 Hz, 1 H), 4.00-3.96 (m, 1 H), 3.11-2.82 (comp, 6 H), 1.97 (s, 3 H), 1.67-1.62 (m, 1 H), 1.48-1.42 (m, 1 H), 0.87 (t, *J* = 7.3 Hz, 3 H); ¹³C NMR (125 MHz, CD₃OD) δ 176.9, 176.8, 175.6, 172.3, 153.5, 135.1, 133.2, 123.3, 59.8, 58.2, 52.5, 51.3, 38.8, 36.5, 27.1, 24.3, 12.0; mass spectrum (FAB +) *m/z* 488.1926 [C₁₉H₃₀N₅O₈P (M+1) requires 488.1910, 461, 369, 277 (base)].

NMR Assignments. ¹H NMR (500 MHz, D₂O) δ 7.27 (d, *J* = 8.1 Hz, 2 H, C15-H or C16-H), 7.16 (d, *J* = 8.1 Hz, 2 H, C15-H or C16-H), 4.52 (t, *J* = 7.8 Hz, 1 H, C10-H), 4.27 (dd, *J* = 7.3, 5.0 Hz, 1 H, C5-H), 4.00-3.96 (m, 1 H, C1-H), 3.11-2.82 (comp, 6 H C4-H, C6-H & C13-H), 1.97 (s, 3 H, C12-H), 1.67-1.62 (m, 1 H, C2-H), 1.48-1.42 (m, 1 H, C2'-H), 0.87 (t, *J* = 7.3 Hz, 3 H, C3-H); ¹³C NMR (125 MHz, CD₃OD) δ 176.9 (C7, C8, C9, or C11), 176.8 (C7, C8, C9, or C11), 175.6 (C7, C8, C9, or C11), 172.3 (C7, C8, C9, or C11), 153.5 (C14 or C17), 135.1 (C14 or C17), 133.2 (C15 or C16),

123.3 (C15 or C16), 59.8 (C5), 58.2 (C10), 52.5 (C4), 51.3 (C1), 38.8 (C6 or C13), 36.5 (C6 or C13), 27.1 (C2), 24.3 (C12), 12.0 (C3).

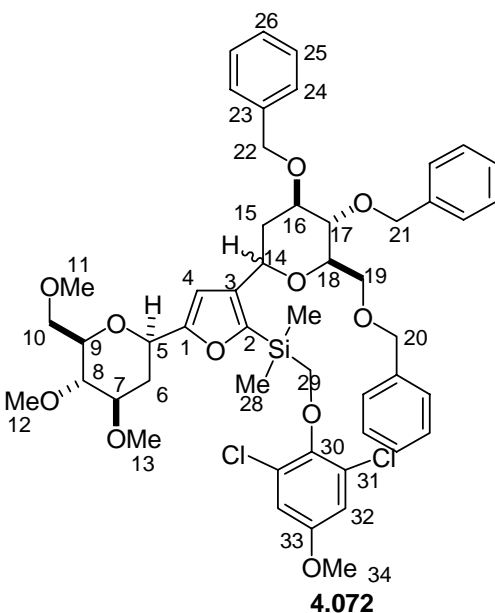


Bromomethyl-6(*R*)-([4-(4(*R*),5(*S*)-Bis-benzyloxy-6(*R*)-benzyloxymethyl-tetrahydro-pyran-2(*R*)-yl)-furan-2-yl]-3(*S*),4(*R*)-dimethoxy-2(*R*)-methoxymethyltetrahydropyran) dimethyl silane (4.071). (hrp3-177). A solution of lithium diisopropylamide (LDA) in a THF (0.4 M, 2 mL, 0.782 mmol) was added to a solution of **4.070^{180,181} (263 mg, 0.391 mmol) in THF (4 mL) at -78 °C, and the mixture was stirred for 4 h at -78 °C. Freshly distilled (bromomethyl)chlorodimethylsilane (107 μL, 0.782 mmol) was added, and the reaction was stirred for 5 min at rt. H₂O (1 mL) was added, and the aqueous mixture was extracted with EtOAc (3 x 10 mL). The combined organic layers were washed with brine (10 mL), dried (Na₂SO₄), and concentrated under reduced pressure. The residue was purified by flash chromatography eluting with EtOAc/hexanes (1:2) to give 11 mg recovered **4.070** and 265 mg of **4.071** [82% (86% brsm)] as a colorless oil: The major diastereomer was isolated by careful flash chromatography and used for characterization: ¹H NMR (500 MHz) δ 7.37-7.25**

(comp, 13 H), 7.21-7.19 (comp, 2 H), 6.29 (s, 1 H), 4.92 (d, $J = 10.8$ Hz, 1 H), 4.70 (d, $J = 11.6$ Hz, 1 H), 4.64 (d, $J = 11.6$ Hz, 1 H), 4.61-4.55 (comp, 2 H), 4.49 (d, $J = 12.1$ Hz, 1 H), 4.41 (d, $J = 1.8$ Hz, 1 H), 4.39 (d, $J = 1.8$ Hz, 1 H), 3.77-3.70 (comp, 3 H), 3.67 (dd, $J = 10.6, 2.0$ Hz, 1 H), 3.63-3.59 (comp, 2 H), 3.57 (s, 3 H), 3.52-3.49 (comp, 1 H), 3.47 (s, 3 H), 3.42-3.37 (comp, 5 H), 3.16 (dd, $J = 9.4, 9.0$ Hz, 1 H), 2.72 (dd, $J = 19.1, 12.8$ Hz, 2 H), 2.35 (ddd, $J = 13.1, 5.0, 1.8$ Hz, 1 H), 2.28 (ddd, $J = 13.1, 5.0, 1.8$ Hz, 1 H), 1.78-1.67 (comp, 2 H), 0.41 (s, 3 H), 0.39 (s, 3 H); ^{13}C NMR (125 MHz) δ 157.7, 152.1, 138.5, 138.4, 138.1, 137.8, 128.4, 128.3, 127.9, 127.7, 127.6, 127.5, 106.5, 82.4, 80.9, 79.8, 79.3, 79.2, 78.0, 75.1, 73.4, 71.8, 71.6, 71.5, 71.2, 69.3, 60.6, 59.3, 57.0, 38.1, 34.5, 17.0, -3.7, -3.8; IR 3163, 2849, 2256, 1796, 1464, 1380, 1265, 1097, 908, 650, 461 cm^{-1} ; mass spectrum (CI) m/z 822.2798 [$\text{C}_{43}\text{H}_{55}\text{BrO}_9\text{Si}$ (M+1) requires 822.2799] 793, 791, 763, 731, 715.

NMR Assignments. ^1H NMR (500 MHz) δ 7.37-7.25 (comp, 13 H, C24-H, C25-H & C26-H), 7.21-7.19 (comp, 2 H, C24-H, C25-H & C26-H), 6.29 (s, 1 H, C4-H), 4.92 (d, $J = 10.8$ Hz, 1 H, C20-H, C21-H or C22-H), 4.70 (d, $J = 11.6$ Hz, 1 H, C20-H, C21-H or C22-H), 4.64 (d, $J = 11.6$ Hz, 1 H, C20-H, C21-H or C22-H), 4.61-4.55 (comp, 2 H, C20-H, C21-H or C22-H), 4.49 (d, $J = 12.1$ Hz, 1 H, C20-H, C21-H or C22-H), 4.41 (d, $J = 1.8$ Hz, 1 H, C14-H or C5-H), 4.39 (d, $J = 1.8$ Hz, 1 H, C14-H or C5-H), 3.77-3.70 (comp, 3 H, C16-H & C19-H), 3.67 (dd, $J = 10.6, 2.0$ Hz, 1 H, C10-H), 3.63-3.59 (comp, 2 H, C10-H & C18-H), 3.57 (s, 3 H, C11-H, C12-H or C13-H), 3.52-3.49 (comp, 1 H, C17-H), 3.47 (s, 3 H, C11-H, C12-H or C13-H), 3.42-3.37 (comp, 5 H, C7-H, C9-H, C11-H, C12-H, C13-H), 3.16 (dd, $J = 9.4, 9.0$ Hz, 1 H, C8-H), 2.72 (dd, $J = 19.1, 12.8$ Hz, 2 H, C29-H), 2.35 (ddd, $J = 13.1, 5.0, 1.8$ Hz, 1 H, C6-H), 2.28 (ddd, $J = 13.1, 5.0, 1.8$ Hz, 1 H, C15-H), 1.78-1.67 (comp, 2 H, C6'-H & C15'-H), 0.41 (s, 3 H, C28-H), 0.39 (s, 3 H, C28'-H); ^{13}C NMR (125 MHz) δ 157.7 (C1, C2, C3 or C23), 152.1 (C1, C2,

C3 or C23), 138.5 (C1, C2, C3 or C23), 138.4 (C1, C2, C3 or C23), 138.1 (C1, C2, C3 or C23), 137.8 (C1, C2, C3 or C23), 128.4 (C24, C25 or C26), 128.3 (C24, C25 or C26), 127.9 (C24, C25 or C26), 127.7 (C24, C25 or C26), 127.6 (C24, C25 or C26), 127.5 (C24, C25 or C26), 106.5 (C4), 82.4(C7 & C9), 80.9 (C16 & C19), 79.8 (C8), 79.3 (C17), 79.2 (C7 & C9), 78.0 (C18), 75.1 (C20, C21 or C22), 73.4 (C20, C21 or C22), 71.8 (C10), 71.6 (C5 or C14), 71.5 (C5 or C14), 71.2 (C20, C21 or C22), 69.3 (C16 & C19), 60.6 (C11, C12 or C13), 59.3 (C11, C12 or C13), 57.0 (C11, C12 or C13), 38.1 (C15), 34.5 (C6), 17.0 (C29), -3.7 (C28), -3.8 (C28').

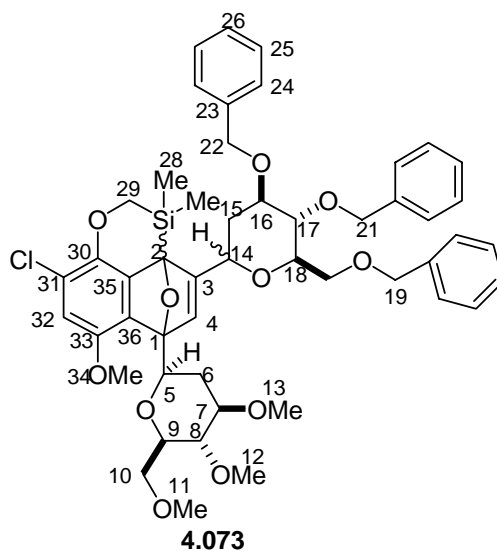


(2,6-dichloro-4-methoxy-phenoxymethyl)-6(R)-[4-(4(R),5(S)-Bis-benzyloxy-6(R)-benzyloxymethyl-tetrahydro-pyran-2(R)-yl)-furan-2-yl]-3(S),4(R)-dimethoxy-2(R)-methoxymethyltetrahydropyranbromomethyl dimethyl silane (4.072). (hrp 3-179). A mixture of tetrabutylammonium iodide (TBAI) (18 mg, 0.048 mmol), K₂CO₃ (30 mg, 0.218 mmol), **4.071** (36 mg, 0.0436 mmol), and **4.033** (12 mg, 0.057 mmol) in acetone (mL) was stirred for 4 d at rt. H₂O (5 mL) was added, and the aqueous mixture

was extracted with EtOAc (3 x 5 mL). The combined organic layers were washed with brine (5 mL), dried (Na₂SO₄), and concentrated under reduced pressure. The residue was purified by flash chromatography eluting with EtOAc/hexanes (1:2) to give 26 mg (88%) of **4.072** as a colorless oil: ¹H NMR (500 MHz) δ 7.38-7.12 (comp, 15 H), 6.81 (s, 2 H), 6.37 (s, 1 H), 4.94-4.90 (m, 1 H), 4.74-4.70 (m, 1 H), 4.66-4.55 (comp, 4 H), 4.51-4.48 (m, 1 H), 4.47-4.43 (m, 1 H), 3.96-3.87 (comp, 2 H), 3.79-3.70 (comp, 6 H), 3.68-3.59 (comp, 2 H), 3.63-3.59 (m, 1 H), 3.57-3.55 (comp, 3 H), 3.54-3.50 (comp, 2 H), 3.47-3.45 (comp, 3 H), 3.43-3.38 (comp, 4 H), 3.21-3.15 (m, 1 H), 2.39-2.35 (m, 1 H), 2.30-2.26 (m, 1 H), 1.79-1.71 (comp, 2 H), 0.49 (s, 1.5 H), 0.47 (s, 1.5 H), 0.49 (s, 3 H); ¹³C NMR (125 MHz) δ 157.1, 155.4, 152.4, 148.0, 138.6, 138.5, 138.3, 137.8, 129.2, 128.4, 128.3, 128.2, 128.0, 127.8, 127.7, 127.6, 127.4, 114.5, 106.5, 82.4, 81.0, 79.8, 79.3, 79.2, 78.1, 75.0, 73.3, 71.8, 71.3, 71.1, 69.4, 66.8, 60.6, 59.3, 57.0, 55.9, 38.1, 34.5, -1.7, -4.1, -4.4; IR (CHCl₃) 3156, 2929, 2837, 2253, 1794, 1766, 1561, 1466, 1380, 1096, 908 cm⁻¹; mass spectrum (CI) *m/z* 935.3350 [C₅₀H₆₀Cl₂O₁₁Si (M + H) requires 935.3360] 903, 827, 763, 447, 433, 419 (base).

NMR Assignments. ¹H NMR (500 MHz) δ 7.38-7.12 (comp, 15 H, C24-H, C25-H & C26-H), 6.81 (s, 2 H, C32-H), 6.37 (s, 1 H, C4-H), 4.94-4.90 (m, 1 H, C20-H, C21-H or C22-H), 4.74-4.70 (m, 1 H, C20-H, C21-H or C22-H), 4.66-4.55 (comp, 4 H, C20-H, C21-H or C22-H), 4.51-4.48 (m, 1 H, C14-H or C5-H), 4.47-4.43 (m, 1 H, C14-H or C5-H), 3.96-3.87 (comp, 2 H, C29-H), 3.79-3.70 (comp, 6 H, C10-H, C16-H & C34-H), 3.68-3.59 (comp, 2 H, C19-H), 3.63-3.59 (m, 1 H, C9-H), 3.57-3.55 (comp, 3 H, C11-H, C12-H or C13-H), 3.54-3.50 (comp, 2 H, C17-H & C18-H), 3.47-3.45 (comp, 3 H, C11-H, C12-H or C13-H), 3.43-3.38 (comp, 4 H, C7-H, C11-H, C12-H or C13-H), 3.21-3.15 (m, 1 H, C8-H), 2.39-2.35 (m, 1 H, C6-H), 2.30-2.26 (m, 1 H, C15-H), 1.79-1.71 (comp, 2 H, C6'-H & C15'-H), 0.49 (s, 1.5 H, C28-H), 0.47 (s, 1.5 H, C28-H), 0.49 (s, 3 H,

C28'-H); ^{13}C NMR (125 MHz) δ 157.1 (C1, C2, C3, C23, C30, C31 or C33), 155.4 (C1, C2, C3, C23, C30, C31 or C33), 152.4 (C1, C2, C3, C23, C30, C31 or C33), 148.0 (C1, C2, C3, C23, C30, C31 or C33), 138.6 (C1, C2, C3, C23, C30, C31 or C33), 138.5 (C1, C2, C3, C23, C30, C31 or C33), 138.3 (C1, C2, C3, C23, C30, C31 or C33), 137.8 (C1, C2, C3, C23, C30, C31 or C33), 129.2 (C1, C2, C3, C23, C30, C31 or C33), 128.4 (C24, C25 or C26), 128.3 (C24, C25 or C26), 128.2 (C24, C25 or C26), 128.0 (C24, C25 or C26), 127.8 (C24, C25 or C26), 127.7 (C24, C25 or C26), 127.6 (C24, C25 or C26), 127.4 (C24, C25 or C26), 114.5 (C32), 106.5 (C4), 82.4 (C7), 81.0 (C16), 79.8 (C8), 79.3 (C17 or C18), 79.2 (C17 or C18), 78.1 (C9), 75.0 (C20, C21 or C22), 73.3 (C20, C21 or C22), 71.8 (C19), 71.3 (C20, C21 or C22), 71.1 (C14), 69.4 (C10), 66.8 (C29), 60.6 (C11, C12 or C13), 59.3 (C11, C12 or C13), 57.0 (C11, C12 or C13), 55.9 (C34), 38.1 (C15), 34.5 (C6), -1.7 (C28), -4.1 (C28), -4.4 (C28).

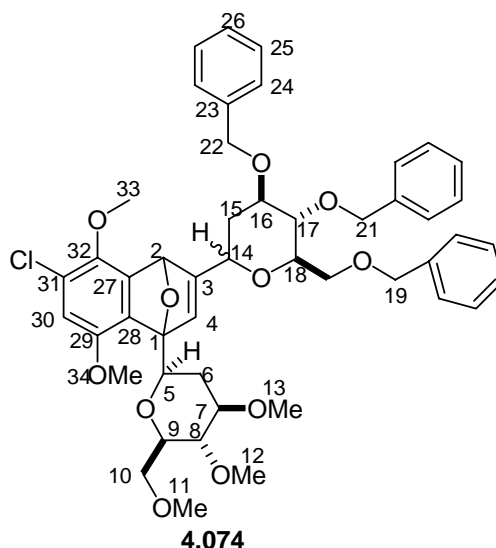


Cycloadduct (4.073). (hrp3-182). Furan **4.072** (171 mg, 0.183 mmol) was dissolved in THF (2 mL), and the solution was cooled to $-95\text{ }^{\circ}\text{C}$ with an $\text{Et}_2\text{O}/\text{Liquid N}_2$

bath. *t*-BuLi (235 μ L of a 1.09 M solution in pentane, 0.256 mmol) was added dropwise, and the bath temperature was maintained below -90 $^{\circ}$ C for 15 min and then allowed to slowly warm to -10 $^{\circ}$ C for 30 min. Saturated aqueous NH_4Cl (2 mL) was added, and the mixture was extracted with EtOAc (3 x 2 mL). The combined extracts were dried (Na_2SO_4) and concentrated. The residue was purified by flash chromatography on silica gel eluting with hexanes/EtOAc (3:2) to afford 101 mg (61%) of cycloadduct **4.073** as a colorless oil. The mixture of two diastereomers was characterized: ^1H NMR (500 MHz) δ 7.37-7.26 (comp, 13 H), 7.21-7.19 (comp, 2 H), 6.69 (d, J = 1.6 Hz, 1 H), 6.61 (s, 1 H), 4.91 (d, J = 11.0 Hz, 1 H), 4.70-4.64 (comp, 1 H), 4.60-4.54 (comp, 1 H), 4.51 (d, J = 11.6 Hz, 1 H), 4.43 (d, J = 11.6 Hz, 1 H), 4.09-3.97 (m, 1 H), 3.90-3.78 (comp, 2 H), 3.75-3.72 (comp, 5 H), 3.71-3.69 (m, 1 H), 3.67-3.60 (comp, 4 H), 3.59-3.54 (comp, 5 H), 3.53-3.45 (m, 1 H), 3.44-3.32 (comp, 8 H), 3.03 (m, 1 H), 2.23 (ddd, J = 12.8, 5.0, 1.9 Hz, 1 H), 2.20 (ddd, J = 12.8, 5.0, 1.6 Hz, 1 H), 1.82-1.75 (m, 1 H), 1.63-1.54 (m, 1 H), 0.41 (s, 3 H), 0.12 (s, 3 H); ^{13}C NMR (125 MHz) δ 171.1, 160.1, 153.7, 149.1, 148.4, 147.3, 145.9, 143.6, 138.7, 138.4, 138.3, 137.9, 136.7, 135.3, 128.4, 128.3, 128.3, 128.0, 127.9, 127.9, 127.8, 127.7, 127.7, 127.6, 127.5, 127.4, 119.4, 113.1, 95.8, 83.2, 81.4, 80.7, 80.4, 79.1, 77.8, 75.1, 73.4, 73.3, 73.2, 72.5, 71.3, 68.9, 61.3, 60.6, 59.3, 56.7, 56.2, 36.2, 31.0, -4.6, -5.6; mass spectrum (CI) m/z 898.3502 [$\text{C}_{50}\text{H}_{59}\text{ClO}_{11}\text{Si}$ (M+H) requires 898.3515] 867, 673, 641, 391.

NMR Assignments: ^1H NMR (500 MHz) δ 7.37-7.26 (comp, 13 H, C24-H, C25-H & C26-H), 7.21-7.19 (comp, 2 H, C24-H, C25-H & C26-H), 6.69 (d, J = 1.6 Hz, 1 H, C4-H), 6.61 (s, 1 H, C32-H), 4.91 (d, J = 11.0 Hz, 1 H, C20-H, C21-H or C22-H), 4.70-4.64 (comp, 1 H, C20-H, C21-H or C22-H), 4.60-4.54 (comp, 3 H, C5-H, C20-H, C21-H & C22-H), 4.51 (d, J = 11.6 Hz, 1 H, C20-H, C21-H or C22-H), 4.43 (d, J = 11.6 Hz, 1 H, C20-H, C21-H or C22-H), 4.09-3.97 (m, 1 H, C14-H), 3.90-3.78 (comp, 2

H, C29-H), 3.75-3.72 (comp, 5 H, C10-H, C19-H & C34-H), 3.71-3.69 (m, 1 H, C17-H), 3.67-3.60 (comp, 4 H, C10'-H & C16-H), 3.59-3.54 (comp, 5 H, C11-H, C12-H or C13-H & C19'-H), 3.53-3.45 (m, 1 H, C9-H), 3.44-3.32 (comp, 8 H, C7-H, C18-H, C11-H, C12-H & C13-H), 3.03 (m, 1 H, C8-H), 2.23 (ddd, $J = 12.8, 5.0, 1.9$ Hz, 1 H, C15-H), 2.20 (ddd, $J = 12.8, 5.0, 1.6$ Hz, 1 H, C6-H), 1.82-1.75 (m, 1 H, C15'-H), 1.63-1.54 (m, 1 H, C6'-H), 0.41 (s, 3 H, C28-H), 0.12 (s, 3 H, C28'-H); ^{13}C NMR (125 MHz) δ 171.1 (C1, C2, C3, C23, C30, C31, C33, C35 or C36), 160.1 (C1, C2, C3, C23, C30, C31, C33, C35 or C36), 153.7 (C1, C2, C3, C23, C30, C31, C33, C35 or C36), 149.1 (C1, C2, C3, C23, C30, C31, C33, C35 or C36), 148.4 (C1, C2, C3, C23, C30, C31, C33, C35 or C36), 147.3 (C1, C2, C3, C23, C30, C31, C33, C35 or C36), 145.9 (C1, C2, C3, C23, C30, C31, C33, C35 or C36), 143.6 (C1, C2, C3, C23, C30, C31, C33, C35 or C36), 138.7 (C1, C2, C3, C23, C30, C31, C33, C35 or C36), 138.4 (C1, C2, C3, C23, C30, C31, C33, C35 or C36), 138.3 (C1, C2, C3, C23, C30, C31, C33, C35 or C36), 137.9 (C1, C2, C3, C23, C30, C31, C33, C35 or C36), 136.7 (C4), 135.3 (C1, C2, C3, C23, C30, C31, C33, C35 or C36), 128.4 (C24, C25 or C26), 128.3 (C24, C25 or C26), 128.3 (C24, C25 or C26), 128.0 (C24, C25 or C26), 127.9 (C24, C25 or C26), 127.9 (C24, C25 or C26), 127.8 (C24, C25 or C26), 127.7 (C24, C25 or C26), 127.7 (C24, C25 or C26), 127.6 (C24, C25 or C26), 127.5 (C24, C25 or C26), 127.4 (C24, C25 or C26), 119.4 (C1, C2, C3, C23, C30, C31, C33, C35 or C36), 113.1 (C32), 95.8 (C1, C2, C3, C23, C30, C31, C33, C35 or C36), 83.2 (C18), 81.4 (C17), 80.7 (C9), 80.4 (C8), 79.1 (C7), 77.8 (C16), 75.1 (C20, C21 or C22), 73.4 (C5, C14, C20, C21 or C22), 73.3 (C5, C14, C20, C21 or C22), 73.2 (C5, C14, C20, C21 or C22), 72.5 (C10), 71.3 (C20, C21 or C22), 68.9 (C19), 61.3 (29), 60.6 (C11, C12 or C13), 59.3 (C11, C12 or C13), 56.7 (C11, C12 or C13), 56.2 (C34), 36.2 (C15), 31.0 (C6), -4.6 (C28), -5.6 (C28')

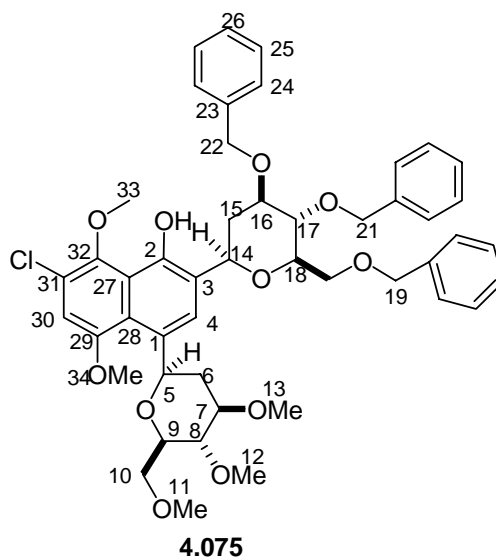


9-(4,5-Bis-benzyloxy-6-benzyloxymethyltetrahydropyran-2-yl)-5-chloro-1-(4,5-dimethoxy-6-methoxymethyltetrahydropyran-2-yl)-3,6-dimethoxy-11-oxatricyclo[6.2.1.0]undeca-2(7),3,5,9-tetraene (4.074). (hrp 3-184). A solution of tetrabutylammonium fluoride (TBAF) in THF (1.0 M, 87 μ L, 0.0867 mmol) was added to a solution of **4.073** (26 mg, 0.0289 mmol) in DMF (0.3 mL) at rt, and the solution was stirred for 15 h at rt. Saturated aqueous NaHCO_3 (1 mL) and H_2O (1 mL) were added, and the aqueous mixture was extracted with EtOAc (2 x 2 mL). The combined organic layers were dried (Na_2SO_4) and concentrated under reduced pressure. The residue was purified by flash chromatography eluting with EtOAc/hexanes (1:1) to give 18 mg of **4.074** (72%) as mixture of diastereomers as a colorless oil: ^1H NMR (500 MHz) δ 7.36-7.25 (comp, 13 H), 7.24-7.21 (comp, 2 H), 6.72 (d, $J = 1.8$ Hz, 1 H), 6.65 (s, 1 H), 6.01 (s, 1 H), 4.91 (d, $J = 11.0$ Hz, 1 H), 4.68 (d, $J = 13.6$ Hz, 1 H), 4.60-4.55 (comp, 4 H), 4.50 (d, $J = 12.1$ Hz, 1 H), 4.07-4.05 (m, 1 H), 3.86 (s, 3 H), 3.76 (s, 3 H), 3.73-3.60 (comp, 5 H), 3.56 (s, 3 H), 3.51-3.41 (comp, 4 H), 3.41 (s, 3 H), 3.40 (s, 3 H), 3.02 (dd, $J = 9.5, 8.7$ Hz, 1 H), 2.31 (ddd, $J = 12.8, 5.0, 1.8$ Hz, 1 H), 2.19 (ddd, $J = 12.8, 5.0, 1.6$

Hz, 1 H), 1.64-1.57 (comp, 2 H); ^{13}C NMR (125 MHz) δ 156.7, 147.8, 144.2, 141.7, 138.5, 138.3, 136.6, 135.2, 128.4, 128.3, 128.0, 127.8, 127.7, 127.7, 127.6, 127.5, 124.7, 112.8, 95.4, 83.0, 80.8, 80.5, 80.2, 80.1, 79.2, 78.2, 75.1, 73.5, 73.1, 72.6, 72.3, 71.3, 69.6, 60.8, 60.6, 59.3, 56.3, 56.1, 34.9, 30.9; IR (CHCl_3) 3003, 2938, 2865, 2837, 2253, 1476, 1454, 1381, 1364, 1103, 908 cm^{-1} ; mass spectrum (CI) m/z 842.3424 [$\text{C}_{48}\text{H}_{55}\text{ClO}_{11}$ (M+H) requires 842.3433] 844, 812 (base).

NMR Assignments: ^1H NMR (500 MHz) δ 7.36-7.25 (comp, 13 H, C24-H, C25-H & C26-H), 7.24-7.21 (comp, 2 H, C24-H, C25-H & C26-H), 6.72 (d, $J = 1.8$ Hz, 1 H, C4-H), 6.65 (s, 1 H, C30-H), 6.01 (s, 1 H, C2-H), 4.91 (d, $J = 11.0$ Hz, 1 H, C20-H, C21-H or C22-H), 4.68 (d, $J = 13.6$ Hz, 1 H, C20-H, C21-H or C22-H), 4.60-4.55 (comp, 4 H, C5-H, C20-H, C21-H & C22-H), 4.50 (d, $J = 12.1$ Hz, 1 H, C20-H, C21-H or C22-H), 4.07-4.05 (m, 1 H, 14-H), 3.86 (s, 3 H, C33-H), 3.76 (s, 3 H, C34-H), 3.73-3.60 (comp, 5 H, C10-H, C16-H & C19-H), 3.56 (s, 3 H, C11-H, C12-H or C13-H), 3.51-3.41 (comp, 4 H, C7-H, C9-H, C17-H & C18-H), 3.41 (s, 3 H, C11-H, C12-H or C13-H), 3.40 (s, 3 H, C11-H, C12-H or C13-H), 3.02 (dd, $J = 9.5, 8.7$ Hz, 1 H, C8-H), 2.31 (ddd, $J = 12.8, 5.0, 1.8$ Hz, 1 H, C15-H), 2.19 (ddd, $J = 12.8, 5.0, 1.6$ Hz, 1 H, C6-H), 1.64-1.57 (comp, 2 H, C6'-H & C15'-H); ^{13}C NMR (125 MHz) δ 156.7 (C1, C3, C23, C27, C28, C29, C31 or C32), 147.8 (C1, C3, C23, C27, C28, C29, C31 or C32), 144.2 (C1, C3, C23, C27, C28, C29, C31 or C32), 141.7 (C1, C3, C23, C27, C28, C29, C31 or C32), 138.5 (C1, C3, C23, C27, C28, C29, C31 or C32), 138.3 (C1, C3, C23, C27, C28, C29, C31 or C32), 136.6 (C4), 135.2 (C1, C3, C23, C27, C28, C29, C31 or C32), 128.4 (C24, C25 or C26), 128.3 (C24, C25 or C26), 128.0 (C24, C25 or C26), 127.8 (C24, C25 or C26), 127.7 (C24, C25 or C26), 127.7 (C24, C25 or C26), 127.6 (C24, C25 or C26), 127.5 (C24, C25 or C26), 124.7 (C1, C3, C23, C27, C28, C29, C31 or C32), 112.8 (C30), 95.4 (C1, C3, C23, C27, C28, C29, C31 or C32), 83.0 (C17), 80.8 (C2), 80.5 (C16), 80.2

(C8), 80.1 (C9), 79.2 (C7), 78.2 (C18), 75.1 (C20, C21 or C22), 73.5 (C20, C21 or C22), 73.1 (C5), 72.6 (C10), 72.3 (C14), 71.3 (C20, C21 or C22), 69.6 (C19), 60.8 (C33), 60.6 (C10, C11, or C12), 59.3 (C10, C11, or C12), 56.3 (C10, C11, or C12), 56.1 (C34), 34.9 (C15), 30.9 (C6).

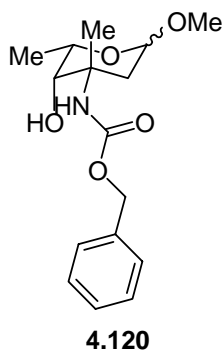


2-(4(R),5(S)-Bis-benzyloxy-6(R)-benzyloxymethyltetrahydropyran-2-yl)-7-chloro-4-(4(R),5(S)-dimethoxy-6(R)-methoxymethyltetrahydropyran-2-yl)-5,8-dimethoxynaphthalen-1-ol (4.075). (hrp3-173). Trifluoroacetic acid (TFA) (1 drop) was added to a solution of **4.074** (4 mg, 0.0019 mmol) in CH₂Cl₂ (0.25 mL) at 0 °C. The reaction vessel was sealed with a glass stopper, warmed slowly to rt, and stirred for 24 h at rt. The reaction mixture was diluted with CH₂Cl₂ (1 mL), and the solution was washed with saturated aqueous NaHCO₃ (1 mL). The organic layer was dried (Na₂SO₄) and concentrated under reduced pressure. The residue was purified by flash chromatography eluting with EtOAc/hexanes (1:2) to give 4 mg of **4.075** (100%) as a single diastereomer as a colorless oil: ¹H NMR (500 MHz) δ 10.07 (s, 1 H), 7.98 (s, 1 H), 7.41-7.23 (comp,

15 H), 6.73 (s, 1 H), 5.21 (d, $J = 10.2$ Hz, 1 H), 5.01 (dd, $J = 11.2, 1.8$ Hz, 1 H), 4.98 (d, $J = 10.8$ Hz, 1 H), 4.77-4.64 (comp, 5 H), 3.97 (s, 3 H), 3.91-3.89 (comp, 4 H), 3.84-3.83 (m, 2 H), 3.67-3.66 (comp, 2 H), 3.62-3.61 (comp, 2 H), 3.57 (s, 3 H), 3.53-3.48 (comp, 2 H), 3.43 (s, 3 H), 3.42 (s, 3 H), 3.11 (dd, $J = 9.5, 8.7$ Hz, 1 H), 2.52 (dd, $J = 4.8, 1.6$ Hz, 1 H), 2.50 (dd, $J = 4.8, 1.6$ Hz, 1 H), 1.74-1.67 (m, 1 H), 1.52-1.45 (m, 1 H); ^{13}C NMR (125 MHz) δ 154.0, 148.3, 145.5, 138.7, 129.7, 128.4, 128.3, 128.3, 128.1, 127.8, 127.7, 127.6, 127.5, 127.4, 124.2, 123.8, 123.5, 121.3, 118.7, 107.2, 83.5, 81.4, 80.2, 79.9, 79.8, 78.5, 75.5, 75.1, 73.5, 72.4, 71.8, 71.3, 69.5, 62.5, 60.6, 59.6, 56.5, 55.8, 39.0, 37.1; IR (CHCl_3) 3320, 3002, 2935, 2862, 2253, 1711, 1598, 1466, 1454, 1359, 1300, 1115, 908 cm^{-1} ; mass spectrum (CI) m/z 842.3444 [$\text{C}_{48}\text{H}_{55}\text{ClO}_{11}$ (M+H) requires 842.3433] 811 (base), 585.

NMR Assignments. ^1H NMR (500 MHz) δ 10.07 (s, 1 H, O-H), 7.98 (s, 1 H, C4-H), 7.41-7.23 (comp, 15 H, C24-H, C25-H & C26-H), 6.73 (s, 1 H, C30-H), 5.21 (d, $J = 10.2$ Hz, 1 H, C5-H), 5.01 (dd, $J = 11.2, 1.8$ Hz, 1 H, C14-H), 4.98 (d, $J = 10.8$ Hz, 1 H, C20-H, C21-H or C22-H), 4.77-4.64 (comp, 5 H, C20-H, C21-H & C22-H), 3.97 (s, 3 H, C33-H), 3.91-3.89 (comp, 4 H, C16-H & C34-H), 3.84-3.83 (m, 1 H, C19-H), 3.67-3.66 (comp, 2 H, C17-H & C18-H), 3.62-3.61 (comp, 2 H, C10-H), 3.57 (s, 3 H, C11-H, C12-H or C13-H), 3.53-3.48 (comp, 2 H, C7-H & C9-H), 3.43 (s, 3 H, C11-H, C12-H or C13-H), 3.42 (s, 3 H, C11-H, C12-H or C13-H), 3.11 (dd, $J = 9.5, 8.7$ Hz, 1 H, C8-H), 2.52 (dd, $J = 4.8, 1.6$ Hz, 1 H, C15-H or C6-H), 2.50 (dd, $J = 4.8, 1.6$ Hz, 1 H, C15-H or C6-H), 1.74-1.67 (m, 1 H, C15'-H), 1.52-1.45 (m, 1 H, C6'-H); ^{13}C NMR (125 MHz) δ 154.0 (C1, C2, C3, C23, C27, C28, C29, C31 or C32), 148.3 (C1, C2, C3, C23, C27, C28, C29, C31 or C32), 145.5 (C1, C2, C3, C23, C27, C28, C29, C31 or C32), 138.7 (C1, C2, C3, C23, C27, C28, C29, C31 or C32), 129.7 (C1, C2, C3, C23, C27, C28, C29, C31 or C32), 128.4 (C24, C25 or C26), 128.3 (C24, C25 or C26), 128.3 (C24, C25 or

C26), 128.1 (C24, C25 or C26), 127.8 (C24, C25 or C26), 127.7 (C24, C25 or C26), 127.6 (C24, C25 or C26), 127.5 (C24, C25 or C26), 127.4 (C24, C25 or C26), 124.2 (C4), 123.8 (C1, C2, C3, C23, C27, C28, C29, C31 or C32), 123.5 (C1, C2, C3, C23, C27, C28, C29, C31 or C32), 121.3 (C1, C2, C3, C23, C27, C28, C29, C31 or C32), 118.7 (C1, C2, C3, C23, C27, C28, C29, C31 or C32), 107.2 (C30), 83.5 (C9), 81.4 (C16), 80.2 (C8), 79.9 (C17 or C18), 79.8 (C9), 78.5 (C17 or C18), 75.5 (C5), 75.1 (C20, C21 or C22), 73.5 (C20, C21 or C22), 72.4 (C10), 71.8 (C14), 71.3 (C20, C21 or C22), 69.5 (C19), 62.5 (C33), 60.6 (C11, C12 or C13), 59.6 (C11, C12 or C13), 56.5 (C11, C12 or C13), 55.8 (C34), 39.0 (C6), 37.1 (C15).



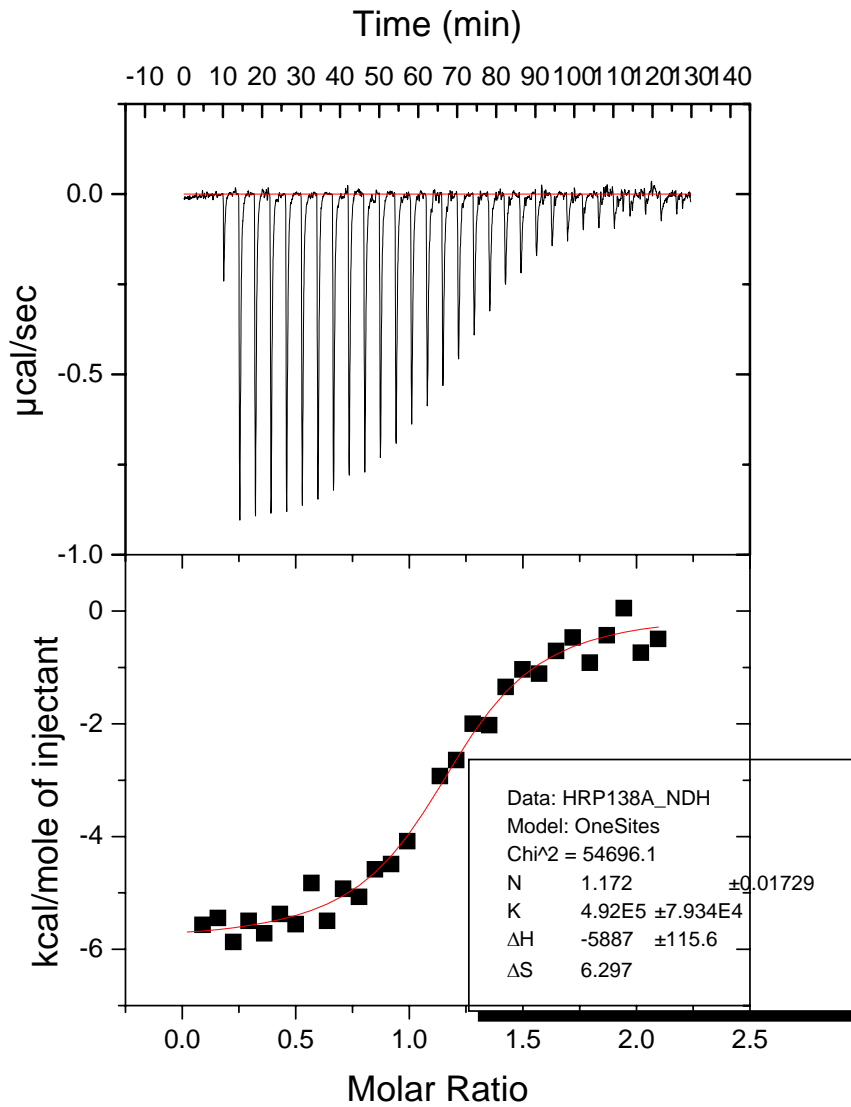
(2'S,3'R,4'S)-(3-Hydroxy-6-methoxy-2,4-dimethyltetrahydropyran-4-yl)carbamic acid benzyl ester (4.120). (hrp4-33 & hrp4-35). A solution containing NaHCO₃ (250 mg, 4.0 mmol) in H₂O (3.0 mL) and Cbz-O-Suc (1.0 g, 3.0 mmol) were added to a solution of vancomycin (1.5 g, 1.0, mmol) in dioxane and H₂O (1:1, 17 mL). The solution was stirred for 2.5 h at rt, and the solution was poured into acetone (200 mL). The mixture was sonicated for 30 min and then the solid was collected by filtration using a finely fritted (F) funnel. The solid was dissolved in MeOH (10 mL) and azeotroped with toluene (3 x 10 mL). The residue was dissolved in MeOH (30 mL), and HCl (4 M in dioxane, 2 mL, 8.0 mmol) was added. The resultant pink solution was stirred for 2.5 h at room temperature (turned cloudy after 30 min), whereupon NaHCO₃

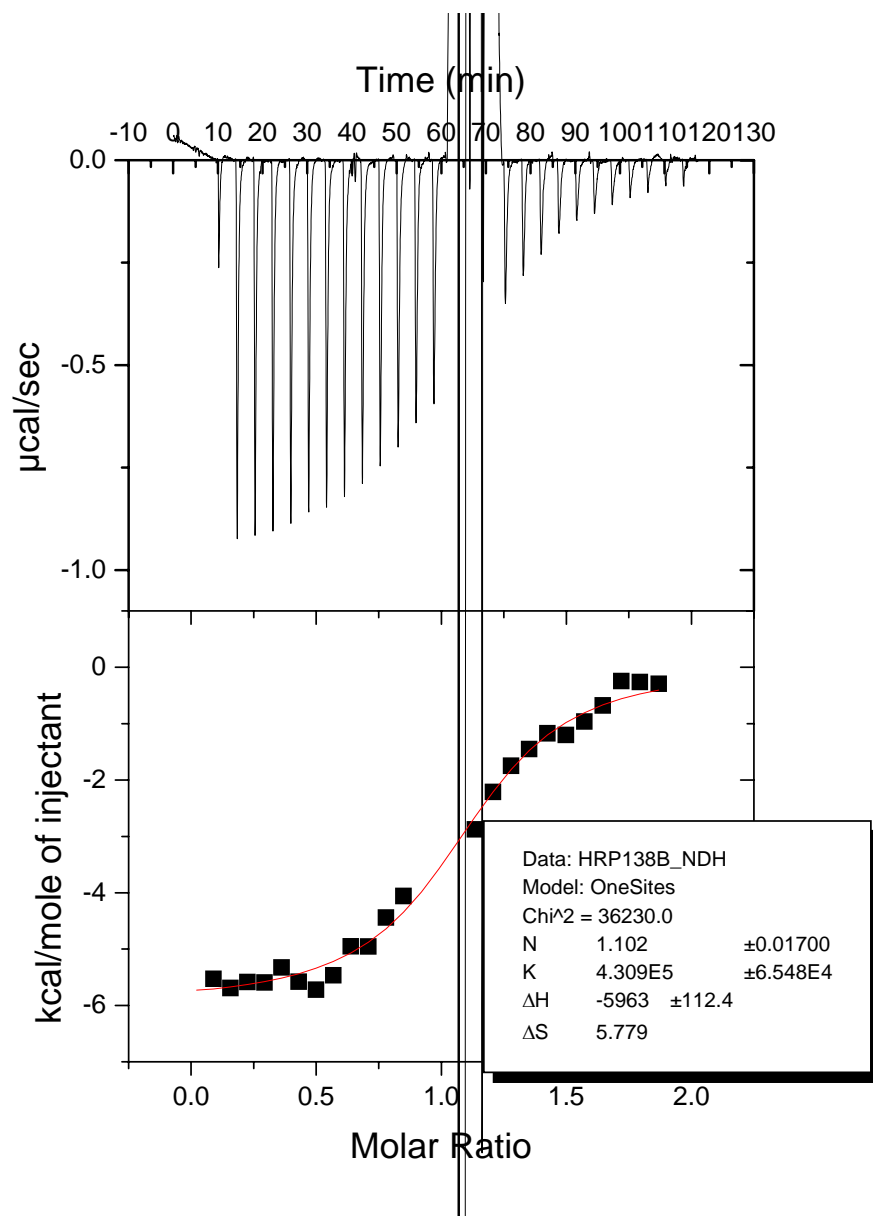
(689 mg, 8.2 mmol) was added. The mixture was concentrated under reduced pressure. The residue was suspended in acetone (100 mL) and sonicated for 30 min. The solid was removed by filtration using a finely fritted funnel (F), and the filtrate was concentrated under reduced pressure. The residue was suspended in EtOAc (40 mL) and sonicated for 30 min. The solid was removed by filtration using a finely fritted funnel (F) and the filtrate was concentrated under reduced pressure and purified by flash column chromatography eluting with hexanes/EtOAc (1:1) to provide 218 mg of **4.120** (71%) as an yellow oil and as a mixture of diastereomers (1:1.5);²²⁴ ¹H NMR (500 MHz) δ 7.35-7.61 (comp m, 5 H), 5.48 (br s, 0.4 H), 5.38 (br s, 0.6 H), 5.07-5.00 (comp m, 2 H), 4.69 (d, $J = 4.7$ Hz, 0.6 H), 4.39 (dd, $J = 9.6, 2.2$ Hz, 0.4 H), 4.07 (dd, $J = 13.3, 6.6$ Hz, 0.6 H), 3.80 (dd, $J = 13.3, 6.4$ Hz, 0.4 H), 3.46 (s, 1.2 H), 3.28 (br s, 0.6 H), 3.29 (s, 1.8 H), 3.25 (br s, 0.4 H), 2.22-2.13 (comp m, 2 H), 1.79 (dd, $J = 14.2, 4.7$ Hz, 0.4 H), 1.62-1.53 (m, 0.6 H), 1.60 (s, 1.8 H), 1.50 (s, 1.2 H), 1.29 (d, $J = 6.4$ Hz, 0.4 H), 1.23 (d, $J = 6.6$ Hz, 0.6 H); ¹³C NMR (125 MHz) δ 155.0, 136.6, 136.5, 128.5, 128.1, 128.0, 103.9, 100.2, 98.1, 98.1, 88.8, 73.1, 72.6, 68.8, 66.2, 62.9, 56.4, 55.0, 54.9, 53.6, 37.4, 35.3, 23.3, 21.6, 17.2, 17.1; IR 3563, 3414, 2988, 2937, 1717, 1499, 1454, 1385, 1274, 1114, 1057 cm^{-1} ; mass spectrum (CI) m/z 310.1664 [$\text{C}_{16}\text{H}_{23}\text{NO}_5$ (M+H) requires 310.1654] 278 (base).

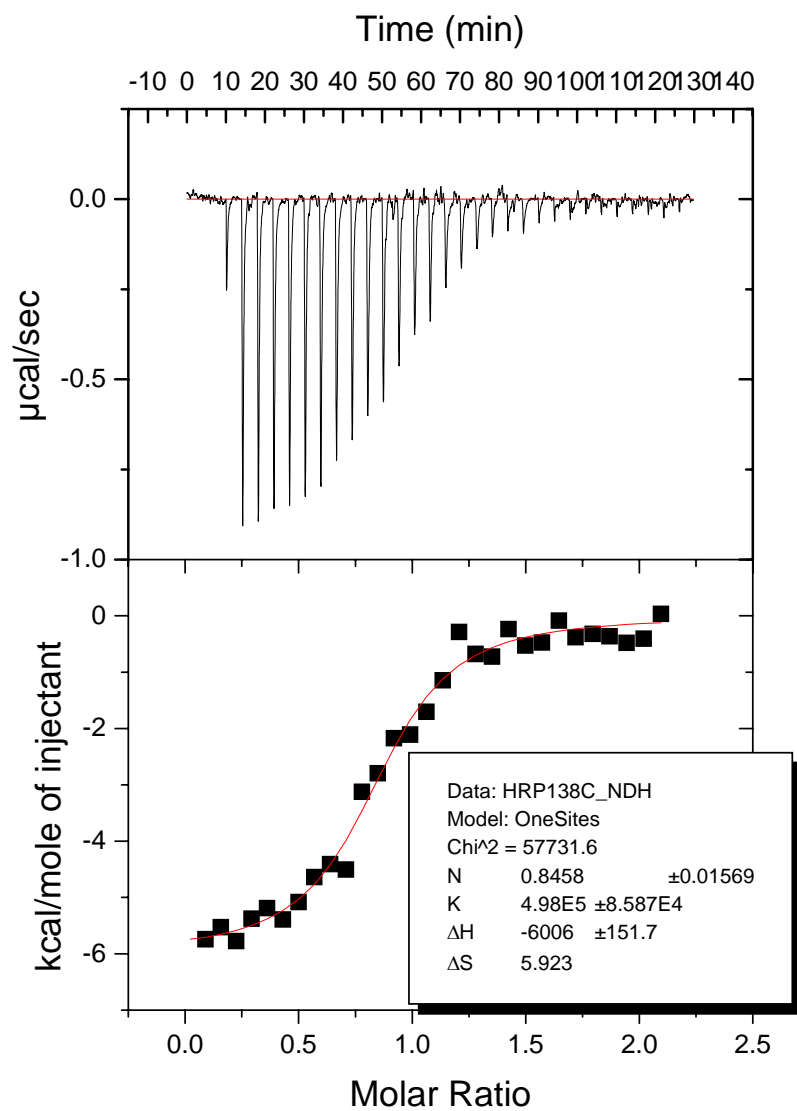
Appendix

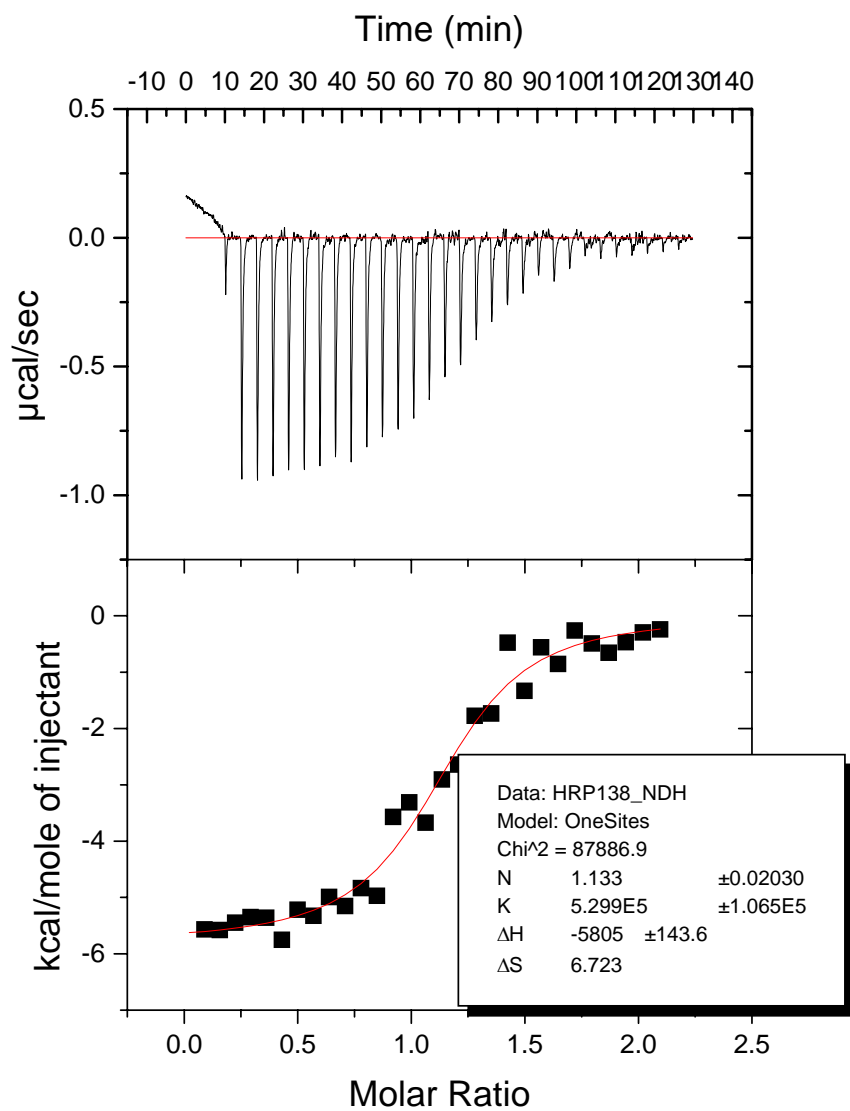
ITC

Data for **2.003** at 25 °C



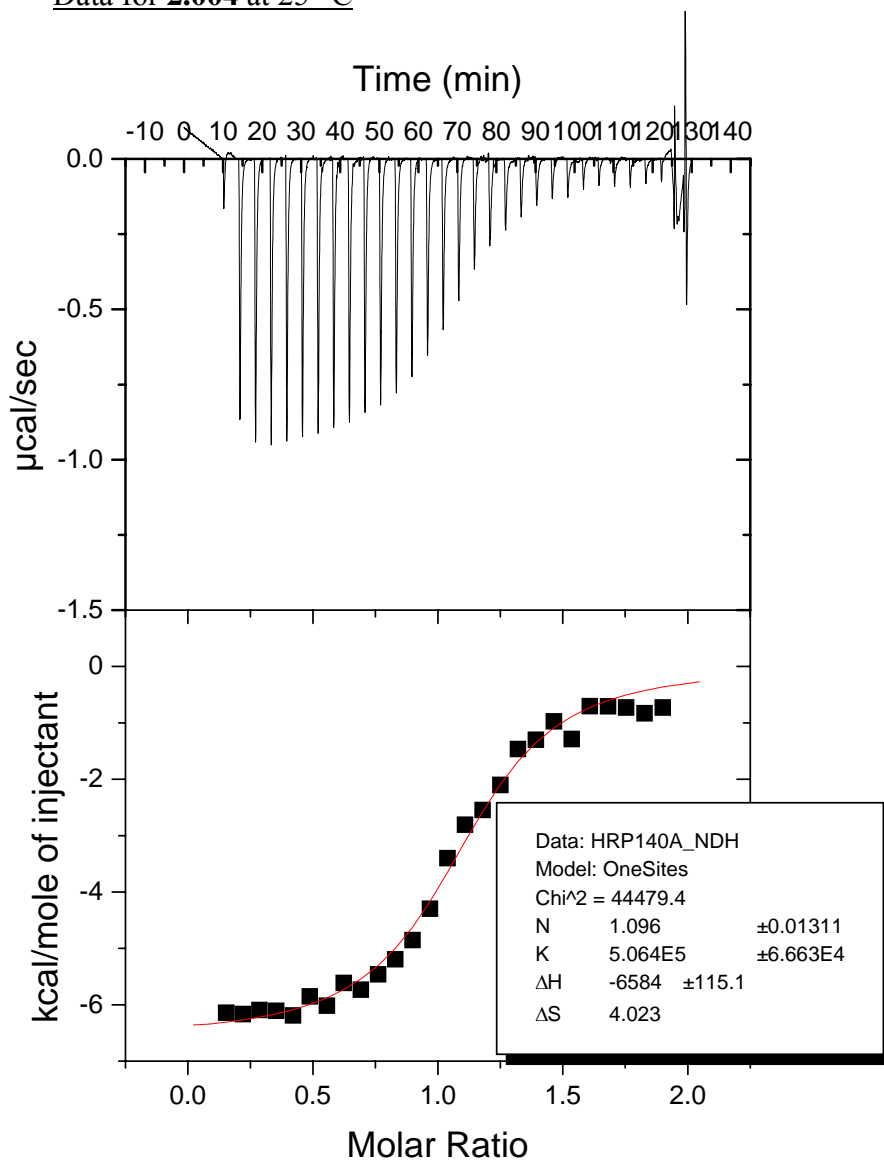


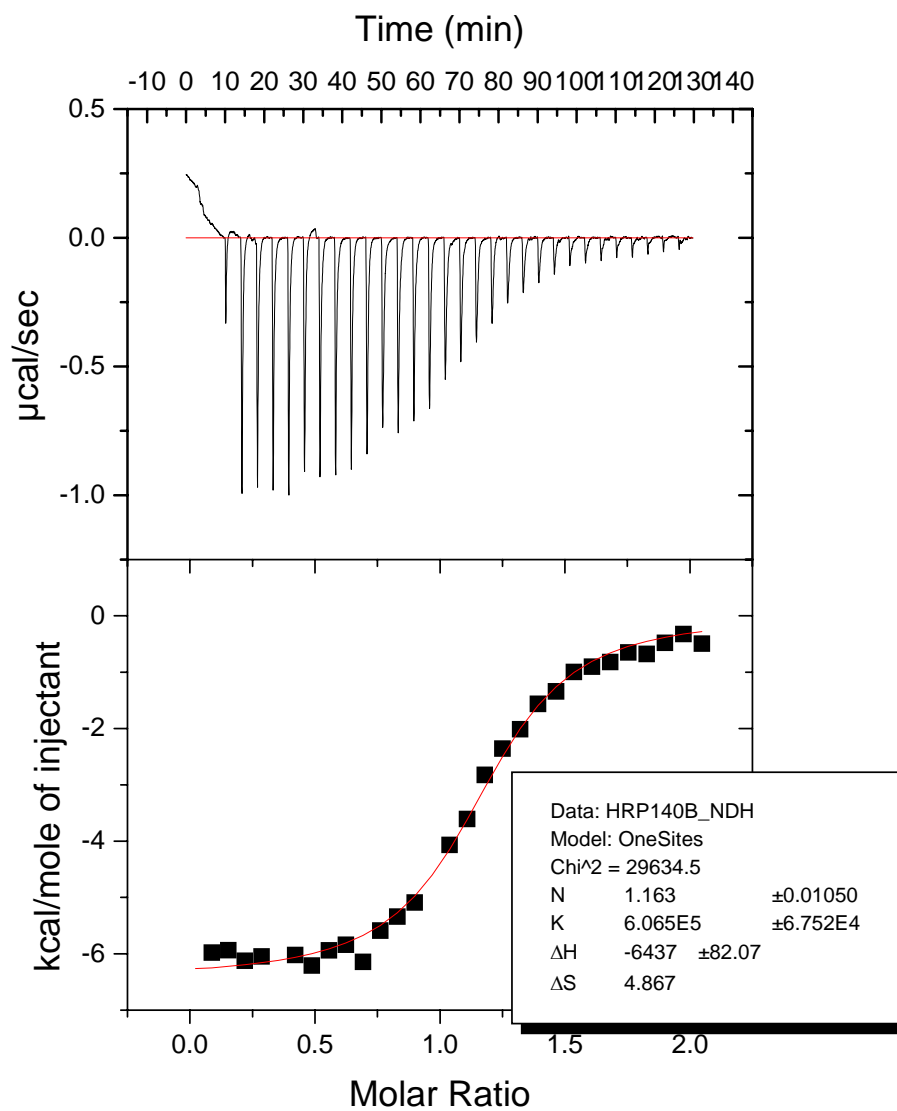


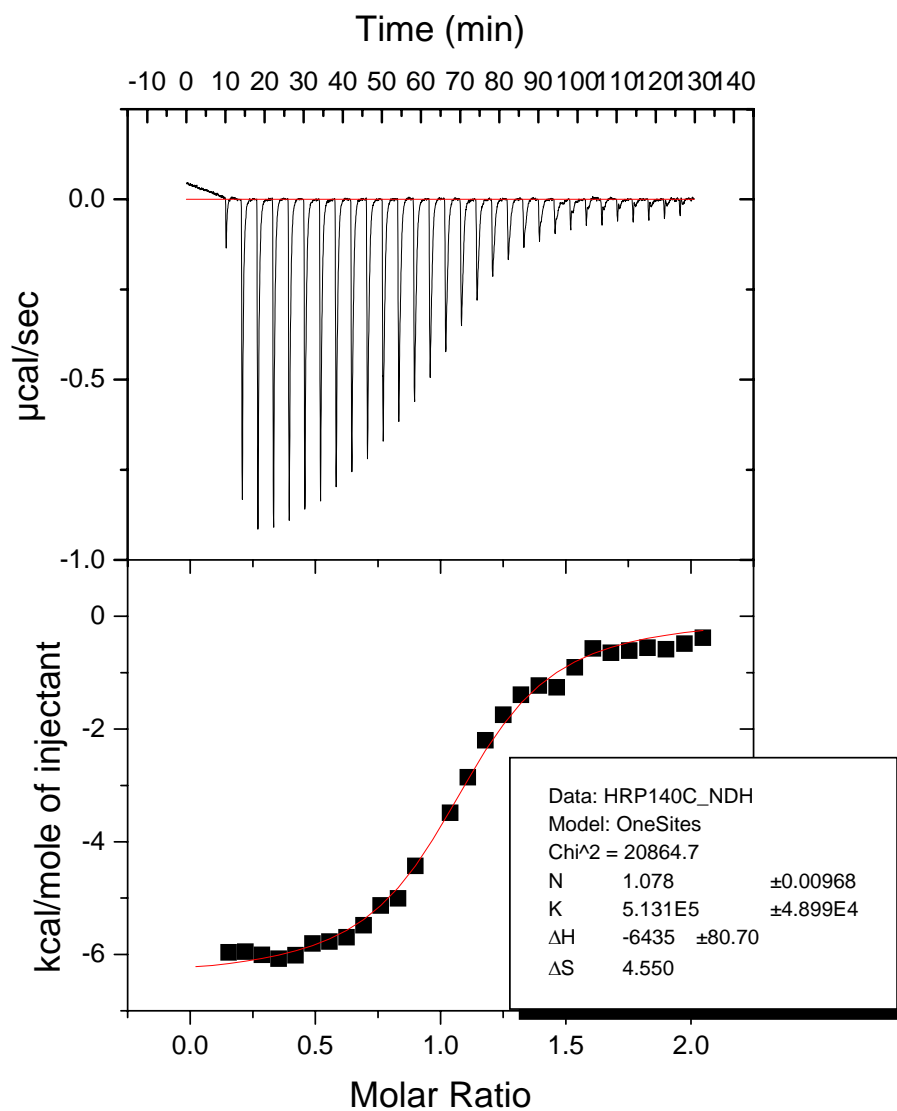


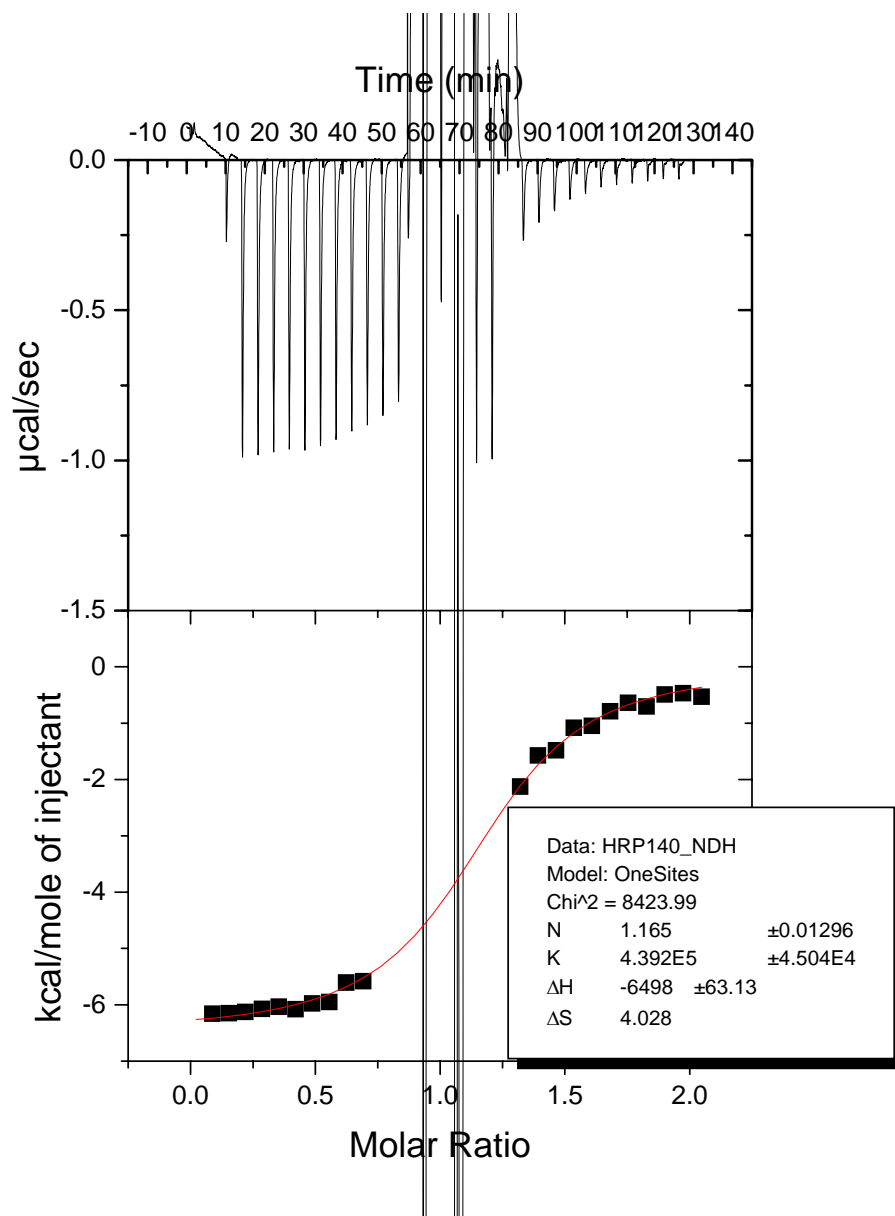
Data at 298 K	2.003
enthaply	-5805 -6008 -5887 -5963
aver	-5915.75
stdv	89.134262
Kb	529990 492500 430900 498000
ave	487847.5
stdev	41407.435
LnKb	13.180613 13.10725 12.973631 13.118355
$\Delta G(J)$	-32674.36 -32492.49 -32161.26 -32520.02
ave	-32462.03
stdev	215.90086
ΔG (kcal mol ⁻¹)	-7.753424 0.051567
Entropy (cal mol ⁻¹ K ⁻¹)	6.1635877 0.4719145

Data for **2.004** at 25 °C



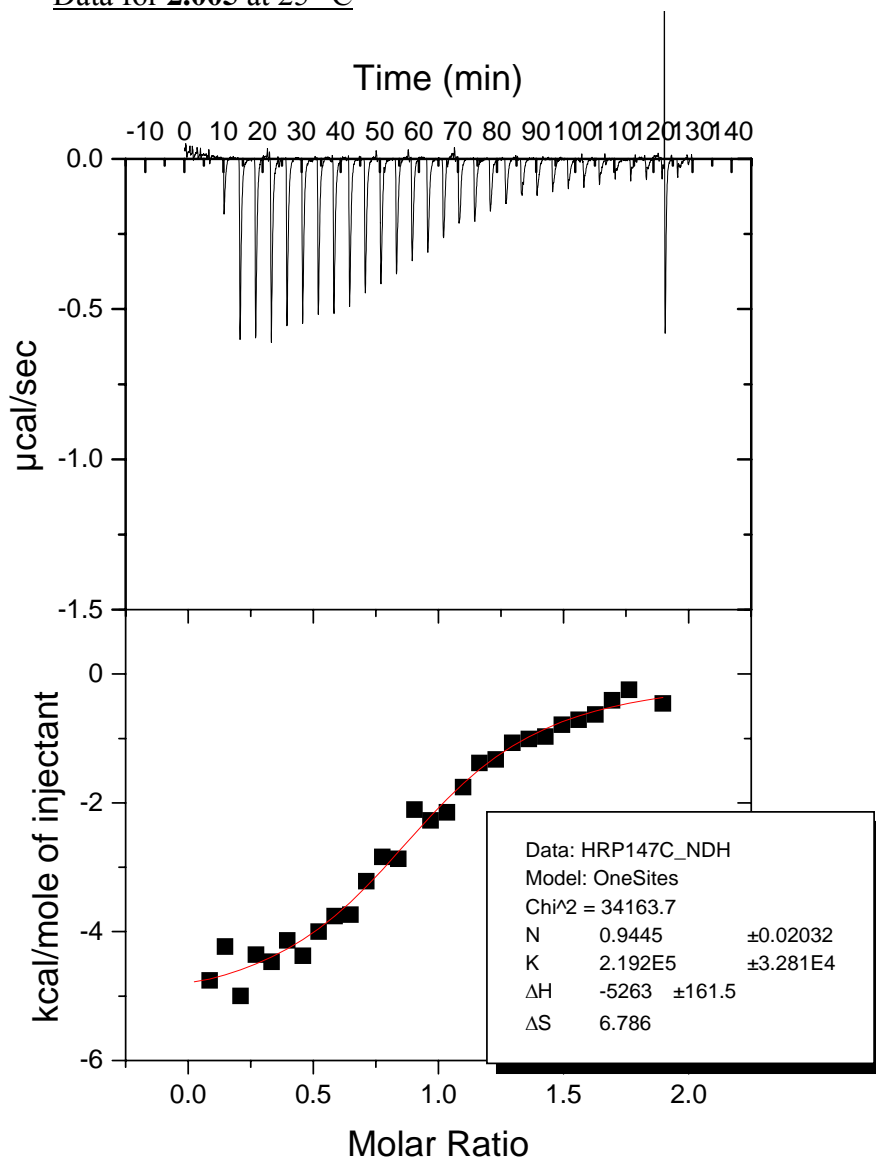


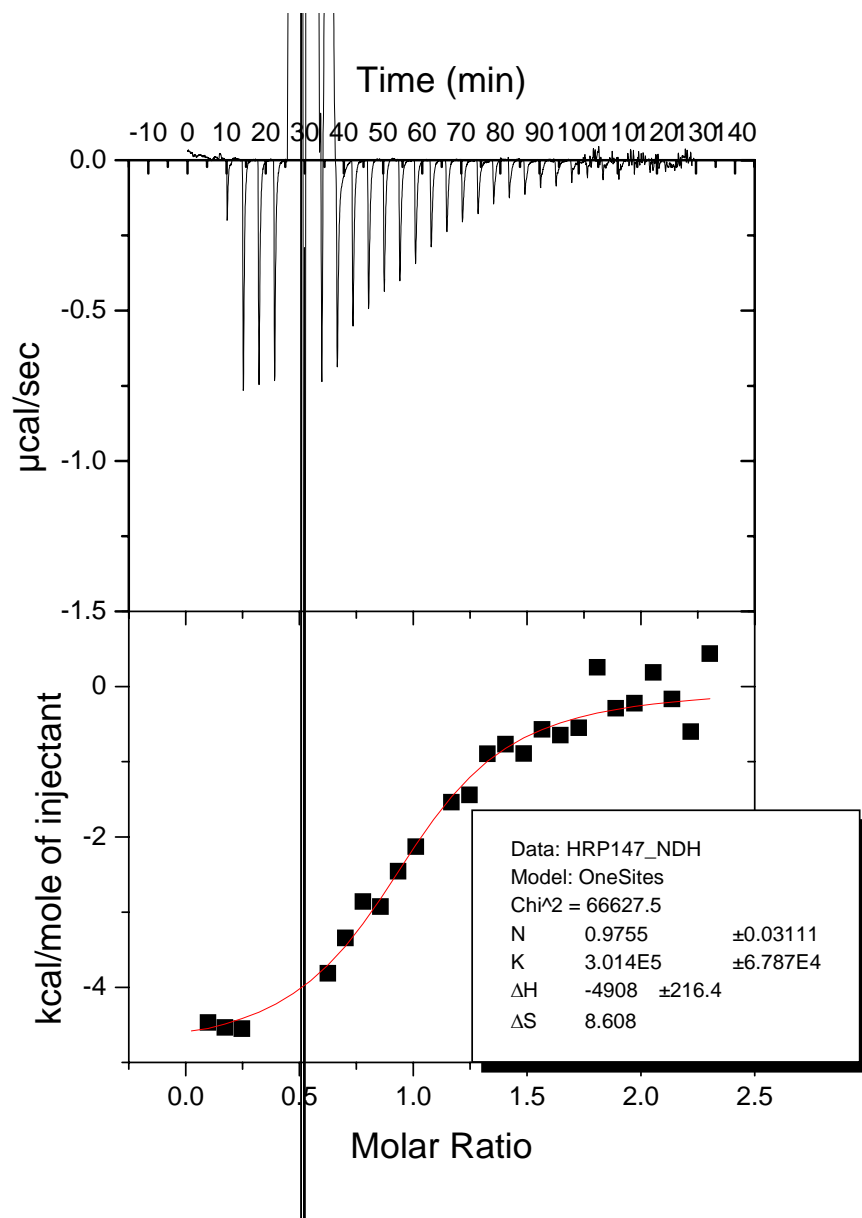


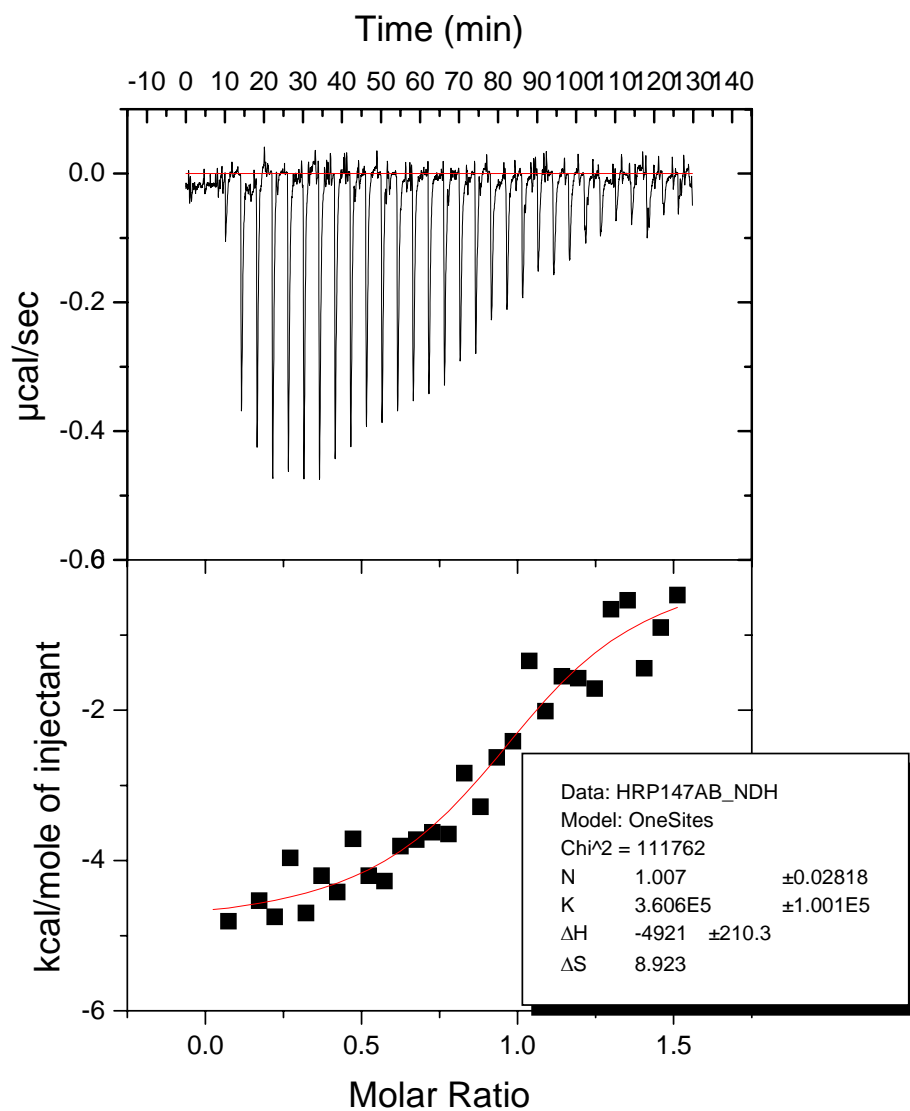


Data at 298 K	2.004
enthaply	-6498 -6554 -6437 -6435
aver	-6481
stdv	56.774407
Kb	439200 506400 606500 513000
ave	516275
stdev	68773.414
LnKb	12.99271 13.135082 13.31546 13.148031
$\Delta G(J)$	-32208.55 -32561.49 -33008.64 -32593.59
ave	-32593.07
stdev	327.38857
ΔG (kcal mol ⁻¹)	-7.784721 0.0781954
Entropy (cal mol ⁻¹ K ⁻¹)	4.3727007 0.452691

Data for **2.005** at 25 °C

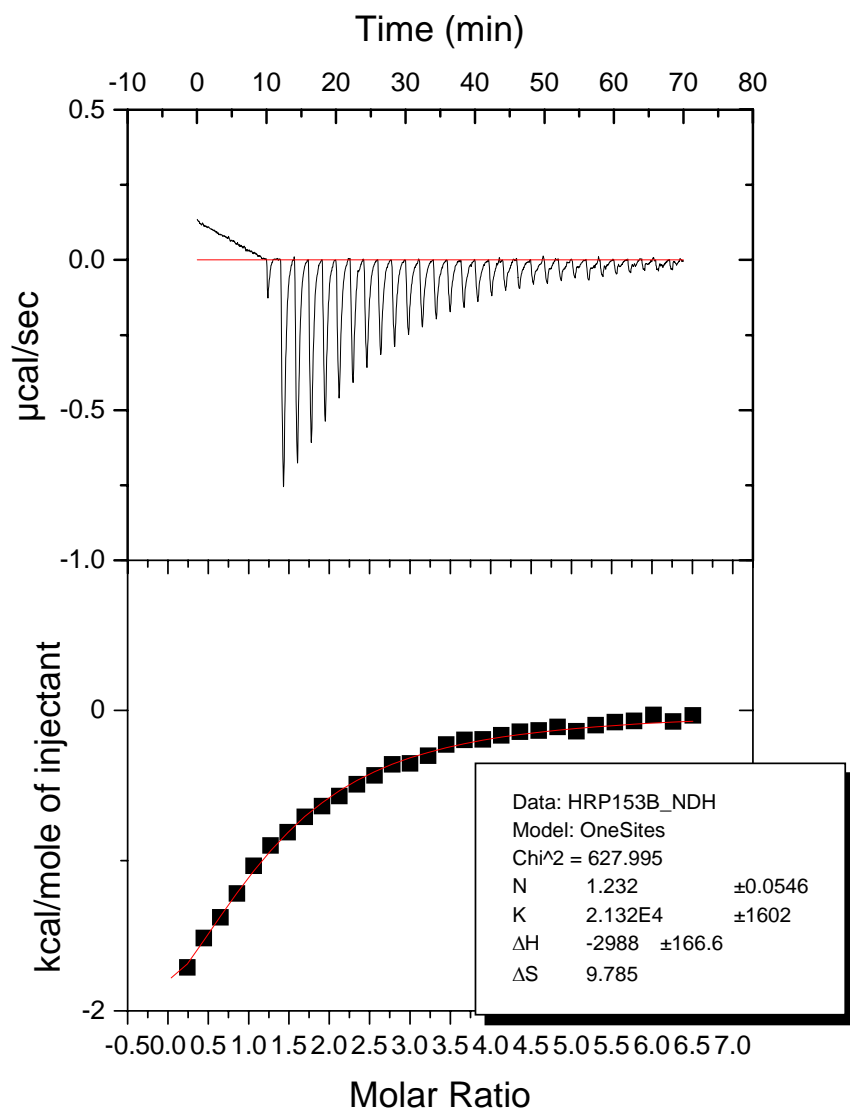


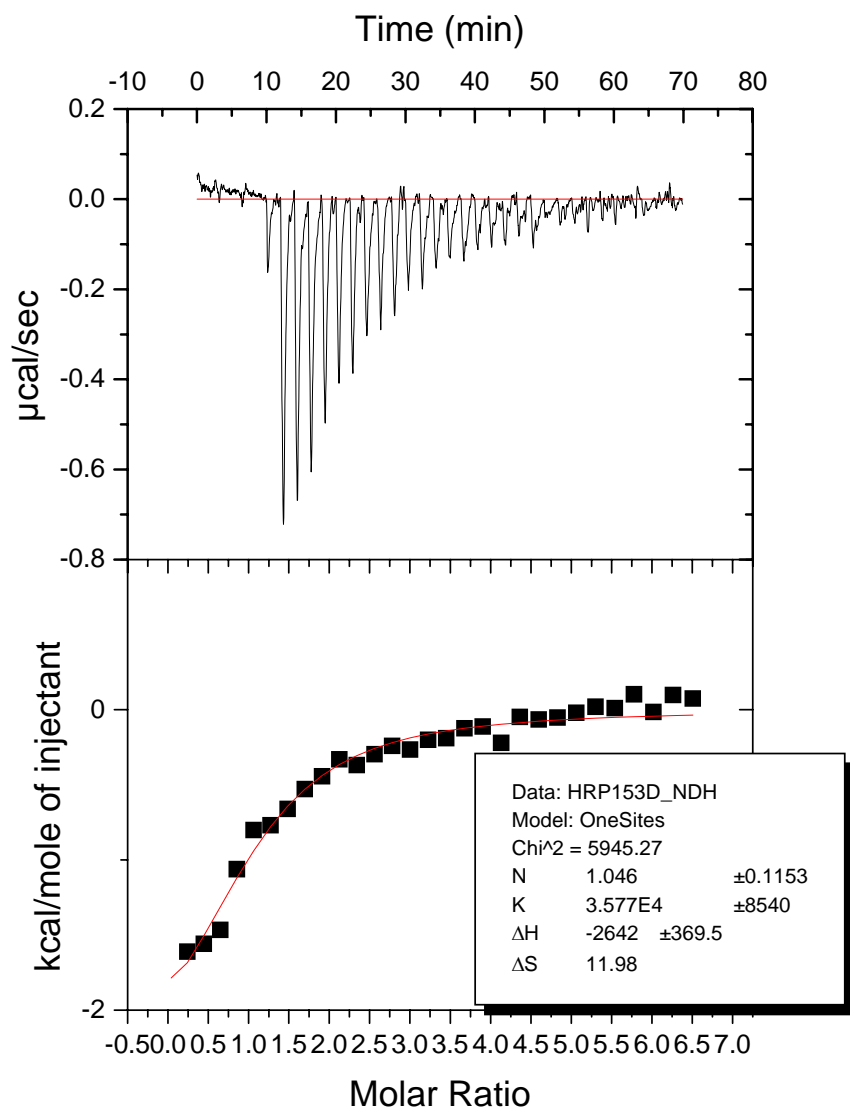


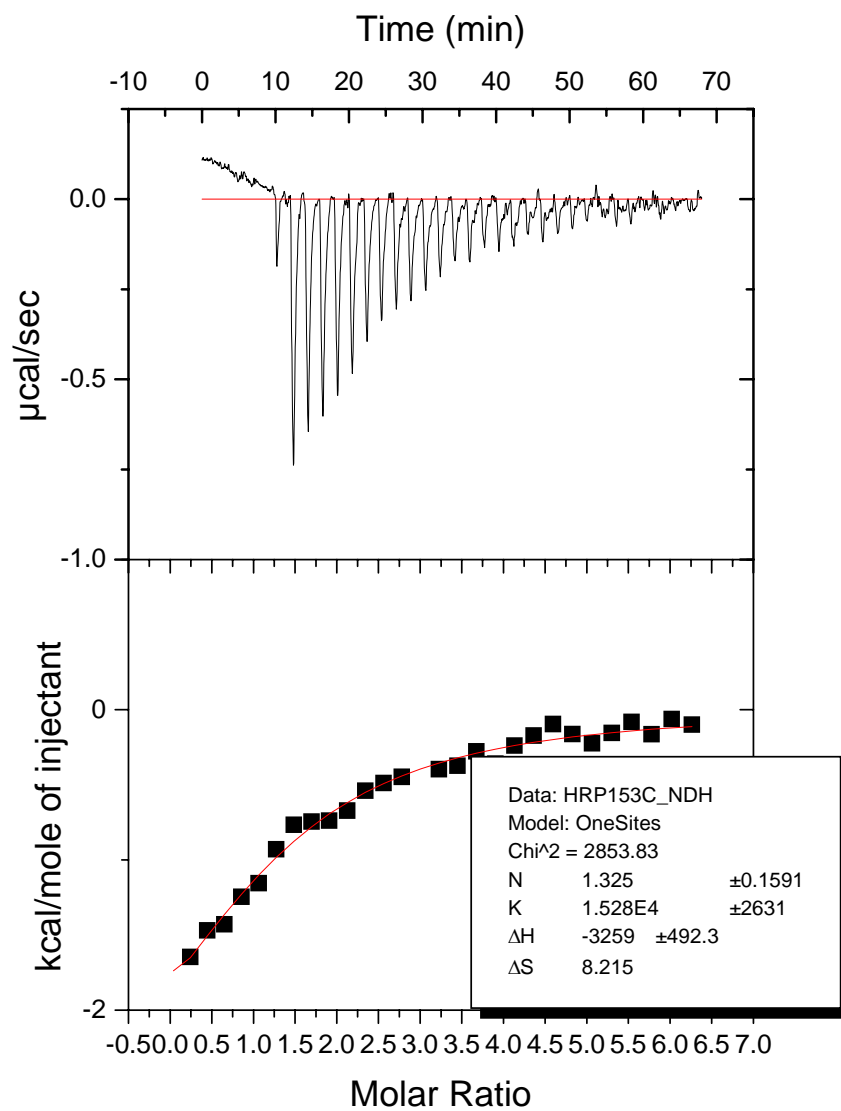


Data at 298 K	2.005
enthaply	-4908 -4921 -5263
aver	-5030.667
stdv	201.31153
Kb	301400 360600 219200
ave	293733.33
stdev	71011.079
LnKb	12.616194 12.795525 12.29774
$\Delta G(J)$	-31275.18 -31719.74 -30485.74
ave	-31160.22
stdev	624.9778
ΔG (kcal mol ⁻¹)	-7.442491 0.1492734
Entropy (cal mol ⁻¹ K ⁻¹)	8.089297 1.1758676

Data for **2.007** at 25 °C







Data at 298 K	2.007
enthaply	-2831 -2988 -3259
aver	-3026
stdv	216.51559
Kb	24280 21320 15280
ave	20293.333
stdev	4586.9961
LnKb	10.097408 9.9674009 9.6343001
$\Delta G(J)$	-25031.18 -24708.9 -23883.15
ave	-24541.08
stdev	592.12935
ΔG (kcal mol ⁻¹)	-5.861536 0.1414277
Entropy (cal mol ⁻¹ K ⁻¹)	9.5104339 1.2005476

References

- 1) Li, P.; Roller, P. P.; Xu, J. "Current Synthetic Approaches to Peptide and Peptidomimetic Cyclization" *Curr. Org. Chem.* **2002**, *6*, 411-440.
- 2) Glenn, M. P.; Fairlie, D. P. "Mimetics of the Peptide B-Strand" *Mini-Reviews in Medicinal Chemistry* **2002**, *2*, 433-445.
- 3) Giannis, A.; Kolter, T. "Peptide Mimetics for Receptor Ligands: Discovery, Development, and Medicinal Perspectives" *Angew. Chem., Int. Ed. Engl.* **1993**, *32*, 1244-1267.
- 4) Gante, J. "Peptide Mimetics - Tailor-Made Enzyme Inhibitors" *Angew. Chem., Int. Ed. Engl.* **1994**, *33*, 1699-1720.
- 5) Hanessian, S.; McNaughton-Smith, G.; Lombart, H.-G.; Lubell, W. D. "Design and Synthesis of Conformationally Constrained Amino Acids as Versatile Scaffolds and Peptide Mimetics" *Tetrahedron* **1997**, *53*, 12789-12854.
- 6) Goodman, M.; Zhang, J. "Peptidomimetic Building Blocks for Drug Design" *Chemtracts-Org. Chem.* **1997**, *10*, 629-645.
- 7) van Holde, K. E.; Johnson, C. W.; Ho, P. S. *Principles of Physical Biochemistry*, Prentice Hall: New Jersey, 1998, 137.
- 8) Andrews, P. R.; Craik, D. J.; Martin, J. L. "Functional-Group Contributions to Drug Receptor Interactions" *J. Med. Chem.* **1984**, *27*, 1648-1657.
- 9) Styer, L. *Biochemistry*, W. H. Freeman and Company: New York, 1995, 7-8.
- 10) Pauling, L.; Corey, R. B. "Configurations of Polypeptide Chains with Favored Orientations around Single Bonds: Two New Pleated Sheets" *Proc. Natl. Acad. Sci., U.S.* **1951**, *37*, 729-740.
- 11) Gohlke, H.; Klebe, G. "Approaches to the Description and Prediction of the Binding Affinity of Small-Molecule Ligands to Macromolecular Receptors" *Angew. Chem., Int. Ed. Eng.* **2002**, *41*, 2645-2676.
- 12) Fersht, A. R. "The Hydrogen-Bond in Molecular Recognition" *Trends Biochem. Sci.* **1987**, *12*, 301-304.
- 13) Williams, D. H.; Searle, M. S.; Mackay, J. P.; Gerhard, U.; Maplestone, R. A. "Toward an Estimation of Binding Constants in Aqueous-Solution - Studies of Associations of Vancomycin Group Antibiotics" *Proc. Natl. Acad. Sci. U.S.A* **1993**, *90*, 1172-1178.

- 14) Searle, M. S.; Williams, D. H. "The Cost of Conformational Order - Entropy Changes in Molecular Associations" *J. Am. Chem. Soc.* **1992**, *114*, 10690-10697.
- 15) Searle, M. S.; Westwell, M. S.; Williams, D. H. "Application of a Generalized Enthalpy-Entropy Relationship to Binding Cooperativity and Weak Associations in Solution" *J. Chem. Soc., Perkin Trans. 2* **1995**, 141-151.
- 16) Kuntz, I. D.; Chen, K.; Sharp, K. A.; Kollman, P. A. "The Maximal Affinity of Ligands" *Proc. Natl. Acad. Sci. U.S.A* **1999**, *96*, 9997-10002.
- 17) Page, M. I.; Jencks, W. P. "Entropic Contributions to Rate Accelerations in Enzymic and Intramolecular Reactions and the Chelate Effect" *Proc. Natl. Acad. Sci. U.S.A* **1971**, *68*, 1678-1683.
- 18) Page, M. I. "Entropy, Binding-Energy, and Enzymic Catalysis" *Angew. Chem., Int. Ed. Eng.* **1977**, *16*, 449-459.
- 19) Williams, D. H.; Cox, J. P. L.; Doig, A. J.; Gardner, M.; Gerhard, U.; Kaye, P. T.; Lal, A. R.; Nicholls, I. A.; Salter, C. J.; Mitchell, R. C. "Toward the Semiquantitative Estimation of Binding Constants. Guides for Peptide-Peptide Binding in Aqueous Solution" *J. Am. Chem. Soc.* **1991**, *113*, 7020-7030.
- 20) Tidor, B.; Karplus, M. "The Contribution of Vibrational Entropy to Molecular Association. The Dimerization of Insulin" *J. Mol. Biol.* **1994**, *238*, 405-414.
- 21) Janin, J.; Chothia, C. "Role of Hydrophobicity in the Binding of Coenzymes. Appendix. Translational and Rotational Contribution to the Free Energy of Dissociation" *Biochemistry* **1978**, *17*, 2943-2948.
- 22) Cole, C.; Warwicker, J. "Side-Chain Conformational Entropy at Protein-Protein Interfaces" *Protein Sci.* **2002**, *11*, 2860-2870.
- 23) Velazquez-Campoy, A.; Luque, I.; Freire, E. "The Application of Thermodynamic Methods in Drug Design" *Thermochim. Acta* **2001**, *380*, 217-227.
- 24) Khan, A. R.; Parrish, J. C.; Fraser, M. E.; Smith, W. W.; Bartlett, P. A.; James, M. N. G. "Lowering the Entropic Barrier for Binding Conformationally Flexible Inhibitors to Enzymes" *Biochemistry* **1998**, *37*, 16839-16845.
- 25) Morgan, B. P.; Holland, D. R.; Matthews, B. W.; Bartlett, P. A. "Structure-Based Design of an Inhibitor of the Zinc Peptidase Thermolysin" *J. Am. Chem. Soc.* **1994**, *116*, 3251-3260.

- 26) Miller, S.; Lesk, A. M.; Janin, J.; Chothia, C. "The Accessible Surface-Area and Stability of Oligomeric Proteins" *Nature* **1987**, *328*, 834-836.
- 27) Murphy, K. P.; Freire, E. "Thermodynamics of Structural Stability and Cooperative Folding Behavior in Proteins" *Adv. Protein Chem.* **1992**, *43*, 313-361.
- 28) Baker, B. M.; Murphy, K. P. "Prediction of Binding Energetics from Structure Using Empirical Parameterization" *Methods in Enzymology* **1998**, *295*, 294-315.
- 29) Lee, B.; Richards, F. M. "The Interpretation of Protein Structures: Estimation of Static Accessibility" *J. Mol. Biol.* **1971**, *55*, 379-400.
- 30) Wang, J. M.; Wang, W.; Huo, S. H.; Lee, M.; Kollman, P. A. "Solvation Model Based on Weighted Solvent Accessible Surface Area" *J. Phys. Chem. B* **2001**, *105*, 5055-5067.
- 31) Gallicchio, E.; Zhang, L. Y.; Levy, R. M. "The Sgb/Np Hydration Free Energy Model Based on the Surface Generalized Born Solvent Reaction Field and Novel Nonpolar Hydration Free Energy Estimators" *J. Comput. Chem.* **2002**, *23*, 517-529.
- 32) Davis, A. M.; Teague, S. J. "Hydrogen Bonding, Hydrophobic Interactions, and Failure of the Rigid Receptor Hypothesis" *Angew. Chem., Int. Ed. Eng.* **1999**, *38*, 737-749.
- 33) Houk, K. N.; Leach, A. G.; Kim, S. P.; Zhang, X. Y. "Binding Affinities of Host-Guest, Protein-Ligand, and Protein-Transition-State Complexes" *Angew. Chem., Int. Ed. Eng.* **2003**, *42*, 4872-4897.
- 34) Chuman, H.; Mori, A.; Tanaka, H. "Prediction of the 1-Octanol/H₂O Partition Coefficient, Log P by Ab Initio Mo Calculations: Hydrogen-Bonding Effect of Organic Solutes on Log P" *Anal. Sci.* **2002**, *18*, 1015-1020.
- 35) Wimley, W. C.; Creamer, T. P.; White, S. H. "Solvation Energies of Amino Acid Side Chains and Backbone in a Family of Host-Guest Pentapeptides" *Biochemistry* **1996**, *35*, 5109-5124.
- 36) Wolfenden, R. "Interaction of Peptide-Bond with Solvent Water - Vapor-Phase Analysis" *Biochemistry* **1978**, *17*, 201-204.
- 37) Sangster, J. *Octanol-Water Partition Coefficients: Fundamentals and Physical Chemistry*, Wiley: New York, 1997, 57-64.
- 38) Liu, L.; Guo, Q. X. "Isokinetic Relationship, Isoequilibrium Relationship, and Enthalpy-Entropy Compensation" *Chem. Rev.* **2001**, *101*, 673-695.

- 39) Cooper, A.; Johnson, C. M.; Lakey, J. H.; Nollmann, M. "Heat Does Not Come in Different Colours: Entropy-Enthalpy Compensation, Free Energy Windows, Quantum Confinement, Pressure Perturbation Calorimetry, Solvation and the Multiple Causes of Heat Capacity Effects in Biomolecular Interactions" *Biophys. Chem.* **2001**, *93*, 215-230.
- 40) Williams, D. H.; Stephens, E.; Zhou, M. "Ligand Binding Energy and Catalytic Efficiency from Improved Packing within Receptors and Enzymes" *J. Mol. Biol.* **2003**, *329*, 389-399.
- 41) Calderone, C. T.; Williams, D. H. "An Enthalpic Component in Cooperativity: The Relationship between Enthalpy, Entropy, and Noncovalent Structure in Weak Associations" *J. Am. Chem. Soc.* **2001**, *123*, 6262-6267.
- 42) Dunitz, J. D. "Win Some, Lose Some - Enthalpy-Entropy Compensation in Weak Intermolecular Interactions" *Chem. Biol.* **1995**, *2*, 709-712.
- 43) Gilli, P.; Ferretti, V.; Gilli, G.; Borea, P. A. "Enthalpy-Entropy Compensation in Drug-Receptor Binding" *J. Phys. Chem.* **1994**, *98*, 1515-1518.
- 44) Sharp, K. "Entropy-Enthalpy Compensation: Fact or Artifact?" *Protein Sci.* **2001**, *10*, 661-667.
- 45) Krug, R. R.; Hunter, W. G.; Grieger, R. A. "Statistical Interpretation of Enthalpy-Entropy Compensation" *Nature* **1976**, *261*, 566-567.
- 46) Sheenan, D. *Physical Biochemistry*, John Wiley & Sons: New York, NY, 2000, 323.
- 47) Gomez, J.; Freire, E. "Thermodynamic Mapping of the Inhibitor Site of the Aspartic Protease Endothiapepsin" *J. Mol. Biol.* **1995**, *252*, 337-350.
- 48) Frisch, C.; Schreiber, G.; Johnson, C. M.; Fersht, A. R. "Thermodynamics of the Interaction of Barnase and Barstar: Changes in Free Energy Versus Changes in Enthalpy on Mutation" *J. Mol. Biol.* **1997**, *267*, 696-706.
- 49) Plum, G. E.; Breslauer, K. J. "Calorimetry of Proteins and Nucleic-Acids" *Curr. Opin. Struct. Biol.* **1995**, *5*, 682-690.
- 50) Jelesarov, I.; Bosshard, H. R. "Isothermal Titration Calorimetry and Differential Scanning Calorimetry as Complementary Tools to Investigate the Energetics of Biomolecular Recognition" *J. Mol. Recognit.* **1999**, *12*, 3-18.
- 51) Wadso, I. "Trends in Isothermal Microcalorimetry" *Chem Soc. Rev.* **1997**, *26*, 79-86.

- 52) Leavitt, S.; Freire, E. "Direct Measurement of Protein Binding Energetics by Isothermal Titration Calorimetry" *Curr. Opin. Struct. Biol.* **2001**, *11*, 560-566.
- 53) McNemar, C.; Snow, M. E.; Windsor, W. T.; Prongay, A.; Mui, P.; Zhang, R.; Durkin, J.; Le, H. V.; Weber, P. C. "Thermodynamic and Structural Analysis of Phosphotyrosine Polypeptide Binding to Grb2-Sh2" *Biochemistry* **1997**, *36*, 10006-10014.
- 54) Wiseman, T.; Williston, S.; Brandts, J. F.; Lin, L. N. "Rapid Measurement of Binding Constants and Heats of Binding Using a New Titration Calorimeter" *Anal. Biochem.* **1989**, *179*, 131-137.
- 55) Ragone, R.; Colonna, G. "Reliability of the Vant Hoff Plots" *J. Phys. Chem.* **1995**, *99*, 13050-13050.
- 56) Miklavc, A.; Kocjan, D.; Mavri, J.; Koller, J.; Hadzi, D. "On the Fundamental Difference in the Thermodynamics of Agonist and Antagonist Interactions with Beta-Adrenergic Receptors and the Mechanism of Entropy-Driven Binding" *Biochem. Pharmacol.* **1990**, *40*, 663-669.
- 57) Veber, D. F.; Holly, F. W.; Nutt, R. F.; Bergstrand, S. J.; Brady, S. F.; Hirschmann, R.; Glitzer, M. S.; Saperstein, R. "Highly-Active Cyclic and Bicyclic Somatostatin Analogs of Reduced Ring Size" *Nature* **1979**, *280*, 512-514.
- 58) Martin, S. F. **2003**, Peptide Mimics and Molecular Bondage. To Constrain or Not to Constrain? *Presentation*.
- 59) Cram, D. J. "Preorganization - from Solvents to Spherands" *Angew. Chem.* **1986**, *98*, 1041-1060.
- 60) Hansen, K. K.; Grosch, B.; Greiveldinger-Poenaru, S.; Bartlett, P. A. "Synthesis and Evaluation of Macrocyclic Transition State Analogue Inhibitors for Alpha-Chymotrypsin" *J. Org. Chem.* **2003**, *68*, 8465-8470.
- 61) Hansen, K. K.; Hansen, H. C.; Clark, R. C.; Bartlett, P. A. "Identification of Novel Macrocyclic Peptidase Substrates Via on-Bead Enzymatic Cyclization" *J. Org. Chem.* **2003**, *68*, 8459-8464.
- 62) Spatola, A. F.; Darlak, K.; Romanovskis, P. "An Approach to Cyclic Peptide Libraries: Reducing Epimerization in Medium Sized Rings During Solid Phase Synthesis" *Tetrahedron Lett.* **1996**, *37*, 591-594.
- 63) Veber, D. F.; Johnson, S. R.; Cheng, H. Y.; Smith, B. R.; Ward, K. W.; Kopple, K. D. "Molecular Properties That Influence the Oral Bioavailability of Drug Candidates" *J. Med. Chem.* **2002**, *45*, 2615-2623.

- 64) Reid, R. C.; Pattenden, L. K.; Tyndall, J. D. A.; Martin, J. L.; Walsh, T.; Fairlie, D. P. "Countering Cooperative Effects in Protease Inhibitors Using Constrained Beta-Strand-Mimicking Templates in Focused Combinatorial Libraries" *J. Med. Chem.* **2004**, *47*, 1641-1651.
- 65) Freidinger, R. M.; Veber, D. F.; Perlow, D. S.; Brooks, J. R.; Saperstein, R. "Bioactive Conformation of Luteinizing-Hormone-Releasing Hormone - Evidence from a Conformationally Constrained Analog" *Science* **1980**, *210*, 656-658.
- 66) Schneider, J. P.; Kelly, J. W. "Templates That Induce α -Helical, β -Sheet, and Loop Conformations" *Chem. Rev.* **1995**, *95*, 2169-2187.
- 67) Degrado, W. F. "Design of Peptides and Proteins" *Adv. Protein Chem.* **1988**, *39*, 51-124.
- 68) Kahn, M. "Peptide Secondary Structure Mimetics: Recent Advances and Future Challenges" *Synlett* **1993**, 821-826.
- 69) Olson, G. L.; Bolin, D. R.; Bonner, M. P.; Bos, M.; Cook, C. M.; Fry, D. C.; Graves, B. J.; Hatada, M.; Hill, D. E.; Kahn, M.; Madison, V. S.; Rusiecki, V. K.; Sarabu, R.; Sepinwall, J.; Vincent, G. P.; Voss, M. E. "Concepts and Progress in the Development of Peptide Mimetics" *J. Med. Chem.* **1993**, *36*, 3039-3049.
- 70) Widlanski, T.; Bender, S. L.; Knowles, J. R. "Dehydroquinase Synthase - a Sheep in Wolf's Clothing" *J. Am. Chem. Soc.* **1989**, *111*, 2299-2300.
- 71) Gerhard, U.; Searle, M. S.; Williams, D. H. "The Free-Energy Change of Restricting a Bond Rotation in the Binding of Peptide Analogs to Vancomycin Group Antibiotics" *Bioorg. Med. Chem. Lett.* **1993**, *3*, 803-808.
- 72) Kawai, M.; Horikawa, Y.; Ishihara, T.; Shimamoto, K.; Ohfuné, Y. "2-(Carboxycyclopropyl)Glycines: Binding, Neurotoxicity and Induction of Intracellular Free Calcium Increase" *Eur. J. Pharmacol.* **1992**, *211*, 195-202.
- 73) Brabet, I.; Parmentier, M. L.; De Colle, C.; Bockaert, J.; Acher, F.; Pin, J. P. "Comparative Effect of L-Ccgl-I, Dcgl-Iv and Gamma-Carboxy-L-Glutamate on All Cloned Metabotropic Glutamate Receptor Subtypes" *Neuropharmacology* **1998**, *37*, 1043-1051.
- 74) Monn, J. A.; Valli, M. J.; Massey, S. M.; Wright, R. A.; Salhoff, C. R.; Johnson, B. G.; Howe, T.; Alt, C. A.; Rhodes, G. A.; Robey, R. L.; Griffey, K. R.; Tizzano, J. P.; Kallman, M. J.; Helton, D. R.; Schoepp, D. D. "Design, Synthesis, and Pharmacological Characterization of (+)-2-Aminobicyclo[3.1.0]Hexane-2,6-Dicarboxylic Acid (Ly354740): A Potent, Selective, and Orally Active Group 2 Metabotropic Glutamate

Receptor Agonist Possessing Anticonvulsant and Anxiolytic Properties" *J. Med. Chem.* **1997**, *40*, 528-537.

75) Gullledge, B. M.; Aggen, J. B.; Eng, H.; Sweimeh, K.; Chamberlin, A. R. "Microcystin Analogues Comprised Only of Adda and a Single Additional Amino Acid Retain Moderate Activity as Pp1/Pp2a Inhibitors" *Bioorg. Med. Chem. Lett.* **2003**, *13*, 2907-2911.

76) Marquis, R. W.; Ru, Y.; LoCastro, S. M.; Zeng, J.; Yamashita, D. S.; Oh, H. J.; Erhard, K. F.; Davis, L. D.; Tomaszek, T. A.; Tew, D.; Salyers, K.; Proksch, J.; Ward, K.; Smith, B.; Levy, M.; Cummings, M. D.; Haltiwanger, R. C.; Trescher, G.; Wang, B.; Hemling, M. E.; Quinn, C. J.; Cheng, H. Y.; Lin, F.; Smith, W. W.; Janson, C. A.; Zhao, B. G.; McQueney, M. S.; D'Alessio, K.; Lee, C. P.; Marzulli, A.; Dodds, R. A.; Blake, S.; Hwang, S. M.; James, I. E.; Gress, C. J.; Bradley, B. R.; Lark, M. W.; Gowen, M.; Veber, D. F. "Azepanone-Based Inhibitors of Human and Rat Cathepsin K" *J. Med. Chem.* **2001**, *44*, 1380-1395.

77) Wang, X. Z.; Yao, Z. J.; Liu, H. P.; Zhang, M. C.; Yang, D. J.; George, C.; Burke, T. R. "Synthesis of a Phosphotyrosyl Analogue Having X-1, X-2 and Phi Angles Constrained to Values Observed for an Sh2 Domain-Bound Phosphotyrosyl Residue" *Tetrahedron* **2003**, *59*, 6087-6093.

78) Ding, J. H.; Fraser, M. E.; Meyer, J. H.; Bartlett, P. A.; James, M. N. G. "Macrocyclic Inhibitors of Penicillopepsin. 2. X-Ray Crystallographic Analyses of Penicillopepsin Complexed with a P3-P1 Macrocyclic Peptidyl Inhibitor and with Its Two Acyclic Analogues" *J. Am. Chem. Soc.* **1998**, *120*, 4610-4621.

79) Smith, W. W.; Bartlett, P. A. "Macrocyclic Inhibitors of Penicillopepsin. 3. Design, Synthesis, and Evaluation of an Inhibitor Bridged between P2 and P1" *J. Am. Chem. Soc.* **1998**, *120*, 4622-4628.

80) Meyer, J. H.; Bartlett, P. A. "Macrocyclic Inhibitors of Penicillopepsin. 1. Design, Synthesis, and Evaluation of an Inhibitor Bridged between P1 and P3" *J. Am. Chem. Soc.* **1998**, *120*, 4600-4609.

81) Smith, R. A.; Coles, P. J.; Chen, J. J.; Robinson, V. J.; Macdonald, I. D.; Carriere, J.; Krantz, A. "Design, Synthesis, and Activity of Conformationally-Constrained Macrocyclic Peptide-Based Inhibitors of Hiv Protease" *Bioorg. Med. Chem. Lett.* **1994**, *4*, 2217-2222.

82) Abbenante, G.; March, D. R.; Bergman, D. A.; Hunt, P. A.; Garnham, B.; Dancer, R. J.; Martin, J. L.; Fairlie, D. P. "Regioselective Structural and Functional Mimicry of Peptides - Design of Hydrolytically-Stable Cyclic Peptidomimetic Inhibitors of Hiv-1 Protease" *J. Am. Chem. Soc.* **1995**, *117*, 10220-10226.

- 83) March, D. R.; Abbenante, G.; Bergman, D. A.; Brinkworth, R. I.; Wickramasinghe, W.; Begun, J.; Martin, J. L.; Fairlie, D. P. "Substrate-Based Cyclic Peptidomimetics of Phe-Ile-Val That Inhibit Hiv-1 Protease Using a Novel Enzyme-Binding Mode" *J. Am. Chem. Soc.* **1996**, *118*, 3375-3379.
- 84) Reid, R. C.; Fairlie, D. P. "Mimicking Extended Conformations of Protease Substrates: Designing Cyclic Peptidomimetics to Inhibit Hiv-1 Protease" *Advances in Amino Acid Mimetics and Peptidomimetics* **1997**, *1*, 77-107.
- 85) Reid, R. C.; March, D. R.; Dooley, M. J.; Bergman, D. A.; Abbenante, G.; Fairlie, D. P. "A Novel Bicyclic Enzyme Inhibitor as a Consensus Peptidomimetic for the Receptor-Bound Conformations of 12 Peptidic Inhibitors of Hiv-1 Protease" *J. Am. Chem. Soc.* **1996**, *118*, 8511-8517.
- 86) Curtin, M. L.; Garland, R. B.; Heyman, H. R.; Frey, R. R.; Michaelides, M. R.; Li, J. L.; Pease, L. J.; Glaser, K. B.; Marcotte, P. A.; Davidsen, S. K. "Succinimide Hydroxamic Acids as Potent Inhibitors of Histone Deacetylase (Hdac)" *Bioorg. Med. Chem. Lett.* **2002**, *12*, 2919-2923.
- 87) Xue, C. B.; Voss, M. E.; Nelson, D. J.; Duan, J. J. W.; Cherney, R. J.; Jacobson, I. C.; He, X. H.; Roderick, J.; Chen, L. H.; Corbett, R. L.; Wang, L.; Meyer, D. T.; Kennedy, K.; DeGrado, W. F.; Hardman, K. D.; Teleha, C. A.; Jaffee, B. D.; Liu, R. Q.; Copeland, R. A.; Covington, M. B.; Christ, D. D.; Trzaskos, J. M.; Newton, R. C.; Magolda, R. L.; Wexler, R. R.; Decicco, C. P. "Design, Synthesis, and Structure-Activity Relationships of Macrocyclic Hydroxamic Acids That Inhibit Tumor Necrosis Factor Alpha Release in Vitro and in Vivo" *J. Med. Chem.* **2001**, *44*, 2636-2660.
- 88) Arttamangkul, S.; Murray, T. F.; Delander, G. E.; Aldrich, J. V. "Synthesis and Opioid Activity of Conformationally Constrained Dynorphin-a Analogs .1. Conformational Constraint in the Message Sequence" *J. Med. Chem.* **1995**, *38*, 2410-2417.
- 89) Arttamangkul, S.; Ishmael, J. E.; Murray, T. F.; Grandy, D. K.; DeLander, G. E.; Kieffer, B. L.; Aldrich, J. V. "Synthesis and Opioid Activity of Conformationally Constrained Dynorphin a Analogues .2. Conformational Constraint in the "Address" Sequence" *J. Med. Chem.* **1997**, *40*, 1211-1218.
- 90) Tsantrizos, Y. S.; Bolger, G.; Bonneau, P.; Cameron, D. R.; Goudreau, N.; Kukolj, G.; LaPlante, S. R.; Llinas-Brunet, M.; Nar, H.; Lamarre, D. "Macrocyclic Inhibitors of the Ns3 Protease as Potential Therapeutic Agents of Hepatitis C Virus Infection" *Angew. Chem., Int. Ed. Eng.* **2003**, *42*, 1355-1360.
- 91) Shi, Z. D.; Wei, C. Q.; Lee, K. O.; Liu, H. P.; Zhang, M. C.; Araki, T.; Roberts, L. R.; Worthy, K. M.; Fisher, R. J.; Neel, B. G.; Kelley, J. A.; Yang, D. J.; Burke, T. R.

"Macrocyclization in the Design of Non-Phosphorus-Containing Grb2 Sh2 Domain-Binding Ligands" *J. Med. Chem.* **2004**, *47*, 2166-2169.

92) Etmayer, P.; France, D.; Gounarides, J.; Jarosinski, M.; Martin, M. S.; Rondeau, J. M.; Sabio, M.; Topiol, S.; Weidmann, B.; Zurini, M.; Bair, K. W. "Structural and Conformational Requirements for High-Affinity Binding to the Sh2 Domain of Grb2" *J. Med. Chem.* **1999**, *42*, 971-980.

93) Greco, M. N.; Maryanoff, B. E. "Macrocyclic Inhibitors of Serine Proteases" *Advances in Amino Acid Mimetics and Peptidomimetics* **1997**, *1*, 41-76.

94) Dekker, F. J.; de Mol, N. J.; Fischer, M. J. E.; Kemmink, J.; Liskamp, R. M. J. "Cyclic Phosphopeptides for Interference with Grb2 Sh2 Domain Signal Transduction Prepared by Ring-Closing Metathesis and Phosphorylation" *Org. Biomol. Chem.* **2003**, *1*, 3297-3303.

95) Edwards, J. V.; Lax, A. R.; Lillehoj, E. B.; Boudreaux, G. J. "Structure-Activity-Relationships of Cyclic and Acyclic Analogs of the Phytotoxic Peptide Tentoxin" *J. Agric. Food Chem.* **1987**, *35*, 451-456.

96) Charifson, P. S.; Shewchuk, L. M.; Rocque, W.; Hummel, C. W.; Jordan, S. R.; Mohr, C.; Pacofsky, G. J.; Peel, M. R.; Rodriguez, M.; Sternbach, D. D.; Consler, T. G. "Peptide Ligands of Pp60(C-Src) Sh2 Domains: A Thermodynamic and Structural Study" *Biochemistry* **1997**, *36*, 6283-6293.

97) Li, T.; Saro, D.; Spaller, M. R. "Thermodynamic Profiling of Conformationally Constrained Cyclic Ligands for the PdZ Domain" *Bioorg. Med. Chem. Lett.* **2004**, *14*, 1385-1388.

98) Hruby, V. J.; BartoszBechowski, H.; Davis, P.; Slaninova, J.; Zalewska, T.; Stropova, D.; Porreca, F.; Yamamura, H. I. "Cyclic Enkephalin Analogues with Exceptional Potency and Selectivity for Delta-Opioid Receptors" *J. Med. Chem.* **1997**, *40*, 3957-3962.

99) Bartosz-Bechowski, H.; Davis, P.; Slaninova, J.; Malatynska, E.; Stropova, D.; Porreca, F.; Yamamura, H. I.; Hruby, V. J. "Cyclic Enkephalin Analogs That Are Hybrids of Dpdpe-Related Peptides and Metenkephalin-Arg-Gly-Leu: Prohormone Analogs That Retain Good Potency and Selectivity for Delta Opioid Receptors" *J. Peptide Res.* **1999**, *53*, 329-336.

100) Collins, N.; Flippen-Anderson, J. L.; Haaseth, R. C.; Deschamps, J. R.; George, C.; Kover, K.; Hruby, V. J. "Conformational Determinants of Agonist Versus Antagonist Properties of [D-Pen2,D-Pen5]Enkephalin (Dpdpe) Analogs at Opioid Receptors. Comparison of X-Ray Crystallographic Structure, Solution 1h Nmr Data, and Molecular

Dynamic Simulations of [L-Ala³]Dpdpe and [D-Ala³]Dpdpe" *J. Am. Chem. Soc.* **1996**, *118*, 2143-2152.

101) Bartosz-Bechowski, H.; Davis, P.; Zalewska, T.; Slaninova, J.; Porreca, F.; Yamamura, H. I.; Hruby, V. J. "Cyclic Enkephalin Analogs with Exceptional Potency at Peripheral Delta-Opioid Receptors" *J. Med. Chem.* **1994**, *37*, 146-150.

102) Boguslavsky, V.; Hruby, V. J.; O'Brien, D. F.; Misicka, A.; Lipkowski, A. W. "Effect of Peptide Conformation on Membrane Permeability" *J. Peptide Res.* **2003**, *61*, 287-297.

103) Lynch, V. M.; Austin, R. E.; Martin, S. F.; George, T. "Determination of the Absolute-Configuration of a Novel Dipeptide Isostere" *Acta Crystallogr., Sect. C* **1991**, *47*, 1345-1347.

104) Martin, S. F.; Dorsey, G. O.; Gane, T.; Hillier, M. C.; Kessler, H.; Baur, M.; Mathae, B.; Erickson, J. W.; Bhat, T. N.; Munshi, S.; Gulnik, S. V.; Topol, I. A. "Cyclopropane-Derived Peptidomimetics. Design, Synthesis, Evaluation, and Structure of Novel Hiv-1 Protease Inhibitors" *J. Med. Chem.* **1998**, *41*, 1581-1597.

105) Davidson, J. P.; Lubman, O.; Rose, T.; Waksman, G.; Martin, S. F. "Calorimetric and Structural Studies of 1,2,3-Trisubstituted Cyclopropanes as Conformationally Constrained Peptide Inhibitors of Src Sh2 Domain Binding" *J. Am. Chem. Soc.* **2002**, *124*, 205-215.

106) De Meijere, A. "Bonding Properties of Cyclopropane and Chemical Consequences" *Angew. Chem.* **1979**, *91*, 867-884.

107) Jorgenson, M. J.; Leung, T. "Photochemistry of α,β -Unsaturated Esters. Iv. Cyclopropyl Conjugation in Olefinic Esters. Conformational Effects on Ultraviolet Absorption" *J. Am. Chem. Soc.* **1968**, *90*, 3769-3774.

108) Doyle, M. P.; Austin, R. E.; Bailey, A. S.; Dwyer, M. P.; Dyatkin, A. B.; Kalinin, A. V.; Kwan, M. M. Y.; Liras, S.; Oalman, C. J.; Pieters, R. J.; Protopopva, M. N.; Raab, C. E.; Roos, G. H. P.; Zhou, Q.-L.; Martin, S. F. "Enantioselective Intramolecular Cyclopropanations of Allylic and Homoallylic Diazoacetates and Diazoacetamides Using Chiral Dirhodium(Ii) Carboxamide Catalysts" *J. Am. Chem. Soc.* **1995**, *117*, 5763-5775.

109) Davidson, J. P.; Martin, S. F. "Use of 1,2,3-Trisubstituted Cyclopropanes as Conformationally Constrained Peptide Mimics in Sh2 Antagonists" *Tetrahedron Lett.* **2000**, *41*, 9459-9464.

110) Martin, S. F.; Dwyer, M. P.; Hartmann, B.; Knight, K. S. "Cyclopropane-Derived Peptidomimetics. Design, Synthesis, and Evaluation of Novel Enkephalin Analogues" *J. Org. Chem.* **2000**, *65*, 1305-1318.

- 111) Hillier, M. C.; Davidson, J. P.; Martin, S. F. "Cyclopropane-Derived Peptidomimetics. Design, Synthesis, and Evaluation of Novel Ras Farnesyltransferase Inhibitors" *J. Org. Chem.* **2001**, *66*, 1657-1671.
- 112) Reichelt, A.; Gaul, C.; Frey, R. R.; Kennedy, A.; Martin, S. F. "Design, Synthesis, and Evaluation of Matrix Metalloprotease Inhibitors Bearing Cyclopropane-Derived Peptidomimetics as P1' and P2' Replacements" *J. Org. Chem.* **2002**, *67*, 4062-4075.
- 113) Martin, S. F.; Austin, R. E.; Oalman, C. J.; Baker, W. R.; Condon, S. L.; DeLara, E.; Rosenberg, S. H.; Spina, K. P.; Stein, H. H.; Cohen, J.; Kleinert, H. D. "1,2,3-Trisubstituted Cyclopropanes as Conformationally Restricted Peptide Isosteres: Application to the Design and Synthesis of Novel Renin Inhibitors" *J. Med. Chem.* **1992**, *35*, 1710-1721.
- 114) Martin, S. F.; Austin, R. E.; Oalman, C. J. "Stereoselective Synthesis of 1,2,3-Trisubstituted Cyclopropanes as Novel Dipeptide Isosteres" *Tetrahedron Lett.* **1990**, *31*, 4731-4734.
- 115) Plake, H. R.; Sundberg, T. B.; Woodward, A. R.; Martin, S. F. "Design and Synthesis of Conformationally Constrained, Extended and Reverse Turn Pseudopeptides as Grb2-Sh2 Domain Antagonists" *Tetrahedron Lett.* **2003**, *44*, 1571-1574.
- 116) Wlodawer, A.; Vondrasek, J. "Inhibitors of Hiv-1 Protease: A Major Success of Structure-Assisted Drug Design" *Annu. Rev. Biochem. Biomol. Struct.* **1998**, *27*, 249-284.
- 117) Wlodawer, A.; Erickson, J. W. "Structure-Based Inhibitors of Hiv-1 Protease" *Annu. Rev. Biochem.* **1993**, *62*, 543-585.
- 118) Waksman, G.; Shoelson, S. E.; Pant, N.; Cowburn, D.; Kuriyan, J. "Binding of a High-Affinity Phosphotyrosyl Peptide to the Src Sh2 Domain - Crystal-Structures of the Complexed and Peptide-Free Forms" *Cell* **1993**, *72*, 779-790.
- 119) Eck, M. J.; Shoelson, S. E.; Harrison, S. C. "Recognition of a High-Affinity Phosphotyrosyl Peptide by the Src Homology-2 Domain of P56(Lck)" *Nature* **1993**, *362*, 87-91.
- 120) Waksman, G.; Kominos, D.; Robertson, S. C.; Pant, N.; Baltimore, D.; Birge, R. B.; Cowburn, D.; Hanafusa, H.; Mayer, B. J.; Overduin, M.; Resh, M. D.; Rios, C. B.; Silverman, L.; Kuriyan, J. "Crystal-Structure of the Phosphotyrosine Recognition Domain Sh2 of V-Src Complexed with Tyrosine-Phosphorylated Peptides" *Nature* **1992**, *358*, 646-653.

- 121) Davidson, J. P. Calorimetric and Structural Studies of 1,2,3-Trisubstituted Cyclopropanes as Conformationally Constrained Peptide Mimics. Dissertation, University of Texas at Austin, 2001.
- 122) Fairlie, D. P.; Abbenante, G.; March, D. R. "Macrocyclic Peptidomimetics - Forcing Peptides into Bioactive Conformations" *Current Medicinal Chemistry* **1995**, *2*, 654-686.
- 123) Hruby, V. J.; Balse, P. M. "Conformational and Topographical Considerations in Designing Agonist Peptidomimetics from Peptide Leads" *Current Medicinal Chemistry* **2000**, *7*, 945-970.
- 124) Hruby, V. J.; Agnes, R. S. "Conformation-Activity Relationships of Opioid Peptides with Selective Activities at Opioid Receptors" *Biopolymers* **2000**, *51*, 391-410.
- 125) Ma, D. "Conformationally Constrained Analogs of L-Glutamate as Subtype-Selective Modulators of Metabotropic Glutamate Receptors" *Bioorganic Chemistry* **1999**, *27*, 20-34.
- 126) Lowenstein, E. J.; Daly, R. J.; Batzer, A. G.; Li, W.; Margolis, B.; Lammers, R.; Ullrich, A.; Skolnik, E. Y.; Barsagi, D.; Schlessinger, J. "The Sh2 and Sh3 Domain Containing Protein Grb2 Links Receptor Tyrosine Kinases to Ras Signaling" *Cell* **1992**, *70*, 431-442.
- 127) Stryer, L. *Biochemistry*, W. H. Freeman: New York, 1995, 351-356.
- 128) Fretz, H.; Furet, P.; Garcia-Echeverria, C.; Rahuel, J.; Schoepfer, J. "Structure-Based Design of Compounds Inhibiting Grb2-Sh2 Mediated Protein-Protein Interactions in Signal Transduction Pathways" *Curr. Pharm. Des.* **2000**, *6*, 1777-1796.
- 129) Etmayer, P.; France, D.; Gounarides, J.; Jarosinski, M.; Martin, M.-S.; Rondeau, J.-M.; Sabio, M.; Topiol, S.; Weidmann, B.; Zurini, M.; Bair, K. W. "Structural and Conformational Requirements for High-Affinity Binding to the Sh2 Domain of Grb2" *J. Med. Chem.* **1999**, *42*, 971-980.
- 130) Rahuel, J.; Gay, B.; Erdmann, D.; Strauss, A.; Garcia, E.; Furet, P.; Caravatti, G.; Fretz, H.; Schoepfer, J.; Gruetter, M. G. "Structural Basis for Specificity of Grb2-Sh2 Revealed by a Novel Ligand Binding Mode" *Nat. Struct. Biol.* **1996**, *3*, 586-589.
- 131) Schiering, N.; Casale, E.; Caccia, P.; Giordano, P.; Battistini, C. "Dimer Formation through Domain Swapping in the Crystal Structure of the Grb2-Sh2-Ac-Pyvnv Complex" *Biochemistry* **2000**, *39*, 13376-13382.
- 132) Furet, P.; Garcia-Echeverria, C.; Gay, B.; Schoepfer, J.; Zeller, M.; Rahuel, J. "Structure-Based Design, Synthesis, and X-Ray Crystallography of a High-Affinity

Antagonist of the Grb2-Sh2 Domain Containing an Asparagine Mimetic" *J. Med. Chem.* **1999**, *42*, 2358-2363.

133) Rahuel, J.; Garcia-Echeverria, C.; Furet, P.; Strauss, A.; Caravatti, G.; Fretz, H.; Schoepfer, J.; Gay, B. "Structural Basis for the High Affinity of Amino-Aromatic Sh2 Phosphopeptide Ligands" *J. Mol. Biol.* **1998**, *279*, 1013-1022.

134) Nioche, P.; Liu, W.-Q.; Broutin, I.; Charbonnier, F.; Latreille, M.-T.; Vidal, M.; Roques, B.; Garbay, C.; Ducruix, A. "Crystal Structures of the Sh2 Domain of Grb2: Highlight on the Binding of a New High-Affinity Inhibitor" *J. Mol. Biol.* **2002**, *315*, 1167-1177.

135) Thornton, K. H.; Mueller, W. T.; McConnell, P.; Zhu, G.; Saltiel, A. R.; Thanabal, V. "Nuclear Magnetic Resonance Solution Structure of the Growth Factor Receptor-Bound Protein 2 Src Homology 2 Domain" *Biochemistry* **1996**, *35*, 11852-11864.

136) Ogura, K.; Tsuchiya, S.; Terasawa, H.; Yuzawa, S.; Hatanaka, H.; Mandiyan, V.; Schlessinger, J.; Inagaki, F. "Solution Structure of the Sh2 Domain of Grb2 Complexed with the Shc-Derived Phosphotyrosine-Containing Peptide" *J. Mol. Biol.* **1999**, *289*, 439-445.

137) Senior, M. M.; Frederick, A. F.; Black, S.; Murgolo, N. J.; Perkins, L. M.; Wilson, O.; Snow, M. E.; Wang, Y.-S. "The Three-Dimensional Solution Structure of the Src Homology Domain-2 of the Growth Factor Receptor-Bound Protein-2" *J. Biomol. NMR* **1998**, *11*, 153-164.

138) Ogura, K.; Tsuchiya, S.; Terasawa, H.; Yuzawa, S.; Hatanaka, H.; Mandiyan, V.; Schlessinger, J.; Inagaki, F. "Conformation of an Shc-Derived Phosphotyrosine-Containing Peptide Complexed with the Grb2 Sh2 Domain" *J. Biomol. NMR* **1997**, *10*, 273-278.

139) Kimber, M. S.; Nachman, J.; Cunningham, A. M.; Gish, G. D.; Pawson, T.; Pai, E. F. "Structural Basis for Specificity Switching of the Src Sh2 Domain" *Molecular Cell* **2000**, *5*, 1043-1049.

140) Bennett, M. J.; Schlunegger, M. P.; Eisenberg, D. "3d Domain Swapping - a Mechanism for Oligomer Assembly" *Protein Sci.* **1995**, *4*, 2455-2468.

141) Garcia-Echeverria, C.; Gay, B.; Rahuel, J.; Furet, P. "Mapping the X+1 Binding Site of the Grb2-Sh2 Domain With .Alpha.,.Alpha.-Disubstituted Cyclic .Alpha.-Amino Acids" *Bioorg. Med. Chem. Lett.* **1999**, *9*, 2915-2920.

- 142) Liu, W.-Q.; Vidal, M.; Gresh, N.; Roques, B. P.; Garbay, C. "Small Peptides Containing Phosphotyrosine and Adjacent .Alpha.Me-Phosphotyrosine or Its Mimetics as Highly Potent Inhibitors of Grb2-Sh2 Domain" *J. Med. Chem.* **1999**, *42*, 3737-3741.
- 143) Llinas-Brunet, M.; Beaulieu, P. L.; Cameron, D. R.; Ferland, J. M.; Gauthier, J.; Ghire, E.; Gillard, J.; Gorys, V.; Poirier, M.; Rancourt, J.; Wernic, D. "Phosphotyrosine-Containing Dipeptides as High-Affinity Ligands for the P56(Lck) Sh2 Domain" *J. Med. Chem.* **1999**, *42*, 722-729.
- 144) Bumagin, N. A.; Bykov, V. V.; Sukhomlinova, L. I.; Tolstaya, T. P.; Beletskaya, I. P. "Palladium-Catalyzed Arylation of Styrene and Acrylic-Acid in Water" *J. Organomet. Chem.* **1995**, *486*, 259-262.
- 145) Ho, G. J.; Mathre, D. J. "Lithium-Initiated Imide Formation - a Simple Method for N-Acylation of 2-Oxazolidinones and Bornane-2,10-Sultam" *Abstracts of Papers of the American Chemical Society* **1995**, *209*, 517-ORGN.
- 146) Humphrey, J. M.; Chamberlin, A. R. "Chemical Synthesis of Natural Product Peptides: Coupling Methods for the Incorporation of Noncoded Amino Acids into Peptides" *Chem. Rev.* **1997**, *97*, 2243-2266.
- 147) Carpino, L. A.; Imazumi, H.; Foxman, B. M.; Vela, M. J.; Henklein, P.; El-Faham, A.; Klose, J.; Bienert, M. "Comparison of the Effects of 5- and 6-Hoat on Model Peptide Coupling Reactions Relative to the Cases for the 4- and 7-Isomers" *Org. Lett.* **2000**, *2*, 2253-2256.
- 148) Carpino, L. A. "1-Hydroxy-7-Azabenzotriazole - an Efficient Peptide Coupling Additive" *J. Am. Chem. Soc.* **1993**, *115*, 4397-4398.
- 149) Bird, J.; Demello, R. C.; Harper, G. P.; Hunter, D. J.; Karran, E. H.; Markwell, R. E.; Mileswilliams, A. J.; Rahman, S. S.; Ward, R. W. "Synthesis of Novel N-Phosphonoalkyl Dipeptide Inhibitors of Human Collagenase" *J. Med. Chem.* **1994**, *37*, 158-169.
- 150) Reichelt, A.; Gaul, C.; Frey, R. R.; Kennedy, A.; Martin, S. F. "Design, Synthesis, and Evaluation of Matrix Metalloprotease Inhibitors Bearing Cyclopropane-Derived Peptidomimetics as P1' and P2' Replacements" *J. Org. Chem.* **2002**, *67*, 4062-4075.
- 151) Doyle, M. P.; Winchester, W. R.; Protopopova, M. N.; Kazala, A. P.; Westrum, L. J. "(1r,5s)-(-)-6,6-Dimethyl-3-Oxabicyclo[3.1.0]Hexan-2-One. Highly Enantioselective Intramolecular Cyclopropanation Catalyzed by Dirhodium(Ii)Tetrakis[Methyl2-Pyrrolidone-5(R)-Carboxylate] - ((3-Oxabicyclo[3.1.0]Hexan-2-One, 6,6-Dimethyl-, (1r-Cis)-)" *Organic Synthesis* **1996**, *73*, 13-24.

- 152) Corey, E. J.; Myers, A. G. "Efficient Synthesis and Intramolecular Cyclopropanation of Unsaturated Diazoacetic Esters" *Tetrahedron Lett.* **1984**, *25*, 3559-3562.
- 153) Jakovac, I. J.; Jones, J. B. "Determination of Enantiomeric Purity of Chiral Lactones - General-Method Using Nuclear Magnetic-Resonance" *J. Org. Chem.* **1979**, *44*, 2165-2168.
- 154) Dwyer, M. P. Cyclopropane-Based Peptidomimetics: Iodocyclopropanes as Versatile Synthetic Intermediates and the Design, Synthesis, and Evaluation of Novel Enkephalin Analogues. Dissertation, University of Texas at Austin, Austin, TX, 1997.
- 155) Olah, G. A.; Gupta, B. G. B.; Narang, S. C.; Malhotra, R. "Synthetic Methods and Reactions .71. Chlorotrimethylsilane Lithium Sulfide and Tert-Butyldimethylsilyl Chloride Lithium Sulfide, Mild and Efficient Silylating Reagents" *J. Org. Chem.* **1979**, *44*, 4272-4275.
- 156) Carlsen, P. H. J.; Katsuki, T.; Martin, V. S.; Sharpless, K. B. "A Greatly Improved Procedure for Ruthenium Tetraoxide Catalyzed Oxidations of Organic-Compounds" *J. Org. Chem.* **1981**, *46*, 3936-3938.
- 157) GodierMarc, E.; Aitken, D. J.; Husson, H. P. "Synthesis of Peptides Containing 2,3-Methanoaspartic Acid" *Tetrahedron Lett.* **1997**, *38*, 4065-4068.
- 158) Roos, E. C.; Bernabe, P.; Hiemstra, H.; Speckamp, W. N.; Kaptein, B.; Boesten, W. H. J. "Palladium-Catalyzed Transprotection of Allyloxycarbonyl-Protected Amines: Efficient One-Pot Formation of Amides and Dipeptides" *J. Org. Chem.* **1995**, *60*, 1733-1740.
- 159) Höegberg, T.; Ströem, P.; Ebner, M.; Räämsby, S. "Cyanide as an Efficient and Mild Catalyst in the Aminolysis of Esters" *J. Org. Chem.* **1987**, *52*, 2033-2036.
- 160) Ainsworth, C. "The Conversion of Carboxylic Acid Hydrazides to Amides with Raney Nickel" *J. Am. Chem. Soc.* **1954**, *76*, 5774-5775.
- 161) Pathak, D.; Laskar, D. D.; Prajapati, D.; Sandhu, J. S. "A Novel and Chemoselective Protocol for the Reduction of Azides Using FeCl₃-Zn System" *Chem. Lett.* **2000**, 816-817.
- 162) Fringuelli, F.; Pizzo, F.; Vaccaro, L. "Cobalt(Ii) Chloride-Catalyzed Chemoselective Sodium Borohydride Reduction of Azides in Water" *Synthesis* **2000**, 646-650.
- 163) Rawal, V. H.; Zhong, H. M. "One-Step Conversion of Esters to Acyl Azides Using Diethylaluminum Azide" *Tetrahedron Lett.* **1994**, *35*, 4947-4950.

- 164) Basha, A.; Lipton, M.; Weinreb, S. M. "A Mild, General Method for Conversion of Esters to Amides" *Tetrahedron Lett.* **1977**, 4171-4174.
- 165) Levin, J. I.; Turos, E.; Weinreb, S. M. "An Alternative Procedure for the Aluminum-Mediated Conversion of Esters to Amides" *Synth. Commun.* **1982**, *12*, 989-993.
- 166) Green, T. W.; Wuts, P. G. M. *Protective Groups in Organic Synthesis*, John Wiley & Sons: New York, 1999, 737.
- 167) Fukuyama, T.; Lin, S.; Li, L. "Facile Reduction of Ethyl Thiol Esters to Aldehydes: Application to a Total Synthesis of (+)-Neothramycin a Methyl Ester," *J. Am. Chem. Soc.* **1990**, *112*, 7050-7051.
- 168) Han, Y.; Chorev, M. "A Novel, One-Pot Reductive Alkylation of Amines by *S*-Ethyl Thioesters Mediated by Triethylsilane and Sodium Triacetoxyborohydride in the Presence of Palladium on Carbon" *J. Org. Chem.* **1999**, *64*, 1972-1978.
- 169) Czech, B. P.; Bartsch, R. A. "Effect of Amines on *O*-Benzyl Group Hydrogenolysis" *J. Org. Chem.* **1984**, *49*, 4076-4078.
- 170) Wojciechowski, M.; Grycuk, T.; Antosiewicz, J. M.; Lesyng, B. "Prediction of Secondary Ionization of the Phosphate Group in Phosphotyrosine Peptides" *Biophysical Journal* **2003**, *84*, 750-756.
- 171) Bradshaw, J. M.; Waksman, G. "Calorimetric Investigation of Proton Linkage by Monitoring Both the Enthalpy and Association Constant of Binding: Application to the Interaction of the Src Sh2 Domain with a High-Affinity Tyrosyl Phosphopeptide" *Biochemistry* **1998**, *37*, 15400-15407.
- 172) Stone, M. J. "Nmr Relaxation Studies of the Role of Conformational Entropy in Protein Stability and Ligand Binding" *Acc. Chem. Res.* **2001**, *34*, 379-388.
- 173) Jaramillo, C.; Knapp, S. "Synthesis of *C*-Aryl Glycosides" *Synthesis* **1994**, 1-20.
- 174) Liu, L.; McKee, M.; Postema, M. H. D. "Synthesis of *C*-Saccharides and Higher Congeners" *Curr. Org. Chem.* **2001**, *5*, 1133-1167.
- 175) Du, Y.; Linhardt, R. J.; Vlahov, I. R. "Recent Advances in Stereoselective *C*-Glycoside Synthesis" *Tetrahedron* **1998**, *54*, 9913-9959.
- 176) Parker, K. A. "Novel Methods for the Synthesis of *C*-Aryl Glycoside Natural-Products" *Pure. Appl. Chem.* **1994**, *66*, 2135-2138.

- 177) Sequin, U. "The Antibiotics of the Pluramycin Group (4h-Anthra[1,2-B]Pyran Antibiotics)" *Progress in the Chemistry of Organic Natural Products* **1986**, 50, 57-122.
- 178) Hansen, M. R.; Hurley, L. H. "Pluramycins. Old Drugs Having Modern Friends in Structural Biology" *Acc. Chem. Res.* **1996**, 29, 249-258.
- 179) Hauser, F. M.; Rhee, R. P. "Anthra[1,2-B]Pyran Antibiotics - Total Synthesis of *O*-Methylkidamycinone" *J. Org. Chem.* **1980**, 45, 3061-3068.
- 180) Kaelin, D. E. Novel Methodologies for the Synthesis of *C*-Aryl Glycosides and Progress toward the Synthesis of the *C*-Aryl Glycoside Natural Products Galtamycinone and Kidamycin. Dissertation, University of Texas at Austin, Austin, Tx., 2002.
- 181) Kaelin, D. E.; Lopez, O. D.; Martin, S. F. "General Strategies for the Synthesis of the Major Classes of *C*-Aryl Glycosides" *J. Am. Chem. Soc.* **2001**, 123, 6937-6938.
- 182) Martin, S. F. "Unified Strategy for the Synthesis of *C*-Aryl Glycosides" *Pure. Appl. Chem.* **2003**, 75, 63-70.
- 183) Matsumoto, T.; Hosoya, T.; Suzuki, K. "Total Synthesis and Absolute Stereochemical Assignment of Gilvocarcin M" *J. Am. Chem. Soc.* **1992**, 114, 3568-3570.
- 184) Hart, H. "Arynes and Heteroarynes" *Chemistry of Triple-Bonded Functional Groups* **1994**, 2, 1017-1134.
- 185) Pellissier, H.; Santelli, M. "The Use of Arynes in Organic Synthesis" *Tetrahedron* **2003**, 59, 701-730.
- 186) Anderson, J. E.; Franck, R. W.; Mandella, W. L. "Peri Interactions in Some 1,8-Di-Tert-Butylnaphthalene Compounds. Rotation and Flipping of the Tert-Butyl Groups" *J. Am. Chem. Soc.* **1972**, 94, 4608-4614.
- 187) Franck, R. W.; Yanagi, K. "Compression Effects in 1,4-Di-Tert-Butylnaphthalenes. Chemistry and Nuclear Magnetic Resonance Spectra" *J. Org. Chem.* **1968**, 33, 811-816.
- 188) Apsel, B.; Bender, J. A.; Escobar, M.; Kaelin, D. E.; Lopez, O. D.; Martin, S. F. "General Entries to *C*-Aryl Glycosides. Formal Synthesis of Galtamycinone" *Tetrahedron Lett.* **2003**, 44, 1075-1077.
- 189) Kaelin, D. E., Jr.; Sparks, S. M.; Plake, H. R.; Martin, S. F. "Regioselective Synthesis of Unsymmetrical *C*-Aryl Glycosides Using Silicon Tethers as Disposable Linkers" *J. Am. Chem. Soc.* **2003**, 125, 12994-12995.

- 190) Crump, S. L.; Netka, J.; Rickborn, B. "Preparation of Isobenzofuran-Aryne Cycloadducts" *J. Org. Chem.* **1985**, *50*, 2746-2750.
- 191) Stork, G.; Sofia, M. J. "Stereospecific Reductive Methylation Via a Radical Cyclization Desilylation Process" *J. Am. Chem. Soc.* **1986**, *108*, 6826-6828.
- 192) Pollart, D. J.; Rickborn, B. "Regioselectivity of Alkoxyisobenzofuran-Aryne Cycloadditions" *J. Org. Chem.* **1987**, *52*, 792-798.
- 193) Gnaim, J. M.; Sheldon, R. A. "Highly Regioselective Ortho-Chlorination of Phenol with Sulfuryl Chloride in the Presence of Amines" *Tetrahedron Lett.* **1995**, *36*, 3893-3896.
- 194) Tamao, K.; Ishida, N.; Tanaka, T.; Kumada, M. "Silafunctional Compounds in Organic Synthesis. Part 20. Hydrogen Peroxide Oxidation of the Silicon-Carbon Bond in Organoalkoxysilanes" *Organometallics* **1983**, *2*, 1694-1696.
- 195) Lopez, J. C.; Gomez, A. M.; Fraser-Reid, B. "Silicon-Tethered Radical Cyclization and Intramolecular Diels-Alder Strategies Are Combined to Provide a Ready Route to Highly Functionalized Decalins" *J. Chem. Soc., Chem. Commun.* **1993**, 762-764.
- 196) Jones, G. R.; Landais, Y. "The Oxidation of the Carbon-Silicon Bond" *Tetrahedron* **1996**, *52*, 7599-7662.
- 197) Kreeger, R. L.; Menaro, P. R.; Sans, E. A.; Shechter, H. "Marked Medium Effects on the Substitution and the Addition-Rearrangement-Ejection Reactions of (Halomethyl)Silanes with Methoxides" *Tetrahedron Lett.* **1985**, *26*, 1115-1118.
- 198) personal communication with Hui Li
- 199) Sparks, S. M. "Final Report" **2003**,
- 200) Soderquist, J. A.; Brown, H. C. "Hydroboration. 56. Convenient and Regiospecific Route to Functionalized Organosilanes through the Hydroboration of Alkenylsilanes" *J. Org. Chem.* **1980**, *45*, 3571-3578.
- 201) Hughes, D. L. "The Mitsunobu Reaction" *Organic Reactions* **1992**, *42*, 335-656.
- 202) Johansson, G.; Sundquist, S.; Nordvall, G.; Nilsson, B. M.; Brisander, M.; Nilvebrant, L.; Hacksell, U. "Antimuscarinic 3-(2-Furanyl)Quinuclidin-2-Ene Derivatives: Synthesis and Structure-Activity Relationships" *J. Med. Chem.* **1997**, *40*, 3804-3819.

- 203) Pocker, Y.; Green, E. "Hydrolysis of D-Glucono-D-Lactone. Ii. Comparative Studies of General Acid-Base Catalyzed Hydrolysis of Methylated Derivatives" *J. Am. Chem. Soc.* **1974**, *96*, 166-173.
- 204) ElOuazzani, H.; Khier, N.; Fernandez, I.; Alcudia, F. "General Method for Asymmetric Synthesis of Alpha-Methylsulfinyl Ketones: Application to the Synthesis of Optically Pure Oxisuran and Bioisosteres" *J. Org. Chem.* **1997**, *62*, 287-291.
- 205) Rollin, P.; Sinay, P. "A Convenient, One-Step Oxidation of Glycals to Lactones Using Pyridinium Chlorochromate" *Carbohydr. Res.* **1981**, *98*, 139-142.
- 206) Furukawa, M.; Iitaka, Y. "Structure of Kidamycin: X-Ray Analysis of Isokidamycin Derivatives" *Tetrahedron Lett.* **1974**, *15*, 3287-3290.
- 207) Furukawa, M.; Iitaka, Y. "The Structures of Kidamycin Derivatives: Triacetylmethoxykidamycin Bis(Trimethylammonium) Iodide and Isokidamycin Bis(M-Bromobenzoate)" *Acta Crystallogr., Sect. B* **1980**, *B36*, 2270-2276.
- 208) Stewart, A. O.; Williams, R. M. "C-Glycosidation of Pyridyl Thioglycosides" *J. Am. Chem. Soc.* **1985**, *107*, 4289-4296.
- 209) Schmidt, R. R.; Effenberger, G. "O-Glycosyl Imidates. 29. Reaction of O-(Glucopyranosyl) Imidates with Electron-Rich Heterocycles. Synthesis of C-Glucosides" *Liebigs Ann. Chem.* **1987**, 825-831.
- 210) Cai, M. S.; Qiu, D. X. "C-Glycosyl Compounds. Xiv. Stereoselective and Mild Method for the Synthesis of C-D-Glucosylarenes in High Yield" *Carbohydr. Res.* **1989**, *191*, 125-129.
- 211) Rousseau, C.; Martin, O. R. "Stereodirected Synthesis of Aryl Alpha-C-Glycosides from 2-O-Arylsilyl-Glucopyranosides" *Org. Lett.* **2003**, *5*, 3763-3766.
- 212) Matsumoto, T.; Katsuki, M.; Suzuki, K. "New Approach to C-Aryl Glycosides Starting from Phenol and Glycosyl Fluoride - Lewis Acid-Catalyzed Rearrangement of O-Glycoside to C-Glycoside" *Tetrahedron Lett.* **1988**, *29*, 6935-6938.
- 213) Matsumoto, T.; Katsuki, M.; Jona, H.; Suzuki, K. "Synthetic Study toward Vineomycins - Synthesis of C-Aryl Glycoside Sector Via Cp2hfcl2-AgclO4-Promoted Tactics" *Tetrahedron Lett.* **1989**, *30*, 6185-6188.
- 214) Matsumoto, T.; Katsuki, M.; Jona, H.; Suzuki, K. "Convergent Total Synthesis of Vineomycinone-B2 Methyl-Ester and Its C(12)-Epimer" *J. Am. Chem. Soc.* **1991**, *113*, 6982-6992.

- 215) Matsumoto, T.; Hosoya, T.; Suzuki, K. "Improvement in *O*-*C*-Glycoside Rearrangement Approach to *C*-Aryl Glycosides - Use of 1-*O*-Acetyl Sugar as Stable but Efficient Glycosyl Donor" *Tetrahedron Lett.* **1990**, *31*, 4629-4632.
- 216) Futagami, S.; Ohashi, Y.; Imura, K.; Hosoya, T.; Ohmori, K.; Matsumoto, T.; Suzuki, K. "Total Synthesis of Ravidomycin: Revision of Absolute and Relative Stereochemistry" *Tetrahedron Lett.* **2000**, *41*, 1063-1067.
- 217) Pihko, A. J.; Nicolaou, K. C.; Koskinen, A. M. P. "An Expedient Synthesis of D-Callipeltose" *Tetrahedron-Asymmetry* **2001**, *12*, 937-942.
- 218) Michael, K.; Kessler, H. "Michael-Type Additions in the Synthesis of Alpha-*O*- and -S-2-Deoxyglycosides" *Tetrahedron Lett.* **1996**, *37*, 3453-3456.
- 219) Kozikowski, A. P.; Li, C. S. "A Nitrile Oxide Based Entry to 2,3-Dihydropyran-4-Ones - Synthesis of a Protected Version of Compactin Lactone in Racemic and Optically-Active Forms" *J. Org. Chem.* **1985**, *50*, 778-785.
- 220) Noecker, L.; Duarte, F.; Bolton, S. A.; McMahon, W. G.; Diaz, M. T.; Giuliano, R. M. "Glycosylation of Branched Amino and Nitro Sugars. 2. Synthesis of the Cororubicin Trisaccharide" *J. Org. Chem.* **1999**, *64*, 6275-6282.
- 221) Abdel-Magid, A. F.; Maryanoff, C. A.; Carson, K. G. "Reductive Amination of Aldehydes and Ketones by Using Sodium Triacetoxyborohydride" *Tetrahedron Lett.* **1990**, *31*, 5595-5598.
- 222) Mai, A.; Artico, M.; Esposito, M.; Sbardella, G.; Massa, S.; Befani, O.; Turini, P.; Giovannini, V.; Mondovi, B. "3-(1h-Pyrrol-1-Yl)-2-Oxazolidinones as Reversible, Highly Potent, and Selective Inhibitors of Monoamine Oxidase Type A" *J. Med. Chem.* **2002**, *45*, 1180-1183.
- 223) Thompson, C.; Ge, M.; Kahne, D. "Synthesis of Vancomycin from the Aglycon" *J. Am. Chem. Soc.* **1999**, *121*, 1237-1244.
- 224) dkahne@princeton.edu or cleimkuh@princeton.edu
- 225) Eliel, E. L.; Satici, H. "Conformational-Analysis of Cyclohexyl Silyl Ethers" *J. Org. Chem.* **1994**, *59*, 688-689.
- 226) Hosoya, T.; Ohashi, Y.; Matsumoto, T.; Suzuki, K. "On the Stereochemistry of Aryl *C*-Glycosides: Unusual Behavior of Bis-Tbdps Protected Aryl *C*-Olivosides" *Tetrahedron Lett.* **1996**, *37*, 663-666.
- 227) Evans, D. A.; Ratz, A. M.; Huff, B. E.; Sheppard, G. S. "Total Synthesis of the Polyether Antibiotic Lonomycin-a (Emericid)" *J. Am. Chem. Soc.* **1995**, *117*, 3448-3467.

- 228) Tellinghuisen, J. "A Study of Statistical Error in Isothermal Titration Calorimetry" *Anal. Biochem.* **2003**, *321*, 79-88.
- 229) personal communication with MicroCal Corp. Northampton, MA.
- 230) Lyon, R. P.; Hill, J. J.; Atkins, W. M. "Novel Class of Bivalent Glutathione S-Transferase Inhibitors" *Biochemistry* **2003**, *42*, 10418-10428.
- 231) Still, W. C.; Kahn, M.; Mitra, A. "Rapid Chromatography Technique for the Preparative Separations with Moderate Resolution" *J. Org. Chem.* **1978**, *43*, 2923-2925.

Vita

Hilary Ruth Plake was born on December 14, 1976 to Donald H. Plake and Dr. Barbara S. Plake. In 1995, she graduated in the top 1% from Lincoln Southeast Highschool, Lincoln, NE. She then attended Boston University and was fortunate to serve as an undergraduate research assistant in the labs of Prof. Kosta Steliou. She was also employed at ARIAD pharmaceuticals in the summer and fall of 1997. She graduated *magna cum laude* with distinction from Boston University with a Bachelor of Arts in Chemistry in 1999. In the fall of that same year, she entered Graduate School at the University of Texas at Austin and joined the labs of Prof. Stephen F. Martin. She is currently an American Cancer Society postdoctoral fellow in the labs of Prof. Michael T. Crimmins at the University of North Carolina, Chapel Hill.

Permanent address: 2300 Camelot Court, Lincoln, NE 68512

This dissertation was typed by the author.